NASA TECHNICAL TRANSLATION

NASA TT F-599

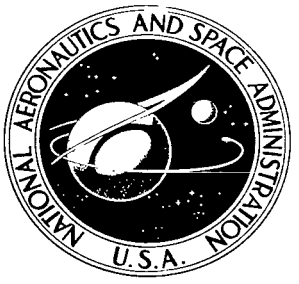

ASTROMETRY AND ASTROPHYSICS, NO. 4, PHYSICS OF COMETS

Edited by V. P. Konopleva

"Naukova Dumka" Press, Kiev, 1969

NATIONAL AERONAUTICS AND SPACE ADMINISTRATION • WASHINGTON, D. C. • JUNE 1970

NASA TT F-599

ASTROMETRY AND ASTROPHYSICS, NO. 4, PHYSICS OF COMETS

Edited by V. P. Konopleva

Translation of "Astrometriya i Astrofizika, 4, Fizika Komet"
"Naukova Dumka" Press, Kiev 1969

NATIONAL AERONAUTICS AND SPACE ADMINISTRATION

For sale by the Clearinghouse for Federal Scientific and Technical Information
Springfield, Virginia 22151 – CFSTI price $3.00

This collection contains the results of original investigations on the physics and activity of comets, the data of laboratory experiments modeling the physical processes in comets, the materials of review articles read at the All-Union Conference on Comets (Kiev, October, 1966), the most recent data concerning the interplanetary magnetic fields, the solar corpuscular radiation, and the interactions between the solar wind and the Earth's magnetosphere and the atmospheres of comets.

Information is given on observations of the Ikey-Seki comet of 1965*f*.

The book is intended for scientists at astronomical and geophysical institutions, undergraduate and graduate students with the corresponding specialties, and all those who are interested in astronomy.

TABLE OF CONTENTS

SOLAR CORPUSCULAR RADIATION ACCORDING TO THE DATA OF MEASUREMENTS ON SATELLITES AND ROBOT SPACE STATIONS

A.S. Dvoryashin†

ABSTRACT: Data on corpuscular radiation which have been obtained from geophysical observations and space probes are reviewed. The existence of a four-streamer structure bringing about four sequences of geomagnetic disturbances is established. Each streamer carries a magnetic field of mainly one polarity. The four-streamer model of the interplanetary magnetic field which has definite boundaries and exists during several revolutions of the Sun is described.

The first information on solar corpuscular radiation, obtained /7* during studies of geophysical phenomena occuring at high and low latitudes, have been made more precise by the direct measurements which are carried out in interplanetary space with the aid of satellites and robot space stations. An analysis of the variations in intensity of cosmic rays of solar and galactic origin has shown that there is a movement of extended magnetic fields at the same time as a corpuscular stream in the solar system. The arisal of the magnetic field in interplanetary space can be considered solely as the result of an increase in the total magnetic field of the Sun and the field of active regions by the corpuscular radiation of the Sun. This radiation brings about either variations in the magnetic fields in the polar cap or magnetic storms with a gradual or sudden beginning (*SC*) on the Earth, accompanied by variations in intensity of the cosmic rays of galactic origin. The differences in nature of the storms with gradual or sudden beginnings are due to the difference in physical characteristics (density, velocity, magnetic field) of the corpuscular streams, which reflects the difference in their sources and, correspondingly, in the emission mechanisms responsible for different streams.

All the data on corpuscular radiation which have been obtained from geophysical observations and experiments carried out with the aid of satellites and automatic interplanetary stations allow us to single out the following components in corpuscular radiation:

(a) "solar wind", or a continuous mild stream of particles

---

* Numbers in the margin indicate pagination in the foreign text.

† Crimean Astrophysical Observatory, Academy of Sciences of the USSR.

from the Sun;

(b) corpuscular streams which are an intensification of the solar wind over the regions of a local magnetic field and are identified as coronal streams;

(c) plasma clouds which are thrown out of active regions with the development of solar flares and which generate a shock wave during their movement;

(d) high-energy corpuscular radiation ($E \sim 10 - 100$ MeV), the spectrum of which sometimes extends to the region of relativistic energy.

The streams of particles, which move away from the Sun at a high speed, also meet other bodies of the Solar System on their way toward the Earth, as is indicated by a number of phenomena observed in the atmospheres of planets and comets. /8

Let us examine the characteristics of each of the components of solar corpuscular radiation.

Solar Wind

The constant disturbance of the magnetic field in the polar caps of the Earth (for an almost stable field at middle and low latitudes [1]) shows that we can single out a constantly effective component in the corpuscular radiation (solar wind), or a continuous mild stream of particles from undisturbed solar regions [2, 3]. It is difficult to draw any definite conclusions on the characteristics of the solar wind from an investigation of geophysical phenomena. Most of the information on the solar wind has been obtained by direct measurements with the aid of satellites and automatic interplanetary stations. The streams of particles in interplanetary space were first measured during the flight of the second Soviet space rocket to the Moon, with "Luna-2" on board, when all the collectors recorded streams of positively charged particles reaching orders of magnitude of $2 \cdot 10^8$ $cm^{-2} \cdot sec^{-1}$ at a long distance from the Earth, in a completely quiet state of the magnetic field [4]. Analogous results were obtained in measurements of the particle flux density during the flight of the automatic station "Venera-1" to Venus in February of 1961 [5, 6].

Somewhat later, the data obtained from the Soviet automatic stations were collaborated by measurements carried out on the American satellite "Explorer-10" [16,17]. It was established that, beyond the boundaries of the Earth's magnetic field, the average velocity of the particles is $3 \cdot 10^7$ cm/sec in order of magnitude, while the streams observed fluctuated around an average value of roughly $3 \cdot 10^8$ protons/$cm^2 \cdot sec$. It was shown that the proton fluxes observed in interplanetary space move in a direction away from the

Sun.

The rather short period for the measurements of the stream of particles (lifespan of the satellite, 53 hours) and the closeness of the trajectory of "Explorer-10" to the Earth's magnetosphere (so that the satellite apparently intersected the region of interaction between the solar wind and the Earth's magnetosphere several times) shows that we should view the measurements carried out on this satellite with a critical eye. Therefore, the results obtained during investigations of the plasma flux in interplanetary space with the apparatus installed on the Soviet automatic interplanetary station "Mars-;" [3] and the American space probe "Mariner-2" [18-22] are of particular great significance. /9

The measurements on "Mariner-2" were the longest. The energy spectrum of the radial component of the solar plasma was measured every 220 sec for more than 100 days. The data from the measurements from August 27 to the end of December show that plasma fluxes from the Sun existed almost constantly during this period. The fluxes which were measured varied substantially in time, which is completely natural since "Mariner-2" also intersected solar corpuscular streams during the flight, as indicated by the magnetic storms on the Earth recorded during this period.

Naturally, a plasma flux can be described at any particular moment by the distribution of the number of particles over the velocity spectrum. Obviously, this distribution may be such that particles of some definite velocity make the greatest contribution to the current measured for some moment of time. In obtaining the average daily velocity of the plasma (as a characteristic of the plasma in interplanetary space), it is wise to take the velocity of the particles which produce the greatest current for each definite moment of time, and to average these values over 24 hours (Fig. 1).

It can be seen from Figure 1 that the average daily velocity underwent substantial fluctuations; however, its value never fell below 350 - 400 km/sec, remaining on this level for 3-4 days. The periods during which the velocity was minimal coincided with the time when the Earth's magnetic field was quiescent (minimal value of K_p). The number of particles in the stream averaged about 2 proton/cm^3. Correspondingly, the average flux of solar plasma was close to the order of magnitude of 10^8 protons/cm^2 sec, which corroborates the measurements carried out earlier on Soviet space rockets [4-6]. Analogous results were obtained on the satellite "IMP-1"; a plasma flux directed away from the Sun which did not exceed $2 \cdot 10^8$ protons/cm^2 sec was constantly observed beyond the boundaries of the Earth's magnetic field (with the field on the surface at rest) [23].

The measurements on "Mariner-2" were carried out during a

rather high activity period of the Sun [1962). Let us discuss a long period of observations of the solar wind with respect to the minimum solar activity (June-October, 1964). /10

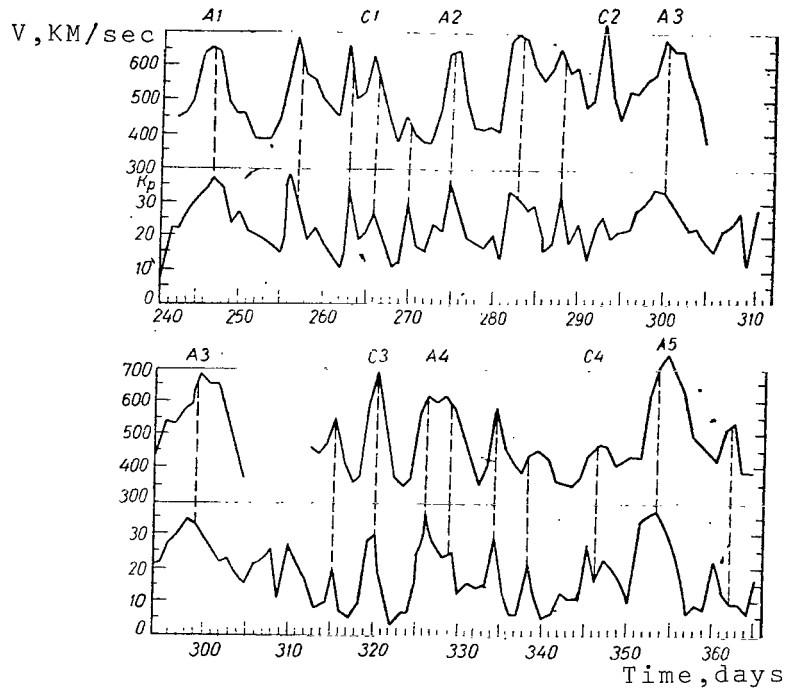

Fig. 1. Average Daily Values of the Plasma Velocity v and Disturbance of the Earth's Magnetic Field K_p From August to December of 1962. (A and C) Sequences of Maxima repeated every 27 Days.

The measurements were carried out on satellites of the "Vela" series. During one revolution, the satellites entered interplanetary space from the solar side of the Earth, where the effect of the Earth and its magnetosphere were not felt, intersected the transition regions behind the shock wave, entered the magnetosphere and intersected its magnetic tail (Fig. 2). The circular orbit with radius of about 17 R (R is the radius of the Earth) was selected so that the satellites would not enter the Earth's radiation belts. One of the tasks of the satellites was to detect nuclear explosions in space.

The electrostatic analyzers of the "Vela-2" satellites measured the energy spectrum, flux density and ion velocity distribution over the directions in the solar wind. Conclusions can be drawn from these observations on the velocity, flux direction, ion density, effective temperature and percentage of α-particles in the solar wind. /11

During roughly 25% of the period from July 27, 1964 to February, 1965, at least one of the "Vela-Hotel" satellites measured

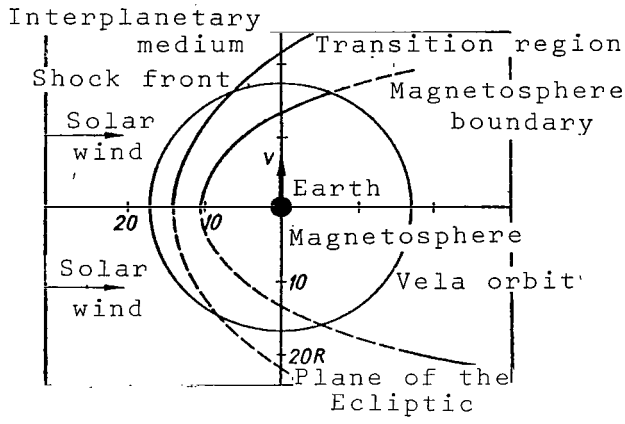

Fig. 2. Cross Section of the Magnetosphere, Transition Region and Front of the Shock Wave Falling Behind the Plane of the Ecliptic (The Circle Approximately Designates the Geometrical Location of Points Collected in the Ecliptic Plane During the Six Months of Operation of the Satellite [24]).

the characteristics of the solar wind. For an example, Figure 3 shows the spectra of ion fluxes recorded in interplanetary space by the "Vela-2" satellites [24]. These spectra indicate that the characteristics of the solar wind change in time and are similar to the spectra observed earlier on "Mariner-2" [19-21] "Explorer-10" [17] and "IMP-1" [25]. In seven months of observations, 10^5 energy spectra and direction-velocity distributions were obtained. The important characteristics of the spectra shown in Figure 3 are the following:

(a) the width of the spectrum, determined by the temperature (however, it was found that even the principal group in the velocity distribution is usually described by a Maxwellian distribution only positively, and even this is not always true); /12

(b) the absolute values for the energy of the protons, from which the average proton velocity, a measure of the plasma velocity as a whole, can be obtained;

(c) the integral of the curve, which determines the flux

density.

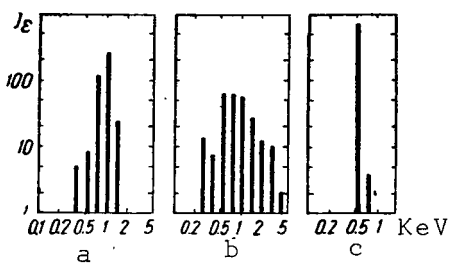

Fig. 3. Ion Spectra Obtained by the "Vela-2" Satellite in Interplanetary Space on July 21 and 26 and August 20, 1964; The Position of the Successive Energy Channels (Vertical Lines) is Plotted in Logarithmic Scale Along the Abscissa Axis. The Width of the Vertical Lines Corresponds to the Width of the Instrumental Channels. The Instrument does not React to the Intermediate Energies Between the Vertical Lines (J_ε is the Differential Flux, $cm^{-2} \cdot stere^{-1} \cdot ReV^{-1}$).

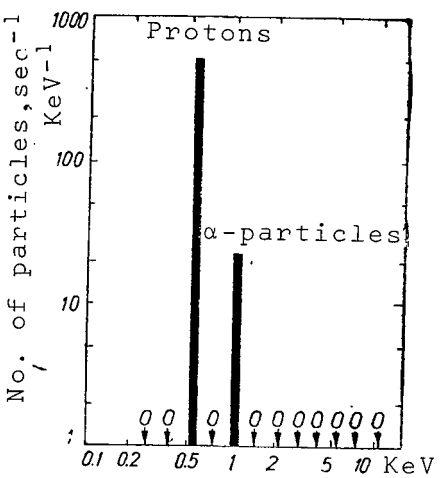

Fig. 4. Energy Spectrum of the Solar Wind with a Sharply Pronounced Maximum of Alpha Particles for August 24, 1964 (The Zeros Show the Position of Those Energy Channels where the Observed Flow Rate Was Equal to Zero).

On the three spectra shown in Figure 3, spectrum (a) is intermediate, and the two others are examples of broad and narrow spectra. Figure 4 shows a spectrum of another type, where we can clearly see the proton and helium components in the solar wind. The α-particles were recorded in the channel where the energy per unit charge is twice greater than the proton energy. Since the energy widths of the channels are less than the intervals between them, it is possible that not all the particles were detected. Obviously, the spectrum shown in Figure 4 was taken at a moment when the fluxes of protons and α-particles were characterized by a narrow energy interval directly incident in the cited channels. An analysis of numerous observations shows that the percentage of α-particles in the solar wind changes in time roughly from 1 to 20%, and the average value according to the measurements on the "Vela-Hotel" satellites is somewhere in the range of 3-6%. /13

The plasma velocity determined from energy spectra for a three-month interval of observations is shown in Figure 5 [24]. The lower values for the disturbance A_p (quiet magnetic fields) corresponded to lower plasma velocities in the interplanetary space.

These velocities are characteristic of the solar wind. The results are close to those obtained on "Mariner-2"; the velocity of the quiescent solar wind is 300-330 km/sec.

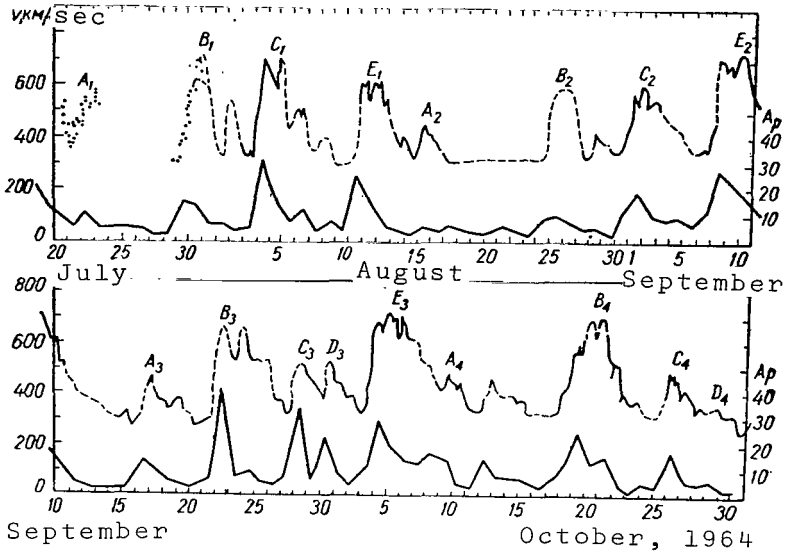

Fig. 5. Plasma Velocity of the Solar Wind in Interplanetary Space During the Period from July to October of 1964. (· Signifies Several Measurements Carried Out Every Two Minutes; —— Signifies Measurements According to These Points; ---- Corresponds to Variations Obtained According to Observations in the Transition Region, When No Velocity in Interplanetary Space Was not Distorted By the Presence of the Leading Shock Wave; A_p Signifies the Disturbance of the Earth's Magnetic Field).

Long-term observations of the characteristics of the plasma in interplanetary space were carried out on the "IMP-1" satellite /14 [25]. The data obtained show that the quiet magnetic field on the Earth (see values of K_p for 6-7 days in Fig. 6[1], corresponds to a velocity of the wind in interplanetary space of $v \sim 280$-300 km/sec (Fig. 7) [26-28]. The measurements refer to the period from October 27, 1963 (date of satellite launching) to February 20, 1964.

[1] The position of the Earth inside the major sector (of 24 hours) during its passage by the Earth is represented along the abscissa axes in Figures 6, 7, 16 and 22.

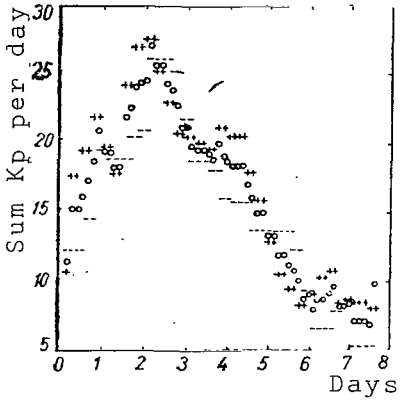

Fig. 6. Changes in Disturbance of the Geomagnetic Field During Passage of a Sector by the Earth (+) Field Directed Away from the Sun; (-) Toward the Sun; (0) From the Sun and Toward the Sun.

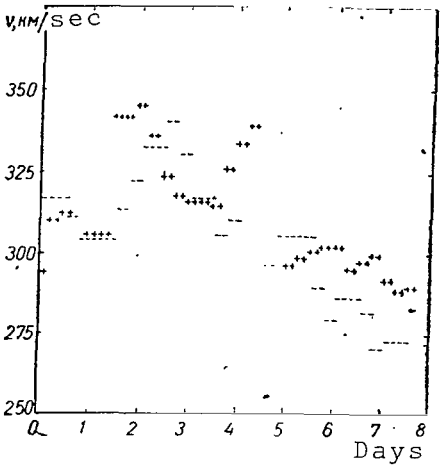

Fig. 7. Change in Solar Wind Velocity During Passage of a Sector by the Earth [28]. (+) Field Directed Away from the Sun; (-) Toward the Sun.

In revolution 1488, the characteristics of the solar wind were noted on the space probe "Pioneer-6", which was launched on heliocentric orbit on December 16, 1965. The results which have been published refer to the period from December 16 to 20, 1965 [29]. It can be seen from Figure 8 that the velocity of the quiescent solar wind is about 350 km/sec. Roughly the same wind velocities were obtained according to the measurements on "Mariner-4" [30].

Thus, the solar wind velocity, measured at different times on all the spacecraft, is within the following range:

350-400 km/sec	"Mariner-2", August-December, 1962;	/15
280-300 km/sec	"IMP-1", December 1963 to February, 1964;	
300-330 km/sec	"Vela-Hotel", July-October, 1964;	
~ 350 km/sec	"Pioneer", December, 1965.	

The lowest velocity occurs at the minimum of the cycle of solar activity, but the difference in the velocities is very small and it is impossible to draw a reliable conclusion on a decrease in wind velocity toward the minimum of the cycle. We can speak only of a tendency.

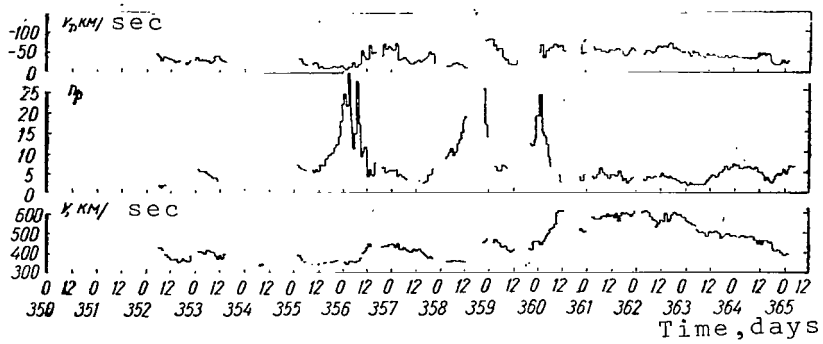

Fig. 8. Data on Velocity of Solar Wind, Density n_p and Thermal Velocity of Protons, Averaged Per Hour (The Blank Spaces Correspond to Times When the Measurements Were Not Carried Out or the Measured Values Were Not Analyzed), The Values of the Velocity v Cited Have an Accuracy of 15 km/sec, and the Density 20%; The Data on the Thermal Velocity v_T Are Very Preliminary.

Geometry of the Interplanetary Magnetic Field Under Average Undisturbed Conditions

Investigations of the interplanetary medium have shown that the solar wind acts constantly. Consequently, we can assume that its comes from each point on the undisturbed surface of the Sun. Measurements of the magnetic fields on the Sun with high-sensitivity and high-resolution apparatus have shown [7-9,31] that the magnetic fields span almost the entire surface of the Sun. Consequently, when the field is carried away by the wind, all the interplanetary space seems to be filled with a plasma with density of $n_p \sim 5$ protons/sec^3, which flows from the Sun at a velocity of about 350 km/sec and entrains a frozen magnetic field with it. If the field remains connected to the Sun while the wind velocity is radial, then the field component occurring in the plane of the ecliptic should twist up into a spiral. /16

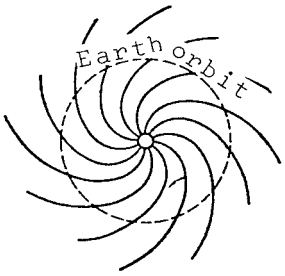

Fig. 9. Spiral Structure of Magnetic Field.

The conclusion on the spiral structure of the field (Fig. 9) was obtained by "transillumination" of the interplanetary space by high-energy particles from outbursts of protons [2, 3, 10, 11, 32]. The time of the formation of high-energy particles [12] is determined by the time of the arisal of a radio outburst of type IV. The moment of the precipitation of such particles at high geomagnetic latitudes of the Earth is determined

according to the time of the beginning of increase in minimal frequencies of reflection during a vertical probe of the ionosphere. It is found that the calculated time for the movement of these high-energy particles from the Sun to the Earth depends on the coordinates of the flare-up on the Sun (Fig. 10).

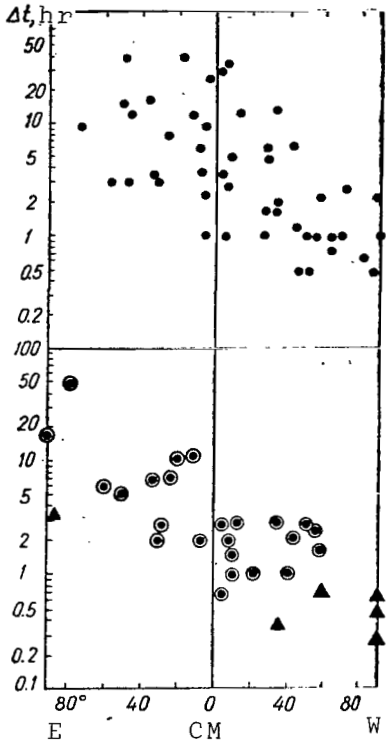

Fig. 10. Delay Δt in the Beginning of the Precipitation of High-Energy Protons on the Polar Cap of the Earth by f_{min} as a function of the Coordinates of a Solar Flare. (●) Mild Proton Outbursts; (⊙) Strong Proton Outbursts; (Δ) Outbursts Causing an Increase in the Intensity of Cosmic Rays at Sea Level.

In the case of flare-ups arising at longitudes in the neighborhood of 60° west of the central meridian of the Sun, the time for movement of high-energy particles from the Sun to the Earth is about 30 min, or the shortest delay. However, for flare-ups in the east, the delay time reaches roughly five hours. The rapid motion of the particles to the Earth from flare-ups in the west can be considered as the result of the fact that the active region which is the source of the particles and is located roughly 60° west of the central meridian is connected by the lines of force of the magnetic fields to the vicinity of the Earth, and the particles move along the field in this case. Actually, for those velocities of the solar wind which were measured directly in interplanetary space with the aid of satellites and rockets, the magnetic field which is carried away by the solar wind from regions near the central meridian reaches the Earth when the region which is the source of this field is roughly 60° west of the central meridian. /17

Satellite and rocket measurements have aided largely in making this first rough model of the interplanetary magnetic field more precise [33-40] and in studying its fine filamentary structure [41-47].

The first measurements of the interplanetary magnetic fields were carried out on the space probe "Pioneer-1" in October of 1958 [33]. Only one field component, that perpendicular to the axis of rotation of the apparatus, was measured. Beyond the limits of 13.5 R "Pioneer-1" reached regions where the field was relatively stable and underwent mild fluctuations around a mean value of $B \sim 5\gamma$ ($1\gamma = 10^{-5}$Oe). It was assumed

that "Pioneer-1" was in interplanetary space during the time when the characteristics of the field and the plasma were not distorted by the effect of the magnetosphere and the outgoing shock wave.[2]

More complete measurements were carried out on the space probe "Pioneer-5" [34] from March 11 to April 30, 1960. A first analysis of the measurements obtained on "Pioneer-5" indicated that the field acts constantly in interplanetary space and has a substantial component on the order of 3γ directed at an angle of 60-90° to the plane of the ecliptic. This field was not included within the framework of the theoretical models, and it contradicted the results obtained from "transillumination" of the interplanetary magnetic fields by high-energy particles from proton beams. A second examination of the measurements on "Pioneer-5" showed [35,36] that the interplanetary field is closer to the plane of the ecliptic and has magnitude of $B \sim 5\text{-}10\gamma$. /18

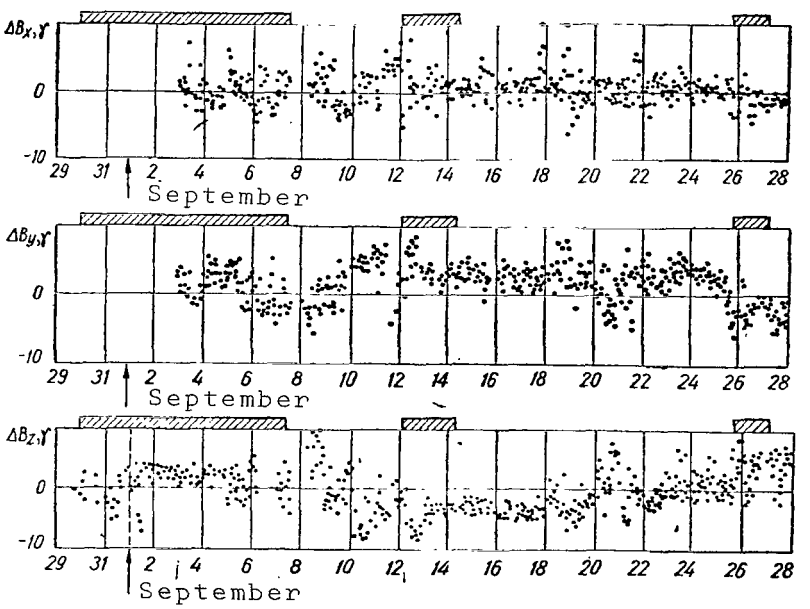

Fig. 11. Magnetic Data According to the "Mariner-2" Measurements; Average Hourly Values of the Three Field Components (Shaded Strips) Correspond to the Arisal of Magnetic Storms.

The magnetic measurements on "Explorer-10" do not give any valuable information on the interplanetary field, since the satellite trajectory apparently passed along the boundary of the magnetosphere and, during its motion (due to variations in the solar wind), the satellite was either in the Earth's magnetosphere, in the

[2] The characteristics of the shock wave and the transition regions will be discussed in a separate study.

transition region, or in "pure" interplanetary space. With regard to the abrupt changes in magnitude and direction of the field and the relatively short period for obtaining the data, the analysis of these satellite measurements did not make a substantial contribution to the model of the interplanetary magnetic field.

The "Mariner-2" measurements were carried out on a higher level [37-39] (August-December, 1962). Measurements of all three components of the field were obtained every 37 sec for more than 100 days: B_z is the field component which occurs in the plane of the ecliptic and is directed along the radius away from the Sun; B_x is the component which is perpendicular to the plane of the ecliptic; B_y is the component in the plane of the ecliptic in the direction in which the Earth moves. The average hourly values of the three components for September of 1962 are given in Figure 11. /19

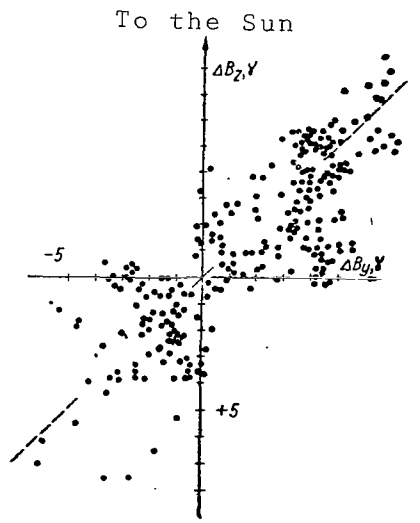

Fig. 12. Magnetic Data of "Mariner-2".

The field component which is perpendicular to the plane of the ecliptic averaged zero over several days. This means that the interplanetary magnetic field is parallel to the plane of the ecliptic on the average. The direction of the field in the plane of the ecliptic is shown in Figure 12, on which the field components, averaged for three hours and smoothed out by calculating the moving averages over nine successive values (in order to decrease the effect of small-scale variations), are plotted. Since the vertical line in Figure 12 corresponds to the solar radius vector, the position of the points shows that the preferable direction for large-scale changes in the magnetic field corresponds to an angle of about 45° with respect to the radial direction.

Thus, although the "Mariner-2" measurements of the magnetic field met with a number of experimental difficulties (the presence of a large, $B \sim 100\gamma$, magnetic field induced near the magnetometer by the craft itself, the insufficient absolute accuracy because of the change of this field during the period between calibration and beginning of the experiment in space), an analysis of the data allows us to draw conclusions on the existence and properties of the large-scale magnetic fields because of the long measurement period and the large amount of information gathered. On the average, the interplanetary field occurs in the plane of the ecliptic and composes an angle of about 45° with the direction toward the Sun.

The first precise measurements of the interplanetary magnetic field, as seen clearly from the statement of the authors themselves [41,42], were carried out on the "IMP-1" satellite. The satellite /20

was put into high elliptical orbit with apogee roughly equal to 31.7 R. In the first loops the apogee-Earth-Sun angle was equal to 25° west of the direction toward the Sun, so that the satellite entered interplanetary space on the day side of the Earth. According to the second Kepler law, the satellite passed in the vicinity of the apogee most of the time in an interplanetary space which was not distorted by the presence of the Earth and its magnetosphere. The magnitude and direction of the field were measured every 20 sec (sessions of 4.8 sec). In order to investigate the large-scale regularities in the field, the measured values were averaged over three hours. The statistical distribution of the directions of the field for this average are shown in Figure 13 [41-44]. As can be seen from Figure 13, the large-scale magnetic field is inclined with respect to the plane of the ecliptic at an angle of 15-20°, while the lines of force in the projection onto the plane of the ecliptic make up an angle of about 50° with the direction toward the Sun. The latter result is particularly important: it indicates

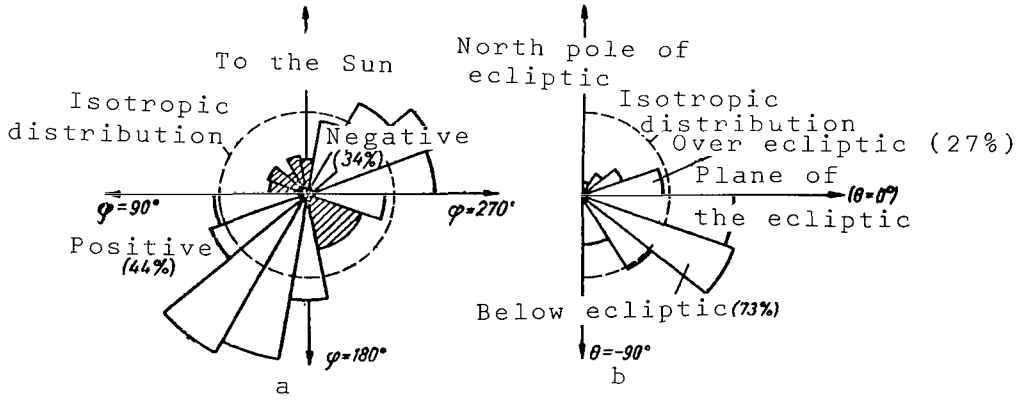

Fig. 13. Statistical Distribution of the Directions of the Interplanetary Magnetic Field: (a) In the Plane of the Ecliptic; (b) in the Plane Perpendicular To It; The Shaded Region Corresponds to Isotropic Distribution; The Angular Intervals in which the Field is Directed Primarily Away from the Sun or Toward the Sun are Designated as Positive or Negative.

that, at a distance of the Earth's orbit, the direction of the large-scale interplanetary magnetic field coincides with the Archimedes spiral, i.e., with the geometry of the corpuscular stream in space. /21

The field intensity measured during this period varies within the range of 3-8γ, and the average value $B \sim 5\gamma$. Note the change in field intensity with the time. It was found that fields of higher intensity (around 6-8γ) are reported in interplanetary space during periods of magnetic storms of the Earth. Obviously, the corpuscular streams, which are considered as an intensification of the solar wind over an active region, transport stronger fields.

Small-scale fluctuations are superposed over the large-scale picture for the regular interplanetary field. This problem will be discussed subsequently.

Corpuscular Streams

A certain amount of information on the corpuscular streams was obtained from studies of geophysical phenomena even before the launching of the first satellites and space rockets. The well-known 27-day recurrence period of storms with gradual beginning indicates that the corpuscular stream causing it is connected with a specific season on the Sun. The 27-day variation in cosmic rays show that the recurrent corpuscular streams transport magnetic fields of high intensity. A roughly correct estimate of the particle density in the flux on the order of 10 protons/cm^3 [51] is given in a number of studies. The average flux velocity corresponding to the beginning of a disturbance is determined according to the delay time for a magnetic storm on the Earth with respect to the passage of an active region through the central meridian of the Sun, assuming an approximately radial escape of gases from the active region. It was found to be on the order of 450 km/sec, which has been confirmed by rocket and satellite measurements in interplanetary space.

Satellite and rocket measurements have aided in clarifying the velocity distribution in the flux (according to the section of the flux perpendicular to the radius vector from the Sun), the density of the plasma at various points of the flux, the geometry of the field in the fluxes and other characteristics.

Characteristics of Corpuscular Streams According to the Data of Satellite and Rocket Measurements /22

Velocity. During the flight of "Mariner-2", several magnetic storms were recorded on the Earth, which indicates that the Earth passed through corpuscular streams. An increase in the disturbance of the magnetic field (see Fig. 1) coincides with an increase in the velocity of the solar wind. Consequently, one of the signs of a corpuscular stream producing disturbances in the magnetic field on the Earth is a higher plasma velocity. If velocities of 350-400 km/sec were observed in the quiet solar wind, sometimes decreasing to 320-240 km/sec, then velocities of 450-700 km/sec were recorded in corpuscular streams. A number of maxima in Figure 1 form sequences with 27-day recurrence intervals. The maxima of Series A appear every 1-2 days after passage through the central meridian of a calcium flocculus located 10° north of the solar equator and observed on the Sun during seven successive revolutions. The maxima of Series C follow every one or two days after the passage of a calcium flocculus north of the equator, and this flocculus is observed during 5 revolutions of the Sun. Considering that the maxima on the curve are reached 2-3 days after the beginning of the increase in velocity, a number of authors conclude that the increase in plasma velocity around the Earth begins practically on the day

the flocculus passes through the central meridian. However, E.R. Mustel' [14] showed that this conclusion is simply the consequence of an incorrect identification of the source of the flux.

The higher plasma velocity as a distinguishing aspect of corpuscular streams producing recurrent magnetic disturbances was also established by the measurements carried out on satellites on the "Vela" Series [24]. A higher velocity of the solar wind (see Fig. 5) is observed during periods of geomagnetic disturbances (increased values of A_p). Just as in the data of "Mariner-2", the velocity measured in the fluxes was within the range of 450-700 km/sec. The highest value of the velocity was around 720 km/sec. The velocity maxima are repeated in 27-day intervals, and this is traced through three revolutions of the Sun. We should mention that the maxima in A_p coincide in time with the periods of rapid increase in velocity. This possibly may be explained by the fact that the disturbance in /23 the magnetic field is characterized by a value averaged over 24 hours.

Very convincing results were obtained on the "IMP-1" satellite with regard to the disturbance in the magnetic field and plasma velocity in corpuscular streams [25]. As the authors show, velocities from 570 to 750 km/sec were obtained during the perturbation periods, which agrees with the measurements on "Mariner-2" and the "Vela-Hotel" satellites.

The measurements of the plasma velocity which were carried out on "Pioneer-6" showed that the periods of magnetic storms on the Earth corresponded to velocities of the fluxes of about 400-600 km/sec (See Fig. 8).

Thus, the data of numerous measurements indicate that, first of all, the increase in plasma velocity up to 450-700 km/sec is a characteristic sign of corpuscular streams producing geomagnetic disturbances. Secondly, these more rapid plasma fluxes originate from long-lasting localized regions in the corona which exist during several revolutions of the Sun and are responsible for the 27-day sequences in geomagnetic disturbances.

Density. According to the "Mariner-2" data, the average density at a distance of 1 Au is roughly 5 protons/cm^3. The variations in density with the time are shown in Figure 14 [48]. The velocity and density are connected by a reciprocal dependence. The maxima on the velocity curve correspond to density minima. Substantial variations in the density, from 1 to 80 protons/cm^3, are very noticeable. The highest values of the density vary within the range of 70-88 protons/cm^3.

Finally, because of the long period of measurements, the change in density with the distance could be determined. Naturally, such an evaluation can be carried out by averaging over a long interval of time. Figure 15 shows proton densities n_p (protons/cm^3), proton fluxes npv (10^8 protons/cm^{2}sec) and kinetic energy $1/2(m_p n_p + m_\alpha n_\alpha)y^2$

(10^{-8} erg/cm^3) averaged over one revolution as a function of the distance. It can be seen that an increase in all the cited values is observed as the distance to the Sun decreases. The density changes roughly as the inverse square of the distance.

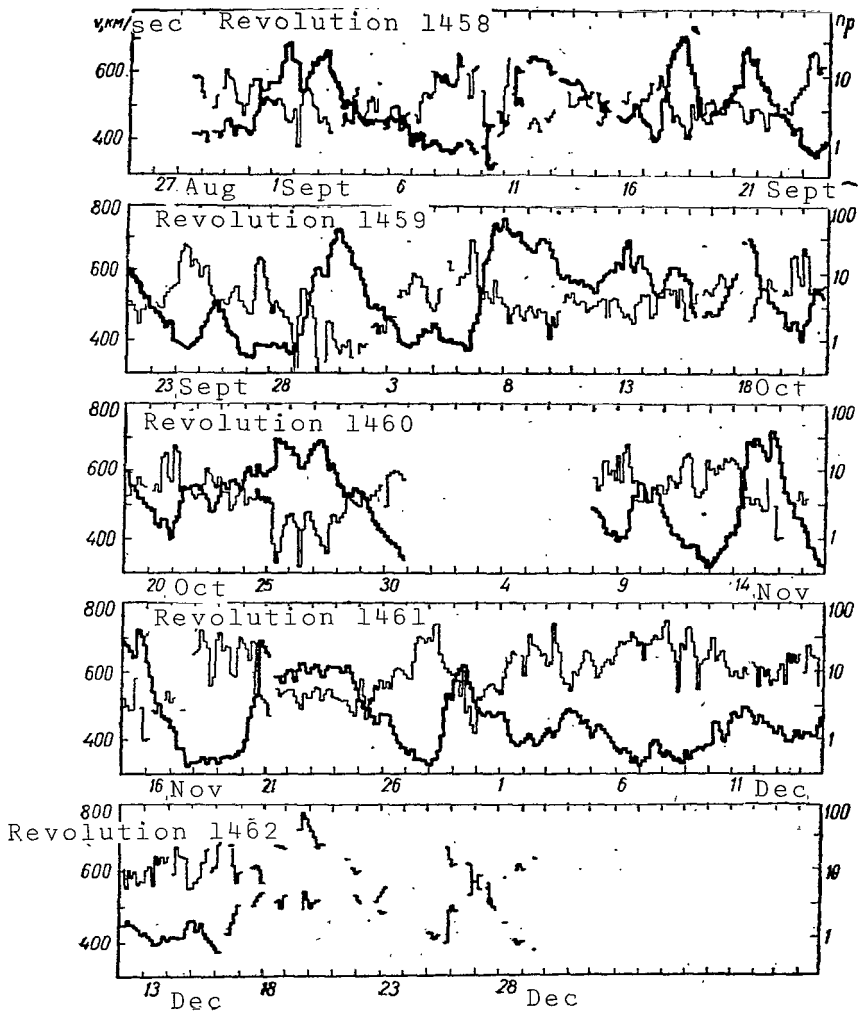

Fig. 14. Three-Hour Average Values of the Magnitude of Plasma Velocity v and Density n_p (Logarithmic Scale) as a Function of the Time [48].

Detailed measurements of the density were carried out on the "IMP-1" satellite [28]. The variation in density with the time is shown in Figure 16. During the flight of "IMP-1", densities from 1 to 15 protons/cm^3 were observed in the solar wind. During roughly 30% of the time when the satellite was in interplanetary space, the instruments installed on the satellite did not detect any solar wind. This apparently can be explained by the narrowness of the energy windows of the receiving channels, divided by wide breaks.

If the distribution function of the proton velocities in the solar wind is very narrow (monoenergetic flux) and the average velocity occurs in a break between neighboring energy channels, then the instrument obviously will not detect the plasma of the solar winds.

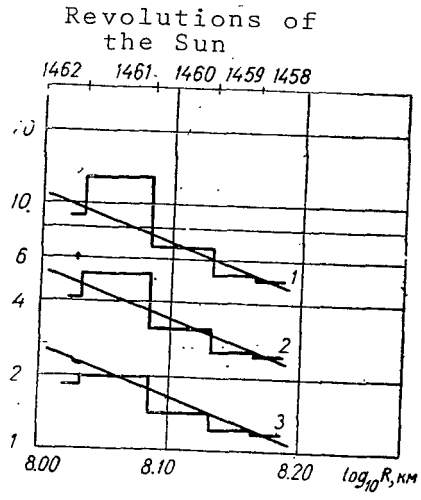

Fig. 15. Averaged (Over 27 Days) Daily Values of the Density of Protons (1), Flux of Protons (2), and Density of Kinetic Energy of the Plasma (3), as a Function of the Distance from the Sun [48].

A systematic analysis of the plasma density of the solar wind was then carried out according to the data of the "Vela" satellites. It was merely established that the average density is roughly equal to 3-5 protons/cm^3 [24], which agrees with other observations [19,22,25]. The measurements of the solar wind which were carried out at the end of 1964 on the "IMP-2" satellite [50] showed that, when the magnetic field is disturbed (the Earth is in a corpuscular stream), a value of $n_p \sim 5$ cm^{-3} is recorded in interplanetary space.

During the end of 1964 and the beginning of 1965, measurements of the solar-wind plasma were carried out on the space probe "Pioneer-6" [29]. In the analysis of the measurements, it was assumed that there is a system of coordinates in which the positive plasma components can be described by an isotopic Maxwell-Boltzmann distribution. Obviously, the velocity of this system of coordinates relative to the instrument is the velocity of the plasma as a whole. The data (see Fig. 8) indicates that there are α-particles moving at the proton velocity. The accuracy in the cited values is the following: plasma velocity as a whole equal to ± 15 km/sec; density, ± 20%; the data on the thermal velocity are preliminary. The following conclusions may be drawn:

(1) the high plasma densities at the maximum can reach 25-30 /26 protons/cm^3;

(2) velocity maxima follow density maxima;

(3) since the high correlation between the velocity of the fluxes and the disturbance of the magnetic field K_p is known, it can be seen (see Fig. 8) that the plasma density in corpuscular streams producing geomagnetic storms is $n_p \sim 5$ cm^{-3}.

Thus, according to the data of numerous measurements carried out directly in interplanetary space, we can conclude that the

plasma density in corpuscular streams generating disturbances in the Earth's magnetic field is lower than the plasma density of the solar wind and averages $n_p \sim 5$ cm^{-3}.

Temperature. The temperature, which is one more characteristic of the solar wind, can be determined from the spectra obtained with the aid of electrostatic analyzers installed on the spacecraft and from measurements of the density and velocity of the plasma of the solar wind. For this purpose, the velocity of the plasma as a whole, and then in the system of coordinates moving at the plasma velocity and the deviation in velocities of single ions, are determined from the energy spectra. It is found that this deviation in velocities can be described by a Maxwellian distribution at some definite temperature. This temperature is also attributed to the solar wind.

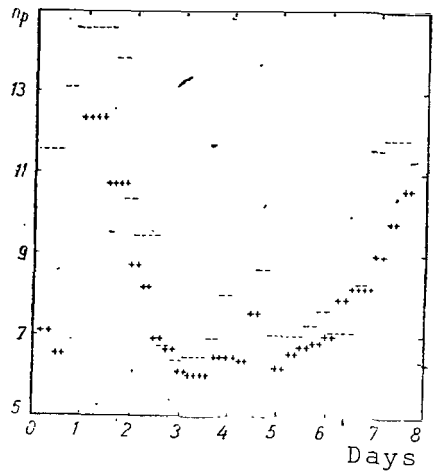

Fig. 16. Proton Density of Solar Wind Recorded Around the Earth During Passage of Sector by the Earth [28]. (+) Field Directed Away from the Sun; (-) Field Directed Toward the Sun.

It was found that the temperature T is not identical in different directions. For the first spacecraft, conclusions on the thermal motions of the particles were drawn from energy spectra characterizing a stream of particles in some fixed direction. Another method of determining the temperatures was based on measurements of the particles in different directions, as on the "Vela" satellites and the "Pioneer-6" space probe. /27

The temperature which was determined during the flight of "Mariner-2" according to energy spectra (Fig. 17) refers to one-dimensional motion. Note the very similar behavior of the velocity and temperature functions of the time. The more rapid plasma jets are found to be "hotter" than the surrounding plasma. A comparison of the velocity and temperature curves shows that the temperature increases more rapidly than does the velocity, and it reaches the maxima a few hours earlier than do the velocity maxima; when the velocity decreases, the temperature decreases, while the minimum temperature, roughly equal to $3 \cdot 10^4$°K, corresponds to quiet solar wind passing at minimal velocity between faster and hotter plasma jets.

The average daily temperature over the entire measurement period was between $1.51 \cdot 10^5$ and $1.85 \cdot 10^5$°K (lower and upper limits). Thus, the proton temperature at the base of the corona. The temperature of the quiet solar wind (between fast plasma streams) was found to be lower by a factor of 50 than the temperature of the corona.

The following question naturally arises: could we use the regularity found in the temperature and velocity changes in order to identify regions in the corona which eject fast plasma streams or are the sources of the quiet solar wind? It is impossible to answer the question of whether or not the temperature measured at a distance of 1 AU reflects the conditions for the origin of corpuscular streams or if it is the result of the heating of positive ions in interplanetary space due to the passage of shock fronts, the propagation of hydromagnetic waves or the development of instabilities of different types. It was found from a comparison of simultaneous measurements of the magnetic field and plasma velocity in interplanetary space from "Mariner-2" [49] that the fluctuations in plasma velocity and field intensity can be explained in terms of hydromagnetic waves superposing in the current of the quiet solar winds and faster plasma streams, and it can be assumed with great reliability that there are accelerated Alfven waves. According to the "Mariner-2" data, the spectrum for the fluctuations in magnetic field is constructed within the range from 1 to 116 oscillations per day. Extrapolating this spectrum to higher frequencies (detected by measurements on "Mariner-4" and the Orbital Geophysical Observatory), we find [49] that the velocity was roughly 4 km/sec for all oscillations with frequency higher than 116 oscillations per day. This is one order less than the "thermal velocity" measured according to the deviation in velocity.

One of the reasons for the proton heating in the faster plasma streams could be the collisionless shock waves which arise when the faster plasma stream enters into the quiet solar wind [13]. However, this mechanism could prove to be necessary only at the leading (western) edge of the stream, which overtakes the quiet solar wind. At the same time, the high temperature values are observed 4-5 days after the passage of the front, i.e., in those plasma streams which belong to the corona when the front passes over into interplanetary space. Consequently, the possibilities of heating up interplanetary plasma, which consists of solar wind and faster plasma jets, are very limited because of the passage of shock waves, and this is completely impossible under certain conditions.

We are inclined to view the very close correspondence between the changes in temperature and velocity (see Fig. 17) as the result of the origination of faster plasma streams, corpuscular streams, in "hotter" regions of the corona, or active regions. This conclusion must be considered as preliminary.

The temperature which was determined according to the data of other satellites agree with the measurements on "Mariner-2". Thus, according to "IMP-2" data, during geomagnetic storms, when the Earth was in a corpuscular stream, the temperatures were determined as $T \sim 2 \cdot 10^5$ °K.

/28

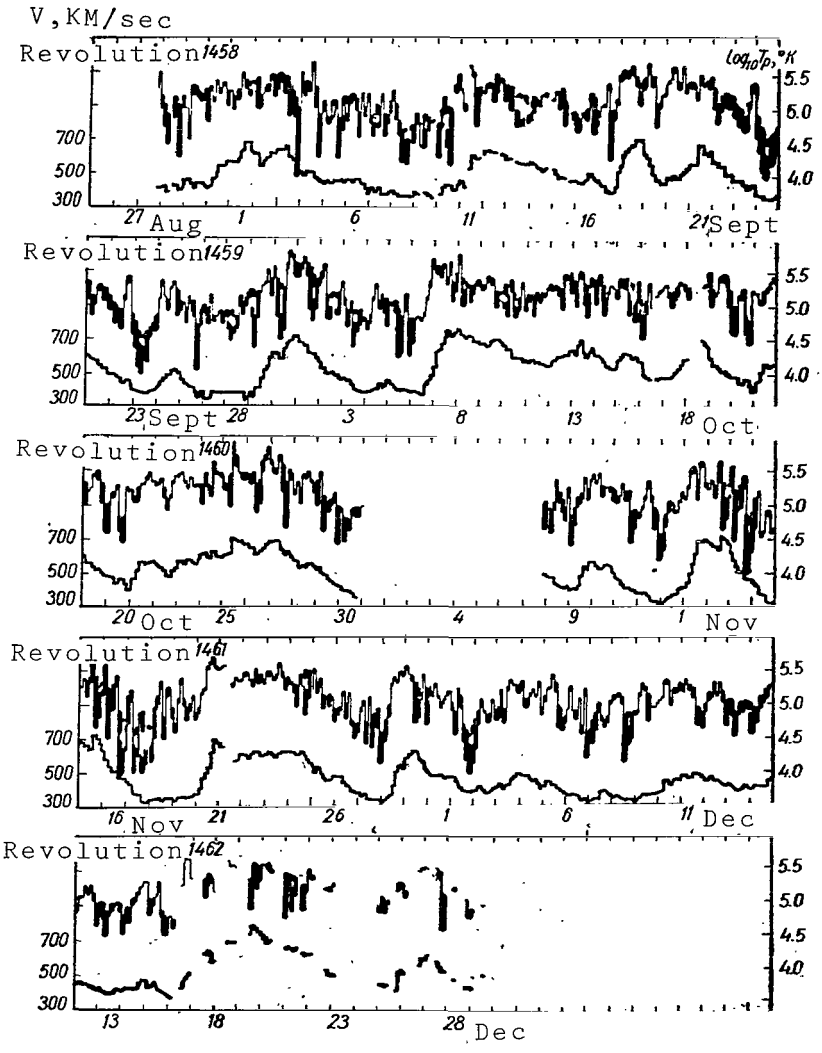

Fig. 17. Three-Hour Average Velocity Values v and Proton Temperature Tp (Logarithmic Scale) as a Function of the Time for Each Revolution of the Sun, Upper and Lower Limits to the Temperature Calculated (The Latter Are Not Designated If They Are Less Than 10^4 °K [48]).

/29

Reliable temperature measurements were carried out with the aid of the "Vela-Hotel" satellites. A low temperature ($T \sim 2 \cdot 10^4$°K) was observed when the solar wind velocity near the lower boundary ($v \sim 325$ km/sec) was very stable. At the beginning of the magnetic perturbation periods, when the Earth is in a fast plasma stream ($v \sim 700$ km/sec), the temperature increases up to values higher than 15^5 °K.

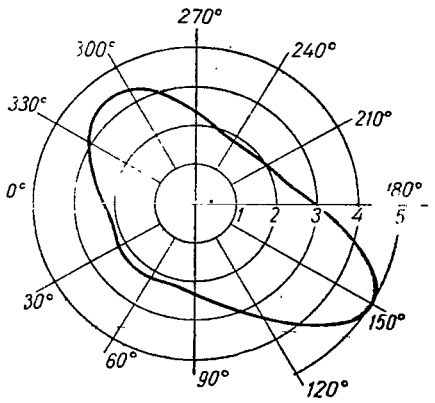

Fig. 18. Temperature in Polar Diagram as a Function of the Angle Φ (The Angle Φ is Equal to 0 if the Direction in which the Proton Temperature of the Solar Wind is Measured Coincides with the Direction Toward the Sun); "Vela-3V", August 5, 1965.

The "Vela-3" satellite investigated the temperature in different directions. In Figure 18, T is given as the function of the angle Φ on the plane $v_1 v_2$ (in 10^4 °K).

A histogram illustrating the repetition frequency of the measured values Φ_m is depicted in Figure 10. It can be seen that the average direction for the greatest velocity differential of the ions is close to the average direction of the magnetic fields. This means that the ion temperature along the field $T_{\parallel}$ is higher than in the transverse direction $T_{\perp}$.

It follows from the data obtained from "Pioneer-6" [16] which have been published that the ion temperature parallel to the field can sometimes exceed the temperature in the transverse direction by one order of magnitude. As a rule, $T_{\parallel}/T_{\perp} \sim 5$. /30

We should mention that the energy density of random motions of the ions is only a small percentage of the energy density of radial motion of the plasma as a whole. However, the thermal energy is comparable to the energy density of the magnetic field. According to numerous measurements carried out in interplanetary space, the variance in velocities of single ions with respect to the plasma velocity as a whole can be described by a Maxwellian distribution for a corresponding temperature roughly equal to $2 \cdot 10^5$ °K for the faster plasma streams and corpuscular streams, (2-4) 10^4 °K for the quiet solar wind with minimum velocity. The author considers that the higher temperature of the corpuscular streams (compared to the quiet solar winds) shows the sources from which they originate.

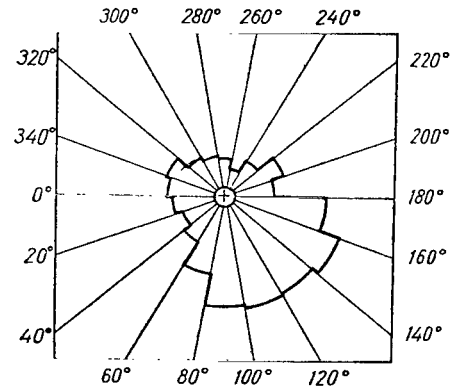

Fig. 19. Histogram Showing the Rate of Measurement of the Maximum Temperature in a Given Direction (July 24 - August 29, 1965).

Sectorial Structure of the Field and Streams In Interplanetary Space /31

The spiral structure of the interplanetary magnetic field (see Fig. 9) was found to have definite regularities

in the distribution of field polarity. A determination of the field's polarity played an important role in identification of the sources of corpuscular streams, since it aided in "tying in" reliably the corpuscular stream to the active region with same field polarity, while a determination of the intensity and polarity of the field, as well as a measurement of the plasma density during several revolutions of the Sun at a distance of the Earth's orbit, aided in constructing the structure of the solar corona (for a time near the minimum of the cycle of solar activity), with coronal streamers extended to the Earth's orbit. In this case, the role of coronal streamers as corpuscular streams is clarified.

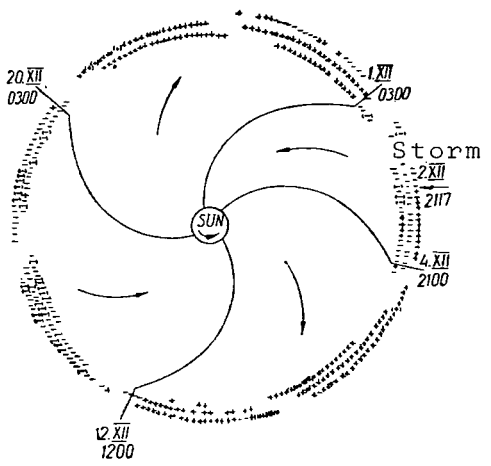

Fig. 20. Sectorial Structure of the Interplanetary Magnetic Field (The Parentheses Around the Signs Show the Time Interval During Which the Field Had a Direction Other than In the "Resolved" Regions Shown in Figure 13).

Sectorial Structure During the End of 1963 and Beginning of 1964. The polarity of the interplanetary magnetic field which was measured on "IMP-1" from November 27, 1963 to February 19, 1964 is shown in Figure 20. The measurements of the magnitude and polarity of the field were carried out every 20 sec (sessions of 4.8 sec), but the data were averaged over 3 hours for the sake of convenience in analysis.

It can be seen that the interplanetary field is divided into four sectors. Within the limit of each sector the field has primarily either a positive (the field is directed away from the Sun) or negative polarity (the field is directed toward the Sun).

Within the limits of each sector, the polarity of the field is repeated from revolution to revolution. The interval of recurrence of polarity of the field is reproduced particularly well in Figure 21. The sequences of geomagnetic disturbances corresponding to the passage of the Earth through corpuscular streams are very poorly pronounced. Each stream producing a certain sequence carries with it a field of primarily one polarity (the lines of force are directed away from the Sun in one stream and toward the Sun in another). Three large sectors, each with duration of about 7-3/4 days, and one small sector with duration of 4 days, pass by the Earth during every revolution of the Sun. It seems improbable that a field of one polarity observed in space during 5-7 days in the passage of the Earth through a stream acquired this structure in "rearrangement" in interplanetary space during the movement of the stream from the Sun to the Earth. It seems natural that the inter-

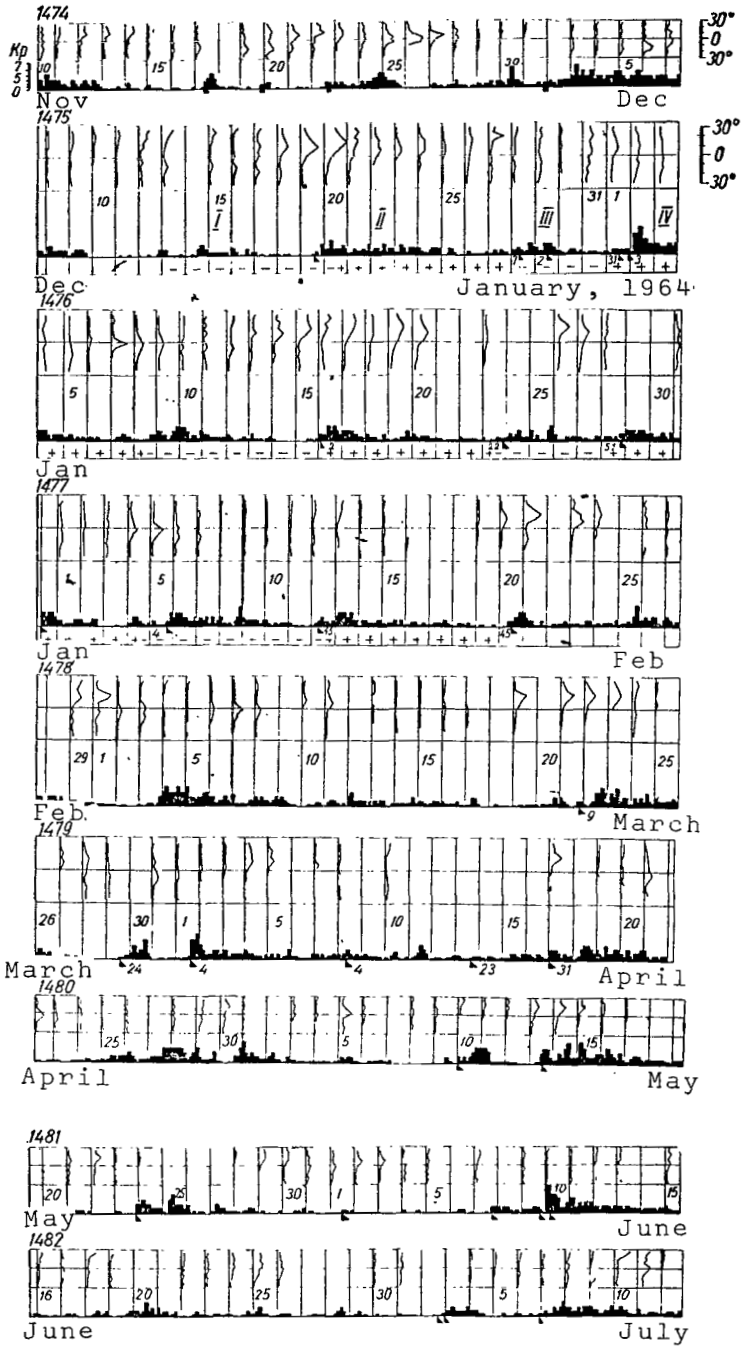

Fig. 21. Steady Sequences in Magnetic Disturbances and Corresponding Sectorial Structure of the Interplanetary Magnetic Field During the 1474-1482 Revolutions of the Sun.

planetary magnetic field observed around the Earth, for example one of positive polarity, was transferred out of solar regions of the same polarity [13]. Ness and Wilcox [42-43] investigated the correlation in the time function between the polarity of the field at the photospheric level (central meridian of the Sun) and the polarity measured at the distance of the Earth's orbit. It was found that the maximum correlation occurs on the 4th and 5th day. This corresponds to an average velocity of the solar wind roughly equal to 385 km/sec. We sould mention that the average velocity of the solar wind which was measured directly by plasma detectors during the first seven satellite orbits was equal to 398 km/sec. This result is, first of all, a direct indication of the origination of the interplanetary magnetic field and, secondly, a proof of the spiral structure of the field.

The fact that the interplanetary magnetic field intensity changes regularly within the limits of each sector is very important. Figure 22 shows the change in field intensity during the passage of a sector by the Earth. After the beginning and end of a sector, the field reaches the maxima, while the field is minimal in the middle, roughly on the 5-th day. Let us note that the change in field occurs in a similar way over all these sectors during all the revolutions. This indicates that there is a stable structure not only in the position of the sectors as a whole but also in the field and streams inside each sector. /34

Let us examine the change in field from one sector to another. Having increased at the end of the outgoing sector, the field abruptly decreases to zero at the boundary. The width of the region of the zero field (boundary between sectors) is about 150,000 km. An increase of the fields which is just as sudden is observed at the beginning of the approaching sector. We are given the impression that the region of the zero field is bounded. It can be seen in Figure 21 that the position of the boundary between sectors (shift in polarity of the field) remains steady during several revolutions.

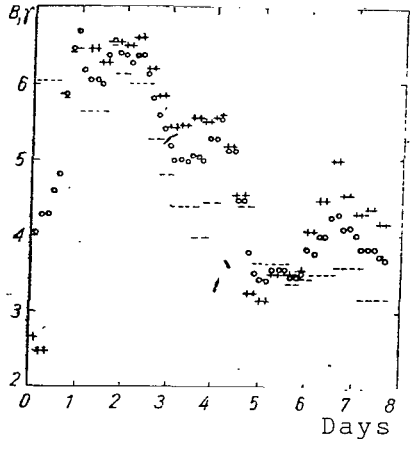

Fig. 22. Changes in Disturbance of the Geomagnetic Field as a Sector Passes by the Earth. (+) Field Directed Away from the Sun; (-) Field Directed toward the Sun; (O) Both Field Directions are Found.

Thus, it has been established experimentally that, at least during three revolutions of the Sun, a steady sector of the field and streams in interplanetary space is observed. The number of spectra, the relative position, the distribution of velocity and density of the plasma of the solar wind and the intensity of the field inside each sector remain stable.

Stability of the sectorial structure according to geophysical data. There are reasons to assume that the sectorial structure of the interplanetary magnetic field established by the satellite measurements at the end of 1963 and the beginning of 1964 is a characteristic of interplanetary space which is found not only in a given period of time. Actually, a steady structure of the field and streams can be traced during several revolutions by using the same rules: /35

(1) the disturbance of the magnetic field K_p shows high correlation with the velocity of this stream;

(2) each stream transports a field of one certain polarity;

(3) the polarity shift occurs at the velocity minimum (minimum of K_p).

It can be seen from Figure 21 that a corpuscular stream which transports a field of negative polarity and produces sequence I of magnetic disturbances clearly begins with revolution 1475 (negative sector from December 12th to December 19) and lasts all during 1964. The shift in sequence toward the left by 1-2 days in revolution 1484 is notable. However, the polarity of the field entrained by the stream remains the same.

Sequence II (second stream in interplanetary space which transports a field of positive polarity) clearly begins with revolution 1474 (positive sector from December 19 to December 27). The stream can be traced by the disturbance of the Earth's field up to revolution 1480. In revolution 1481, we see only a slightly noticeable storm, the sudden start of which is marked by a triangle for June 1. In revolution 1482, the disturbance of the Earth's magnetic field is more clearly distinguishable. It begins on June 24 and 27 and ends on July 1.

The third sequence (negative sector from December 26-27 to December 31, 1963) was observed reliably by the satellite during revolutions 1475 and 1476. The sequence is traced reliably in revolution 1477 by the disturbance of the magnetic field. Traces of it can be seen in revolution 1478. Since a shift of the fourth sequence to the left is noted in revolution 1479, the third sequence is "lost" in revolution 1480.

The fourth sequence (positive sector beginning roughly on December 31 in revolution 1475) is clearly distinguishable during many revolutions. We can see a shift at the beginning of this sequence in revolutions 1478 and 1480, but the variation of the disturbance (width of the sector) is constant during the entire time in which the sequence holds.

Thus, the four-sector structure of the interplanetary magnetic fields which was established by satellite measurements is followed by sequences of magnetic disturbances roughly up to the middle of

the year. At the middle of the year, the stable sectorial structure of the field (streams) seems to be missing, which is possibly /36
connected with the transition of the projection of the apparent center of the Earth from the southern hemisphere of the Sun to the northern one. It is also very probable that the four-sector structure of the field is preserved, but only two fast plasma streams can be noted according to the disturbance of the geomagnetic field (revolution 1481). This assumption is more probable, since steady geomagnetic sequences and a corresponding four-sector structure of the fields are again observed in interplanetary space in the second half of the year.

Stability of the Sectorial Structure Constructed According to Geophysical Data and Satellite Measurements. The four sequences of magnetic perturbations (correspondingly, four corpuscular streams) are traced clearly from revolution 1482 to revolution 1488 (Fig. 23). Assuming that each stream entrains a field of primarily one definite polarity, we can obtain the sectorial structure for the interplanetary magnetic field. The boundaries of the proposed sectors are designated in Figure 23 by two vertical lines. In revolution 1482, the position of the boundaries is determined according to the minimum of magnetic field disturbance (K_p curve). The measurements of the plasma velocity which were carried out on the "Vela-Hotel" satellites and interplanetary space were also used to determine the boundaries for revolutions 1483-1485 (the minimum velocity is observed near the boundary of the sector). Finally, for revolutions 1486, 1487 and the beginning of 1488, we have the measurements of the field polarity which were carried out on the "IMP-2" satellite [50].

It can be seen from Figure 23 that the extreme left sequence begins roughly on June 17 (revolution 1482). The boundary for the beginning of the sector, which is determined according to the minimum velocity and Kp, is identified reliably up to revolution 1487. A field of negative polarity is connected with the stream.

The corpuscular stream producing weak magnetic disturbances from June 24 to June 31 in revolution 1482 (second sequence) is traced reliably from July 21 to 27 (revolution 1483), from August 17 to 24 (revolution 1484) and clearly up to revolution 1488. The field transported by it forms a positive sector.

The position of the two right-hand sequences is determined particularly clearly. The boundaries of the positive or negative sectors of the interplanetary magnetic fields produced by them are very steady during seven revolutions of the Sun. Using the geophysical data and satellite measurements for the second half of 1964, we can construct a theoretical four-sector model of the interplanetary magnetic field with clearly defined boundaries which last for several revolutions of the Sun.

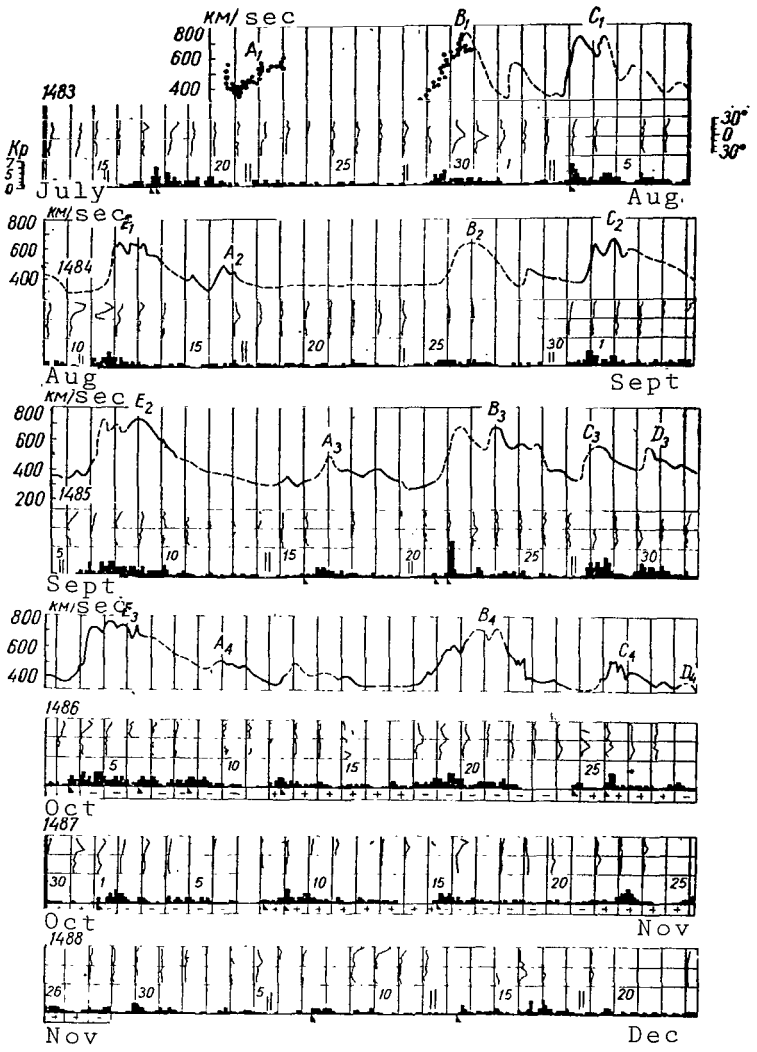

Fig. 23. Sequences of Geomagnetic Disturbances and Sectorial Structure of Interplanetary Magnetic Field During Revolutions 1483-1488 of the Sun. (+ and -) Predominance of Positive or Negative Polarity, Respectively.

References

1. Eygenson, M.S., M.N. Gnevyshev, A.I. Ol' and B.M. Rubashev: Solnechnaya aktivnost' i yeye zemnyye proyavleniya (Solar Activity and Its Terrestrial Manifestations). Moscow, "Gostekhizdat", p. 240, 1948.
2. Dvoryashin, A.S.: Izvest. Krymskoy Astrofizicheskoy Observatorii, Vol. 30, p. 221, 1963.
3. Dvoryashin, A.S.: In the book: Solnechnaya aktivnost' (Solar Activity). Moscow, "Nauka", 1965.
4. Gringauz, K.I., V.V. Bezrukikh, V.D. Ozerov and R.Ye. Rybchinskiy: Doklady Akad. Nauk. S.S.S.R., Vol. 131, No. 6, p. 1301, 1960.
5. Gringauz, K.I., V.G. Kurt, V.I. Moroz and I.S. Shklovskiy: Doklady Akad. Nauk S.S.S.R., Vol. 132, No. 5., p. 1062, 1960.
6. Gringauz, K.I.: Iskusstvennyye Sputniki Zemli, Vol. 12, 1962.
7. Severnyy, A.B.: Astron, zhur., Vol. 42, No. 2, p. 217, 1965.
8. Severnyy, A.B.: Uspekhi Fiz. Nauk, Vol. 88, No. 1, p. 3, 1966.
9. Severnyy, A.B.: Vestnik Akad, Nauk S.S.S.R., Vol. 9, 1964.
10. Dvoryashin, A.S., O.S. Levitskiy and A.K. Pankratov: Izvest. Krymskoy Astrofizicheskoy Observatorii, Vol. 26, p. 90, 1961.
11. Dvoryashin, A.S., L.S. Levitskiy and A.K. Pankratov: Astron. zhur., Vol. 38, No. 3, p. 419, 1961.
12. Dvoryashin, A.S.: Izvest. Krymskoy Astrofizicheskoy Observatorii, Vol. 28, p. 293, 1962.
13. Dvoryashin, A.S.: In the book: Elektromagnitnyye yavleniya v more (Electromagnetic Phenomena in the Sea). Kiev, "Naukova Dumka", 1968.
14. Mustel', E.R.: Astron. zhur., Vol. 42, No. 2, p. 276, 1965.
15. Vsekhsvyatskiy, S.K.: Informatsionnyy Byulleten', Vol. 5, p. 216, 1963.
16. Bonetti, A. et al: J. Geophys. Res., Vol. 68, No. 13, p. 4017, 1963.
17. Bonetti, A. et al: Space Research III, Symposium COSPAR, Washington, p. 540, 1962.
18. Mustel E.R.: Space Research IV. North-Holland Publishing Company. Amsterdam, p. 77, 1964.
19. Snyder, C.W., M. Neugebauer: Science, Vol. 138, p. 1095, 1962.
20. Snyder, C.W., M. Neugebauer: Space Research IV, North-Holland Publishing Company, Amsterdam, p. 89, 1964.
21. Snyder, C.W., M. Neugebauer, and U.R.Rao: J. Geophys. Res., Vol. 68, No. 24, p. 6361, 1963.
22. Snyder, C.W., M. Neugebauer: Proceedings of the Plasma Space Science Symposium Ed. by C.C. Chang, S.S. Huang, D. Reidel Publishing Company Dordrecht, Holland, p. 67, 1965.
23. Bridge, H. et al: Space Research V. North-Holland Publishing Company, p. 969, 1965.
24. Coon, J.H.: Radiation Trapped in the Earth's Magnetic Field, Ed. by B.M. McCormac, D. Reidel Publishing Company Dordrecht, Holland, p. 231, 1966.

25. Wolfe, J.H., R.W. Silva, M.A. Myers: J. Geophys, Res., Vol. 71, No. 5, p. 1319, 1966.
26. Ness, N.F., J.M. Wilcox: Science, Vol. 148, p. 1592, 1965.
27. Ness N.F.: Measurements of the Magnetic Fields in Interplanetary Space and Magnetosphere, London, September 6-17, 1965.
28. Wilcox, J.H., N.F. Ness: J. Geophys. Res., Vol. 70, No. 23, p. 5793, 1965.
29. Lazarus, A.J., H.S. Bridge, J. Davis: J. Geophys. Res., Vol. 71, No. 15, p. 3787, 1966.
30. Lazarus, A.J. et al: Paper presented at the COSPAR meeting, Vienna, 1966.
31. Severny, A.: Space Sci. Rev., Vol. 3, No. 2, p. 454, 1964.
32. Dvoryashin, A.S.: J. Phys. Soc., Japan, Vol. A-11, p. 17, 1962.
33. Sonett, C.P. et al: J. Geophys. Res., Vol. 65, No. 1, p. 55, 1960.
34. Coleman, P.J., L. Davis, C.P. Sonett: Phys. Rev. Letters, Vol. 5, No. 1, p. 43, 1960.
35. Greenstadt, E.W.: Astron. J. Vol. 68, No. 8, p. 536, 1963.
36. Greenstadt, E.W.: Astrophys. J., Vol. 145, No. 1, p. 270, 1966.
37. Colemann, P.J. et al: Science, Vol. 138, p. 1099, 1962.
38. Sonett, C.P.: Space Sci. ed. by D.P. LeCalley, New York, London, Vol. 10, p. 374, 1963.
39. Smith, E.J.: Space Physics. Ed. by D.P. LeCalley and A. Rosen, New York, London, Sydney, Vol. 10, p. 350, 1964.
40. Cahill, L.J.: Science, Vol. 147, No. 3661, p. 991, 1965.
41. Ness, N.F., J.M. Wilcox: G.S.F.C.Report, Vol. X-612, No. 65, p. 302, 1965.
42. Ness, N.F., J.M. Wilcox: Phys. Rev. Letters, Vol. 13, No. 15, p. 461, 1964.
43. Ness, N.F., J.M. Wilcox: Astrophys.J., Vol. 143, No. 1, p. 23, 1966.
44. Ness, N.F. et al: J. Geophys. Res., Vol. 69, No. 17, p. 3531, 1964.
45. Behannon, K.W. et al: Forth-Sixth Annual Meeting, April 19-22, Washington, 1965.
46. Ness, N.F. et al: J. Geophys. Res., Vol. 71, No. 13, p. 3305, 1966
47. Ness, N.F.: J. Geophys. Res., Vol. 71, No. 13, p. 3319, 1966.
48. Neugebauer, M., C.W. Snyder: J.Geophys, Res., Vol. 71, No. 19, p. 4469, 1966.
49. Colemann, P.L.: Phys. Rev. Letters, Vol. 17, No. 4, p. 207, 1966.
50. Fairfield, D.H., N.F.Ness: Magnetic Field Measurements with the IMP-2 Satellite, Prepr., 1966.
51. Mustel, E.R.: Space Sci. Rev., Vol. 3, No. 2, p. 139, 1964.

A FOUR-STREAMER MODEL OF THE SOLAR CORONA NEAR THE ACTIVITY MINIMUM

A.S. Dvoryashin

ABSTRACT: A four-streamer model of the solar corona was constructed for a period near a minimum of solar activity on the basis of satellite and rocket measurements of the plasma and field. The characteristic features of the magnetic disturbances in the Earth's magnetic field may be explained by the complex structure of the coronal streamers. This structure reflects the distribution of sources.

An analysis of the data obtained in observations [1] has shown /40
that the solar corpuscular radiation in the neighborhood of a minimum in the cycle of the solar activity is characterized by a stable four-sector structure of the field and streams in each solar system (at least in the plane of the ecliptic). The plasma characteristics (velocity, density, magnetic field intensity) change in a similar way in all the sectors (this shows stability in the sector of the field and streams in each separate sector and allows us to construct a four-streamer model of the solar corona near an activity minimum.)

Characteristics of Active Regions, Sources of the Sectorial Structure of the Field and Corpuscular Streams

Since the stream comes from a region of the field of the same polarity [1], then, following along the line of force, we can arrive at its source, i.e., the active region from which the corpuscular stream leaves. The range of emission should be extended by latitude. This statement is based on the following facts.

First of all, as has been shown, a sector with primarily one field polarity passes by the Earth during the course of five to seven days (width of the sector at the distance of the Earth's orbit). In the plane of the ecliptic, the set of sectors fills an entire circle with center at the Sun. Since the flow of the plasma and the field is radial, the surface of the sectors should be extended by longitude.

Secondly, it is well known that one geomagnetic disturbance can last five to seven days. This means (considering the delay in the beginning of the disturbance, which is equal to four days) that the velocity of that plasma stream in which the Earth is found, for example, on the third day of a magnetic perturbation, should be about 250 km/sec. However, according to direct measurements, the velocity of the plasma stream producing the magnetic disturbances

is generally greater than 400 km/sec. Consequently, the plasma /41
stream was emitted in the direction toward the Earth by part of the active region moving toward the central meridian after a lag by 2-3 days relative to the western boundary of the region (causing the beginning of the disturbance). Thus, we again can conclude that the region which emits the corpuscular stream and is responsible for the sectorial structure of the interplanetary magnetic field has substantial expanse in terms of longitude.

Thirdly, satellite measurements have shown that the deviation in velocities in a stream, measured at a given moment of time, is relatively small. Consequently, the assumption of the high dispersion in velocity in a stream, which was made earlier to explain prolonged magnetic disturbances, proved to be untenable.

Because of the rotation of the Sun, prolonged disturbances of the Earth's magnetic field are found to be simply the result of irradiation of the Earth by new jet streams emitted in the direction toward the Earth by active regions extended in longitude. The principal characteristic of these regions is the presence of a field of primarily one polarity. The sectorial structure of the interplanetary magnetic field imposes this requirement of the active regions.

Extended regions of primarily positive or negative field polarity (according to photospheric measurements) are actually observed on the Sun. A regularity has been established in the distribution of regions with positive and negative field polarities in each hemisphere of the Sun [27-29]. It was found that the distribution of the regions is due to their origination.

It is well known that a well-developed active region consists of a group of spots with fields of positive or negative polarity. The spots with fields of a certain polarity are sometimes distributed so that a line can be drawn to divide a field of one polarity from fields of the other polarity (the neutral line is the line of the zero longitudinal field). The head spot (leader) in the active regions in the northern hemisphere had a field directed away from the Sun (positive polarity) at the preceding maximum and on the descending branch of the cycle of solar activity, while the tail part had a field directed toward the Sun (negative polarity).

Having investigated the distribution of large-scale solar magnetic fields, Bumba and Howard found the existence of regions on the Sun with primarily negative or positive polarity, extended in latitude and longitude [27-29]. A comparison of these regions during /42
several successive revolutions showed that they are the result of the evolution of complex activity centers including several active regions. The extended regions of primarily negative polarity are formed from the "tail" part of the active regions. Consequently, these regions have negative polarity in the northern hemisphere. The leading part of the active regions develops in time into an

extended region of positive polarity. In the southern hemisphere, these regions correspond to their mirror reflections with opposite field polarity. A precise determinatino of the boundaries of regions with a field of positive or negative polarity is a complex problem, particularly for the time of a maximum in the cycle of solar activity, since almost the entire surface of the Sun is covered during this time by weak magnetic fields [2-4, 25] which change continuously in time and space, forming the so-called background. The background fields are the result of the expansion, diminishment and distension, by differential rotation of the Sun, of the magnetic fields of old active regions, their interaction with the neighboring fields, and the continuous development of magnetic fields of new regions. Nevertheless, the regions with a field of primarily positive or negative polarity are identified reliably against this complex background during several revolutions of the Sun.

A certain regularity is observed in the distribution of field intensity over the area occupied by a unipolar region. Regardless of the polarity, the field intensity is higher in the leading (western) part of the region and it decreases at the "tail", toward the east. It has been found that a brighter chromospheric prominence and a flocculus are observed in the chromosphere over regions with a stronger field in the photosphere. A facula is observed in the region of the stronger field. This fact is important, since it allows us to determine the configuration of the field according to the position of the flocculus. An almost unambiguous correspondence in the position of the magnetic fields and calcium flocculi in the chromosphere was found in [30-32]. This correspondence is valid all the way to the very smallest bright details observed at the resolution limit of the instruments, and the correlation factor reached 0.99 for fields on the order of 2.5 G. The fact that there is a high correlation between the brightness of individual structural elements of a flocculus and the intensity of the magnetic field which was established by V.Ye. Stepanov [5,6] is noteworthy.

It is difficult to determine the lifetime of unipolar regions /43
with a field of positive or negative polarity, particularly near a maximum in the cycle of solar activity. For a period of low activity, there must be 2-3 revolutions for the preliminary development of a unipolar region with magnetic "tail" extended toward the east, after which the region is observed during 5-7 revolutions. A unipolar region with its weak local fields can remain during several revolutions after the emission of the calcium flocculus and of the brighter calcium prominence in the chromosphere ceases.

It follows from this analysis that the active regions which have a relation with the origin of corpuscular streams are unipolar. Their extent by longitude is 70-90° and more. The field intensity is higher in the western (leading) part of the region and decreases toward the east. The emission of a calcium flocculus and a brighter chromospheric prominence is observed over a region with high field intensity. The position of the regions remains steady during several

revolutions of the Sun.

Evolution of an Active Region and Formation of a Coronal Streamer

The unipolar regions with field of positive or negative polarity which are in one hemisphere may be very closely adjacent. It is natural to expect that part of the field of one region will close over the field of another. This assumption seems to be all the more valid in that regions with a field of primarily positive and negative polarities were a single active region (or several regions) in the past, with closely-spaced fields and spots of the opposite polarities. Naturally they were closed. In observing such a region on the limb, systems of the arcs of loop prominences, etc., can be seen, which shows the closure of the field.

Considering the extension of fields of a certain polarity (now in the unipolar stage of development), we must expect that, in the closure of one field on another, the lines of force will not only pass through the hemisphere, but will also ascend over it, forming arcs high in the corona. We should mention that, according to the data of [27, 28], regions of positive and negative polarity (in observations of the Sun) are almost always divided by a quiet filament. Consequently, this filament on the limb will appear to be a quiet prominence "sitting" at the base of the arcs. /44

Thus, we can draw the following conclusion: at the boundary layer between two unipolar regions, some of the field of one polarity is linked over a field of the other polarity. The lines of force which connect the more remote regions of the field of opposite polarity should come from the chromosphere, forming the arcs and bends high in the corona. A quiescent prominence underlies the system of arcs and bows.

The entire field of one polarity cannot be completely closed in the form of a system of arcs and bends over the field of another polarity, since in this case the farthest arcs going high into the corona are in the region where the solar wind is found and, consequently, should be carried into interplanetary space. Two streams of the field of opposite polarity which are parallel and divided by a zero-field region are formed.

The system of arcs and bends which we constructed at the boundary layer between fields of opposite polarity, together with the quiet filament dividing these polarities, have much in common with a plume. Consequently, the stream coming from the corona over the system of arcs and bends is none other than a coronal streamer.

Four-Steamer Model of the Solar Corona and Four Coronal Streams in Interplanetary Space

Since the four-sector structure of the interplanetary magnetic field corresponds to four unipolar regions on the Sun, we can construct four coronal streamers and, consequently, four coronal streams. This picture is shown schematically in Figure 1.

It can be shown that the coronal streams, which are a continuation of the streamers in interplanetary space, reach the Earth's orbit and move beyond its boundaries. Actually, an analysis of satellite measurements of the plasma density and velocity and the interplanetary magnetic field intensity shows that coronal streams /45 are reliably observed at a distance of the Earth's orbit.

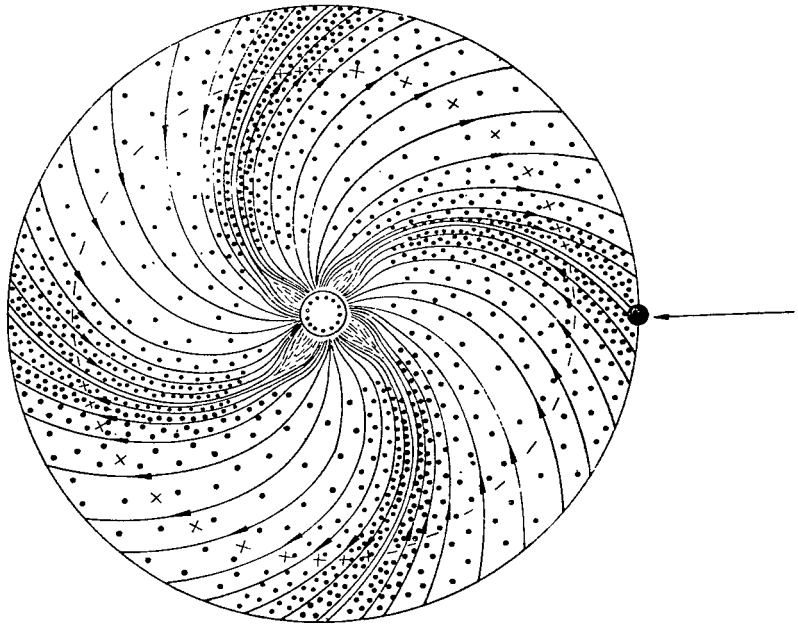

Fig. 1. Four-Streamer Model of the Solar Corona with Coronal Streamers Extending to the Earth's Orbits (View from Polar Axis, the Arrow Shows the Position of the Earth at the Moment of its Passage Through the Center of a Streamer on March 2, 1964).

In our model, the streamer is found at the boundary layer between fields of opposite polarity. The lines of force which pass over the higher arcs, the closure of which is still seen in the corona, form two fields of opposite polarity in expanding interplanetary space, which are divided by a region with a field equal to zero. A field of positive polarity is found at one side of the zero-field region (for example, western), while that of negative polarity is found on the other side. Following along the zero-field regions to the Earth's orbit (along a spiral trajectory),

we can see the same zero-field region with corresponding distribution of polarities to the west and east (see Fig. 1). The zero field region is the original center of the coronal streamer. /46

In discussions of the sectorial structure of the interplanetary magnetic field, particular attention is usually given to the sector as a whole. In the proposed model, the sectors are considered as regions of the field and plasma which compose the streamer, while it is not the entire sector, but the half adjacent to the zero-field region which belongs to the specified streamer. Particular attention is given to the boundary between the sectors, to the zero-field region, which is identified as the middle of the coronal streamer.

When near the Sun, the magnetic field "organizes" the streamer. As Ye.A. Ponomarev [7] showed, the presence of a magnetic field must be assumed for the very existence of coronal streamers during some substantial amount of time. The external appearance of the plumes, and the shape of the arcs and bends, indicate that the field is concentrated in the center of the streamer and is greater in the streamer than in interplanetary space. Following along the zero-field region of the streamer constructed up to the Earth's orbit, we find that the field is maximum at the boundary of the sectors (in the vicinity of the streamer center) and minimum at the middle (between the streamers) of the sectors (see Figures 1 and 22 of [1]).

A coronal streamer can be seen on photographs made during an eclipse because of the high density. Following along the centers of the cited streamer up to Earth's orbit, we can see that higher density is observed at the boundary of the sectors (at the middle of the streamer) and decreases at the middle of the sector (between the streamers) (see Figures 1 and 16 of [1]).

The model reconstructed for the corona, with four coronal streams extending to Earth's orbits, is collaborated by an analysis of the data obtained during direct satellite measurements.

The correctness of the proposed picture for the origination of coronal streamers and their correspondence with corpuscular streams could be tested by comparing the model we have constructed to observations of the corona during an eclipse. Unfortunately, a total eclipse was not observed during the period being discussed in this study, but on March 5, 1964, we obtained a photograph of the corona with the aid of a coronagraph, from a height roughly of 32 m over the ground [33]. A large equatorial streamer was detected on the western limb. This streamer was apparently on the central meridian on February 27. Since the streamer has the shape of a spiral on the plane of the solar equator, its center should pass by the Earth roughly 4.5 days later, i.e., March 2. The center of /47 the streamer corresponds to the zero-field region between the sectors, or the sector boundary. Direct measurements in outer space

have shown that the maximum plasma density is concentrated around the sector boundary (see Fig. 16 of [1]). Consequently, in our model of the coronal streamers and streams, the Earth should pass through the densest part of the coronal streamer on March 2.

This statement is based on the following facts:

It follows from Figure 21 of [1] that a minimum in the disturbance of the magnetic field (minimum of K_p) is observed on March 2. According to measurements carried out on "Mariner-2", "IMP-1" and the "Vela-Hotel" satellites [1], the K_p minima coincides with the velocity minima (see Figures 1, 5, 6 and 7 of [1]), while the velocity minima correspond to density maxima (see Figures 8 and 14 of [1]). Consequently, the Earth actually passes through the densest part of the coronal streamer on March 2.

We identified the center of the streamer as a zero-field region, i.e., a boundary region between the sectors. Consequently, if the Earth actually passes through the center of the coronal streamer on March 2, then a shift in field polarity should be observed during this time. The polarity of the interplanetary field was not measured in revolution 1478. However, the measurements were carried out in revolution 1476 and 1477, and the field polarity was shown in Figure 27 of [1]. In revolutions 1476 and 1477, the polarity shift occurs roughly 4.5 days after the beginning of the revolution, i.e., March 2. Consequently, the Earth actually passed through the center of the coronal streamer on March 2.

Thus, knowing the position of the coronal streamer on the photograph obtained during an eclipse, we can determine (within the framework of the model constructed) the time of the passage of the streamer past the Earth. It was found that this time agrees with the satellite measurements, which shows the correctness of the model.

Let us give some arguments in favor of the correctness of the proposed origin of a coronal streamer. It was shown above that the center of the streamer (zero-field region) passed by the Earth on March 2. Knowing the polarity of the fields in the sectors, i.e., the field's polarity in the streamer on the right (to the west) and left (to the east) of the center of the streamer (viewed from the Earth, facing the streamer), we can determine the field polarity at the level of the photosphere to the west and east of the streamer center, which, as we have established, was on the central meridian /48 on February 27. It can be seen from Figure 21 of [1] that the western section of the streamer passed by the Earth until March 2 and had a field of positive polarity, while the eastern section passed after March 2 and had a field of negative polarity. Consequently, a region with a field of positive polarity should occur on the Sun before February 27, and a region of negative polarity should occur later.

Let us compare our assumptions with the true picture for the magnetic fields on the Sun.

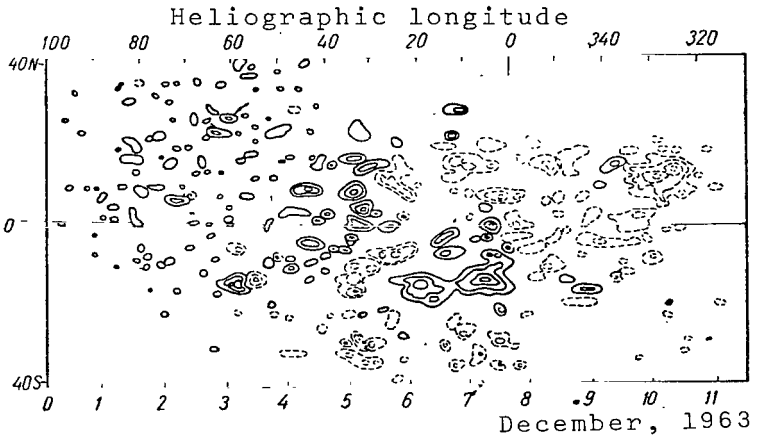

Fig. 2. Synoptic Map of the Magnetic Field at the Level of the Photosphere (The Solid Line Shows Regions with Field of Positive Polarity, and the Dashed Line Shows Those with Negative Polarity; The Contour Lines Correspond to 2, 4, 8, 12 and 25 G).

There is no synoptic map of the magnetic fields on the Sun for revolution 1478, but [26] gives a map of the fields during the period from December 1 to December 11, 1963 (Fig. 2). In Figure 2, we can see two regions of primarily one field polarity (the fields are plotted in the regions ±40° of the equator). In the northern hemisphere, the region of positive polarity passes the central meridian from December 1 to 6, and the region of negative polarity passes from December 6 to 11. South of the equator, the region of positive polarity is more extended. Here the polarity shift occurs /49 on December 7-8. This corresponds to the beginning of revolution 1475. It follows from the stability of the position for unipolar regions that the field polarity shifts in revolution 1478 also occurs at the beginning of the revolution, i.e., on February 27. The region of positive polarity passes the central meridian before February 27, and that of negative polarity passes later. This is what we have to prove.

Thus, knowing the position of the streamer during a total eclipse and the field polarity measured at a distance of the Earth's orbit, we can determine the field polarity in the region underlying the streamer, when the streamer passes the central meridian of the Sun. The distribution of the field polarity at the base of the streamer observed on the western limb on March 5, 1964 was stretched, as follows from the model under discussion. This agreement speaks in favor of our suggestion for the origin of a coronal streamer, and it also shows how the streamer can extend to Earth's orbit.

Role of Coronal Streamers as Corpuscular Streams

The idea of corpuscular streams as coronal streamers extending into planetary space up to the Earth's orbit and beyond its limits was proposed in 1943-1944 by S.K. Vsekhsvyatskiy [8, 9] and later developed in [10-17]. In this case, it was assumed that the solar corona was similar to a dynamic formation [18, 19]. The development of the dynamic model of the solar corona (for the case of spherical symmetry) was accomplished by Parker [20-24, 34-42], who began to develop this problem in 1958 apart from other authors, and, using the results of measurements of the plasma density and velocity, as well as of the interplanetary magnetic fields measured with the aid of satellites and rockets, constructed a model whose principal characteristics are presently well known [43-48].

Recent measurements of the plasma density in interplanetary space allow us to find the change in density with time during the course of one revolution. A regularity has been established in the passage of denser plasma streams past the Earth. In 1964, four such streams were detected. Each of them lasted at least one year, passing by the Earth with 27-day recurrence intervals. It is completely reasonable to identify these corpuscular streams as coronal streamers which are observed at equatorial latitudes of the Sun during total solar eclipses and which extend to the Earth's orbit, according to the previously-developed concept [15]. /50

At the same time, measurements of the plasma velocity and polarity of the interplanetary magnetic field allow us to make some details in the preliminary picture of streams more specific, and to put the first models in agreement with the physical and solar observations.

The plasma velocity in the streamer is not identical along the cross section perpendicular to the radius of the Sun (see Fig. 7 of [1]). The velocity first increases with the distance from the center of the streamer in places, reaches a maximum value roughly between the first and second days, and then decreases again to the minimum near the sector boundary (center of the following streamer). If we face the streamer, the velocity is lower on the western side, which intersects the Earth before the center, and it is greater on the eastern side, which intersects the Earth after the center. This particular characteristic in the behavior of the velocity can be explained by the distribution of the sources underlying the streamer.

Let us mention that regions with a field of primarily one polarity underlie a streamer, while the middle of the streamer (zero-field region) is directly over the line dividing these regions. In each unipolar region [27-29], the field intensity is higher in the western (leading) part of the region and lower in its "tail" (eastern part). Since the center of the coronal streamer is above the boundary between the unipolar regions, the western section of the streamer rests on the tail (eastern) part of the unipolar region, while the eastern section rests on the leading (western) part. However, the

western section of the unipolar region of any polarity has a high-intensity field. A disturbed chromosphere and, naturally, a hotter corona are observed over a region with a high-intensity field. Consequently, the eastern section of the coronal streamer, which rests on the hotter corona, contains a faster (and hotter) plasma stream, which agrees with direct satellite measurements.

This particular characteristic of the structure of each coronal streamer involves one important geophysical effect. Since the disturbance of the Earth's magnetic field Kp correlates with the velocity (see Figures 1 and 5 of [1]), then a great perturbation of the magnetic field should be recorded during the passage of the Earth through the eastern half of the coronal streamer, which includes the fast plasma stream. This also explains the characteristic observed in the course of magnetic disturbances; the disturbance begins when the Earth is at the center of the streamer and increases as the faster jet passes by the Earth. The disturbance of the magnetic field diminishes when the velocity decreases. This is observed in all the sequences in geomagnetic disturbances.

An increase in the disturbance of the magnetic field with an increase in velocity is obviously a characteristic of the "reaction" of the magnetosphere to the streamline flow of a fast plasma jet. This assumption can be accepted, since the energy which the center of the streamer transfers is comparable to the energy of a fast plasma jet or greater than it (the velocity in the jet is 1.5 times greater, while the density is 4 times greater at the center of the streamer). Consequently, these parts of the streamer are equal from the point of view of energy. /51

It is well known that, when the disturbance of the Earth's magnetic field increases at high geomagnetic latitudes, a complex set of geophysical phenomena (particularly aurorae) which owe their origin to high-energy particles is developed. It is possible that the arisal of these particles is connected with a more intensive development of a plasma instability under the conditions when the Earth is in a faster and less dense plasma jet than is the center of the streamer.

A comparison of the geophysical data and those obtained from satellites allowed us to establish the stability in the sequences of geomagnetic disturbances, stability in the sectorial center of the interplanetary magnetic fields, and uniform distribution of the characteristics of the solar wind and magnetic fields within the limits of each sector. Thus, we can conclude that the sources of corpuscular radiation in the corona, chromosphere and photosphere are stable.

The prolonged existence of radiation source leads to their expansion by differential rotation of the Sun: the regions become less extended in longitude, while the base of the streamer and, consequently, the streamer itself are found to be wide. This

explains the length of magnetic disturbances and the width of the sectors.

The extended regions underlying streamers cannot be strictly uniform in terms of field intensity. A certain regularity in the field distribution in the photosphere to the right and left of the streamer center leads to a corresponding distribution of the velocity over the streamer. The streamer is not uniform in terms of density, field or velocity. The center of the streamer transfers energy comparable to the energy of a faster plasma jet (or even more). The correlation between the disturbance of the Earth's magnetic field and the velocity of the streams reflects the characteristic feature of the "reaction" of the magnetosphere to the streamline flow of a fast plasma jet. /52

References

1. Dvoryashin, A.S.: This Collection.
2. Severnyy, A.B.: Astron. Zhur, Vol. 42, No. 2, p. 217, 1965.
3. Severnyy, A.B.: Uspekhi Fiz. Nauk, Vol. 88, No. 1, p. 3, 1966.
4. Severnyy, A.B.: Vestnik Akad, Nauk S.S.S.R., Vol. 9, 1964.
5. Stepanov, V.Ye.: Izvest. Krymskoy Astrofizichekoy Observatorii, Vol. 20, p. 52, 1958.
6. Petrova, N.N. and V. Ye. Stepanov: Izvest, Krymskoy Astrofizicheskoy Observatorii, Vol. 21, p. 152, 1959.
7. Ponomarev, Ye.A.: In the book: Fizika solnechnykh korpuskulyarnykh potokov i ikh vozdeystviye na atmosferu Zemli (Physics of Solar Corpuscular Radiation and its Effect on the Earth's Atmosphere). Moscow, Izdat. Akad. Nauk S.S.S.R., p. 69, 1957.
8. Vsekhsvyatskiy, S.K.: Astron, Zhur., Vol. 20, No. 5-6, p. 34, 1943.
9. Vsekhsvyatskiy, S.K.: Astron, Zhur., Vol. 21, No. 4, p. 149, 1944.
10. Vsekhsvyatskiy, S.K.: In the book: Zemnoy magnetizm i elektrichestvo (Terrestrial Magnetism and Electricity). Moscow, "Gidrometizdat", Vol. 6, No. 3, p. 47, 1946.
11. Vsekhsvyatskiy, S.K.: Publikatsii Kiyevskoy Observatorii, Vol. 1, pp. 26-97, 1946.
12. Vsekhsvyatskiy, S.K., Ye. A. Ponomarev, G.M. Nikol'skiy and V.I. Cherednichenko: Astron. Zhur., Vol. 32, No. 2, p. 165, 1955.
13. Nikol'skiy, G.M.: In the book: Polnyye solnechnyye zatmeniya (Total Solar Eclipses). Moscow, Izdat, Akad. Nauk S.S.S.R., p. 115, 1958.
14. Nikol'skiy, G.M.: In the book: Polnyye solnechnyye zatmeniya (Total Solar Eclipses). Moscow, Akad. Zauk S.S.S.R., p. 133, 1958.
15. Veskhsvyatskiy, S.K., Ye.A. Ponomarev, G.M. Nikol'skiy and V.I. Cherednichenko: In the book: Fizika solnechnykh korpuskulyarnyk potokov i ikh vozdeystviye na verkhnyuyu atmosferu Zemli (Physics of Solar Corpuscular Streams and their Effect on the Earth's Upper Atmosphere). Moscow, Izdat, Akad. Nauk S.S.S.R., p. 51, 1957.

16. Vsekhsvyatskiy, S.K.: Informatsionnyy Byulleten', No. 5, p. 216, 1963.
17. Vsekhsvyatskiy, S.K.: Geomagnetizm i Aeronomiya, Vol. 4, No. 2, p. 328, 1964.
18. Ponomarev, Ye.A.: Author's Abstract of Doctoral Dissertation, Kiev, 1957.
19. Ponomarev, Ye.A.: Astronomicheskiy Sbornik. L'vov, L'vov University Press, No. 2-4, p. 12, 1960.
20. Parker, E.: In the book: Eksperimental'noye issledovaniye okolozemnogo kosmicheskogo prostranstva (Experimental Investigation of the Space Around the Earth). Moscow, Foreign Literature Publishing House, p. 31, 1961.
21. Parker, E.: Uspekhi Fiz. Nauk., Vol. 84, No. 1, p. 169, 1964.
22. Parker, E.: Dinamicheskiye protsessy v mezhplanetnoy srede (Dynamic Processes in the Interplanetary Medium). Moscow, "Mir", 1965.
23. Scarf, F.L.: In the book: Kosmicheskaya fizika (Space Physics). "Mir", p. 452, 1966.
24. Scarf, F.L. and L.M. Noble: In the book: Raketnaya tekhnika i kosmonavtika (Rocket Technology and Astronautics). Moscow, "Mir", No. 6, p. 233, 1964.
25. Severny, A.: Space Sci. Rev., Vol. 3, No. 2, p. 454, 1964.
26. Ness, N.F., J.M. Wilcox: Astrophys. J., Vol. 143, No. 1, p. 23, 1966.
27. Bumba, V., R. Howard: Astrophys. J., Vol. 141, No. 4, p. 1502, 1965.
28. Bumba, V., R. Howard: Science., Vol. 149, No. 3690, p. 1331, 1965.
29. Bumba, V., R. Howard, E. Smith: Astron. J., Vol. 69, No. 8, p. 535, 1964.
30. Babcock H.W., H.D. Babcock: Astrophys. J., Vol. 121, p. 349, 1955.
31. Howard, R.: Astrophys. J., Vol. 130, No. 1, p. 193, 1959.
32. Leighton, R.: Astrophys. J., Vol. 130, p. 366, 1959.
33. Newkirk, G., J.D. Bohlin: Sky and Telescope, Vol. 28, No. 1, p. 16, 1964.
34. Parker, E.N.: J. Geophys. Res., Vol. 64, p. 11, 1959.
35. Parker, E.N.: Astrophys. J., Vol. 132, p. 821, 1960; Vol. 134, p. 20, 1961; Vol. 132, p. 821, 1950; Vol. 134, p. 20, 1961; Vol. 139, No. 1, p. 72, 1964; Vol. 139, No. 1, p. 93, 1964; Vol. 139, No. 2, p. 690, 1964; Vol. 141, No. 4, p. 1469, 1965.
36. Parker, E.N.: Vistas in Astronomy, 3, New York, Vol. 178, 1960.
37. Parker, E.N.: Space Astrophysics, Ed. by W. Lieller, Vol. 157, 1961.
38. Parker, E.N.: Plan. Space Sci., Vol. 9, p. 461, 1962.
39. Parker, E.N.: Interplanetary Dynamical Processes, Interscience Publishers, Inc., New York, 1963.
40. Parker, E.N.: Sci. Amer., Vol. 210, p. 7, 1964.
41. Parker, E.N.: Research in Geophysics. Ed. by H. Odishaw, Massachusetts Institute of Technology, Cambridge, Massachusetts, Vol. 1, No. 4, p. 99, 1964.

42. Parker, E.N.: Proceedings of the Plasma Space Science Symposium Ed. by C.C. Chang and S.S. Huang. D. Reidel Publishing Company Dordrecht, Holland, p. 99, 1965.
43. Noble, L.M., F.L. Scarf: Astrophys. J., Vol. 138, p. 4, 1963.
44. Scarf, F.L., L.M. Noble: Astrophys. J., Vol. 141, p. 4, 1965.
45. Scarf, F.L., L.M. Noble: AIAA Bull. Vol. 1, p. 1, 1964.
46. Scarf, F.L., L.M. Noble: AIAA Bull, Vol. 2, No. 6, p. 1158, 1964.
47. King, J.H., R.L. Carovillano: Bull. Amer. Phys. Soc. Vol. 9, No. 2, p. 161, 1964.
48. Carovillano, R.L.,J.H. King: Astrophys. J., Vol. 141, p. 2, 1965.

SECULAR DECREASE IN THE ABSOLUTE BRIGHTNESS OF THE COMET ENCKE†

Z. Sekanina

ABSTRACT: The brightness curves of Comet Encke are investigated in detail in this study on the basis of the returns from 1805 to 1961. The secular decrease of its absolute brightness ranges from 2^m to 4^m per century, which agrees with the author's results. Vsekhsvyatskiy's definition of the absolute magnitude, H_{10}, is found to be a good approximation of the comet's luminosity when the observations span a rather wide range of heliocentric distances. The method which Kresak suggested, and which leads to a decrease of 1-1.1^m per century, is shown to be absolutely erroneous.

The problem of the secular variations in the brightness of /54
Comet Encke from short-period comets was reviewed by L. Kresak [12]. He concluded that the secular decrease in brightness of the Comet Encke and of others, which was derived from the data of the "General Catalogue of Absolute Magnitudes" by S.K. Vsekhsvyatskiy [2, 3, 4, 5] and obtained in a previous study by [16], is strongly increased. According to Kresak, it does not achieve 1.0-1.1^m. Our investigation leads to an estimate from 2.0 in 1850.0 to 2.9^m in 1900.0. L. Kresak determined the absolute magnitude of Comet Encke according to the maximum value of its observed brightness, i.e., according to a single evaluation of the brightness of the comet in each return. The indefiniteness in this estimate often reaches 1^m and even more. He assumed that he could disregard the instrumental effects arising when long-focus telescopes and photographic methods are used to determine the integral brightness of comets, but he nevertheless introduces a number of undesirable errors in his original observational data: (a) the effect of a single evaluation, which makes smoothing of random errors in the estimate impossible; (b) the indefiniteness of the reduction of observed brightnesses to absolute magnitudes; (c) the effect of strong atmospheric extinction for low altitudes over the horizon; (d) the effect of evening and morning twilights on the measured values; (d) the effect of perihelion asymmetry.

† Translation from the English by D.A. Andriyenko, S.K. Vsekhsvyatskiy, G.A. Garazdo-Lesnykah, V.P. Konopleva. ** This is not the original in English, but a translation from the Russian.

Photometric Parameter n of Comet Encke Approximation of Its Absolute Magnitude

The absolute magnitude is usually called its stellar magnitude, relative to a unit of geocentric Δ and heliocentric r distance. The most reliable value for the absolute magnitudes are obtained by interpolating the observed data obtained when r is very close to 1 AU. However, the perihelion distance of Comet Encke is only equal to 0.34 AU, while the time of the maximum observed brightness of the comet is on the average at a distance of about 0.5 AU from the Sun. The importance of the parameter n for deriving the absolute magnitude at such short distances is obvious. /55

If the suggested average value $n = 4$ is applied to a number of evaluations obtained for a large range of heliocentric distances, particularly longer and shorter than 1 AU, as was done by S.K. Vsekhsvyatskiy, the effect of n is largely decreased. When only a few estimates, or even one estimate, is used, particularly if the heliocentric distance of the comet under investigation is no more than 0.5 AU, systematic errors can appear in the absolute magnitude because of the inaccuracy of n. This effect is demonstrated numerically in Table 1.

The effect of secular variations in the heat of desorption L on the absolute magnitude which is derived both according to a single observations and according to a number of observations can be studied theoretically on the basis of the gas model. The photometric parameter n_g depends on the heliocentric distance in the following way:

$$n_g = \frac{\alpha}{2} + \alpha \frac{L}{RT_0} r^{\alpha}, \qquad (1)$$

where α is the coefficient characterizing the dependence of the temperature T over the surface of the nucleus on the heliocentric distance; R is the universal gas constant; T_0 is the temperature at a distance of 1 AU. Keeping the symbols of S.K. Vsekhsvyatskiy and L. Kresak, and assuming that $B = L/RT_0$, we can find the deviations of the data they gave from the absolute magnitude of the gas model H_{0g}:

$$H_{10} - H_{0g} = 2.5 \bmod B\left(\frac{1}{\alpha}\cdot\frac{r_2^{\alpha} - r_1^{\alpha}}{\ln r_2/r_1} - 1\right) + (1.25\alpha - 10)\frac{\bmod \ln (r_1 r_2)}{2}, \qquad (2)$$

If the observations are carried out at a distance between r_1 and r_2, while mod = 0.43429..., and

$$M_{4p} - H_{0g} = 2.5 \bmod B(r^{\alpha} - 1) + (1.25\alpha - 10) \bmod \ln r, \qquad (3)$$

if a single observation at a distance of r from the Sun is used. If we take another value of n instead of $n = 4$, then (3) is valid only with the following correction: $(4.343 - 1.086\,n)\ln r$.

TABLE 1 /56

r	$\alpha=0.5$				$\alpha=0.3$				$\alpha=0.1$			
	$B=8$	$B=10$	$B=12$	$B=14$	$B=13.7$	$B=17$	$B=20.3$	$B=23.7$	$B=42$	$B=52$	$B=62$	$B=72$
	$M_{4p}-H_{0g}$											
0.4	$+0.54^m$	-0.26^m	-1.06^m	-1.86^m	$+0.26^m$	-0.61^m	-1.48^m	-2.35^m	-0.06^m	-1.01^m	-1.96^m	-2.91^m
0.6	+0.12	−0.37	−0.86	−1.35	+0.03	−0.49	−1.00	−1.52	−0.08	−0.62	−1.16	−1.70
0.8	−0.01	−0.24	−0.47	−0.70	−0.03	−0.26	−0.50	−0.73	−0.05	−0.29	−0.53	−0.77
	$H_{10}-H_{0g}$											
0.4−0.8	+0.20	−0.33	−0.86	−1.39	+0.07	−0.49	−1.05	−1.62	−0.07	−0.67	−1.27	−1.87
0.4−1.0	+0.15	−0.28	−0.71	−1.14	+0.05	−0.40	−0.86	−1.31	−0.06	−0.54	−1.03	−1.51
0.4−1.6	+0.15	−0.04	−0.23	−0.42	+0.07	−0.14	−0.35	−0.56	−0.01	−0.24	−0.48	−0.71
0.6−1.0	+0.02	−0.24	−0.49	−0.75	−0.01	−0.28	−0.54	−0.80	−0.05	−0.32	−0.60	−0.87
0.6−1.6	+0.08	+0.08	+0.08	+0.08	+0.05	+0.04	+0.03	+0.02	+0.01	0.00	−0.02	−0.04
0.8−1.0	−0.01	−0.13	−0.25	−0.36	−0.02	−0.14	−0.26	−0.37	−0.03	−0.15	−0.27	−0.39
0.8−1.6	+0.10	+0.25	+0.40	+0.55	+0.07	+0.21	+0.36	+0.50	+0.05	+0.18	+0.32	+0.46
1.0−1.6	+0.15	+0.43	+0.70	+0.98	+0.11	+0.38	+0.65	+0.92	+0.08	+0.34	+0.60	+0.86
1.2−1.6	+0.22	+0.61	+0.99	+1.38	+0.17	+0.54	+0.91	+1.29	+0.11	+0.48	+0.84	+1.20

As can be seen from Table 1, the values of M_{4p} increase more /57 and more when L increases as one approaches the Sun. On the other hand, even a very disadvantageous distribution of observations between 1.2 - 1.6 AU from the Sun brings about a systematic decrease in the absolute magnitude which is roughly equal to half the magnitude of overestimation of the value M_{4p} at a distance of 0.5 AU. Moreover, the data for r = 1.0 - 1.6 and 1.2 - 1.6 AU are increased, since the increase of n at great heliocentric distances ($\log r \geq 0.2$) according to the gaseous model is replaced by its decrease, as was observed for the comet Encke. This is to the advantage of the gas-dust model. If the observations encompass an interval from 0.6 to 1.6 AU, then the distance in magnitudes H_{10} and H_{0g} is 0.1^m, while the error in the value of M_{4p} can exceed 1^m.

The agreement between the value of H_{10} and the gas model is still insufficient to confirm its reliability, and there is still no certainty that the model is plausible. The applicability of the gas model to Comet Encke at $r < 1.5$ AU is demonstrated below.

Thus, all the above, which is based on calculations, speaks in favor of Vsekhsvyatskiy's values of H_{10}, compared to Kresak's values of M_{4p}, at least for distances less than 1.5 - 2 AU. A reduction to 1 AU for long heliocentric distances should be analyzed solely on the basis of the curves obtained for the gas-dust model.

Kresak admitted that there were difficulties due to the poor values of n; therefore, he attempted to discuss the problem of the photometric parameter of Comet Encke. However, his conclusion that the "characteristic" parameter n of Comet Encke was approximately equal to four, which is based on average values of the parameters n for different returns in [16], is not convincing. Kresak admits that this coefficient depends to a great extent on r, but he holds that its "instrumental effects arise because of the inclusion of observations obtained at great heliocentric distances, which relate more to nuclear condensation than to the integral magnitude". However, he does not give any proof for this statement. His arguments are based only on the results of these calculations, without an analysis of the observational data. The curves for the change in brightness of Comet Encke according to which the average values of n were calculated are shown in Figure 1. The pre-perihelion observations were used solely in order to decrease the effect of perihelion asymmetry. Information on the observations carried out in this century is given in [1].

Figure 1 shows a substantial dependence of the parameter n on the heliocentric distance, even in those parts of the curve where estimates of the brightness made with identical instruments were used. The same results were obtained from an analysis of the observations of M. Beyer during the apparitions of Comet Encke in 1937, 1947, 1951 and 1961 [7, 8]. The change in the value of n from 2.5 at r = 0.8 AU to n = 8 at r = 1-1.5 AU in the apparition of 1947, for example, can hardly be explained by Kresak's argument, attributing the brightness estimates used to nuclear condensation First of all, it is well known from Beyer's observations of stable diffuse objects that the method he used yield integral values (in a system which is practically identical to the international photovisual system) and, secondly, Beyer mentioned in his comments on the observations of 1947 that only a rather extended coma without any nucleus was observed at distances from 1.5 to 1.3 AU; the nuclear condensation became visible only at r less than 1.1 AU. This case is completely opposite to that held by Kresak. The same is also valid for a number of other returns of Comet Encke. Moreover, the explicit decrease of the characteristic n with r appears at $r >$ 1.5-2 AU. This agrees with the assumption of the gas-dust model of a comet, and indicates that the effects responsible for the changes in the parameter n are connected with processes occurring in the comet itself, and are not instrumental.

We should mention that the dependence given in Figure 1 in the article by Kresak for the parameter n, as a function of the

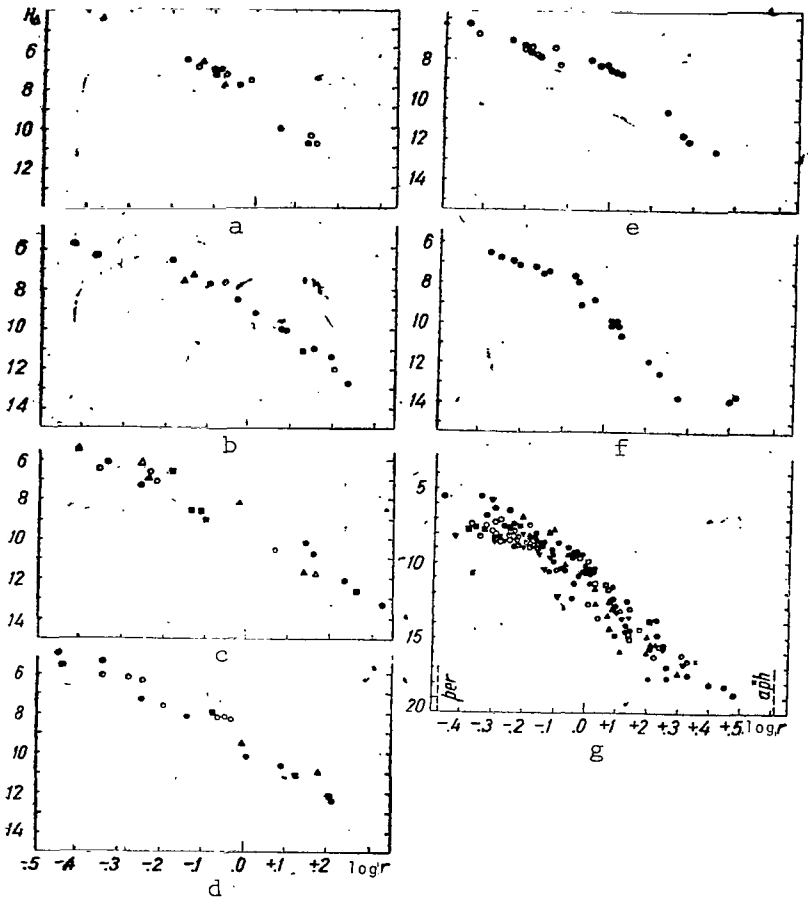

/58

Fig. 1. Change in Brightness of Comet Encke with Heliocentric Distance According to Observations Before Perihelion in the Apparitions: a-1805 (▲) 1819 (■), 1825 (●) and 1829 (○); b-1835 (▲) 1838 (●) 1842 (■) and 1848; c-1852 (▲) 1858 (△) 1862 (●) 1868 (○) and 1871 (■); d-1875 (▲) 1882 (●) 1885 (■) and 1891 (○); e-1895 (●) and 1901 (○); f-1905 (●) and 1911 (○); g-1914 (■) 1918 (■) 1924 (⊙) 1928 (▽) 1934 (▼) 1937 (▽) 1937 (▲) 1941 (△), 1947 (●), 1951 (○), 1954 (x) 1957 (◓) and 1961 (◒) (without the observations of M. Beyer).

maximum value of the heliocentric distance, in the interval for which the observations were used, has no significance, since the value of n resulting at the minimum heliocentric distance is distorted to the same extent as is the maximum value, while the value of n should refer to the middle of the interval used log r. /59

Kresak refers to an article by V. Vanysek and F. Hrebik [19] published long ago as a possible support of his conclusions with respect to the characteristic n. However, the results of this study do not indicate at all that Kresak's assumption (n = 4) is valid.

Moreover, there has been substantial progress in the photometry of comets since 1954.

Kresak's interpretation of the observed increase in n with time contradicts his principal results, because it leads to a gradual decrease in the region in which the comet is easily accessible to observations, due to the decrease in its absolute magnitude. /60

The data of Table 1 (for B = 12) in Kresak's study do not show the effect of "gradual contraction". On the other hand, the difficulties disappear if the observational data are studied from the point of view of the existence of secular variations in the value of the parameter n. A disregard of these changes brings about an underestimation of the absolute brightness of the comet in earlier apparitions, and an increase for recent returns, if based on estimates obtained at $r < 1$ AU. This also gave Kresak a decreased estimate of the rate of the secular decrease in brightness of the comet.

The Effects of Twilights and Atmospheric Absorption

Every photometric observation at low altitudes is aggravated by strong atmospheric absorption. It is practically forbidden to disregard this effect, particularly if a diffuse object is being observed. Similar difficulties arise in observations near the Sun against the bright sky background. In this case, the estimates of the total brightness are of a particularly subjective nature and are burdened with additional errors. Therefore, we should prefer observations relating to high altitudes, as well as observations carried out against the dark background of the night sky. However, L. Kresak rejected these observations immediately.

Effect of Perihelion Asymmetry

This effect also greatly complicates a determination of the absolute magnitude from observations close to the perihelion. Kresak found this obstacle and attempted to decrease it by introducing the deviations of ΔM from the average law and by considering them as a function of the time. His method leads to results about which the following comments can be made.

(1) We can take the statistical systematic nature of the values of M between $t - T$ as equal to -25 and -5 days (Fig. 4), but it is difficult to make them agree with the corrections which are applied by using the "smoothed" curve for individual values of M_{42} in order to obtain the "corrected" values of M' (without considering the sign of ΔM in Fig. 4, which is opposite to the sign in the text). The indefiniteness introduced in this correction is found to be of the same order as the rate of the secular decrease. /61

(2) If we turn to the unreliability of M', we should mention that the average secular decrease derived from these values for the period between 1805 and 1931 is close to 2m for one century,

which is definitely closer to my values than to Kresak's (about 1^m per 100 years). Nothing definite can be said about the data for the period from 1934 to 1964 (see Fig. 5 of Kresak's article).

(3) The perihelion asymmetry for Comet Encke which follows from Figure 4 of Kresak's article absolutely does not correspond to the observed brightness curves. The decrease by 2 or 3^m is the result of the

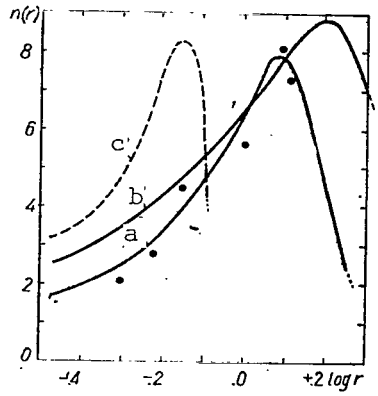

Fig. 2. Change of Photometric Parameter n as a Function of the Heliocentric Distance of the Comet. (a - n_α = 2, α = 2, B = 3, k = 0.1; b - n_α = 2, α = 1, B = 6, k = 0.01; c - Corrections of ΔM Introduced by Kresak; the Curves of the Dots are Values Obtained from Beyer's Observations). (a) and (b) were Obtained Theoretically for the Gas-Dust Model, and the Last Two Relate Directly to Comet Encke.

erroneous photometric law which Kresak used. This can be easily demonstrated.

For each r, the "osculating" law

$$H_\Delta = H_0 + 2.5n \log r \tag{4}$$

was replaced by Kresak by the following artificial relationship:

$$H_\Delta = H_0 + 10 \log r. \tag{5}$$

Using the correction of ΔM, Kresak assumed that he thereby reduced M_{42} by the value burdened by "perihelion asymmetry" to the true absolute magnitude H_0, i.e.,

$$\Delta M = M_{42} - H_0. \tag{6}$$

Comparing (4) and (5), we find that

$$n = 4\left(1 + \frac{0.1\,\Delta M}{\log r}\right). \tag{7}$$

The changes of n with the heliocentric distance which were derived from the corrections of ΔM and which are represented in Figure 2 absolutely did not correspond to the nature of the observed brightness curves or to the theoretical exponential curves. /62

Rate of Secular Variation

It follows from the above that the substantial errors in the values of M_{42}, M_{62} and M_{41} given in Kresak's article are at least equal to, and probably greater than, the values of the secular decrease he found, so that no definite conclusion can be drawn from the data he collected. These data are not uniform, and are characterized by substantial dispersion and large systematic errors which have nothing in common with the secular variation. This is also seen in the lower degree of correlation of the dependence $M_{42} = M_{42}(t)$ (also for the values of M_{41} and M_{62}) which Kresak represented, as well as in the almost complete absence of a difference between the decrease in reduced values of M_{42}, on the one hand, and the absolutely unreduced (either for $\Delta = 1$ or for $r = 1$) maximum apparent magnitudes of the comet M_m, on the other hand. The latter yields a "secular decrease" of 0.0^m per century. We can draw the same conclusion by noting the standard deviations of ε from M_{42} with respect to the averaged difference of O-C produced by the rate of the secular change. From this point of view, it is interesting that Kresak did not consider the correlation of n with time, on the one hand, since the average deviation decreases only from ±0.53 to ±0.41, but, on the other hand, he needed about three pages to describe and discuss the method of "reducing" the deviations of M_m from ±1.13 to $\pm 1.06^m$ for M_{42}, to $\pm 1.08^m$ for M_{41} and to $\pm 1.29^m$ for M_{62}. The magnitude M_m has nothing in common with the absolute brightness of comet Encke. The same can be said of the magnitude M_{np}. All these data are put in Table 2 of this study, where we find, from the combination of M_m and M_{42} (according to Kresak) and H_{10} (according to S.K. Vsekhsvyatskiy), the secular changes in brightness of the comet per revolution, the correlation factor ψ, the standard deviation for the set of values of ε under study and the average O-C differential derived from the time dependence.

TABLE 2

Magnitudes	ΔH_0	ψ	ε	$\overline{O-C}$	$\varepsilon-(\overline{O-C})$
M_m	$0^m.028 \pm 0^m.012$	0.33 ± 0.13	$\pm 1^m.20$	$\pm 1^m.13$	$0^m.07$
M_{42}	0.032 ± 0.012	0.39 ± 0.13	± 1.15	± 1.06	0.09
H_{10}	0.075 ± 0.008	0.83 ± 0.04	± 1.26	± 0.68	0.58

We must add that, in Table 1, Kresak does not give values for /63 the absolute magnitudes for two new and very important apparitions of the comet in 1941 and 1954, when it was exceptionally weak. Kresak holds that Comet Encke was not observed at heliocentric distances less than 1 AU in either of the cited apparitions. This is valid only for the apparition of 1941, during which all the observations were obviously carried out $r \geq 1.1$ AU. In 1954, Jones estimated the brightness of the comet as 9.7^m when it was at a distance of 0.6 AU from the Sun. The corresponding brightness of M_{42} is less than it should be according to Kresak's law, at least by 2^m for the secular decrease in brightness. It's magnitude for

the apparition of 1964 was greatly increased, as was already noted by V. Vanysek [18]. The correct value is at least 2.5^m, and probably 3.5-4^m weaker than that given for it, even when the perihelion asymmetry and the "instrumental effects" are taken into account. All these facts show the high rate of the secular decrease in brightness of Comet Encke, compared to that obtained by Kresak.

Let us now examine the quantitatively emperical relationship $M_{np} = M_{np}(t)$ digressing from the fact that it can be easily replaced by the expression $M_m = M_m(t)$, which has no physical significance. There is a close relationship between the correlation factor ψ, the inclination of the relationship (weight of secular decrease) of ΔH_0 and the square root of the deviation in each of the two statistical sets under investigation (time and absolute magnitude) ε_t and ε_{H_0}. Using the least-square method, we find that

$$\frac{\Delta H_0}{\psi} = \left(\frac{n\Sigma M_{np}^2 - \Sigma M_{np}\,\Sigma M_{np}}{n\Sigma t^2 - \Sigma t\,\Sigma t}\right)^{1/2} = \frac{\varepsilon_{M_{np}}}{\varepsilon_t}, \tag{8}$$

since

$$n\Sigma x^2 - \Sigma x\,\Sigma x = n^2\varepsilon_x^2, \tag{9}$$

where n is the number of pairs in (t, M_{np}), which must be summated. Since ε_t does not depend on M_{np}, the following relationship should occur between the characteristics of S.K. Vsekhsvyatskiy (B) and L. Kresak (K):

$$\frac{\Delta H_0(\mathrm{K})}{\Delta H_0(\mathrm{B})} = \frac{\psi(\mathrm{K})\,\varepsilon_{M_{np}}(\mathrm{K})}{\psi(\mathrm{B})\,\varepsilon_{M_{np}}(\mathrm{B})}. \tag{10}$$

The data of Table 2 actually satisfy (10), which would be expected. /64

Thus, the value of the systematic decrease in brightness which was obtained by Kresak as equal to 1^m per century does not relate to Comet Encke, but is the result of the large dispersion of his data.

Early and Recent Observations of Comet Encke. Independent Evaluations of the Disintegration Rate

The most complete observational data on the brightness of Comet Encke before 1965 were collected by J. Holetschek [11]. During the observations, he attempted to select that instrument in which the comet would appear as an almost pointed object.

The photometric observations of comets during apparitions in 1918-1964 were carried out by different observers in the majority

of cases either by comparing the comet to extrafocal stellar images or by some photographic methods. Moreover, we should mention the special method which Beyer developed and applied systematically in 1932. He used it for observations of Comet Encke in the apparitions of 1937, 1947, 1951 and 1961. As Vanýsek noted [18], the absolute magnitudes of Comet Encke which Beyer derived from his observations corresponded to the estimates which J. Holetschek and others reported at the beginning of the century. This fact could be a strong argument in favor of the assumption that there is a moderate secular decrease in the brightness of the comet in 20 centuries. However, Beyer's method obviously gives higher estimates of the brightness of comets than do other methods. This is apparent from the data of Table 3, which contains estimates of the absolute magnitude derived by Beyer and other authors, independently. As is well known, the absolute magnitude of the comet, calculated according to the observed curve for the change in brightness with the aid of a power law $(1/r^n)$, depends on the interval of heliocentric distances used or on the photometric parameter n itself. In order to avoid this effect, we have included only those data for which the values of the photometric parameter derived by Beyer differ from the values of other authors by no more than 25%. This criterion was used because, in the majority of cases, information on the intervals of r could not be found, or nothing was said of the "effective" heliocentric distance. The data of Table 3 were taken from the study of S.K. Vsekhsvyatskiy [2], its supplements [3, 5] and the studies of M. Beyer. Table 3 contains the designations of the comets, the

TABLE 3 /65

Comet	q	A	X	A—X	Author
1932 V	1.04	7.5	7.6	—0.1	Vsekhsvyatskiy
1932 VI	2.31	3.2	3.6	—0.4	
1935 I	0.81	9.5	9.8	—0.3	Bobrovnikov
1937 II	0.62	10.3	10.3	0.0	
			10.4	—0.1	Konopleva
1937 IV	1.73	3.9	4.7	—0.8	
1937 VI*	0.34	10.0	11.5	—1.5	Vsekhsvyatskiy
1939 III	0.53	6.4	7.2	—0.8	Shavik
1941 VIII	0.87	6.9	6.9	0.0	Konopleva
1947 XI*	0.34	9.9	10.9	—1.0	Vodop'yanova
1948 I	0.75	6.3	6.6	—0.3	
1948 IV	0.21	7.5	8.0	—0.5	Bouska
1948 V	2.11	4.4	5.3	—0.9	
1949 IV	2.06	5.6	6.4	—0.8	
			7.1	—1.5	Vodop'yanova
1950 I	2.55	4.9	3.5	+1.4	
1950 VII	1.39	8.9	9.4	—0.5	
1952 I	0.74	8.9	9.3	—0.4	
1954 VII	0.68	4.7	5.7	—1.0	
1954 VIII	5.05	3.9	6.2	—2.3	Vsekhsvyatskiy
1955 IV	1.48	4.8	6.7	—1.9	
			5.4	—0.6	Bouska
1957 III	0.32	5,1	5.9	—0.8	Richter
			6.7	—1.6	Ruzechkova, Valnicek
			5.9	—0.8	Bouska
			6.3	—1.2	Van Verden
1957 V	0.35	3.6	4.2	—0.6	Grigard
1958 III	1.32	6,8	7.4	—0.6	Sinton
1960 II	0.50	7.6	8.7	—1.1	Vsekhsvyatskiy

*Comet Encke

perihelion distances, the absolute magnitudes determined by Beyer (A) and other authors (X), the differences in these estimates and the last names of the authors. Of the 29 differences, the average

$$A - X = -0.72^m \pm 0.13^m \qquad (11)$$

is also a value which does not depend on the perihelion distance of the comet. The existence of differences (A-X) does not mean that Beyer's estimates are systematically erroneous. On the other hand, they can characterize the integral magnitude much better than do the magnitudes obtained by the extrafocal method. They cannot be compared to the data obtained the other way, without introducing the corresponding corrections. When discussing with me, M. Beyer suggested that the estimates he obtained for the brightness of comets are systematically higher than the data of other observers, since the luminosity of the weaker peripheral regions of the visible coma is considered in his method (in contrast to all the others). This statement was based on his 30 years of experience. /66

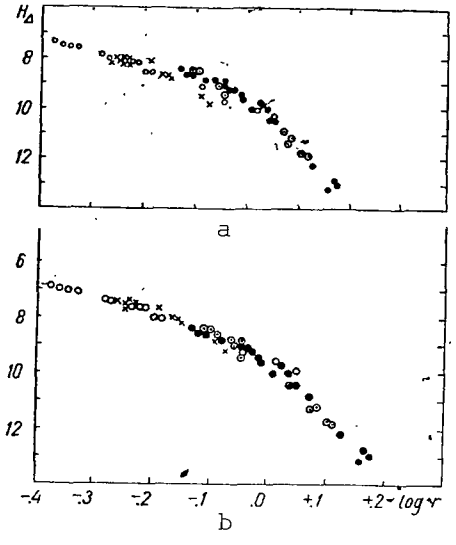

Fig. 3. Variation in Brightness of Comet as a Function of r in the Apparitions of 1937 (⊙), 1947 (●), 1951 (○), 1961 (x). (a) According to the Data of Beyer's Pre-Perihelion Observations; (b) With a Correction for the Secular Decrease in Brightness as Equal to 3.5^m per Century, 1937.

As for the phase of observations of Comet Encke, it follows from Figure 3a that the brightness curves coincide only for the apparitions of 1937 and 1947. The absolute magnitude of the comet of 10.2^m for the apparition of 1961 which Beyer obtained by extrapolation of the value for r_{max} = 0.84 AU is increased. Because of the change in the photometric parameter n with distance from the Sun, the true value of H_0 can be almost one stellar magnitude lower. Therefore, we can expect a decrease in the brightness of the comet reduced to r = 1 AU by almost a whole stellar magnitude between 1937 and 1947, on the one hand, and 1961, on the other hand, or roughly $3\text{-}4^m$ per century. Figure 3a is a graphic demonstration of how important it is to compare the changes in the characteristic n with r. It is a very great pity that Beyer's observations stopped at r = 1.5 AU. For the sake of a comparison, Figure 3b gives estimates of the brightness of Comet Encke which were carried out in 1937-1961. They refer to the apparition of 1937, with the following corrections added: 0.0^m for 1947, -0.6^m for 1951 and 0.8^m for 1961. It follows from the

data in this figure that the secular decrease in brightness of the comet is 3.5^m. The remaining differences are obviously smaller than in the case presented in Figure 3a. /67

If the effect of the geocentric distance is considered according to the formula of E. Opik [14], then, as can be seen from Figure 4, a sharp decrease in the brightness of the comet occurred between 1937 and 1961. There is no doubt that the law of Δ^{-1} is not correct, at least for the observations which were not carried out according to Beyer's method.

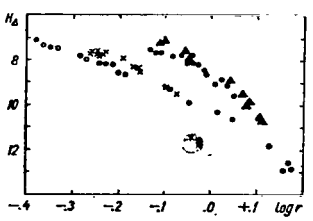

Fig. 4. Observations of M. Beyer, Reduced to r = 1 AU According to the Formula of E. Opik. (▲) 1937; (●) 1947; (○) 1951; (x) 1961.

TABLE 4

Returns	H_0
1825	8^m.6
1829	8 .5
1838	9 :0
1848	8 .8
1858	9 .0:
1868	9 .8:
1871	9 .8:
1875	9 .7
1881	9 .9
1895	8 .6
1905	9 .8
1914	<10 .4

Since the interval of 23.1 years between the perihelion passages of Comet Encke in 1937 and 1961 cannot be considered to be sufficiently long to derive a reliable value for the secular decrease in brightness, we can consider the problem from other points of view.

First of all, we can use the data which J. Holetschek collected for those apparitions of the comet in which it is observed roughly at r = 1 AU or, if possible, the observed values are reduced rather reliably to this distance from the Sun. A list of the magnitudes H_0, including systematic deviations between the photometric scales of individual observations, is given in Table 4. The data of Table 4 show that the brightness decrease between 1825 and 1914 was more than 2^m per century. Only in one apparition (1895) was the comet brighter than would follow from this conclusion.

In order to make the photometric data sufficiently uniform, it is desirable to connect previous observations with recent ones, i.e., to connect the series of observations of the two most experienced observers Holeschek and Beyer. Unfortunately, there were no /68 simultaneous estimations of the brightness of comets made by these observers. However, we can establish an indirect relationship. For this, we will use the advise of Vanysek. At one time, Holetschek published a catalogue of stellar magnitudes of certain diffuse objects [10], including estimates of the brightnesses of brighter globular clusters. These data were re-examined by Graff [9]. The globular clusters are similar in appearance to a comet and therefore can serve as photometric standards to connect a

series of observations carried out by Holetschek and Beyer. Holetschek observed Comet Encke in the apparitions of 1891, 1895, 1901 and 1905, while Beyer's observations refer to four apparitions between 1937 and 1961. Using the photoelectric values for globular clusters given in the catalogue of Kron and Mayall [13], the estimates of both observers can be reduced to the standard international system of star magnitudes. Beyer suggests that the author be requested to measure the magnitude of the globular clusters selected. Seven estimates of the brightness of nebulae and globular clusters which were published in [8] and a few estimates from an unpublished study were used in order to obtain the preliminary results. It was found that the scales of both observers were close for objects of 6^m, while they were brighter than 5 and weaker than 7^m for diffuse objects. Holetschek gives lower estimates of the brightness than does Beyer. The difference reaches 1^m. The highest value for the apparent brightness of Comet Encke, reduced to r = 1 AU according to Holetschek, is close to 8^m.

This effect is confirmed qualitatively by a comparison of the simultaneous visual observations by M. Beyer and A.M. Bakharev in 1951 and 1961. The comet seems to be less bright to Bakharev. The difference in the estimates of Bakharev and Beyer averages 0.5^m, while the extreme values are 0.2 and 1.5^m.

The results of a study of this effect and the magnitude of the secular decrease in brightness will be published after the observations are terminated. The preliminary value for the brightness decrease, with respect to 1925, is equal to at least 2.5^m per century.

An additional comparison of the estimates of Holetschek and those of his contemporaries [11] shows (compared to Beyer) that they decreased the brightness of the comet even more. It is possible that the absolute magnitude of the comet in the return of 1895 (based /69
almost completely on the observations of Holetschek) is due to this effect.

The set of approximately 150 individual pre-aphelion and pre-perihelion estimates of the brightness of Comet Encke which were obtained for 1914 and later returns (Fig. 1, g) is so non-uniform that it is impossible to study it by more precise methods than that which S.K. Vsekhsvyatskiy uses.

Thus, the following conclusions can be drawn.

(1) The observations span almost the entire interval from aphelion to perihelion. The record was made in 1953, when the comet was seen for 10 months before its passage through the perihelion at r = 3.53 AU. The aphelion distance was equal to 4.08 AU.

(2) There doubtlessly is a secular decrease in brightness. The dispersion in values of H_Δ from 2 to 4^m (for different r) does not allow us to estimate the magnitude of the secular decrease in graphic terms.

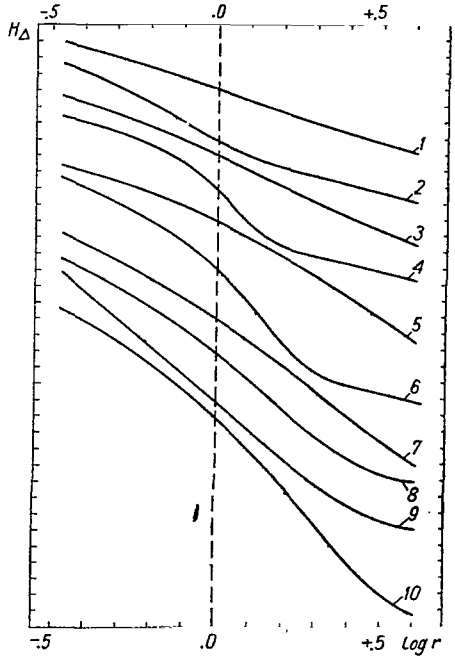

Fig. 5. Curves for the Variation in Brightness for the Gas-Dust Model of the Comet. The following Combinations of the Parameters $n\alpha$, α, B, k Are Given: 1-2, 0.5, 8, 1; 2-2, 0.7,8.5,1; 3-2, 0.3, 12, 0.1; 4-2, 2, 3.5, 0.1; 5-2, 0.5, 7, 0.01; 6-2, 1, 7, 0.01; 7-3, 0.3, 17, 0.01; 8-2, 0.5, 12, 0.01; 9-2, 0.1, 70, 0.01; 10-3, 0.5, 14, 0.001.

(3) Although individual magnitudes have great dispersion, the changes in average brightness with distance from the Sun are demonstrated convincingly by Figure 1g, which shows the dependences of the photometric characteristic n or r. The maximum value of this parameter corresponds to r = 1.5 AU, which is in complete agreement with the gas-dust model, and these changes will not be explained by assuming that there is a strong instrumental effect.

(4) The average curve can be described by the following parameters of the gas-dust model (Fig. 5, Curve 6): /70

$$H_0 = 11.2^m;\ n_d = 2;\ \alpha = 1;\ L = 14T_0, \text{cal/mole};\ k = 0.01$$

(T_0 is expressed in degrees Kelvin). A comparison with the observations of Holetschek at the end of the 19th century and the beginning of the 20th century gives approximately 3^m per century for the secular decrease in brightness of the comet, while, for the returns of the first half of the 19th century it gives a value from 2 to 2.5^m per century.

(5) Visual evaluations obtained at short heliocentric distances make up most of the observations. Only 40% of the total number of observations relate to r > 1 AU, 7% are obtained for r > 1.5 AU and only 6% for r > 2 AU.

(6) The combination of observations under investigation, which is close in nature to the data which Vsekhsvyatskiy used, together with (2), showed that the instrumental techniques, and particularly the photographic observations, cannot have a substantial effect on the determination of the absolute magnitudes of Comet Encke or their secular variations.

Gas-Dust Model of the Comet

In order to show the complete agreement between the data of observations and the physical hypothesis, we will compare the curves for the change in brightness shown in Figures 1 and 3 to some theoretical curves based on the concept of a gas-dust model of the comet, which was formulated mathematically by Vanýsek [17]. Figure 5 shows theoretical curves for an arbitrary absolute magnitude H_0 and for different combinations of the fundamental physical parameters of the comet according to the equations in [15], which the author derived during the process of improving the model. The corresponding curves are given in Figure 6, where the following four parameters were used: n_d is the photometric characteristic for the dust component of the cometary atmosphere; α is the exponent characterizing the change in temperature over the surface of the nucleus with heliocentric distance $T(r) = T_0 r^{-\alpha}$, the product of the heat of desorption and the temperature T_0 [see (1)]; k is the ratio between absolute brightnesses of the dust and gas coma.

TABLE 5

/71

n_d	α	B	k	r_{max}	n_{max}
2	2	3	1	0.99	4.50
		3	0,01	1.47	11.80
		3.5	0.1	1.18	8.35
		3.5	0.001	1.60	16.75
	1	6	0.1	1.22	6 55
		6	0.001	1.97	11.20
		7	0.01	1.47	9.64
		7	0.0001	2,13	14.33
	0.7	8.5	1	0 80	4.42
		8.5	0.01	1.64	7.89
		8.5	0.001	2.13	9.63
	0.5	7	1	1.06	2.88
		7	0.1	1.78	4.12
		7	0.01	2.87	5.47
		7	0.001	(4.27)	6.82
		12	1	0.72	4.59
		12	0.1	1 13	5.95
		12	0.01	1.64	7.29
		12	0.001	2.24	8.61
	0.3	12	0.1	1.69	3.83
		12	0.001	(5.39)	5.68
		24	0.1	0.97	6.87
		24	0.001	1.94	8.56
	0.1	35	0.01	3.73	3.85
		70	0.01	1.22	7.05
3	0.5	10	0.01	2.33	7.11
		14	0.001	2.20	9.94
	0.3	17	0.01	2.49	6.33
		24	0.001	2.25	8.90
	0.1	50	0.01	2.63	5.34

H_Δ (see Fig. 5) is a value which corresponds to a distance of r from the Sun and a unit distance from the Earth for the comet model. Table 5 contains the maximum values of the photometric parameters n_{max}, calculated for different combinations of the cited parameters, and the corresponding heliocentric distances r_{max}. They were obtained from the following relationships, which are valid for

constant values of n_d and:

$$r^{\alpha}_{\max} = 1 + \frac{1}{B}\left(n_d - \frac{\alpha}{2}\right)\ln r_{\max} - \frac{1}{B}\ln\frac{k\left(\alpha^2 B^2 r^{2\alpha}_{\max} - 2n_d \alpha B r^{\alpha}_{\max} + \frac{1}{4}\alpha^2 - n_d\alpha + n_d^2\right)}{\alpha^2 B r^{\alpha}_{\max}}, \quad (12)$$

$$n_{\max} = \left(\frac{n_d^2 + \alpha^2 k^{-1}\left(\frac{1}{4} + B^2 r^{2\alpha}_{\max}\right) r^{n_d - 1/2\alpha}_{\max} \exp\left[B\left(1 - r^{\alpha}_{\max}\right)\right]}{1 + k^{-1} r^{n_d - 1/2\alpha}_{\max} \exp\left[B\left(1 - r^{\alpha}_{\max}\right)\right]}\right)^{1/2}, \quad (13)$$

/72

A comparison of Figures 1 and 3 with Figures 2, 5 and 6 and the data of Table 5, shows the validity of the gas-dust model for describing any curve of a brightness variation observed. Moreover, comparative calculations show that the curve for the brightness change corresponding to the gas-dust model for $r < 1.5$ AU, for comets with low values of k (similar to the comet Encke), is very similar to the corresponding curve for the gas model.

Both in the gas model and in the gas-dust model, the curvature of the brightness curves is a characteristic aspect, while the existence of a salient point is typical of the gas-dust model. From this point of view, it is very significant in analyzing the observed brightness curves for Comet Encke that the curvature of the brightness curves is more significant in the more recent apparition of the comet than in earlier ones. This fact is partly connected with the circumstance that a wider range of r was spanned in recent returns, while in the case of the observations of Holetschek and Beyer there was a lower intrinsic dispersion. However, the main reason is the doubtless decrease of the parameter k and increase of L in time, which are responsible for the secular variations in the physical behavior of the comet. The first is due to the gradual depletion of the porous dust layer on the surface, and the latter is due to the selective effect of the liberation of different volatile gases from the nucleus: the more volatile molecules are evaporated or desorbed before the less volatile ones. Both of these factors bring about substantial changes in the photometric parameter n in dependence on the heliocentric distance and, thus, a more

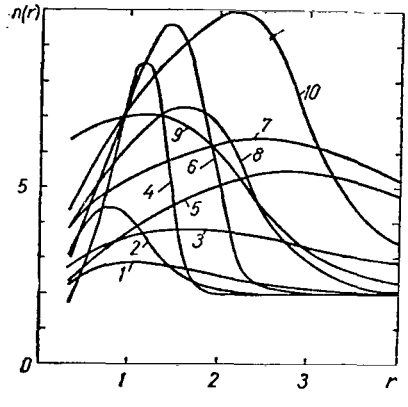

Fig. 6. Curves for the Change in the Parameter n as a Function of r for the Gas-Dust Model of the Comet (the Combinations of Parameters are the Same as in Fig. 5).

significant curvature of the brightness curves. /73

The effect of the perihelion asymmetry of the brightness curves is connected with the same phenomena. The abrupt decrease in the parameter n observed during recent returns, from the rather high values at distances of $r > 1$ AU to values of $n \sim 2$-3 at distances close to the perihelion, can be described by the relatively high values of α equal to or greater than unit, i.e., the abrupt increase in the temperature as the comet approaches the Sun. On the other hand, the theoretical curve of the photometric parameter n for low r occurs outside the curves obtained from observations. The same holds for the corresponding brightness curves.

That the perihelion asymmetry actually should bring about an abrupt increase in the values of α is obvious for the following reasons. The solar radiation incident on the comet acts in two directions, causing an increase in temperature of the comet's nucleus and liberation of frozen gases from the nucleus. The more the gases are enclosed in the nucleus, the greater the energy necessary for their liberation, and because of this the increase in temperature of the nucleus should be less, and the inverse. The perihelion asymmetry, which is due to the decrease in concentration of molecules over the surface of the nucleus, thus leads to a change in the thermal balance so that the nucleus is heated.

According to the data of observations carried out during 32 pre-perihelion and 20 post-perihelion periods (some of them correspond to the same return), it was found that the average difference in pre-perihelion and post-perihelion absolute magnitudes of Comet Encke is 1-1.5^m. This difference can be attributed to the effect of perihelion asymmetry. If we assume that the effect begins to act at a distance approximately equal to 1 AU, then the change in H_0 is equivalent to the decrease before perihelion and the increase after perihelion of the parameter n, at least by 0.4, but averaging somewhat more than unity.

Conclusions

(1) An analysis of the photometric curves of Comet Encke obtained at the end of the 19th century and the beginning of the 20th century leads to several independent estimates of the secular decrease in absolute brightness of the comet. As has been shown, the magnitude of the decrease is of a progressive nature and is equal to 2 to 4^m per century.

(2) The absolute magnitude H_{10} which S.K. Vsekhsvyatskiy determined allow us in the majority of cases to characterize the "intrinsic" luminosity of the comet completely reliably. /74

(3) The disintegration of the comet is unavoidable, but is not of a uniform nature. Periods of a rapid decrease in brightness alternate with periods of a moderate decrease. The magnitudes cited

above are averaged over rather long periods of time. Even the destruction of Comet Encke which was recently predicted by F. Whipple [20], and D. Douglas-Hamilton [21] seems to be completely realistic.

(4) If we cannot use the assumption of a sudden decrease in brightness of Comet Encke by 2^m between 1947 and 1951, then the law of Δ^{-1} proposed by E. Opik [14] must be rejected. O.V. Dobrovol'skiy and Osherov [6] recently found the statistically most probable reduction formula of $\Delta^{-2.1}$, using a vast amount of observational data. Therefore, we preferred the classic law of Δ^{-2} over Opik's formula.

(5) A comparison of the theoretical and observational curves for the brightness of Comet Encke allows us to consider that there is a systematic decrease in the parameter n before the perihelion and an increase after it. This change, which is due to the effect of perihelion asymmetry, does not exceed unity on the average.

(6) The magnitude for the decrease in brightness of comet Encke which L. Kresak recently obtained as equal to $1\text{-}1.1^m$ per century is not reliable, since the method he used cannot give any results at all.

(7) Although there are about 400 estimates of the brightness of Comet Encke at present, and 47 observed returns, Kresak's results are based only on 45. In each of these returns, he used only a single estimate to determine the absolute brightness of the comet, while he completely ignored the last two returns.

(8) The observational data which Kresak used are very non-uniform. They are burdened with the effects of morning and evening twilights, atmospheric extinction and perihelion asymmetry, and contain systematic errors which necessarily appear because of the unsuccessful law selected for the change in brightness. The resulting error in each value of M_{np} is either equal to or exceeds the estimate Kresak derived for the secular decrease in brightness of the comet.

(9) Since the "working" distance from the Sun is much less than 1 AU, the accuracy of the photometric parameter n in Kresak's method is of principal significance. The "intrinsic" value of the /75
parameter n of Comet Encke which he used (equal to 4), which is the basis of all his results, is absurd. Actually, the "characteristic" value of this parameter does not exist at all, since the parameter n is a function of the heliocentric distance, changing from two to eight and more, and undergoing the effects of secular variations in a way similar to the brightness of the comet. These changes can be explained completely on the basis of the gas-dust model.

(10) A reduction of estimates of the maximum apparent brightness to $r = \Delta = 1$ AU is of a purely formal nature. Kresak's method

decreases the average deviations from ±1.13 to ±1.06^m for M_{42}. The insufficient accuracy for the values of M_{np} brings about a low degree of correlation of $M_{np} = M_{np}(t)$, and a slow rate of disintegration of Comet Encke because of the close relationship between the correlation factor ψ and the inclination of the relationship under investigation.

(11) Kresak's arguments, which are based on the relative stability of the maximum apparent magnitude of the comet, are unsound and unreliable. This can be easily explained by the combination of effects due to the observational conditions, the secular variations in physical parameters of the comets, the perihelion asymmetry and the geometrical relationships in the comet-Sun-Earth system.

(12) One of the most important factors interfering with a determination of the more precise value for secular decrease in brightness of the comet is the systematic difference in photometric scales of different observers. Kresak did not consider this problem. Some important comments are made in this article relative to this problem, but it will be considered in more detail when Beyer's observations are at the disposal of the author.

The meager amount of observational data does not allow us to carry out a similar investigation for other short-period comets.

References

1. Vsekhsvyatskiy, S.K.: Astron, Zhur., Vol. 31, p. 281, 1954.
2. Vsekhsvyatskiy, S.K.: Fizicheskiye kharakteristiki komet (Physical Characteristics of Comets). Moscow, "Fizmatgiz" 1958.
3. Vsekhsvyatskiy, S.K.: In the book: Issledovaniya komet po programme MGSS (Studies of Comets According to the IQSY Program) Kiev, "Naukova Dumka", 1964.
4. Vsekhsvyatskiy, S.K.: Komety v period MGSS (The Comets During the IQSY Period). Moscow, Akad. Nauk S.S.S.R., 1964.
5. Vsekhsvyatskiy, S.K.: Fizicheskiye kharakteristiki komet, nablyudavshikhsya v 1954-1960 gg (The Physical Characteristics of Comets Observed in 1954-1960). Moscow, "Nauka" 1966.
6. Dobrovol'skiy, O.V. and R.S. Osherov: This Collection.
7. Beyer, M.: Astron. Nachricht, Vol. 265, p. 37, 1937; Vol. 282, p. 145, 1955; Vol. 286, p. 219, 1962.
8. Beyer, M.: Astron, Nachricht, Col. 278, p. 217, 1950.
9. Graff, K.: Mitt, Sternw. Wien, Vol. 4, p. 1, 1944.
10. Holetschek, J.: Ann. Sternw. Wien, p. 20, 1907.
11. Holetschek, J.: Denk.math.nat.Klasse Akad. Wien., Vol. 93, p. 201, 1916.
12. Kresak, L.: Bull. Astr. Inst. Czechoslov, Vol. 16, p. 348, 1965.
13. Kron, G.E., N.U. Mayall: Astron, J., Vol. 65, p. 581, 1960.
14. Opik, E.J.: Irish Astr., J., Vol. 6, p. 93, 1963.
15. Sekanina, Z.: Publ. Astr. Inst. Charles Univ. Prague, Vol. 36A, p. 37, 1962.

16. Sekanina, Z.: Bull. Astr. Inst. Czech. Vol. 15, p. 1, 1964.
17. Vanysek, V.: Contr. Astr. Inst. Masaryk Univ., Brno. Vol. 1, p. 9, 1952.
18. Vanysek V.: Bull. Astr. Inst. Czechoslov., Vol. 16, p. 355, 1965.
19. Vanysek, V., F. Hrebik: Bull. Astr. Inst. Czech., Vol. 5, p. 65, 1954.
20. Whipple, F.L.: Astron,J., Vol. 69, p. 152, 1964.
21. Whipple, F.L. and D.H. Douglas-Hamilton: Nature et Origine des Cometes (The Nature and Origin of Comets). Coll. Inst. Liege, p. 469, 1966.

AN ANALYSIS OF THE SURFACE BRIGHTNESS DISTRIBUTION IN THE TAIL OF THE COMET 1956h

G.K. Nazarchuk

ABSTRACT: Photometry was used to analyze the high-quality large-scale photographs of the comet Arend-Roland which were obtained by S.K. Vsekhsvyatskiy with the 40cm-telescope of the Crimean Astrophysical Observatory. A simple model was used for the data on the kinematic and physical parameters of the streams, with a consideration of the constant acceleration and dissocation of the luminous molecules and the expansion of the matter in the tail. All the parameters were determined by a comparison between the photometric and calculated results. It was found that the expansion of the matter in the tail was anisotropic; this may be due to the presence of a longitudinal magnetic field of order of 10^{-6} -10^{-5} G.

The classic mechanical theory of comet shapes [14] was developed mainly for the purpose of interpreting the geometrical characteristics of the tails of comets (curvatures, deviations from the radius vector, etc.) and the kinematic parameters determined according to them (velocities and accelerations of cloud formations, etc.). The same holds true for studies on the magnetohydrodynamic phenomena in plasma tails [11], in which it is mainly the geometrical and kinematic properties of the tails observed which are interpreted [15]. /77

Photometric data are used indirectly for an analysis of the geometric structure of the tail: the lines of maximum (in cross section) brightness and the axes of the stream are plotted, and the points of local brightness increases (cloud formations) are marked. Obviously, this kind of analysis of the tail structure has its disadvantages, and is necessarily connected with some subjectivity and a substantial loss in the information included in the photometric picture of the comet.

A great deal of the studies on the photometry of comets relate either to integral photometry and data concerning the evolution of comets [2], or to surface photometry of the heads [9]. There have been repeated investigations of the definition of surface brightness of the heads, the laws for the brightness decrease in the radial direction, and the shape and the contraction of the isophotes [9]. The photometric structure of a comet head has been calculated theoretically in numerous studies [3, 9].

In the photometry of cometary tails, there are only a few studies where the authors either limit themselves to publications of the isophotes [18, 20] or find empirical laws for the brightness decrease along selected directions of the type r^{-n}. Of particular note is the work of Thiessen [21], in which there is an attempt at linking the photometric and kinematic characteristics of the tail, as well as several other studies of the same nature [7, 5].

The following dependence was obtained in [21] as a result of photometry of Comet Arend-Roland:

$$C\int n dx = I(y), \tag{1}$$

where x and k are the transverse and longitudinal coordinates of the plane of reference, respectively; n is the surface density of the radiating ions; C is the proportionality factor between the surface density and the surface brightness. The integral in (1) encompasses practically the entire tail, and its formal limits range from $-\infty$ to $+\infty$. /78

Assuming that the number of radiating particles decreases exponentially in time, while the particles themselves move with uniform acceleration, Thiessen wrote out the law of conservation of the radiating particles in the following form:

$$I(y)\, e^{t/\tau} v(y) = \text{const}, \tag{2}$$

where t is the age of the particles, i.e., the time during which the particles have passed a distance of y; τ is the mean lifespan; v is the velocity of the particles in a section drawn to the distance from the nucleus. Using the equations of uniformly accelerated motion, i.e.,

$$v^2 = v_0^2 + 2ay, \tag{3}$$

$$y = v_0 t + \frac{at^2}{2}, \tag{4}$$

where a is the acceleration and v_0 is the initial velocity of the particles, as well as the law of conservation in (2) for any four sections of the tail, it is easy to obtain a closed system of equations to determine v_0, τ and a.

Using this method, Thiessen, and then Dobrovol'skiy and Ibadinov, determined the acceleration, initial velocities and lifespanss for Arend-Roland and Halley's Comet, while Yegibekov determined the same parameters for Comet Mrkos [7, 5, 21].

The assumption that there is no dispersion of the velocities of the particles over the entire tail underlies Thiessen's method. This assumption narrows the range of applicability of the method extensively since, if it is valid, there are particles of different ages in any cross section and (2) becomes unreliable. Before using (2) - (4) to estimate the kinematic parameters and mean life span of the particles, we must find whether or not all the particles of one age are actually grouped in the neighborhood of one cross section. A check of this assumption in [12] showed that it is not valid.

A model which took account of the splitting of a bunch of particles of the same age was constructed in [12], and it was shown that there was satisfactory agreement with observations. Only axial sections of single streams of the tail of the Arend-Roland comet /79 were used for the comparison with observations. The possibility of reciprocal superposition of single streams was not considered, which had to affect the reliability of the parameters determined.

This study, which is a continuation of [12, 13], contains an analysis of the brightness distribution both along and across the steams. Using the diffusion model assumed in [12], we have attempted to divide single streams and to make the values for the model parameters more accurate, with a consideration of the partial overlapping of streams. Moreover, an investigation of the surface brightness distribution allows us to find anisotropic expansion of the matter in the tail of the Comet Arend-Roland, and to make a quantitative determination of the degree of anisotropy.

Construction and Significance of the Diffusion Model of a Tail

A theoretical model of the brightness distribution in the tail of a comet can be constructed by two methods. The first is to integrate a system of kinetic equations for the particles of the tail without a consideration of cross collisions but with regard for the interaction between solar corpuscular radiation and self-consistent electric and magnetic fields. The non-magnetic state was examined by A.Z. Dolginov with respect to comet heads.

The second method is based on the use of Green's function for an instantaneous source. The small size of the nucleus, compared to the tail, allows us to consider the nucleus and the adjacent region to be a point source of the matter. Let the surface density of the particles in the cloud which is emitted instantaneously by the point source change according to the following law in the reference system connected with the gravity center of the cloud:

$$n = G(X, Y, t), \qquad (5)$$

where X and Y are the coordinates on the plane of the comet's orbits.

In order to obtain the surface density in the tail, we must know the law of motion of the cloud after it is emitted and the dependence of the escape velocity of the matter from the source (source power) on the time $f(t)$. If the cloud's gravity center describes /80 the curve below in the plane of the orbit

$$X=\varphi(t),\ Y=\psi(t), \tag{6}$$

then the surface brightness distribution in the plane of the tail is determined by the following expression at the moment of observation:

$$I(X,Y)=C\int_0^t f(t^*)\,G[X-\varphi)(t^*),\ Y-\psi(t^*)]\,dt^*$$

on the condition that the escape of particles from the source had begun at the moment t, while $f(t)$ is the number of particles emitted by the source in one second t seconds ago. Selecting different functions of G, ϕ, ψ and f, we can find different models for the distribution of surface brightness.

We will assume in this discussion that the escape of matter is stable ($f(t)$ = const) and was begun infinitely long ago ($t \to \infty$). We will consider that each elementary cloud moves, after its appearance, with uniform acceleration, with zero initial velocity along the Y axis, i.e.,

$$\varphi(t)=0;\ \psi(t)=\frac{at^2}{2}. \tag{7}$$

The assumption of uniformly accelerated motion was based on the fact that numerous observations of the motion of cloud formations yield some average values of the acceleration for the entire interval of observations. With these assumptions, the specific model of the tail depends only on the selection of Green's function, i.e., the law of expansion of the elementary cloud.

For a rigorous determination of Green's function, we must resolve the stochastic problem of the behavior of the cometary ion in a corpuscular stream i.e., we must determine the probability density $W(r - r_0, t, v_0)$ that the ion whose initial position and velocity were r_0 and v_0 will diverge in a time of t by the vector of $r - r_0$. Obviously, the trajectory of the ion is a random curve whose mathematical expectation is the following:

$$\langle r\rangle=\int F(v_0)\,rW(r,t,v_0)\,dv_0\,dr, \tag{8}$$

where $F(v_0)$ is the distribution function of the initial velocities, describing the motion of the center of gravity of the elementary cloud. In correspondence with the initial assumption, /81

$$\langle r \rangle = \left\{0, \frac{at^2}{2}, 0\right\}. \tag{9}$$

Let us define the new probability density $W_1(r - \langle r \rangle, v_0, t)$ as the probability of divergence of the particle from the center of gravity of the cloud. Obviously, the unknown Green function will then be equal to the following:

$$G(X, Y, t) = \int e^{-\frac{t}{\tau}} f(v_0) W_1(r - \langle r \rangle, t, v_0)\, dv_0\, dr. \tag{10}$$

In those cases when the trajectory of the particle is not random, but a completely definite curve, i.e.,

$$r = r_1(t), \tag{11}$$

the probability density is

$$W = \delta[r - r_1(t)]. \tag{12}$$

Thus, Green's function for free molecular dispersion in the absence of external fields is easily obtained: it coincides with equation (17) in [8] by S.A. Kaplan and V.G. Kurt. If a gravitational field acts on the particles, then it is sufficient to substitute r by $r - \frac{gt^2}{2}$ into Green's function for free molecular dispersion.

The particles of cometary tails are subjected to the accelerating effect of the proton and corpuscular radiation of the Sun. If the acceleration occurs when small percentages of an impulse are frequently imparted to the cometary molecules or ions, then we can disregard the dispersion of the particle trajectories corresponding to identical conditions, i.e., we can consider the trajectories to be completely definable and we may use Green's function, with the cited substitution for the accelerated motion. This approximation, the criterion for applicability of which is

$$\langle |r - \langle r \rangle|^2 \rangle \ll |\langle r \rangle|^2, \tag{13}$$

should be best satisfied with tails of dust and of gas, since their principal acceleration mechanism is photon radiation.

A model of the tail of a comet was constructed in this approximation in [13]. A check showed that the distribution of surface brightness in axial sections of the streams of the tail of Comet Arend-Roland does not correspond to this model. /82

The motion of the ion in a corpuscular stream appears to be much more complex. Because of infrequent collisons with ions of the stream, the cometary ion has relatively high increases in impulse and the self-consistent fields take part in the pulse transfer. It can be said that the process of ion acceleration by the stream is a Markov process, i.e., the ion trajectory depends slightly on the initial velocity.

The problem of determining the probability characteristics of the motion of an ion in a corpuscular stream, even in the absence of a magnetic field, is connected with great mathematical difficulties; therefore, without calculating the probability density W, we will determine Green's function, assuming that, if the average ion acceleration is compensated, then the probability of its divergence by the vector of r after each collision is determined by a normal Gaussian law, i.e.,

$$W(r) \sim e^{\frac{r^2}{e^2}}. \qquad (14)$$

As Chandrasekhar [17] showed, Green's function has the appearance of a normalized Gaussian curve in this case, regardless of the frequency of collisions, so that

$$G = \frac{1}{2\pi (Dt)^{3/2}} e^{-\frac{r^2}{2Dt}}, \qquad (15)$$

i.e., it coincides with Green's function for the equation of diffusion. We should mention that the movement of the ion by the effect of infrequent collisions is not a diffusion process in the ordinary sense of the word. The diffusion occurs in rather frequent collisions and, as Chandrasekhar showed, the expression for Green's function has the form of (15) regardless of the nature of the particle interaction, i.e., for any form of the probability density of (14). Since there is visual averaging of the surface brightness in observations, we can rightfully use Green's function for infrequent collisions when calculating macroscopic characteristics of the tail.

The process of turbulent diffusion leads to Green's functions. The turbulent diffusion of ions in a cometary tail can occur if the magnetic field of the corpuscular stream has a sufficient random component. Dolginov considered random magnetic fields to be an accelerating factor [6]. In addition to acceleration, they should cause scattering of the cometary ions, or collisionless magneto-turbulent diffusion. /83

Let us examine the source of the matter at the origin of the coordinates. The possibility that the coordinates of a particle in the turbulent flow are included in the interval $(X, X + dX)$, $(Y, Y + dY)$ is then

$$W(X, Y)\,dX'\,dY = \frac{dX\,dY}{2\pi\sqrt{\langle X^2\rangle\,\langle Y^2\rangle}}\,e^{-\frac{X^2}{\langle X^2\rangle}-\frac{Y^2}{\langle Y^2\rangle}}$$

The mean squares $\langle X^2\rangle$ and $\langle Y^2\rangle$ depend on the time. The specific form of the dependence is determined by the correlation characteristics of the magnetic field in the stream; however, there are general properties of $\langle X^2\rangle$ and $\langle Y^2\rangle$ which occur in any case.

Let $v(t)$ be the velocity of a cometary ion which has age of t; we then have the following according to the relationship of Campa de Ferier [1]:

$$\langle X^2\rangle = 2\int_0^t (t-t')\,\langle v_x(t''-t')\,v_x(t'')\rangle\,dt'. \qquad (16)$$

The time scale of the turbulence is determined as:

$$L_{tx} = \int_0^\infty R_x(t)\,dt, \qquad (17)$$

where the correlation factor

$$R_x(t) = \frac{\langle v_x(t+t')\,v_x(t')\rangle}{\langle v_x^2\rangle} \qquad (18)$$

does not depend on t'.

At $t >> L_{tx}$,

$$\langle X^2\rangle = 2\langle v_x^2\rangle L_{tx}\,t - 2\langle v_x^2\rangle\int_0 tR(t)\,dt =$$

$$= 2\langle v_x^2\rangle L_{tx}\,t - \text{const} \approx 2\langle v_x^2\rangle L_{tx}\,t, \qquad (19)$$

while at $t << L_{tx}$ we will find an estimate for $\langle X^2\rangle$, based on the fact that $R_x(t)$ is by definition an even function of t and $R_x(0) = 1$. An extension of $R_x(t)$ into a series in the neighborhood of $t = 0$ obviously has the following form: /84

$$R(t) = 1 - \frac{1}{2}R''(0)\,t^2. \tag{20}$$

from which

$$\langle X^2 \rangle \approx \langle v_x^2 \rangle t^2. \tag{21}$$

Analogous relationships can also be written for $\langle Y^2 \rangle$.

It follows from (19) and (21) that young particles are distributed around the center of the cloud, as in free molecular scattering, while the particle distribution in a rather "old" cloud is the same as in ordinary diffusion, except that the following product plays the role of the diffusion factor:

$$D_{tx} = 2 \langle v_x^2 \rangle L_{tx}. \tag{22}$$

Using these concepts, let us select a Green function of the type in (15), assuming for the sake of generality that the process of expansion of the bunch of particles is anisotopic and considering that, because of the dissociation and ionization, the number of radiating particles in the bunch decreases exponentially, i.e.,

$$G = \frac{1}{2\pi t \sqrt{D_\perp D_\parallel}} e^{-\frac{X^2}{2D_\perp t} - \frac{Y^2}{2D_\parallel t} - \frac{t}{\tau}}, \tag{23}$$

where $D_\perp$ and $D_\parallel$ are the transverse and longitudinal diffusion factors.

We will call the tail model which is based on Green's function a diffusion one. The distribution of surface density of the particles in the diffusion model can be obtained by substituting (23) and (9) into (6) and assuming that $t \to \infty$, f = const:

$$n(X, Y) = \frac{f}{2\pi \sqrt{D_\perp D_\parallel}} \int_0^\infty \frac{dt}{t} e^{-\frac{X^2}{2D_\perp t} - \frac{\left(Y - \frac{at^2}{2}\right)^2}{2D_\parallel t} - \frac{t}{\tau}}. \tag{24}$$

In order to decrease the number of parameters, we will convert to the dimensionless variables

$$x = \frac{X}{L_\perp}, \quad y = \frac{Y}{L_\parallel}, \quad \theta = \frac{t}{2\tau}, \tag{25}$$

where /85

$$L_{\perp} = 2\sqrt{D_{\perp}\tau};\ L_{\parallel} = 2\sqrt{D_{\parallel}\tau}, \tag{26}$$

and we will introduce the dimensionless parameter

$$\Gamma = a\sqrt{\frac{\tau^3}{D_{\parallel}}}. \tag{27}$$

The surface density of the particles is determined, with these symbols, by the following expression:

$$n(x, y) = \frac{f}{2\pi\sqrt{D_{\perp} D_{\parallel}}}\int_0^{\infty}\frac{d\theta}{\theta}e^{-\frac{x^2+(y-\Gamma\theta^2)^2}{2\theta}-2\theta}. \tag{28}$$

It depends only on the single essential parameter Γ.

Thus, for a theoretical determination of the surface brightness in the tail of the comet, we must calculate the single-parameter group of surfaces, i.e.,

$$\Phi_{\Gamma}(x, y) = \int_0^{\infty}\frac{d\theta}{\theta}e^{-\frac{x^2+(y-\Gamma\theta^2)^2}{2\theta}-2\theta} \tag{29}$$

The values of this integral were determined in a rather dense three dimensional system (x, y, Γ) with the aid of numerical integration on the "Razdan-2" computer. The integration method guarantees four-six reliable significant digits, depending on the combination of variables, which exceeds the observations even in the worst cases. Figure 1 shows some transverse sections, and Figure 2 shows some longitudinal sections of a set of $\Phi_{\Gamma}(x, y)$.

Let us make some comments on the applicability of the diffusion model. Since Green's function in (23) is essentially postulated, and not obtained from a solution to the problem of the ion motion in a corpuscular stream, then (28) should be considered as a working hypothesis which needs proof from observations. By testing the diffusion model, we will thereby test the validity of the original assumption in (14). The fact that this hypothesis merits a check follows from the results of [12], where there is a satisfactory agreement between the observed change in brightness in axial sections of streams of Comet Arend-Roland and that predicted theoretically by the diffusion model.

What divergences of the law in (28) from the brightness distribution actually observed should be anticipated even in the case /86

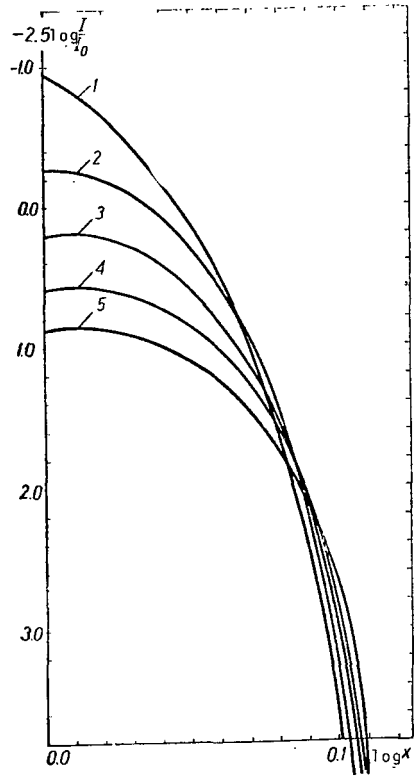

Fig. 1. Cross Sections of a Group of Surfaces $\Phi_\Gamma(x, y)$ (at G = 10 y = 0.10 (1); 0.3 (2); 0.5 (3); 0.7 (4); 0.9 (5).

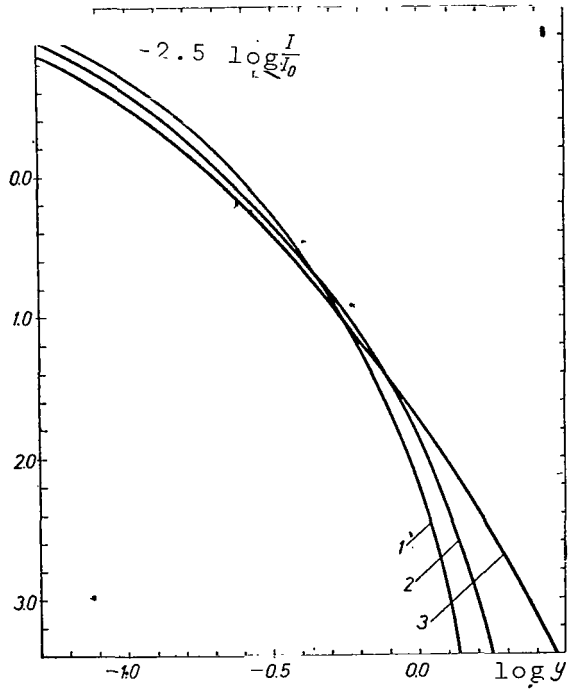

Fig. 2. Longitudinal Sections of a Group of Surfaces $\Phi_\Gamma(x, y)$ (Γ = 0.1 (1); 2.5 (2); 10.0 (3)).

of validity of (40)? First of all, some discrepancies arise as the result of the initial assumption on the steady-state flow of matter from the source. The model does not predict fluctuations in the density of the particles of the material or a regular density change due to a change in the heliocentric distance of the comet.

Secondly, in deriving the law of (28), it was assumed that the illumination of the tail was due to excitation of particles of a single kind. Only in this case can we speak of proportionality of the surface brightness and surface density of the particles, or use a single average lifetime. Consequently, the greatest deviation from observations should be expected in regions close to the head. Deviations of the model from observations should also be detected here if the true law for splitting of the bunch is not a diffusion process but a turbulence-diffusion one. /87

Role of the Spatial Orientation of the Tail /88

The preceding discussions referred to the case when the plane of reference coincides with the plane of the cometary orbit. Only in this case is the distribution of surface density of the particles determined by (28), where the parameter Γ is expressed in terms of the lifetime of the particles, while the coefficient of longitudinal diffusion is determined by (27).

Let us show that the surface density is expressed in terms of the integral in (28) for any orientation of the tail with respect to the observer, but with a change in the value of Γ.

Actually, we will convert from the system of coordinates in which (28) was defined to a new system of x^*, y^*, z^*, selecting the direction of the z^* axis along the line of sight. The old coordinates are expressed in the terms of the new ones by a system of linear relationships.

$$\begin{aligned} x &= \alpha_{11}x^* + \alpha_{12}y^* + \alpha_{13}z^*, \\ y &= \alpha_{21}x^* + \alpha_{22}y^* + \alpha_{23}z^*, \\ z &= \alpha_{31}x^* + \alpha_{32}y^* + \alpha_{33}z^*. \end{aligned} \tag{30}$$

The surface density of the number of radiating particles is obtained by integration of the volume density along the line of sight. It is equal to the following, with accuracy up to a constant factor:

$$\int_{-\infty}^{+\infty} dz^* \int_0^{\infty} \frac{d\Theta}{\Theta^{7/2}} \exp\left\{-2\Theta - \frac{1}{2\Theta}[x^2 + (y - \Gamma\Theta^2)^2 + z^2]\right\}. \tag{31}$$

We will require that this expression be equal to the following, with accuracy up to a constant factor:

$$\int_0^{\infty} \frac{d\Theta}{\Theta} \exp\left\{-2\Theta - \frac{1}{2\Theta}[x^{*2} + (y^* - \Gamma'\Theta^2)^2]\right\}. \tag{32}$$

Substituting (30) into (31) and integrating by z^*, we find the sufficient conditions of proportionality for (31) and (32):

$$\alpha_{11} = 1, \tag{33}$$

$$\alpha_{12} = \alpha_{13} = \alpha_{21} = \alpha_{31} = 0, \tag{34}$$

$$\alpha_{33} = -\alpha_{22}, \tag{35}$$

$$\alpha_{23} = \alpha_{32} = \sqrt{1 - \alpha_{22}^2}. \tag{36}$$

The transformation is orthogonal and /89

$$\alpha_{22} = \cos\beta, \tag{37}$$

where β is the angle between the axis of the stream and the plane of reference, while the transformation itself is a turn of the

coordinate system around the x axis up to coincidence of the z axis with the direction of the line of sight. Consequently, if we select the direction of the y axis in the plane of reference along the stream, the direction of the x axis perpendicular to the stream, and the origin of the coordinates in the nucleus of the comets, then the distribution of surface brightness in this system is proportional to the value

$$\Phi_{\Gamma a_{22}}(x, y) = \int_0^\infty \frac{d\Theta}{\Theta} e^{-\frac{x^2+(y-\Gamma a_{22}\Theta^2)^2}{2\Theta}} \cdot 2\Theta$$

regardless of the orientation of the comet tail with respect to the observer. We must also take account of the contrast of the diffusion factor in the direction perpendicular to the plane of the orbit $D_\wedge$ from the other two factors $D_\perp$ and $D_\parallel$, and we must replace the coefficients of longitudinal dispersion in the plane of reference by $(D_\parallel \cos\beta + D_\wedge \sin\beta)$ in (26) - (28). We ultimately find that

$$n\left(\frac{X}{L_\perp}, \frac{Y}{L_\parallel}\right) = \frac{f}{2\pi\sqrt{D_\perp}(D_\parallel \cos\beta + D_\wedge \sin\beta)} \Phi(x, y, \Gamma), \tag{38}$$

where

$$\Gamma = \frac{a\cos\beta \cdot \tau^{3/2}}{\sqrt{D_\parallel \cos^2\beta + D_\wedge \sin^2\beta}}; \tag{39}$$

$$L_\perp = 2\sqrt{D_\perp \tau}; \tag{40}$$

$$L_\parallel = 2\sqrt{(D_\parallel \cos^2\beta + D_\wedge \sin^2\beta)\tau}. \tag{41}$$

Determination of the Model Parameters According to the Surface Brightness Distributions

We had at our disposal photographs of Comet Arend-Roland obtained by S.K. Vsekhsvyatskiy on the 16" astrograph of the Crimean Astrophysical Observatory on the night of May 2-3, 1957. A photometric chart of the comet was obtained according to these photographs. There is no need to discuss the method of processing and describing the observational materials and reductions, since this information can be found in [12]. The isopycnic lines of the comet /90 are also contained there.

Photometric sections which satisfy the requirement of the preceding paragraph were selected for the analysis. The distances from the sections to the nucleus of the comet (in space) are given in

Table 1. The brightness distribution along these sections is shown in Figure 3.

It can be seen from Figure 3 that the tail of the comet consists of a few (four) largely superposing streams. The extreme stream is not found in all the cross sections because of the limitedness of the photometered portion. The brightness maxima are clearly seen on the cross sections, and they correspond approximately to the axial point of single streams. There is no precise correspondence between the brightness maxima and the center of the streams, since the brightness maxima move toward a brighter neighboring stream because of the reciprocal superposition. The maximum can be unbiased only in a random case, if both neighboring streams have identical brightness.

TABLE 1

Section No.	Y·10⁶, км
1	0.0
2	1.11
3	2.33
4	3.34
5	4.56
6	5.72
7	6.84
8	7.95

Let us find to what extent the diffusion model described in the preceding paragraph can represent the distribution of surface brightness in the tail, and let us determine the parameters of the model by (39) - (40). If the tail of the comet were to consist of one streak or several streaks which are widely spaced, then the solution to the problem we have formulated would be relatively simple. Actually, the tail of Comet Arend-Roland had a complex multiple-stream structure while the observational conditions were such that single streams overlapped. The need for dividing the streams, each of which can be characterized by its set of parameters Γ, $L_\perp$, $L_\parallel$ is the principle difficulty encountered in this study.

Mathematically, the problem can be formulated as such: determine that set of parameters Γ_i, $L_{\perp i}$, $L_{\parallel i}$ and

$$K_i = \frac{c_i f_i}{2\pi\sqrt{D_{\perp i}(D_{\parallel i}\cos\beta_i + D_{\wedge i}\sin\beta_i}}, \qquad (42)$$

where i is the number of the corresponding stream (I-IV) and the magnitude x_{ik} (k is the number of the cross section), so that the following equality takes place for any transverse photometric section:

$$I_k = \sum_{i=1}^{4} K_i \Phi[(x - x_{ik}) L_{\perp i}, y_k, L_{\parallel i}, \Gamma_i], \qquad (43)$$

/91

while the positions of the centers of the streams in the cross sections of x_{ik} should satisfy the condition of rectilinearity of these streams,

$$\frac{X_{ik} - X_{jk}}{X_{il} - X_{jl}} = \frac{Y_k}{Y_l}. \qquad (44)$$

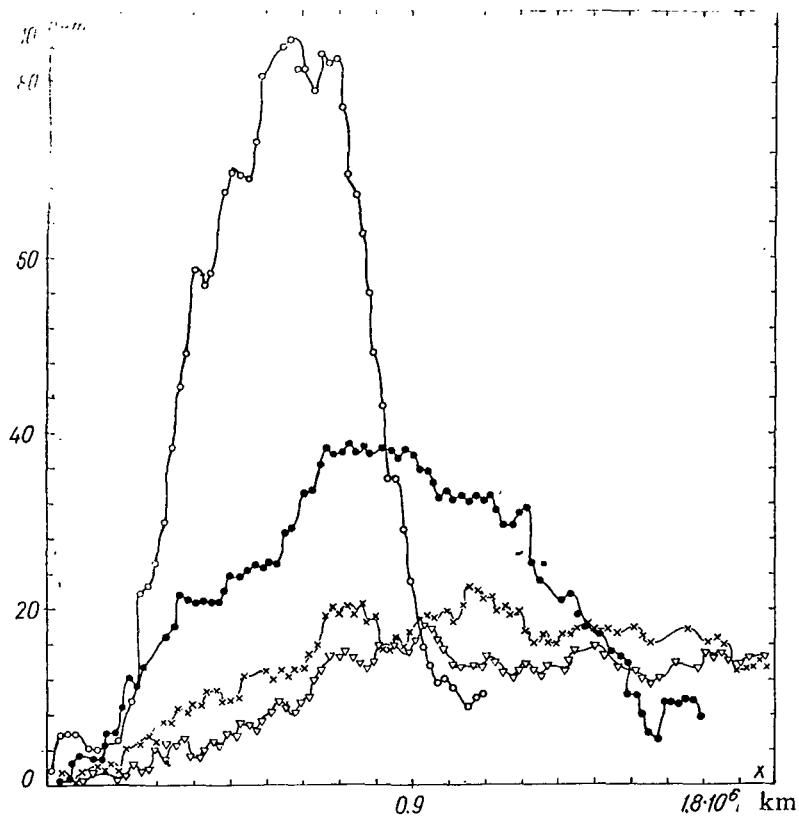

Fig. 3. Brightness Distribution in Cross Sections. (O) Section 2; (●) Section 4; (X) Section 6; (∇) Section 8.

In principle, an analytical solution to the problem is possible, for example, by the least-square method; however, we will not carry /92 it out, since it is time-consuming and little applicable because of the calculation difficulties which arise. The difficulties in a numerical analysis of the graph (Fig. 3) are due to the fact that functions of the type in (38), by the superposition of which we would like to represent the distribution of surface brightness over the entire tail, are not orthogonal with respect to each other, which involves a high loss in accuracy in the calculations [10]. The cross sections were analyzed graphically according to these concepts: the method involved a repetition of several stages. In the first stage, we considered that the center I of the stream in the initial approximation coincides with the brightness maximum in the cross sections. Let us construct the curves

$$\log I_k(x_l, \max) = \Psi_0(\log Y). \qquad (45)$$

i.e., the longitudinal section of the first stream in logarithmic coordinates. By shifting the origin of the coordinates, we arrived at a coincidence between the curve in (45) and one of the curves of the set

$$\log \Phi(0, y, \Gamma) = \Psi_c (\log y). \tag{46}$$

The values for the shift of the abscissa and ordinate axes are given by $\log L_{\parallel i}$ and $\log K_i$, respectively, and we can thereby determine the initial approximation of Γ. Using the curve for the brightness differential in the transverse section at the edge of the tail, we will select the value $L_{\perp i}$. Let us subtract the following value from the observed brightness values:

$$K_i \Phi[(x - x_{ik}) L_{\perp i}, y_k, L_{\parallel i}, \Gamma_i],$$

We then obtain the cross sections, from which the contribution I of the stream is eliminated in the initial approximation. Performing this operation over all the cross sections, we will make the preliminary values of the parameters more accurate. After this, we will carry out the same procedure on the following, apparently extreme stream. In order to be certain that (44) is satisfied, it was convenient to change the scales of the abscissa axes in different cross sections so that the brightness maxima occurred one after another. Controlling the results continuously, we will repeat the sequential stages until there is coincidence between the calculated and observed curves. The criterion for coincidence is the appearance of the O-C curve, which should represent the line O-C = 0 in the ideal case, while its points should be scattered at random around the abscissa axis in the real case, because of the fluctuations in brightness and the errors in photometry.

We should mention that the process described here for the division of the photometric structure into single streams is very laborious, and involves the need for considering certain fine details: insignificant deviations of the axes of the streams from straight lines, local intensifications of the brightness in single cross sections, etc. Therefore, in carrying out the studies, we often had to turn to the photometric map and photograph of the comet in order to obtain additional information which was not contained in the sections analyzed, and in order to check the correctness of the operations used.

As would be expected, a satisfactory coincidence between the observed brightness distribution and that calculated according to the diffusion model was found on the basis of the results of [12], i.e., we succeeded in selecting those values of the parameters for which the theoretical brightness distribution coincided with the smoothed observed values (see Fig. 4). The values of the parameters for all four streams are given in Table 2. The values Γ and $L_{\parallel}$

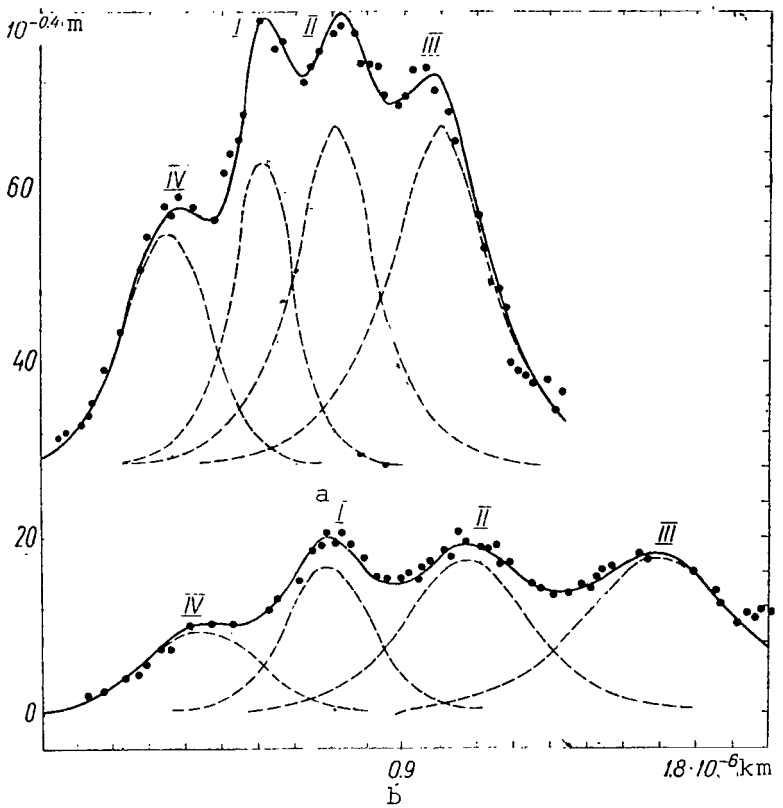

/93

Fig. 4. Comparison of the Theoretical (Solid Curve Distribution of Brightness with that Observed) (Points). Two Transverse Sections are Given (a - No. 3; b - No. 6). The Streams are Designated by the Numerals I, II, III, IV (The Dashed Curve is the Contribution of Single Streams).

for the first two streams differ somewhat from those previously published in [12], since the reciprocal overlapping of streams is not considered in the preliminary investigation. /94

TABLE 2

Stream No.	r	$L_\parallel/\cos\beta$, см	$L_\perp$, см	K	β
I	10	$1{,}1 \cdot 10^{12}$	$8.64 \cdot 10^{9}$	20	25°16′
II	6	$1.1 \cdot 10^{12}$	$1.15 \cdot 10^{10}$	20	49.52
III	6	$1.1 \cdot 10^{12}$	$1.44 \cdot 10^{10}$	20	66.00
IV	2	$2.5 \cdot 10^{11}$	$2 \cdot 10^{9}$	52	8.27

In the photometric sections closest to the nucleus, the coincidence between theoretical and observational data is not satisfactory; this apparently can be explained by the cited factors - particle ionization of the gas, numerous kinds of radiating particles in the region of the head and coma, and deviations from the law of diffusion.

Analysis and Conclusions

No one has succeeded in obtaining a positive spectrum of a comet at the distances from the head of interest to us. Liller advanced further than the others in this respect; however, his best spectrogram, for April 30, 1957, which was published in [19], was obtained with low resolution (width of the output slit of the photoelectric spectrometer of 47 Å) and with a substantial noise level. Against the background of the noise path, we can see maxima corresponding to the bands N_2^+ (3914Å), CO^+ (3580; 4001.5 + 4024; 4231 + 4251 + 4274; 4544 + 4568; 5048 Å); however, the identification is not reliable and it is very difficult to trace the level of the continuous spectrum correctly. Liller himself considers that no molecular emissions were observed in the tail; however, this statement must be viewed with a critical eye, since the resolution of the spectrometer was less than the distance between neighboring bands, which should have brought about a blurring of the bands, together with the noise, as well as an apparent conversion of the spectrum into a continuous one. /95

Since there are no reliable spectral data, the proportionality factor C between the surface density and the surface brightness, which depends on the Einstein coefficient of the observed transitions and populations of the corresponding levels, has remained indefinite. Therefore, despite the fact that absolute photometry of the tail has been carried out, the density of the particles in the tail has not been determined. However, the parameters Γ, $L_\perp$, $L_\parallel$ and K are found without using the absolute values of the particle density, and relative photometry is sufficient.

It is not the physical parameters of the tail a, τ, $D_\perp$, $D_\parallel$, f, which are determined directly from observations but the values Γ, $L_\perp$, $L_\parallel$, K, which are dependent on them. The angle β is easily calculated according to the known coordinates of the comet at the moment of observation and the element of its orbit on the basis of the generally accepted assumption that the plane of orbit of a comet is the plane of symmetry of each stream. After Γ, $L_\perp$, $L_\parallel$ and K are found, we have four equations (39) - (42) with five unknowns a, τ, $D_\perp$, $D_\parallel$, f.

In order to determine these values, it is necessary to use some additional considerations. For example, we can evaluate the lower acceleration limit by considering the practically unnoticeable curvature of the tail, since this is done when determining the type of tail in the mechanical theory of cometary forms. On the plates under investigation, the tail remained straight all the way to a distance of 10^7 km, with a consideration of the projection. Consequently, $1 + \mu > 10$.

The heliocentric distance of the comet at the moment of observation was 0.727 AU, which gives the following estimate for acceleration:

$$a > 10 \text{см/сек}^2 \tag{47}$$

From (39) and (41),

$$\Gamma \frac{L_\parallel}{\cos\beta} = 2a\tau^2, \tag{48}$$

where the unknown values are found in the left-hand part of the equation (see Table 2). This relationship gives the upper limit to the mean lifetime of the particles, i.e., /96

$$\tau < \sqrt{\frac{\Gamma L_\parallel}{2\cos\beta}} \approx 5 \div 7.5 \cdot 10^5 \text{ сек} \tag{49}$$

We can obtain the lower estimated values of the diffusion factors in a similar way:

$$D_\perp > L_\perp^2 \sqrt{\frac{5\cos\beta}{4\Gamma L_\parallel}}, \tag{50}$$

$$D_\parallel > \left(\frac{L_\parallel}{\cos\beta}\right)^{3/2} \sqrt{\frac{5}{4\Gamma}} \tag{51}$$

We can obtain opposite estimates by assuming that the mean lifetime of the particles can hardly be less than 24 hours. Considering that $\tau > 10^5$, we find the following from (48):

$$a < \frac{1}{2}\Gamma \frac{L_\parallel}{\cos\beta} 10^{-10} [\text{см/сек}^2] \tag{52}$$

$$D_\perp < 0.25 \cdot 10^{-5} L_\perp^2, \tag{53}$$

$$D_\parallel < 0.25 \cdot 10^{-5} L_\parallel^2 / \cos^2\beta [\text{см}^2/\text{сек}] \tag{54}$$

The estimates obtained from (50) - (54) are shown in Table 3 for each stream.

The abrupt difference in longitudinal and transverse scales, whose magnitudes are given in Table 3 for all the streams, indicates that there is anisotropy to a great extent in the expansion of the matter in each stream. It can be seen from Table 3 that the longitudinal diffusion factor is on the average 3 orders greater than the transverse factor, while it follows from (40) and (41) that

$$\frac{D_\perp}{D_\parallel} = \frac{(L_\perp \cos\beta/L_\parallel)^2}{1-(L_\perp \cos\beta/L_\parallel)^2 \tan^2\beta} \approx \left(\frac{L_\perp \cos\beta}{L_\parallel}\right)^2. \qquad (55)$$

TABLE 3

Stream No	a, cm/sec^2	τ, sec	$D_\parallel$, cm^{2}sec^{-1}	$D_\perp$, cm^{2}sec^{-1}	$\frac{L_\parallel}{L_\perp \cos\beta}$	H, G
I	550	10^5	$3.0\cdot10^{18}$	$1.75\cdot10^{15}$	42	$2.0\cdot10^{-5}$
	10	$7.4\cdot10^5$	$4.1\cdot10^{17}$	$1.89\cdot10^{14}$		$0.26\cdot10^{-6}$
II	660	10^5	$3.0\cdot10^{18}$	$3.08\cdot10^{15}$	31	$1.1\cdot10^{-5}$
	10	$5.7\cdot10^5$	$5.3\cdot10^{17}$	$5.36\cdot10^{14}$		$0.2\cdot10^{-6}$
III	660	10^5	$3.0\cdot10^{18}$	$5.08\cdot10^{15}$	25	$1.0\cdot10^{-5}$
	10	$5.7\cdot10^5$	$5.3\cdot10^{7}$	$8.84\cdot10^{14}$		$0.16\cdot10^{-6}$
IV	25	10^5	$1.6\cdot10^{17}$	$1.27\cdot10^{15}$	11	$2.26\cdot10^{-5}$
	10	$1.6\cdot10^5$	$1.0\cdot10^{17}$	$8.02\cdot10^{14}$		$1.3\cdot10^{-6}$

We should emphasize that this conclusion depends most slightly /97 on all the original assumptions, including the specific form of Green's function selected for constructing the model. Actually, any Green function should decrease to infinity and, consequently, should be characterized by some spatial dimension. Even if the true Green function differs in some details from that we selected, the anisotropy of the expansion, which is expressed as the difference in characteristic dimensions in two measurements, should remain, since this is a rather rough property of the requisite Green function.

The conclusions and estimates which have been made to this time are based directly on observations and can be considered as sufficiently sound; starting with an interpretation of the anisotropy in expansion and further, we will have to resort to some untested hypotheses, and we will use theories whose applicability in the case of interest to us is, at least, problematic.

The difference in the coefficients of longitudinal and transverse diffusion indicates that the direction of the axes of the stream is separate from and physically unequivalent to the other two directions. The acceleration vector is directed along the axis, and it can be assumed that the vector of the regular component of the magnetic field is directed along the axis.

The anisotropic expansion during collisions of cometary ions with the solar corpuscles, the difference between the mean free path and the Larmor radius in the regular longitudinal magnetic field, the anisotropy of the statistical properties of the random magnetic field component, all these are different reasons for the anisotropy in the expansion of the matter. We will not examine

the first of these reasons, since the classic theory of collisions of charged particles gives the reverse effect; transverse diffusion should be stronger than longitudinal. Observations show that this effect overlaps with the stronger effect of the magnetic field. One more argument in favor of the presence of a magnetic field is /98 the existence of several streams in the tail, including the extended leading radius vector.

At the moment the photograph of the comet was taken, the heliocentric distance was equal to 0.73 AU. The section of the tail under investigation, which had length of about 0.05 AU, was closer than 0.09 to the Sun. As is known from rocket investigations [4], the random magnetic field in the solar wind is recorded at heliocentric distances which exceed 1.5 AU. Considering this, we will assume that the magnetic field in each stream is regular and directed along the axis of the stream.

To evaluate the intensity of the magnetic field, we will use the following relationship [16]:

$$\frac{D_\perp}{D_\parallel} = \frac{1}{1+\frac{\lambda^2}{r_i^2}}. \qquad (56)$$

the mean free path of the electron λ along the field will be evaluated from the relationship below

$$\lambda \approx \frac{D_\parallel}{v_e}, \qquad (57)$$

while the Larmor radius of the ions is

$$r_i = \frac{m_i c \bar{v}_i}{eH}, \qquad (58)$$

where $\bar{v}_i$ and $\bar{v}_e$ are the average thermal velocities of the ions and electrons. Substituting (57) and (58) into (56), and considering that

$$\frac{D_\perp}{D_\parallel} = \frac{L_\perp^2 \cos^2\beta}{L_\parallel^2} \ll 1, \qquad (59)$$

we will obtain the following constant after substituting the numerical values:

$$H \approx 2\cdot 10^{-6} \frac{T}{D_\parallel} \cdot \frac{L_\parallel}{L_\perp \cos\beta}. \qquad (60)$$

In order to evaluate the magnetic field from above, we will use the minimum value of $D_{\parallel}$ and assume that $T = 10^5$ °K. We will obtain the lower limit by substituting the values of $D_{\parallel_{max}}$ into (60), and we will assume that $T = 10^4$ °K. The estimates obtained for all the streams are given in Table 3. As can be seen, to explain the anisotropy observed, it is sufficient to have a rather weak magnetic field H (10^{-6} - 10^{-5} G). /99

We should mention that the model is valid only if the magnetic field in the stream is purely longitudinal. The anisotropy detected allows us to consider that the magnetic field did not have a substantial regular transverse component, which could play a role in the acceleration of the matter in the tail.

In principle, we could close the system of equations in order to determine the physical parameters of the tail and to find the acceleration, lifetime, and diffusion factors, since these values depend on the parameters of the corpuscular stream. An attempt at this was made in [12], on the assumption that the mechanism for acceleration of the ions was collision with solar corpuscles; this yielded values for the stream parameters which did not agree with the data of rocket measurements.

In order to realize this possibility, we must use the strict theory of interaction of the solar wind and photon radiation with the matter of the cometary tail. Let us mention that this theory should describe not only the acceleration of the cometary ions, but also their decay and splitting in space.

References

1. Bay, Shi-i: Turbulentnoye techeniye zhidkostey i gazov (The Turbulent Flow of Liquids and Gases). Moscow, Foreign Literature Publishing House, p. 212, 1962.
2. Vsekhsvyatskiy, S.K.: Fizicheskiye kharakteristiki komet (The Physical Characteristics of Comets). Moscow, "Fizmatgiz", 1958.
3. Gnedin, Yu.N. and A.Z. Dolginov: Astron. Zhur., Vol. 43, p. 181, 1960.
4. Dvoryashin, A.S.: This Collection.
5. Dobrovol'skiy, O.V. and Kh.Ibadinov: Byull. Institut. Astrofiziki Akad. Nauk Tadzh. S.S.R., Vol. 46, No. 7, 1966.
6. Dolginov, A.Z.: This Collection.
7. Yegibekov, P.: Byull. Institut. Astrofiziki Akad. Nauk Tadzh. S.S.R., Vol. 30, No. 8, 1961.
8. Kaplan, S.A. and V.G. Kurt: Astron. Zhur., Vol. 37, p. 536, 1960.
9. Konopleva, V.P.: In the book: Problemy kometnoy astronomii. Inform. Byul. MGK AN USSR (Problems of a Cometary Astronomy. Information Bulletin of the International Geological Congress of the Academy of Sciences of the Ukrainian S.S.R). Kiev, "Naukova Dumka", p. 10, 1966.
10. Lantsosh, K.: Prakticheskiye metody prikladnogo analiza (Practical Methods of Applied Analysis). Moscow, "Fizmatgiz", 1961.
11. Marochnik, L.S.: Uspekhi Fizicheskikh Nauk, Vol. 82, p. 221, 1964.
12. Nazarchuk, G.K.: In the book: Fizika komet i meteorov (Physics of Comets and Meteors). Kiev, "Naukova Dumka", 1965.
13. Nazarchuk, G.K.: In the book: Aktivnyye protsessy v kometakh (Active Processes in Comets). Kiev, "Naukova Dumka", 1967.
14. Orlov, S.V.: Komety (Comets). Moscow, United Scientific and Technical Presses, 1935.
15. Ptitsyna, N.I.: Byull. komiss. po kometam i meteoram (Bulletin of the Commission on Comets and Meteors). Siberian Divsion of the Academy of Sciences of the U.S.S.R. Press. No. 9, p. 12, 1964.
16. Frank-Kamenetskiy, D.A.: Lektsii po fizike plazmy (Lectures on Plasma Physics). Moscow, "Atomizdat", p. 200, 1964.
17. Chandrasekhar, S.: Stokhasticheskiye problemy v fizike i astronomii (Stochastic Problems in Physics and Astronomy). Moscow, Foreign Literature Publishing House, p. 23, 1947.
18. Ceplecha, Z.: Publ. Astron. Inst. Czech., Vol. 34, p. 13, 1958.
19. Liller, W.: Astron. Journ. Vol. 132, No. 3, p. 867, 1960.
20. Ruzickova, B., M. Plavec: Publ. Astron. Inst. Czech, Vol. 34, p. 35, 1958.
21. Thiessen, G.: Z. Astroph. Vol. 44, P. 3, 1958, 1969.

HYDRODYNAMICS OF THE CIRCUM-NUCLEAR REGION OF A COMET

L.M. Shul'man

ABSTRACT: The flow in the region of a comet's head around the nucleus is examined. Intermolecular collisions in this region are substantial, and the movement of the substance there is described in terms of hydrodynamics. It is shown that only supersonic flows can occur if the heating due to external radiation is not too great. The brightness distribution is found for the case of an adiabatic flow. The problem of the motion of dust particles in a supersonic flow is solved. It is found that the velocity of the particles is somewhat higher in a gas flow than in a free molecular one. The effect of heating the gases by external radiation is considered qualitatively. It is shown that a discontinuity in the density produces haloes which surround the nucleus of the comet under certain conditions.

Even those who constructed the classic mechanical theory of /101
cometary forms understood that the sphere of its applicability excludes that part of the comet where the collisions of particles cannot be disregarded. The estimates given by O.V. Dobrovol'skiy [3] show that the collisions are substantial only for rather bright comets, in a region directly adjacent to the nucleus. This region can reach $5 \cdot 10^4$ km, which is an insignificant part of the entire comet. According to Jackson's estimates [7], for maximum density of the NH_3 molecules in the inner coma ($2 \cdot 10^{13}$ cm^{-3}), one molecule undergoes 10^4 - 10^5 collisions.

To establish Maxwellian distributions by velocities, it is sufficient to have only a few collisions per molecule; therefore, we should expect that the distribution of molecules by initial velocities for most bright comets differs substantially from that which occurs when they evaporate from the surface of the nucleus. This shows that we should have a critical approach to the results of a number of model studies [5], in which the brightness distribution in the head of a comet was calculated by integration over the trajectories of molecules escaping from the side of the nucleus which was turned toward the Sun.

Because of the collisions, the distribution of molecules by velocities tends to be isotropic. If the dimensions of the region where collisions are substantial are greater than the radius of the nucleus, then, studying the distribution of matter in the tail, we can consider the nucleus to be a spherically symmetrical point

source of the matter. A departure from spherical symmetry should be expressed in a relatively small solid angle behind the nucleus ("shadow" region) and at distances which are comparable to the mean free path of the molecules at the surface of the nucleus.

The model of the comet's head depends on the initial conditions for the motion of the molecules in free molecular flow. These conditions should be found by an investigation of the flow of the matter in the region where the collisions are substantial, not the process of evaporation of the molecules from the surface of the nucleus. The nature of the gas flow in the neighborhood of the nucleus also affects the initial conditions for motion of dust particles, since the latter are accelerated by the gas stream. Our study is an investigation of these problems.

Isentropic Flow of Matter

/102

By the term "circum-nuclear region" (CNR), we mean that part of the coma which is adjacent to the nucleus of the comet and in which molecular collisions cannot be disregarded and the flow of matter can be described in terms of hydrodynamics. The real gas flow in the CNR is the flow of the reacting and relaxing mixture of substances with supply and emission of heat. The rules for this flow are very complex; therefore, we must begin our explanation of the role of intermolecular collisions with the simplest case, that of spherically symmetrical isentropic steady flow. The regularities of this type of flow are well known [1].

The following laws should be obeyed in the gas flow in the CNR:

(1) Law of conservation of matter

$$\bar{\rho}\bar{v}\bar{r}^2 = \bar{\rho}_0 \bar{v}_0 \bar{r}_0^2 = J/4\pi, \tag{1}$$

where $\bar{\rho}$, $\bar{v}$, $\bar{r}$ are the density, velocity, and distance from the center of the nucleus, respectively; J is the total mass flux passing through the surface of the nucleuses; the subscript "0" is written for values referring to the surface of the nucleus;

(2) The Bernoulli equation

$$\frac{\bar{v}^2}{2} + \frac{\gamma}{\gamma - 1} \cdot \frac{\bar{p}}{\bar{\rho}} = \frac{\bar{v}_0^2}{2} + \frac{\gamma}{\gamma - 1} \cdot \frac{\bar{p}_0}{\bar{\rho}_0} = H_0, \tag{2}$$

where γ is the adiabatic exponent depending on the number of degrees of freedom of the molecules; $\bar{p}$ is the pressure; H_0 is the stagnation enthalpy of a unit mass of the matter;

(3) The equation for the adiabatic curve

$$\bar{p} = K\bar{\rho}^{\gamma}, \tag{3}$$

where K is connected with the entropy and specific heat capacity for constant volume c_V by the following relationship:

$$K = \exp[(s - s_0)/c_V].$$

Equations (1) - (3) give a complete discription of the gas flow under given conditions at the surface of the nucleus. It is convenient to use them in dimensionless form. In order to reduce (1) - (3) to a dimensionless form, we will introduce the initial Mach number, i.e.,

$$M_0 = \bar{v}_0 / \sqrt{\gamma \frac{\bar{p}_0}{\rho_0}}. \tag{4}$$

According to the theory of sublimation, /103

$$M_0 = \frac{\alpha}{\sqrt{\gamma}} \left(\frac{p_S}{p_0} - 1 \right), \tag{5}$$

where p_S is the saturation vapor pressure over the surface of the nucleus at the temperature of the nucleus. The dimensionless parameters of the flow will be defined by the following relationships:

$$\rho = \frac{\bar{\rho}}{\rho_0} \left(1 + \frac{\gamma - 1}{2} M_0^2 \right)^{-\frac{1}{\gamma - 1}}, \tag{6}$$

$$v = \frac{\bar{v}}{v_0} \left(\frac{\gamma - 1}{2} M_0^2 \right)^{1/2} \left(1 + \frac{\gamma - 1}{2} M_0^2 \right)^{-1/2}, \tag{7}$$

$$p = \frac{\bar{p}}{p_0} \left(1 + \frac{\gamma - 1}{2} M_0^2 \right)^{-\frac{\gamma}{\gamma - 1}}, \tag{8}$$

$$T = \frac{\bar{T}}{\bar{T}_0} \left(1 + \frac{\gamma - 1}{2} M_0^2 \right)^{-1}, \tag{9}$$

$$r = \frac{\bar{r}}{\bar{r}_0} \left(\frac{\gamma - 1}{2} M_0^2 \right)^{-1/4} \left(1 + \frac{\gamma - 1}{2} M_0^2 \right)^{\frac{\gamma + 1}{4(\gamma - 1)}}. \tag{10}$$

The initial system now acquires the following form:

$$\rho v r^2 = 1, \tag{11}$$

$$v^2 + \frac{p}{\rho} = 1, \tag{12}$$

$$p = \rho^{\gamma}, \tag{13}$$

from which

$$\rho\sqrt{1-\rho^{\gamma-1}} = \frac{1}{r^2}, \tag{14}$$

$$v(1-v^2)^{\frac{1}{\gamma-1}} = \frac{1}{r^2}, \tag{15}$$

$$p^{\frac{1}{\gamma}}\sqrt{1-p^{(\gamma-1)/\gamma}} = \frac{1}{r^2}, \tag{16}$$

$$T^{\frac{1}{\gamma-1}}\sqrt{1-T} = \frac{1}{r^2}. \tag{17}$$

It can be seen from the latter relationships that all the parameters of the flow (dimensionless) change within the limits from zero to one. There is a value in the right-hand parts of (14)-(17) which decreases during an increase in distance from the nucleus; therefore, the left-hand parts should also decrease. The decrease of the left-hand parts of (14) - (17) can occur, first of all, because of the approach of the parameters of the flow to zero and, secondly, because of their approach to one. Thus, the flow parameters ρ, v, p, T are two-valued functions of the distance. /104

The two branches of the solution to (14) - (17) correspond to two modes of flow. If the initial Mach number $M_0 < 1$, then the velocity of the flow decreases with an increase in distance from the nucleus, while the density and pressure increase. The local Mach number decreases in this case, i.e., the flow remains subsonic throughout. The nature of the change in these values is the opposite if the initial Mach number is greater than one. The velocity in such a flow increases, asymptotically approaching a constant value, while the density and pressure decrease. In this case, the local value for the Mach number increases with an increase in distance from the nucleus, i.e., the flow is supersonic throughout.

Since, under the actual situations which occur in comets, the density should decrease with distance from the nucleus, then $M_0 > 1$ and, consequently, the gas flow in the CNR is always supersonic. In a supersonic flow, the dimensionless velocity reaches a critical value of $v \simeq 1$ rather rapidly, while the density begins to diminish according to the following law:

$$\rho \propto \frac{1}{r^2}, \tag{18}$$

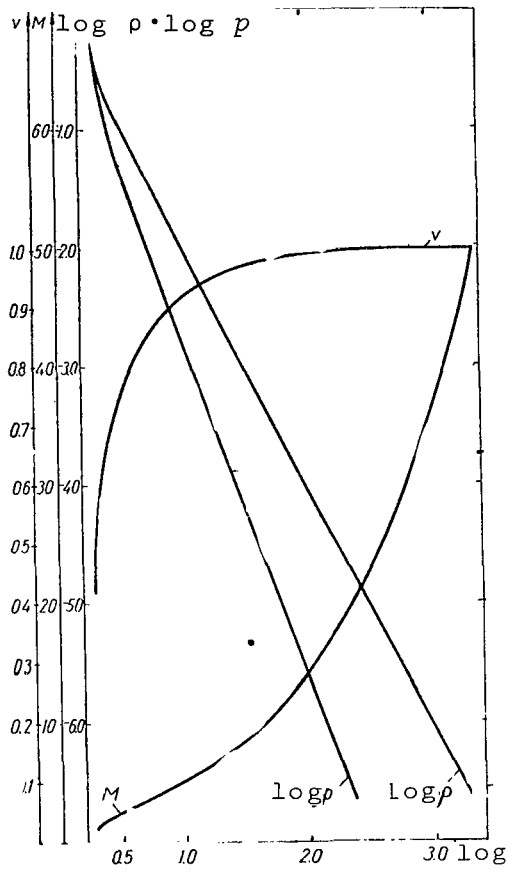

Fig. 1. Parameters of Adiabatic Supersonic Flow at $\gamma = 7/5$.

This has been affirmed repeatedly by observations [4]. This law for the decrease in density is characteristic of free molecular flow [5]. The fact that it is a also obtained from a hydrodynamical examination shows that the hydrodynamical solution also yields correct results where it is not strictly applicable, since the gas pressure at long distances from the nucleus plays almost no role in the motion of the matter. Therefore, a disregard of the anisotropy of the pressure and the higher moments of the distribution function [6] in (1) (2) does not affect the solutions.

Figure 1 shows the dependence of the density, velocity, pressure and temperature on the distance for different values of the adiabatic exponent. It can be seen that the parameters of the cross section in the CNR deviate from the parameters of free molecular flow. In the future, we will be interested in the deviation of the density decrease from the law of r^{-2} and the deviation of the velocity from a constant value. /105

Distribution of Surface Brightness

In order to investigate the distribution of surface brightness, it is necessary to know the chemical composition of the gas mixture and its variation with distance from nucleus because of ionization and issociation. Since the dimensions of the CNR are relatively small, we can assume, within the framework of the suggestions already made, that the matter is homogeneous. In this case, the volume luminosity is proportional to the density and, for the surface brightness,

$$I(R) = 2K \int_R^\infty \frac{r\rho(r)\,dr}{\sqrt{r^2 - R^2}}, \qquad (19)$$

where $I(R)$ is the surface brightness at a distance of R from the center of the nucleus, and K is the coefficient of proportionality between the density and the volume luminosity. /106

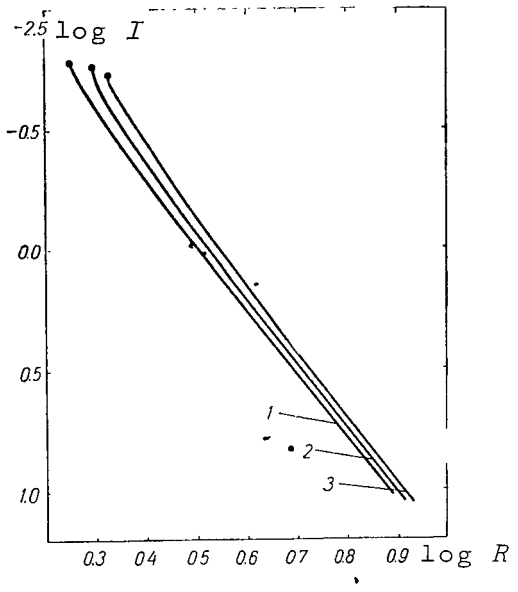

Fig. 2. Distribution of Surface Brightness in CNR. $\left(1-\gamma=\frac{5}{3};\ 2-\gamma=\frac{7}{5};\ 3-\gamma=\frac{9}{7}\right)$

We do not have an explicit dependence $\rho(r)$, but we know the explicit form of the inverse function $r(\rho)$ [14]; therefore, we will turn to integration over ρ in (19). The following expression

$$I(\rho_0)=\frac{K}{2}\int_0^{\rho_0}\frac{2-(\gamma+1)\rho^{\gamma-1}}{\sqrt{\rho}(1-\rho^{\gamma-1})\sqrt{1-R^2\rho}\sqrt{1-\rho^{\gamma-1}}}d\rho. \quad (20)$$

together with the relationship

$$R=\sqrt{\frac{1}{\rho_0\sqrt{1-\rho_0^{\gamma-1}}}} \quad (21)$$

determine the dependence $I(R)$ in parametric form.

Figure 2 shows the dependence of $-2.5 \log I$ on $\log R$ for different values of γ. Depending on the initial conditions, the change in surface brightness is depicted by the section of the corresponding curve which is to the right of the initial point. /107

It can be seen from Figure 2 that the maximum deviation of the surface brightness distribution from the law of R^{-1} should be observed only at very short distances from the nucleus. Therefore, the effects predicted by hydrodynamics can hardly be detected by photometry. However, these effects must be taken into account in attempts at establishing the initial flow data from observations of the comet's head.

Motion of Dust Particles in the Gas Flow

In calculations of the motion of dust particles in the gas flow (review in [3]), the attraction of the nucleus of the comet was taken into account, but it was considered that, first of all, the velocity of the gas flow does not depend on the distance and is equal to the radial component of the thermal velocity of the molecules at the temperature of the nucleus and, secondly, the mass of dust is small, and the dust therefore does not affect the balance of energy and momentum in the molecular flow.

Let us examine the motion of a dust particle in a gas flow in the same approximation, but without a consideration of the attraction of the nucleus. We will explain the effect of the distance dependence of ρ and v, which is characteristic of the gas flow, on the dust dynamics.

The equation of motion of the dust particle has the following form, considering the assumptions made:

$$m\frac{du}{dt}=\frac{1}{2}C_d S\rho(u-v)^2, \tag{22}$$

where m, u, S are the mass, velocity and center section of the dust particles; C_d is the drag coefficient; ρ and v are the density and velocity of the gas. Considering the dust particles to be spheres with radius of h, consisting of a substance of density δ, and selecting r as the independent variable, we will convert this equation into the following form:

$$\frac{du}{dr}=\frac{1}{2}\beta r_0 v_0\frac{(v-u)^2}{uvr^2}, \tag{23}$$

where the dimensionless parameter β depends on the properties of the dust particles:

$$\beta=\frac{3}{4}C_d\left(\frac{r_0}{h}\right)\left(\frac{\rho_0}{\delta}\right). \tag{24}$$

Equation (23) is invariable relative to the selection of scales for the distance and velocity; therefore, its form does not change in a transfer to the dimensionless variables used earlier. Together with the initial condition /108

$$u=0 \text{ at } r=r_0 \tag{25}$$

and (15), Equation (23) determines the law of motion of the dust particle. The dimensionless velocity at the surface of the nucleus

$$v_0=\sqrt{\frac{\frac{\gamma-1}{2}M_0^2}{1+\frac{\gamma-1}{2}M_0^2}}, \tag{26}$$

while the dimensionless radius of the nucleus

$$r_0=\left(\frac{\gamma-1}{2}M_0^2\right)^{-\frac{1}{4}}\left(1+\frac{\gamma-1}{2}M_0^2\right)^{\frac{\gamma+1}{4(\gamma-1)}}. \tag{27}$$

The equation of motion of a dust particle in a free molecular flow differs from (23) only in that, instead of the velocity $v(r)$ determined by (15), we have the constant initial velocity v_0. The effect of the velocity variability can be established qualitatively without solving the equations in (24). Actually, v goes into the right-hand part of (23) in the form of the combination

$$v + \frac{u^2}{v} - 2u. \qquad (28)$$

Since the velocity of the gas flow increases with the distance, the first term of this expression increases, while the second one decreases. At short distances from the nucleus, the second term is much less than the first; therefore, its decrease cannot compensate the increase of the first term. Considering this, we can conclude that the acceleration of the dust particle in the gas flow is greater than in the free molecular flow (for equal density of the flux of matter), and this discrepancy is all the greater when the initial Mach number is lower.

In the case of $v = v_0$, (23) is integrated elementarily:

$$r = r_0\left\{1 - \frac{2}{\beta}\left[\frac{u/v_0}{1-u/v_0} + \ln\left(1 - \frac{u}{v_0}\right)\right]\right\}^{-1}, \qquad (29)$$

while, with variable v, it is determined numerically by the Runge-Kutta method. The results of the numerical integration are shown in Figure 3. This figure also gives the curves for acceleration in a free molecular flow, calculated according to (29). /109

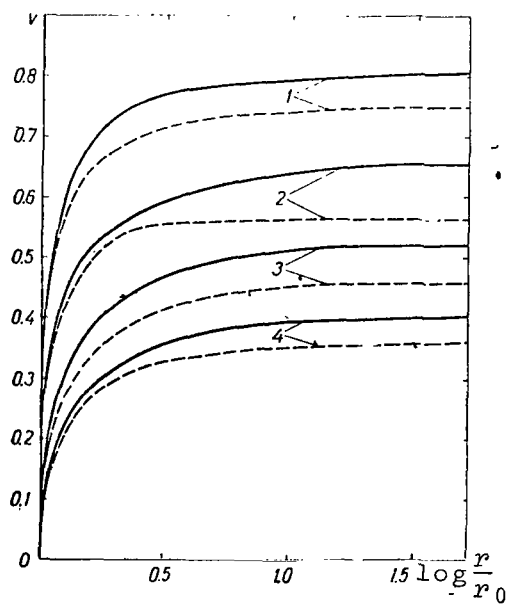

It can be seen from Figure 3 that, even at a distance equal to ten times the radius of the nucleus, the velocity of the dust particle almost reaches its critical value, which depends on M_0 and β. Thus, the process of dust-particle acceleration occurs completely in the CNR, where the variability of gas velocity must be taken into account. Because of the automatic acceleration of the supersonic

Fig. 3. Acceleration of Dust in Supersonic Flow. (1) $M_0 = 5$; $\beta = 10$; (2) $M_0 = 2$, $\beta = 10$; (3) $M_0 = 5$, $\beta = 1$; (4) $M_0 = 2$, $\beta = 1$. Acceleration of Dust in Free Molecular Flow (Dashed Lines).

flow, the dust particles gain a velocity which is somewhat higher than in a free molecular flow, and the velocity of the dust particle which has a rather small radius can exceed the initial flow velocity.

Effect of Nonadiabaticity

/110

It was assumed earlier that the gas flow in the CNR was adiabatic. Actually, the photon and corpuscular radiation of the Sun heats the substance in the CNR. Obviously, the heating is stronger when the heliocentric distance is shorter. The specific heating mechanism is connected with the physical and chemical processes in the CNR. It can be calculated only if we know the chemical composition of the substance; therefore, we will limit outselves to the most general regularities in a nonadiabatic flow and we will analyze them qualitatively.

In a nonadiabatic flow, the law of conservation of matter is written out as before, in the form of (1). However, the remaining laws of conservation are not reduced to (2) and (3). The law of conservation of momentum has the form of

$$dp+\rho v dv=0, \tag{30}$$

while the law of conservation of energy will be written out in the form

$$dQ=c_v dT+pd\left(\frac{1}{\rho}\right), \tag{31}$$

where dQ is the heat supplied to a unit mass; c_V is the heat capacity for constant volume.

After some conversions, (1), (30) and (31) can be written as such:

$$\frac{dv}{v}=\frac{1}{1-M^2}\left(\frac{dQ}{H}-\frac{2dr}{r}\right), \tag{32}$$

$$\frac{dp}{p}=\frac{\gamma M^2}{M^2-1}\left(\frac{dQ}{H}-\frac{2dr}{r}\right), \tag{33}$$

$$\frac{d\rho}{\rho}=\frac{1}{M^2-1}\left(\frac{dQ}{H}-\frac{2dr}{r}\right)-\frac{2dr}{r}, \tag{34}$$

$$\frac{dT}{T}=\frac{1-\gamma M^2}{1-M^2}\left(\frac{dQ}{H}-\frac{2dr}{r}\right)+\frac{2dr}{r}, \tag{35}$$

$$\frac{dM^2}{M^2}=\frac{1+\gamma M^2}{1-M^2}\left(\frac{dQ}{H}-\frac{2dr}{r}\right)-\frac{2dr}{r}, \tag{36}$$

where the entropy of a unit mass H is connected with the heat capacity c_p at constant pressure and temperature by the following relationship:

$$H=c_pT. \tag{37}$$

If heat is supplied to the gas in the CNR, then $dQ > 0$. It /111
can be seen from (32) - (36) that the heat supply acts in a way similar to a compression of the flow, i.e., as a decrease of r. In this case, for a change in velocity and pressure, the heat supply is completely equivalent to a decrease in r. There is no complete equivalent with respect to the remaining variables, since dr/r is found in (34) - (36) not solely in the combination

$$\frac{dQ}{H} \cdot \frac{2dr}{r}.$$

Let us insert the value

$$w=\frac{r}{2H}\cdot\frac{dQ}{dr}-1. \tag{38}$$

In heat supply $w > -1$, in heat transfer $w < -1$, and the case of $w = -1$ corresponds to adiabatic flow. After substituting (38) into (32) - (36), we obtain the following:

$$\frac{d\ln v}{d\ln r}=\frac{2w}{1-M^2}, \tag{39}$$

$$\frac{d\ln p}{d\ln r}=\frac{2\gamma M^2 w}{M^2-1}, \tag{40}$$

$$\frac{d\ln \rho}{d\ln r}=2\left(\frac{w}{M^2-1}-1\right), \tag{41}$$

$$\frac{d\ln T}{d\ln r}=2\left(\frac{1-\gamma M^2}{1-M^2}w+1\right), \tag{42}$$

$$\frac{d\ln M^2}{d\ln r}=2\left(\frac{1+\gamma M^2}{1-M^2}w-1\right). \tag{43}$$

In an adiabatic flow, there can be two regimes which differ by the signs of the derivatives of (39) - (43); subsonic and supersonic. A nonadiabatic flow can occur in one of eleven different regimes, of

which five are supersonic and six are subsonic.

The conditions for realization of supersonic regimes are the following:

$$1.\ w < \frac{1-M^2}{\gamma M^2-1} < \frac{1-M^2}{\gamma M^2+1} < 0 < M^2-1.$$

In this regime, the density, pressure and temperature decrease, while the velocity an Mach number increase. /112

$$2.\ \frac{1}{\gamma M}\ \ 1\ \ w\ \ \frac{1-M^2}{\gamma M^2+1} < 0 < M^2-1.$$

In this regime, the pressure and density decrease, while the velocity, Mach number and temperature increase.

$$3.\ \frac{1-M^2}{\gamma M^2-1} < \frac{1-M^2}{\gamma M^2+1} < w < 0 < M^2-1.$$

The density and Mach number decrease, and the velocity, pressure and temperature increase.

$$4.\ \frac{1-M^2}{\gamma M^2-1} < \frac{1-M^2}{\gamma M^2+1} < 0 < w < M^2-1.$$

The density, Mach number and velocity decrease, and the pressure and temperature increase.

$$5.\ \frac{1-M^2}{\gamma M^2-1} < \frac{1-M^2}{\gamma M^2+1} < 0 < M^2-1 < w.$$

The velocity and Mach number decrease, and the density, pressure and temperature increase.

The conditions for realization of subsonic regimes are the following:

$$6.\ w > \frac{1-M^2}{\gamma M^2-1} > \frac{1-M^2}{\gamma M^2+1} > 0 > M^2-1.$$

The density, pressure and temperature decrease, while the velocity and Mach number increase.

$$7.\ \frac{1}{\sqrt{\gamma}} < M < 1;\ \ \frac{1-M^2}{\gamma M^2-1} > w > \frac{1-M^2}{\gamma M^2+1} > 0 > M^2-1$$

or

$$0 < M < \frac{1}{\sqrt{\gamma}};\ w > \frac{1-M^2}{\gamma M^2+1} > 0 > M^2-1 > \frac{1-M^2}{\gamma M^2-1}.$$

The density and pressure increase, while the velocity, Mach number and temperature increase.

$$8.\ \frac{1}{\sqrt{\gamma}} < M < 1;\ \frac{1-M^2}{\gamma M^2-1} > \frac{1-M^2}{\gamma M^2+1} > w > 0 > M^2-1$$

or /113

$$0 < M < \frac{1}{\sqrt{\gamma}};\ \frac{1-M^2}{\gamma M^2+1} > w > 0 > M^2-1 > \frac{1-M^2}{\gamma M^2-1}.$$

The density and Mach number decrease, while the velocity, pressure and temperature increase.

$$9.\ \frac{1}{\sqrt{\gamma}} < M < 1;\ \frac{1-M^2}{\gamma M^2-1} > \frac{1-M^2}{\gamma M^2+1} > 0 > w > M^2-1$$

or

$$0 < M < \frac{1}{\sqrt{\gamma}};\ \frac{1-M^2}{\gamma M^2+1} > 0 > w > M^2-1 > \frac{1-M^2}{\gamma M^2-1}.$$

The density, velocity and Mach number decrease, and the pressure and temperature increase.

$$10.\ \frac{1}{\sqrt{\gamma}} < M < 1;\ \frac{1-M^2}{\gamma M^2-1} > \frac{1-M^2}{\gamma M^2+1} > 0 > M^2-1 > w$$

or

$$0 < M < \frac{1}{\sqrt{\gamma}};\ \frac{1-M^2}{\gamma M^2+1} > 0 > M^2-1 > w > \frac{1-M^2}{\gamma M^2-1}.$$

The velocity and Mach number decrease, while the density, pressure and temperature increase.

$$11.\ 0 < M < \frac{1}{\sqrt{\gamma}};\ \frac{1-M^2}{\gamma M^2+1} > 0 > M^2-1 > \frac{1-M^2}{\gamma M^2-1} > w.$$

In this regime, the velocity, temperature and Mach number decrease while the density and pressure increase.

Regimes 1 and 10 can occur when heat is either supplied or transferred, regime 11 can occur only when heat is transferred, and the remaining regimes occur only when heat is supplied.

The flow regime can change with the distance from the nucleus, since the Mach number and the values of w are variables which depend on r. The regions where different regimes exist are adjacent to one another; however, some transitions between neighboring regimes are impossible (for example, there cannot be transition from the first regime to the tenth, and the inverse).

A subsonic flow can transfer from regime to regime only with a change in the number of the regime by one. If the local Mach /114
number in an adiabatic subsonic flow (regime 10 at $w = -1$) can only decrease, then there are two regimes with heat supply (regimes 6 and 7) in which the Mach number increases in this case. Similarly, in supersonic regimes, a transition from one to another is possible only when the regime number changes by one and there are two regimes (regimes 4 and 5) in which the Mach number decreases.

Another contrast to adiabatic flows is the possibility of a continuous transition of a subsonic flow (regimes 6 and 7) into a supersonic one (regime 1 or 2), or a transition of a supersonic flow (regimes 3, 4 and 5) into a subsonic one (regimes 8, 9 and 10). In this case, the condition $w = 0$ must necessarily be obeyed at the sonic point $M = 1$. Moreover, there can be discontinuous transitions of a supersonic flow into a subsonic flow (for example, from regime 5 to regime 6) through the front of the shock waves which is stationary with respect to the nucleus.

In correspondence with the boundary conditions, the density, pressure and temperature should tend toward zero in an infinite increase in distance from the nucleus. This means that regime 1 should be realized in the outer part of the CNR.

If the flow occurs in this regime from the surface of the nucleus itself, then the picture observed is similar to that which was examined in the adiabatic approximation. However, for a sufficiently intensive heat supply, $w > 0$ and the flow cannot begin in regime 1. We will not examine all the possible variations of an alternation in regimes by which the flow can convert into regime 1, but we will mention one variation which is, in our opinion, most interesting.

Let the flow begin in regime 4 by strength of the conditions on the surface of the nucleus. Since the Mach number in this regime decreases along the flow, regime 4 tends to convert into regime 5 (if w does not decrease substantially), in which the Mach number decreases as before, but the density of the substance increases with an increase in distance from the nucleus. After this, a discontinued

transition through the front of the shock wave to regime 6 remains the sole possibility for adjunction with the zero boundary conditions to infinity. After the discontinuity, the Mach number increases continuously and the flow converts into the supersonic regime 1 through the point $w = 0$. If the variation in flow parameters with distance from the nucleus is represented schematically (Fig. 4), we find that the nucleus of the comet is surrounded by a ring of compressed gas, which is observed as a halo.

This qualitative analysis is not a proof that such a regime of gas flow is realized in the CNR. For a specific calculation, it is necessary to know the gas-heating mechanism. In particular, it would be expedient to find how the dissociation of the parent molecules by the effect of external radiation, which is connected with the conversion of some amount of absorbed energy into heat, affects the gas flow. /115

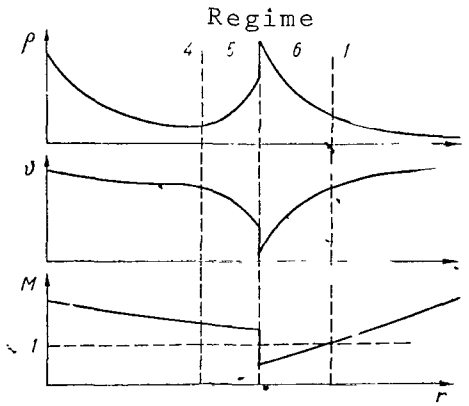

Fig. 4. Schematic Representation of the Variation in Density, Velocity and Mach Number in a Heated Flow.

Another interesting problem which must be solved in order to develop the CNR theory is that of the flow in the boundary layer of the nucleus which is directly adjacent to the sublimable surface. Having examined the adiabatic flow, we must decide on the initial value for the Mach number, in terms of which all the dimensionless initial values are expressed. In order to calculate a specific variation, we must know the values of the dimensional initial parameters: density, velocity and pressure at the surface of the nucleus and radius of the nucleus. At the same time, it follows from physical concepts that the flow should be determined completely for a given nucleus by one parameter, or the illuminance of the nucleus. It is not sufficient to have the one sublimation equation (5), which expresses the law of conservation of the particles, to solve the problem we have formulated. The flow in the boundary layer and the flow with dissociative heating will be examined in other studies.

References

1. Bay Shi-i: Vvedeniye v teoriyu techeniya szhimayemoy zhidkosti (Introduction to the Theory of the Flow of a Compressible Fluid). Moscow, Foreign Literature Publishing House, 1962.
2. Dobrovol'skiy, .V.: Nestatsionarnyye protsessy v kometakh i solnechnaya aktivnost' (Non-Stationary Processes in Comets and Solar Activity). Trudy Dushanbinskoy Astron. Observ., Vol. 8, 1961.
3. Dobrovol'skiy, O.V.: Komety (Comets). Moscow, Nauka, 1966.
4. Konopleva, V.P.: Inform. Byulletin' MGK Ukr. S.S.R., Vol. 10, p. 77, 1966.
5. Mokhnach, D.O.: Byull. Instit. Teoret. Astron., Vol. 6, p. 269, 1966.
6. Grad, H.: Commn. on Pure and Appl. Math, Vol. 2, p. 331, 1949.
7. Jackson, W.M. and B.D. Donn: Nature et Origine des cometes (The Nature and Origin of Comets). Comm. coll. intern. d'astrophysique (Liege, 1965), Belgium, 1966.
8. Wallace, L.V., F.D. Miller: Astr. J., Vol. 63, p. 213, 1958.

THE PHYSICAL CONDITIONS IN THE BOUNDARY LAYER OF A COMETARY NUCLEUS

L.M. Shul'man

ABSTRACT: A connection is found between the initial parameters of the gaseous flow in the nucleus of a comet (density, velocity, temperature and pressure) and the temperature of the cometary nucleus on the basis of the laws of conservation. It is shown that the initial Mach number depends solely on the sublimation and accomodation coefficients. The initial velocity of the flow is found to be somewhat higher than that calculated on the basis of the assumption that a free molecular flow begins at the very surface of the nucleus and that the initial temperature is equal to the surface temperature of the nucleus.

Let us establish a relation between the density, radial velocity and temperature of the gas at the surface of a nucleus, on the one hand, and the temperature of the nucleus surface, on the other hand. We will examine the stationary process of sublimation of the gases from the ice (generally contaminated) surface of the nucleus, the model of which has been discussed a great deal in the literature. Using the assumption that the sublimation process is stationary, we will assume the temperature of the nucleus to be constant in time; however, all the results of this study are also applicable, without any changes, to the case of non-stationary sublimation if the temperature of the nucleus does not change catastrophically rapidly. /117

It is usually considered [2] that the temperature of the nucleus T_n is equal to the temperature of the gas at the surface of the nucleus T_0, and the radial velocity of the flow v_0 at the surface of the nucleus is a hemispherical average velocity of Maxwellian distribution, i.e.,

$$v_0 = \sqrt{\frac{kT_n}{2\pi m}}, \tag{1}$$

where m is the mass of a molecule. The density of the gas at the nucleus can then be obtained from the equation of sublimation:

$$\rho_0 v_0 = \alpha \frac{m p_s}{\sqrt{2\pi m k T_n}} \tag{2}$$

The saturation vapor pressure at the temperature of the nucleus p_s, which is introduced in (2), is connected with the temperature of the nucleus by the following relationship:

$$p_s = AT_n^{\frac{c_p - c}{k}} e^{-\frac{L}{kT_n}}, \qquad (3)$$

where A is a constant, c_p and c are the heat capacity of the vapor (at constant pressure) and solid phase, respectively, and L is the latent heat of transition at absolute zero temperature.

The relationships in (1)-(3) exhaust the problem of the initial conditions for outflow of the gases from the surface of the nucleus only if the mean free path of the molecule at the surface of the nucleus is much greater than the dimensions of the nucleus itself, i.e., the free scattering of molecules begins directly at the surface of the nucleus. This circumstance is not necessarily realized in the circum-nucleus regions of bright comets [3,5], where collisions between molecules are substantial. In order to find the initial parameters of the flow in this case, we would have to solve a kinetic equation with a boundary condtion which describes the distribution of evaporated molecules and molecules reflected from the surface of the nucleus. Instead, let us examine a simplified model of a boundary layer which is thin in comparison to the radius of the nucleus and whose thickness is comparable in order of magnitude to the mean free path of the molecule in the same region. /118

We will consider that a local-Maxwellian distribution of molecules by velocities has been established on the outer limit of the boundary layer, i.e.

$$f_0 = n_0 \left(\frac{m}{2\pi k T_0}\right)^{3/2} e^{-\frac{m\left[(v_r - v_{r0})^2 + v_\varphi^2 + v_\theta^2\right]}{2kT_0}} \varphi\left(\frac{U}{kT}\right), \qquad (4)$$

where v_0, T_0, and n_0 are the initial flow parameters and $\phi(U/kT)$ is the distribution function of molecules by energies U of the intrinsic (rotational and vibrational) degrees of freedom.

The Maxwellian distribution is absent at the inner limits of the boundary layer (surface of the nucleus), but we will approximate ti by the sum of hemispherical Maxwellian distribution for the molecules which are incident on the surface of the nucleus, reflected and evaporated.

In statistical equilibrium, the evaporated molecules are distributed by velocities as if there were a gas with the parameters of saturated vapor at the given temperature below the subliming surface, and there were thermal effusion of the gas through a number of apertures, the total area of which is some percentage of the

total area of the nucleus. The non-equilibrium case under investigation differs only in that there is no compensation for the flow of evaporated molecules by a reflux of condensed molecules; however, it follows from the principle of detailed balance that the coefficient of condensation is equal to the coefficient of sublimation.

Thus, there is the following distribution of molecules in the apertures in the model under investigation /119

$$F_1 = \alpha n_{\text{s}} \left(\frac{m}{2\pi k T_n}\right)^{3/2} e^{-\frac{m\left(v_r^2+v_\varphi^2+v_\theta^2\right)}{2kT_n}} \varphi\left(\frac{U}{kT_n}\right)\sigma(v_r) + \\ + \alpha n_0 \left(\frac{m}{2\pi k T_0}\right)^{3/2} e^{-\frac{m\left(v_r^2+v_\varphi^2+v_\theta^2\right)}{2kT_0}} \varphi\left(\frac{U}{kT_0}\right)[1-\sigma(v_r)], \tag{5}$$

where (x) is a Heaviside step function, i.e.,

$$\sigma(x) = \begin{cases} 1 & \text{at } x \geq 0, \\ 0 & \text{at } x < 0. \end{cases} \tag{6}$$

The molecules are reflected from the remaining part of the surface, which is (1-α) of the total surface of the nucleus. We will represent the distribution function of the reflected molecules in the following form:

$$F_2 = (1-\alpha) n_{\text{ref}} \left(\frac{m}{2\pi k T_{\text{ref}}}\right)^{3/2} e^{-\frac{m\left(v_r^2+v_\varphi^2+v_\theta^2\right)}{2kT_{\text{ref}}}} \varphi\left(\frac{U}{kT_{\text{ref}}}\right)\sigma(v_r) + \\ + (1-\alpha) n_0 \left(\frac{m}{2\pi k T_0}\right)^{3/2} e^{-\frac{m\left(v_r^2+v_\varphi^2+v_\theta^2\right)}{2kT_0}} \varphi\left(\frac{U}{kT_0}\right)[1-\sigma(v_r)]. \tag{7}$$

The surface of the nucleus in the model used was replaced by the equivalent perforated diaphragm with saturated vapor on one side and, on the other side, a non-equilibrium gas consisting of molecules escaping beyond the diaphragm, reflected from it and incident on its surface and in the apertures (condensation model).

Within the framework of the model of the nucleus-conglomerate, this representation can be taken literally, considering the process of the release of gases from the nucleus by their infiltration through the pores between solid particles. However, the same distribution functions can also be used for the pure ice model, which gives the coefficient α the ordinary probability significance.

Our problem is to express T_0, ρ_0, p_0 and v_0 in terms of T_n and α.

Laws of Conservation in the Boundary Layer

/120

We are not interested in the change in flow parameters inside the boundary layer. We will find the values for the flow parameters at the outer limit of the boundary layer. In order to solve this problem, we will use the laws of conservation of matter, energy and momentum during a transition through the layer (as is done in the elementary flow of gas-dynamic discontinuities).

The following values should be identical both at the inner and outer limits of the boundary layer:

(1) Flux of matter

$$m\int \boldsymbol{v} f_0(\boldsymbol{v})\,d\boldsymbol{v}\,dU = m\int \boldsymbol{v} f_i(\boldsymbol{v})\,d\boldsymbol{v}\,dU; \tag{8}$$

(2) Flux of momentum

$$m\int v^2 f_0(\boldsymbol{v})\,d\boldsymbol{v}\,dU = m\int v^2 f_i(\boldsymbol{v})\,d\boldsymbol{v}\,dU; \tag{9}$$

(3) Flux of energy

$$\int \boldsymbol{v}\left(\frac{mv^2}{2}+U\right) f_0(\boldsymbol{v})\,d\boldsymbol{v} = \int \boldsymbol{v}\left(\frac{mv^2}{2}+U\right) f_i(\boldsymbol{v})\,d\boldsymbol{v}. \tag{10}$$

Substituting the values of f_0 from (4) and $f_i = F_1 + F_2$ from (5) and (6) into these relationships, and carrying out integration by velocities and intrinsic energies, we will find the laws of conservation of matter, momentum and energy in the following form:

$$\rho_0 v_0 = \alpha\left[p_s\left(\frac{m}{2\pi k T_n}\right)^{1/2} - p_0\left(\frac{m}{2\pi k T_0}\right)^{1/2}\right] + (1-\alpha)\left[p_{\text{ref}}\left(\frac{m}{2\pi k T_{\text{ref}}}\right)^{1/2} - p_0\left(\frac{m}{2\pi k T_0}\right)^{1/2}\right]; \tag{11}$$

$$p_0 + \rho_0 v_0^2 = \frac{\alpha}{2}(p_n + p_0) + \frac{1-\alpha}{2}(p_{\text{ref}} + p_0), \tag{12}$$

$$\rho_0 v_0\left(\frac{v_0^2}{2} + c_p T_0\right) = \frac{\alpha}{\pi}\left(1+\frac{i}{4}\right)\left[p_s\left(\frac{2\pi k T_n}{m}\right)^{1/2} - p_0\left(\frac{2\pi k T_0}{m}\right)^{1/2}\right] + \frac{1-\alpha}{\pi}\left(1+\frac{i}{4}\right)\left[p_{\text{ref}}\left(\frac{2\pi k T_{\text{ref}}}{m}\right)^{1/2} - p_0\left(\frac{2\pi k T_0}{m}\right)^{1/2}\right]. \tag{13}$$

In these relationships, $p = nkT$, while i in (13) is the sum of the number of rotational and twice the number of vibrational degrees of freedom of the molecule. The heat capacity of the gas at constant pressure can also be expressed in terms of i: /121

$$c_p = \frac{k}{m} \cdot \frac{5+i}{2}. \tag{14}$$

The equation of energy in (13) was obtained on the assumption that the intrinsic state of the molecule does not change either in evaporation or in reflection from the surface.

As is well known [1], the translational part of the energy of molecules changes to the greatest extent in reflection; the change in rotational energy requires multiple successive reflections from the wall. As for the vibrational degrees of freedom, they can be considered as either completely unexcited ($i = i_{rot}$) or semi-excited ($i = i_{rot} + i_{vib}$) at the temperature of interest to us.

The unknown values p_{ref}, T_{ref}, p_0, ρ_0, T_0 and v_0 are introduced in (11)-(13); their number exceeds the number of equations. For additional relationships we will select the Clapeyron equation

$$p_0 = \frac{k}{m} \rho_0 T_0, \tag{15}$$

and the condition that the substance coming from reflected molecules does not contribute to the flow, i.e.,

$$\frac{p_{ref}}{\sqrt{T_{ref}}} = \frac{p_0}{\sqrt{T_0}}, \tag{16}$$

Moreover, we will use the relationship between T_{ref}, T_0 and T_n:

$$\frac{T_{ref}}{T_0} = 1 - a + a\frac{T_n}{T_0}, \tag{17}$$

where a is the accomodation coefficient [4]. We now have a closed system of equations to determine all the values.

Solution and Analysis /122

Let us reduce the principal system of equations to a dimensionless form. For this, we will exclude the values of p_{ref} and T_{ref} from the laws of conservation with the aid of (2), (16) and (17), and we will introduce the dimensionless parameters x and y and the Mach number, i.e.,

$$M_0 = v_0/\sqrt{\gamma p_0/\rho_0}, \tag{18}$$

where the adiabatic exponent

$$\gamma = \frac{5+i}{3+i}. \tag{19}$$

The dimensional values are expressed in terms of the dimensionless values, the Mach number and the temperature of the nucleus in the following way:

$$T_0 = y^2 T_n, \tag{20}$$

$$p_0 = x p_s(T_n), \tag{21}$$

$$\rho_0 = \frac{m p_s(T_n)}{k T_n} \cdot \frac{x}{y^2}, \tag{22}$$

$$v_0 = M_0 y \sqrt{\gamma \frac{k T_n}{m}}. \tag{23}$$

After substituting these expressions into the equations of conservation, we have a system which can be used to determine the dimensionless values, i.e.,

$$M_0 = \frac{\alpha}{\sqrt{2\pi\gamma}}\left(\frac{y}{x} - 1\right), \tag{24}$$

$$1 + \gamma M_0^2 = \frac{\alpha}{2}\left(\frac{1}{x} + 1\right) + \frac{1-\alpha}{2}\left(1 + \sqrt{1 - a + \frac{a}{y^2}}\right), \tag{25}$$

$$1 + \frac{\gamma - 1}{2} M_0^2 = \frac{\gamma + 1}{2\gamma} \cdot \frac{x}{y - x}\left\{\alpha\left(\frac{1}{xy} - 1\right) + (1-\alpha)\left[\left(1 - a - \frac{a}{y^2}\right)^{3/2} - 1\right]\right\} \tag{26}$$

It follows from (24)-(26) that the dimensionless parameters depend only on the sublimation and accomodation coefficients. Excluding the Mach number from the system, we can obtain the relationship between the parmeters x and y: /123

$$x = \frac{\alpha y^2}{\alpha y + \frac{\pi}{2} \pm \sqrt{\alpha\pi y + \frac{\pi^2}{4} - \pi y^2\left[1 - (1-\alpha)\sqrt{1 - a + \frac{a}{y^2}}\right]}}, \tag{27}$$

The equation of energy acquires the following form:

$$\frac{2\gamma}{\gamma+1}\left(\frac{y}{x}-1\right)\left[1+\frac{\gamma-1}{4\pi\gamma}\alpha^2\left(\frac{y}{x}-1\right)^2\right]= \\ =\alpha\left(\frac{1}{xy}-1\right)+(1-\alpha)\left[\left(1-a+\frac{a}{y^2}\right)^{3/2}-1\right]. \tag{28}$$

An investigation of these equations shows that two sublimation regimes are possible: subsonic and supersonic.

The subsonic regime corresponds to the minus sign in (27) ($y > 1$), and the plus sign corresponds to the supersonic (in supersonic sublimation $y < 1$).

Using a numerical solution to the systems of (27)-(28), we obtained the functions $x(\alpha)$ and $y(\alpha)$ by the iteration method for an accomodation coefficient of $a = 0.8$, and we then calculated the function $M_0(\alpha)$ according to (24). The value

$$\alpha' = \alpha\left(1-\frac{x}{y}\right), \tag{29}$$

should replace the real value of the sublimation coefficient if the density of the flux of subliming molecules is calculated according to the ordinary formula below:

$$nv_0 = \alpha' \frac{p_s(T_n)}{\sqrt{2\pi m kT_n}}. \tag{30}$$

The results of the calculations are shown in Figures 1 and 2. In the subsonic regime, the effective sublimation coefficient α' does not exceed 0.115, while the Mach number is always less than 0.054.

The supersonic regime should be considered as physically realistic [4]. In this regime, the effective sublimation coefficient is less than 0.8, while the Mach number is greater than 1.25. The temperature of the gas at the boundary is always less than the temperature of the nucleus, while the velocity which is determined according to (23) is a factor of $M_0 y\sqrt{2\pi/\gamma}$ greater than that obtained according to (1). Since $M_0 y \sim 1.15$, this ratio is found to be about 2.5, which shows how necessary it is to consider the gas-dynamic effect in calculating the initial parameters for the outflow of gases from the nuclei of comets.

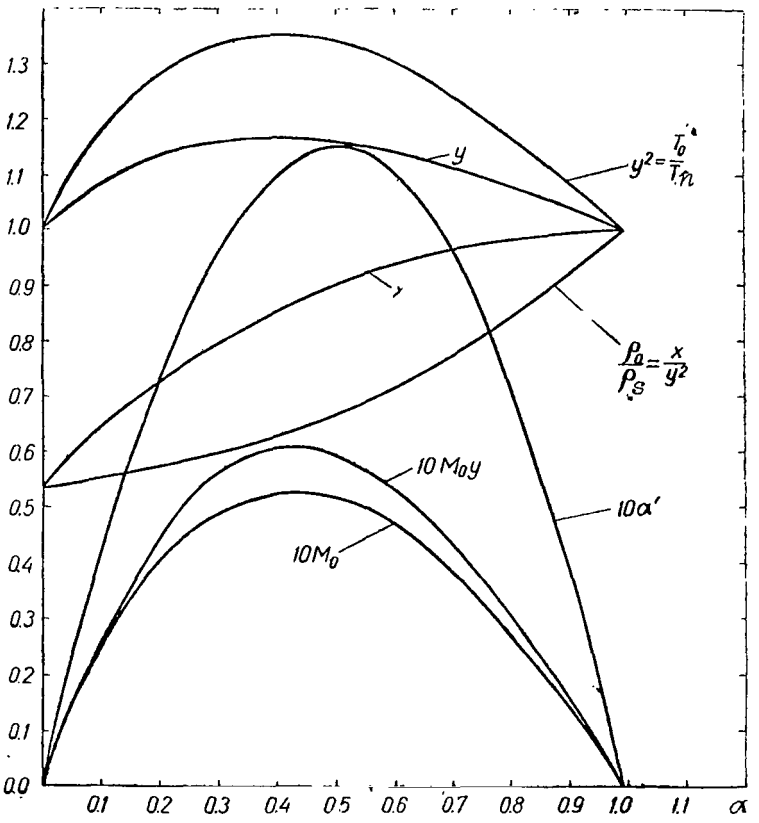

/124

Fig. 1. Initial Parameters of Subsonic Flow.

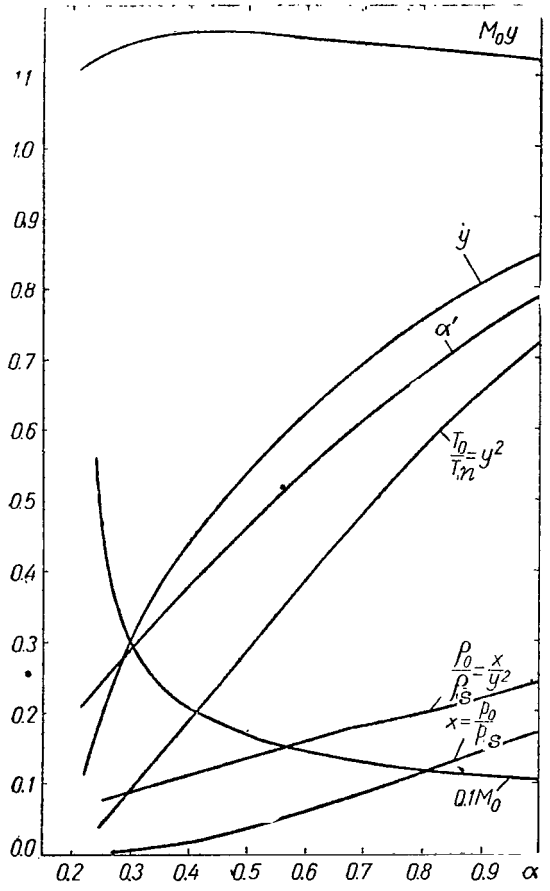

Fig. 2. Initial Parameters of Supersonic Flow.

References

1. Deviyen, M.: Techeniya i teploobmen razrezhennykh gazov (Flow and Heat Exchange of Rarefied Gases). Moscow, Foreign Literature Publishing House, p. 90, 1962.
2. Dobrovol'skiy, O.V.: Komety (Comets). Moscow, "Nauka", 1966.
3. Dobrovol'skiy, O.V.: Nestatsionarnyye protsessy v kometakh i solnechnaya aktivnost' (Non-stationary Processes in Comets and Solar Activity). Trudy dushanbinskoy Astron, Observ., Vol. 8, 1961.
4. Shul'man, L.M.: This Collection.
5. Jackson, W.M. and B. Donn: Nature et origine des cometes (Nature and Origin of Comets). Comm. Coll. Intern. d'Astrophysique. Liege, 1965; Belgium, p. 133, 1966.

SOME PROBLEMS IN PHOTOELECTRIC OBSERVATIONS OF COMETS

V. Vanýsek

ABSTRACT: Methods of photoelectric observations of comets using narrow and wide band filters are discussed. Some possible combinations of filters yield a parameter q as equal to the intensity ratio between the continuous spectrum and the emission bands of CN, C_2 and C_3 molecules and the sodium lines, D_1 and D_2. The new physical classification of comets depends on this parameter. Some information is given on photoelectric observations of comets being carried out in Czechoslovakia (Ondrejov, Skalnate Pleso, Brno, Klet).

The systematic photoelectric investigations of comets were first begun in the Netherlands, and then American astronomers began to carry out observations of some comets. /127

In Czechoslovakia, the photoelectric observations of comets were organized by the author in 1957 (Table 1).

Bright comets, Arend-Roland (1957III) and Mrkos (1957V), were observed with the aid of electrophotometers with FEU-17 photomultipliers (Ondrejov, Brno) in two light systems which did not coincide with the photometric system BV. In 1960, a 30-centimeter reflector equipped with an electrophotometer with an EMI6094B photomultiplier was put into operation at the Observatory of the Astronomical Institute of the Czechoslovakian Academy of Sciences in Ondrejov, and two years later a new photometer with photomultiplier of the IP21 type was designed for the 60-centimeter reflector of the observatory of Skalnate Pleso of the Slovakian Academy of Sciences. Later (1963), a 65-centimeter reflector was constructed at Ondrejov, with which photoelectric observations of stars and comets are carried out. In the photometer, which was made with the aid of P. Mayer, the EMI6094B photomultiplier is used as the radiation receiver. Moreover, two more identical photometers have recently been made for Skalnate Pleso and Ondrejov; these photometers have devices which automatically replace filters and record the measurement results.

Selection of Photometric System

The generally-accepted photometric system, UBV, is not convinient for studying comets, since the equivalent wavelengths do not coincide with the positions of the principal emissions observed in comets (CN and C_2). In order to isolate the CN emission, the Schott filters WG9 (2mm) + UG2 (1 mm) with relative transmission near λ3880 Å of about 34% can be used. A combination of wideband

TABLE 1 PHOTOELECTRIC OBSERVATIONS OF COMETS IN CZECHOSLOVAKIA

Comet	Observatory	Instrument	Photometric System	No. of Nights	Observers	Source
1957 III	Ondrejov	20-centimeter refractor	(*bv*)	7	Růžičkova, Valníček	[2]
	Brno	60-centimeter reflector		8	Vanýsek, Tremko	[3]
1957 V				2		[3]
1960 II	Ondrejov	30-centimeter reflector	BV	1	Vanýsek Smetanova	[4]
1961 *e*	Skalnate Pleso	60-centimeter reflector		5	Vanýsek, Tremko	[5]
1961 *f*				2		
1963 *b*	Ondrejov	65-centimeter reflector	UBV CN	6		
	Skalnate Pleso	60-centimeter reflector	BV	2		
1964 *h*	Ondrejov	65-centimeter reflector	UBV CN	4	Bouska, Mayer	[1]
1965 *f*			Infrared 8000 Å	1	Vanýsek	[6]
1966 *b*			UBV	1	Mrkos, Tremko, Vanýsek	
	Klet*	50-centimeter reflector	UBV (H)	3		
	Skalnate Pleso	60-centimeter reflector	UBV	6		
1966 *c*	Klet	50-centimeter reflector	BV	2		

* Station of the National Observatory in the Czech Budejovitse and Karlov University.

and narrowband filters allows us to determine the ratio between the intensive emission and the continum in the spectrum of the comet. This intensity ratio does not depend on the diameter of the telescope. For a comet of 10^m, the photoelectric method give much higher data on the relative intensities of the emission bands and the continuous spectrum than do spectral observations. It seems at first glance that filters which divide the emission band and a segment of the continuous spectrum of the same width must be required for this purpose. However, the intensity of the continuum outside and inside the emission band may not be identical. Therefore, it is better to measure the emission band in combination with a wide range of the continuum, and then to find the unknown ratio. /129

In the case of CN emission, we can use the standard combination of the filters for the system U and the filter C, which isolates the $\lambda 3880$Å band, as the wideband region. The measured intensity corresponding to the U region is

$$I_U = \int_{\Delta\lambda} F(\lambda_1) S(\lambda_1) d\lambda, \tag{1}$$

and that corresponding to the C filter is

$$I_C = \int_{\Delta\lambda} F(\lambda_2) S(\lambda_2) d\lambda, \tag{2}$$

where $S(\lambda)$ is the transmission coefficient of the filters, and $F(\lambda)$ is the flux of emission from the comet.

If we designate that

$$A = \frac{I_C}{I_U},$$

while the ratio between the transmission coefficients of the filters is

$$B = \frac{S_U(3880)}{S_C(3880)},$$

then the ratio q in intensities of the continuous spectrum I_c and the emission I_e in the spectral region U

$$q = \left[\frac{I_e}{I_c}\right]_U, \tag{3}$$

can be found according to the following formula:

$$\frac{I_U}{I_C} = \frac{A + Bq}{I + q}. \qquad (4)$$

The accuracy in the determination of the value q depends on the values of the parameters A and B. Better results can be obtained if $A < 1$ while $B > 1$. For the photometer which operates at Ondrejov, $A = 0.67 \pm 0.02$ and $B = 2.00 \pm 0.03$. /130

TABLE 2. COMBINATION OF NARROW-BAND FILTERS WITH THE PHOTOELECTRIC SYSTEM FOR PHOTOELECTRIC OBSERVATIONS OF COMETS

Spectral Region	Interference Filters	Width of Transmission Band, Å	Filter Transmission	Relative Sensitivity	Isolated Band
U	388	60	37	0.47	CN
	407	60	37	0.12	C_3
B	388	60	37	0.37	CN
	407	45	39	1.00	C_3
	474	38	39	0.80	C_2
	492	36	40	0.50	Continuous spectrum
V	474	38	39	0.10	
	492	66	40	0.24	Continuous spectrum
	517	45	40	0.77	
	530	47	39	0.82	Continuous spectrum
	589	45	44	0.38	(D_1D_2)

Table 2 contains the possible combinations of wide and narrow band filters which aid in determining the value of q for other emissions in comets. The sensitivity of the cited combinations is calculated with respect to the C_3 band (λ 407 mμ). The data for the interference filters correspond to the photometers at Ondrejov and Skalnate Pleso.

A Classification of Comets According to the Data of Photoelectric Measurements

All the attempts at constructing a classification of comets which might have physical significance have been unsuccessful. At the same time, such a classificiation is necessary.

The possibility of approaching the solution to this problem in a new way was admitted when photoelectric investigations began to be developed. The value of q for CN or C_2 molecules can be taken as the criterion for the classification of comets. In this case, it is convenient to divide the comets into the following groups:

(1) comets with a pure emission spectrum ($0 < 1/q < 0.2$);

(2) comets with a weak continuous spectrum ($1/q$ = 0.2 - 0.5); /131

(3) comets with a sharply pronounced continuous spectrum ($1/q$ = 1 - 2);

(4) comets with a very intensive continuous spectrum or without emission bands ($1/q$ > 2).

It can be expected tha the value of q changes with the heliocentric distance r. At large distances from the Sun, the value of q is low and most of the comets which are far removed from the Sun should belong to group IV. However, the value of q depends not only on r, but also on the processes which occur in the comet itself. This can be seen in the example of Comet Alcock (1963b) (Table 3), for which a flare-up in brightness was observed on May 27, 1963.

TABLE 3. VALUES OF q FOR THE C REGION (RATIO $\frac{\text{CN}}{\text{CONTINUUM}}$)

Comet	q	$\kappa_U - \kappa_B$	Observers
1963 *b* Alcock	0.25	0.15	Vanýsek, Tremko (1964)
	0.33	0.20	
1964 *h* Everhardt	0.15	0.3	Bouska, Mayer
1966 *b* Kylston	—	0.05	

The Effect of the Diaphragm Diameter and the Color

A very interesting effect which the author discovered in 1961 is the systematic increase in positive color index with an increase in the diameter of the diaphragm. This dependence is substantial for comets with an emission spectrum, but is not observed for comets with an intensive continuum or with CO^+ emission alone. Thie effect can be explained by the varying life span of CN and C_2 molecules.

In first approximation,

$$I_B \sim N_{C_2} \rho^{-\varkappa_B}, \tag{5}$$

$$I_U \sim N_{CN} \rho^{-\varkappa_U}, \tag{6}$$

where ρ is the distance from the nucleus of the comet.

In this case, /132

$$\frac{d(U-B)}{d\rho} = -\frac{1}{\rho} 1.08 (\varkappa_U - \varkappa_B). \tag{7}$$

If the color $U-B = (U-B)_0$ for some ρ_0 (for example, $\rho_0 = 1$), then

$$U-B=(U-B)_0+2.5(\varkappa_U-\varkappa_B)\log\ \rho. \tag{8}$$

For comets with an intensive continuous spectrum

$$\varkappa_U-\varkappa_B\approx 0, \tag{9}$$

and if the emission is sharply pronounced, then

$$\varkappa_U-\varkappa_B\leqslant 0.3. \tag{10}$$

as can be seen from Table 3.

Consequently, electrophotometric observations allow us to obtain basic data characterizing the comet, and to make a reliable decision on which of the groups of the classification is involved. It is only necessary that the comet observations be carried out roughly in the same color system for all the observatories, and that the principal photometric standards of stellar magnitudes be used.

References

1. Bouska, J., P. Mayer: Bull. Astr. Inst. Czech., Vol. 16, p. 84, 1965.
2. Valnicek, B., Ruzichkova: Publ. Czech. A. V., Vol. 34-42, p. 53 1958.
3. Vanysek, V., J. Tremko: Publ. Czech.A.V., 34-42, p. 59, 1958.
4. Vanysek, V., M. Smetanova: Circ. IAU, p. 1727, 1960.
5. Vanysek, V., J. Tremko: Bull. AStr. Inst. Czech, Vol. 15, p. 233, 1964.
6. Vanysek, V.: Bull. Astr. Inst. Czech., Vol. 17, p. 212, 1956.
7. Mrkos, A., J.V. Tremko V. Vanysek: Bull. Astr. Inst. Czech. Vol. 19, No. 1, p. 43, 1968.

SOME PROBLEMS IN THE SPECTROSCOPY OF COMETS

V.I. Cherednichenko

ABSTRACT: Some unidentified emissions in the spectra of comets are described, and possible interpretations are given. The existence of certain parent molecules and atoms yet undiscovered in comets is proven by some data. The subject is discussed on the basis of the fact that hydrogen atoms are abundant in the cometary atmosphere. The process of the recombination of negative hydrogen ions with positive ones is assumed to be a source of the continuous spectra of comets. The theoretical and observed brightness in the continuous spectrum and the position of the maximum in the spectral distribution are in good agreement for Comet Mrkos 1957V.

The following are the most important problems in the spectroscopy of comets: interpretation of the still unidentified emissions of the spectra of comets, possible detection of emissions of atomic hydrogen in comets, and the role of negative ions of atomic hydrogen in the formation of the continuous spectrum in comets. This study contains a discussion of the cited problems. /134

Inidentified Emissions in Comets

Many unidentified emissions in comets are found in the ultraviolet and violet spectral regions. Thus, in the spectra of Comets 1941I and 1948I, there was a weak λ3377Å line observed, the λ3383Å which is almost inaccessible to measurements, pronounced λ3378Å emission and weaker λ3388Å. According to Swings and Page [16, 17], these emissions are in the system of the β-bands for the transition (0.9) $^2\Pi \rightarrow {}^2\Pi$ of the NO molecule. Emissions in the vicinity of λλ 3517, 3677, 3837 and 4095Å of these comets are also unidentified. They are apparently caused by the O_2 molecule [16]. For a reliable identification of these emissions with the O_2 molecule, there must be a careful analysis of the rotational structure of the cometary bands observed. For the homonuclear O_2 molecule, the population of the upper rotational levels is higher than for the CO^+ molecule. If this population is of the same order as for the homonuclear O_2 molecule, then the cometary bands of O_2 molecules should be wider than, for example, the λ2675Å band of O_2 molecules in ground laboratories [16].

The λ3675Å emission in Comet Bester can be ascribed either to the CO_2 molecule, the O_2 molecule or O_2^+, O_2^{++} ions [16-21]. In order to explain the presence of λ3675Å emission in the tails of comets

at large distances from the nucleus, it must be assumed that these molecules were formed from the corresponding parent molecules far from the nucleus. Consequently, with respect to the dissociation process $XO_2 \rightarrow X+O_2$, the lifetime of the parent XO_2 molecule in the field of solar radiation should be rather long (X here signifies all the remaining atoms of the parent molecule except for atoms of the O_2 molecule). The anomalously intensive λ4201Å band in cometary spectra can be attributed to the second positive system of N_2 molecules or the system of β-bands of NO molecule [20, 21, 14]. /135

Some emissions in the violet region and the near ultraviolet, namely the bands λ3803.3 (3) (transition 0 → 2), λ4058.2 (3.5) (transition 0 → 3), λ4345.5 (3) (transition 0 → 4) and λ3939.5 (8) (transition 1 → 4) can be attributed to the second positive system of N_2 molecule bands (the number in the parentheses indicates the relative intensities of the cometary bands in the ten-mark scale).

The overly large superpositions of other emissions still prevent us from attributing the lines λλ 3947, 3964, 4480, 4497, 4574 and 4589 Å to the system of β-bands of the NO molecule [14].

Neutral N_2 molecules in comets should be excited by weak ultraviolet radiation of the Sun with wavelength of λ2000Å. In this case, the N_2 molecule transfers to the metastable *A* level. Because of the low frequency of collisions, the excited nitrogen N_2 molecule (*A*) then converts into the ground state X and gives forth emissions, or the Vegard-Kaplan bands. It is interesting that a comparison of airglow, Comet Peltier and laboratory emissions of N_2 molecules showed that some emissions of comets can be attributed to the Vegard-Kaplan bands of the N_2 molecule [14].

The λλ 3377, 3518, 3676 and 3837 Å emission lines of Comet 1940c which were observed on a slit spectrograph with quartz-crystal optics of an 83-inch reflector at MacDonald Observatory are not identified reliably as bands of the molecular CO_2^+ ion for the transition $^2\Pi_u \rightarrow {}^2\Pi_v$ [21]. However, the question of where the ions in the comets come from remains unclear: as a result of direct ionization of the CO_2 molecule, or from dissociation of the complex molecule CO_2X (according to the scheme $CO_2X \rightarrow CO_2^+ + X$). According to Swings, the first process is more probable [19, 20]. In this case, together with the transition bands $^2\Pi_u \rightarrow {}^2\Pi_v$ ($^2\Pi_v$ is the normal level for the CO_2^+ ion), there should be a binary band of λ2883-2896Å corresponding to the transition $^2\Sigma_u^+ \rightarrow {}^2\Pi_v$ observed. This band has still not been identified in comets.

The identification of bands of the molecules CO, NO, N_2, H_2O and SiO_2 is very difficult because of the high excitation energies of the resonance bands of these molecules, which correspond to solar photon radiation at $\lambda \approx 2900$Å. The low intensity of solar radiation in the region of $\lambda \approx 2900$Å brings about a very low intensity in the emission bands of the cited molecules, which complicates

their identification [14, 19].

There is reason to consider that NaH and SiH molecules are present in the atmospheres of comets. The fact that the brightest band of the spectrum of these molecules blends with the λ4050 Å band of the C_3 molecule prevents their identification. /136

We should expect that sulfur compounds and potassium atoms may be identified in cometary spectra. Sulfur is a component of meteorites, or decay products of cometary nuclei. Potassium has the λ7665 and 7669 Å resonance lines. It is very abundant in outer space and has a relatively low boiling point (1035°K).

The question of the two types of CN radicals with completely different rotational-energy distribution in comets is very interesting. One distribution corresponds to a rotational temperature which changes with the distance according to the law $T \approx \frac{300}{\sqrt{r}}$ (r is the heliocentric distance of the comet in astronomical units), while the other corresponds to a constant temperature of $T \sim 50°K$. The fluorescence mechanism of excitation of cyanin molecules cannot explain this characteristic of the cometary spectrum. It is possible that the reason for the two different distributions of rotational energy is either the presence of two types of parent molecules, the composition of which includes the CN molecule in the nuclei of comets, or in the existence of two simultaneously different mechanisms for dissociation of the parent CNX molecules with the formation of rotational excited CN molecules.

Laboratory investigations of the spectra of the molecules NO, N_2O, HCN, HCOO, CH_3O, C_2H_5O, C_2H_5NCO (for the spectral range 4250Å $\leq \lambda \leq$ 4650 Å) and the molecules HCO_2, CH_3O, C_2H_5O, NCO, NCS, CH_3S, CH_3NCS, CH_3SCN (for the spectral region 3800 Å $\leq \lambda \leq$ 4300 Å) and a comparison with the spectra of comets indicate that these molecules are present in cometary nuclei and in the atmospheres of comets [20].

The Problem of Detecting Atmospheric Hydrogen In Comets

Since most of the possible parent molecules in comets (i.e., C_2H_2, C_3H_6, CH_4, NH_3 and H_2O) contain hydrogen, it should be one of the most abundant elements in the cometary atmosphere [9, 10, 15]. To explain why hydrogen is not observed in comets, (despite its great abundance), let us evaluate the brightness of a comet in the $H\alpha$ lines. /137

For example, let us take Halley's Comet, 1910 II, for which the total quantity of molecules in the head at r = 1 AU was evaluated as 10^{34} [44].

Let us assume that the number of hydrogen atoms in this comet

is roughly equal to $N_H = 10^{34}$ atoms, and let us calculate the intensity of the H_α emission (λ = 6563 Å) on the Earth at a geocentric distance of the comet of Δ = 1 AU.

If the concentration of light quanta exciting the hydrogen atoms at the $3p$ level, for heliocentric distance of the comet of r = 1 AU in a unit frequency interval, is designated as ρ_ν, the quantum energy as $h\nu$, and the Einstein conversion factor ($1s \to 3p$) as B_{13}, then the flux of cometary emission $L\beta$(λ = 1026 Å) on the Earth, which is a distance of Δ from the comet, is equal to the following:

$$I_{L_\beta} = \frac{\rho_\nu B_{13} h\nu}{4\pi\Delta^2} N_H \left[\frac{\text{erg}}{c\text{м}^2 \text{ sec} \cdot \text{sterad}}\right]. \qquad (1)$$

Considering that the factor B_{13} is connected with the oscillator strength of the transition $1s \to 3p$ by the relationship

$$B_{13} = \frac{e^2}{mch} \lambda_{13} f_{13} = 4 \cdot 10^{19} \lambda_{13} f_{13}, \qquad (2)$$

in which λ_{13} is expressed in 1000 Å, while the concentration of photons is determined according to the formula below, considering the dilution,

$$\rho_\nu = 1.3 \cdot 10^{-15} \frac{T_\odot^3}{cr^2} \exp\left(-\frac{144}{\lambda T_\odot}\right)\left[\left(\frac{144}{\lambda T_\odot}+1\right)^2+1\right], \qquad (3)$$

Expression (1) can be rewritten in the following way [11]:

$$I_{H_\alpha} = \frac{1.85 \cdot 10^{-31} f_{13} T_\odot^3 \exp\left(-\frac{144}{\lambda T_\odot}\right)\left[\left(\frac{144}{\lambda T_\odot}+1\right)^2+1\right] N_H}{r^2\Delta^2} \cdot \frac{A_{32}}{A_{31}} \cdot \frac{\lambda_{L_\beta}}{\lambda_{H_\alpha}}, \qquad (4)$$

where r is expressed in AU, while T is expressed in 1000° K. Substituting into (4) f_{13} = 0.105 [1], T = 5200° K [9], λ_{L_β} = 1026 Å, $A_{32} = 2.2 \cdot 10^7$ sec^{-1} [1], $A_{31} = 1.65 \cdot 10^8$ sec^{-1} [1], λ_{H_α} = 6563 Å, $N_H = 10^{34}$ atoms, $r = \Delta$ = 1 AU, we find that the intensity of hydrogen emission $I_{H_\alpha} = 5.66 \cdot 10^{-7}$ erg/cm^2 sec sterad = 0.16R.[1]

However, as rocket measurements have shown [12], at an altitude of $h \geq 120$ km, an emission of L_α = 1216 Å with intensity of about 2.5 kR (1 kR = 1000 R) is constantly present in the airglow, as is /138

[1] 1R (Rayleigh) = $3.56 \cdot 10^{-6}$ erg/cm^2·sterad.

the very weak H_α emission with intensity from 5 to 20 R. This emission is due to the scattering of solar light by H atoms in the geocorona [12]. In other words, the H_α emission from bright comets of Halley's type (1910 II) is 30 times weaker than the minimum H_α emission in the night sky. This circumstance greatly complicates detection of hydrogen emission from comets.

Recombination of Negative Hydrogen Ions As A Possible Source of the Continuous Spectrum of Comets

Of all the possible mechanisms for the formation of the continuous spectrum of comets, the recombination of negative hydrogen ions with positive ions merits attention. An effective process for the formation of negative ions is that of charge transfer of neutral hydrogen atoms with carbon, oxygen and nitrogen molecules, which are doubtlessly present in large quantities in the atmospheres of comets.

As the studies of Kharkov physicists have shown [5, 6, 7], the cross section of electron capture by a hydrogen atom with energy on the order of 1-10 KeV in molecular gases of O_2 and N_2 in the processes

$$H + O_2 \rightarrow H^- + O_2^+, \quad (5)$$

$$H + N_2 \rightarrow H^- + N_2^+ \quad (6)$$

is $\sigma_1 \approx 5 \cdot 10^{-17}$ cm^2 i.e., rather large.

The effective cross section of the process below can be taken as the same:

$$H + C_2 \rightarrow H^- + C_2^+. \quad (7)$$

The negative hydrogen ions can further collide with the most abundant ionized components of cometary atmospheres, for example with CO^+ ions or Na^+, and recombine according to the following scheme:

$$H^- + CO^+ \rightarrow H + CO + h\nu, \quad (8)$$

$$H^- + Na^+ \rightarrow H + Na(^2p) + 2.25 \text{ eV} \quad (9)$$

The effective cross section of the processes is very great and increases when the resonance defect (value of the quantum energy of the continuous spectrum in neutralization of negative and positive ions) decreases. /139

Laboratory measurements of the recombination cross section of CO^+ ions with H^- ions gives a value on the order of 3.10^{-13} cm^2 [8]. Let us evaluate the intensity of the continuous spectrum for Comet Mrkos. One of the most abundant ionized atmospheric components for this comet is Na^+ ions, with concentration in the region of the cometary nucleus of

$$n_{Na^+} \approx 0.1\, n_{Na} = 10^7\ см^{-3}.$$

The effective cross section of the process of recombination of Na^+ with H^- ions can be taken as equal to σ_2 $3 \cdot 10^{13}$ cm^2 [18].

A notable characteristic of the process in (9) is that the light quantum released in recombination, with energy of 2.25 eV [22, 23], corresponds to a wavelength of λ = 4850 Å. The maximum of the energy distribution observed in the continuous spectrum of comets is in the vicinity of this wavelength. In order to estimate the brightness of Comet Mrkos in the continuous spectrum in the case of the cited recombination mechanism and to compare it to observations, we must know the number of N_H^- ions in the head of the comet. According to the theory of dissociative transformation [23, 13], the value of N_H^- can be found by solving the following system of differential equations:

$$\begin{aligned} \frac{dN_H}{dt} &= -\lambda_1 N_H, \\ \frac{dN_{H^-}}{dt} &= \lambda_1 N_{H^-} - \lambda_2 N_H, \end{aligned} \qquad (10)$$

where $\lambda_1 N_H$ is the frequency of appearance of the ions, $\lambda_2 N_H^-$ is the frequency of disappearance of the ions, λ_1 and λ_2 are constants of the processes in (7) of formation of H^- ions and the processes of their disappearance with $H^- + Na^+ \rightarrow H + Na(^2p)$, which can be found from the relationships $\lambda_1 = \sigma_1 V_1 n_{C_2}$ and $\lambda_2 = \sigma_2 V_1 n_{Na^+}$.

The value for the concentration of carbon molecules in the region of the cometary nucleus is $n_{C_2} = 10^{10}$ cm^{-3} [4].

The maximum number of H^- ions at a distance of 0.6 AU from the Sun is equal to the following, in correspondence with (1):

$$N_{H^-} = N_H(0)\, \frac{\sigma_1 n_{C_2}}{\sigma_2 n_{Na^+} - \sigma_1 n_{C_2}}. \qquad (11)$$

The total number of hydrogen atoms $N_H(0)$ at the initial moment of time in the head of the comet can be taken as equal to the total number of carbon moleucles, i.e., /140

$$N_H(0) \approx \frac{1}{10} N_{C_2} = 3 \cdot 10^{33} \text{ atoms}.$$

Then, according to (5), $N_{H^-} = 5 \cdot 10^{32}$ ions of H^-. Substituting this value into the expressions for the brightness of the comet in the continuous spectrum, i.e.,

$$m = -2.5 \log \left[N_{H^-} \cdot \frac{1}{r^2 \Delta^2} n_{Na} + \frac{v \sigma_2}{8\pi\lambda} \cdot \frac{h\nu}{M} \right], \qquad (12)$$

where Δ = 1 AU is the distance of the comet from the Earth, M = 1.61×10^4 erg/sec·lu the mechanical light equivalent, $h\nu$ is the quantum energy at wavelength of $\lambda 4850\text{Å}$, we find that $m = 3.5^m$. This value is close to that observed, or $m_0 = 4.1^m$ [2].

References

1. Allen, K.W.: Astrofizicheskiye velichiny (Astrophysical Magnitudes). Moscow, Foreign Literature Publishing House, 1960.
2. Vsekhsvyatskiy, S.K.: Fizicheskiye kharakteristiki komet, nablyudavshikhsya v 1954-1960 gg (Physical Characteristics of Comets Observed in 1954-1960). Moscow, "Nauka", 1966.
3. Dobrovol'skiy, V.: Komety (Comets). Moscow, "Nauka", 1966.
4. Poloskov, S.M.: Soobshcheniya Gosudarstv. Astron. Instit. imeni Shtenrberg, Moskovsk. Universit., Vol. 60, No. 3, 1951.
5. Fogel', Ya.M. and R.V.Mitin: Zhur. Eksp. i Teoret. Fiz., Vol. 30, No. 3, p. 454, 1956.
6. Fogel', Ya.M., V.A. Ankudinov, D.V. Philipenko and N.V. Topolya: Zhur. Eksp. i Teoret. Fiz., Vol. 34, No. 3, p. 585, 1958.
7. Fogel', Ya.M., A.G. Koval' and Yu.Z. Levchenko: Zhur. Eksp. i Teoret. Fiz., Vol. 40, No. 1, p. 13, 1961.
8. Hasted, J.: Fizika atomnykh stolknoveniy (The Physics of Atomic Collisions). Moscow, "Mir", 1964.
9. Cherednichenko, V.I.: Fizika verkhney atmosfery Zemli (Physics of the Earth's Upper Atmosphere). Kiev, Kiev University Press, 1965.
10. Cherednichenko, V.I.: Astron, Zhur., Vol. 36, No. 2, p. 254, 1959.
11. Cherednichenko, V.I.: Izvest. Glavn. Astron. Observ. Akad. Nauk Ukr.S.S.R., Vol. 3, No.1, p. 112, 1960.
12. Chamberlain, J.: Fizika polyarnykh siyaniy i izlucheniya atmosfery (The Physics of Aurorae and Atmospheric Radiation). Moscow, Foreign Literature Publishing House, 1963.
13. Cherednichenko, V.I.: In the book: Astronomicheskiy sbornik (Astronomics Collection), No. 3 and 4. L'vov University Press, p. 84, 1960.
14. Dufay, M.J.: C.R., Vol. 204, No. 9, p. 744, 1937.
15. Delsemme, A.H.: Nature et Origine des Cometes (Nature and Origin of Comets). Institut d'Astrophysique, Cointe-Selessin, Belgique, 1966.
16. Swings, P.: Bull.Acad.Roy. Belg., Vol. 35, p. 432, 1949.
17. Swings, P.: J. Roy Astron. Soc., Vol. 6, p. 53, 1965.
18. Swings, P.: Thornton Page Ap. J., Vol. 108, p. 526, 1948; Vol. 111, p. 203, 1950.
19. Swings, P.: Space age Astronomy, 1962.
20. Swings, P.: In the book: The Moon, Meteorites and Comets, ed. G. Cooper and B. Middlehurst, No. 4, p. 580, 1964.
21. Swings, p.: Bull. Acad. Belg. Col.35, p. 938, 1939.
22. Swings, p.: Norvegica, Vol. 9, No. 19, p. 3, 1964.
23. Wurm, K.: Mitt. Hamburg Stern. Berg., Vol. 8, p. 81, 1943.

THE SPECTRUM OF THE TAIL OF COMET IKEYA-SEKI (1965f)

Z.V. Karyagina

ABSTRACT: The energy distribution in the spectrum of the tail of Comet Ikeya-Seki was obtained in absolute units ($erg^{+1} \cdot cm^{-1} sterad^{-1} \Delta\lambda = I$ cm) for November 1 and 2, 1965. A comparision with the energy distribution in the solar spectrum shows that the spectral characteristics of the continuum of the tail are similar to those of the Sun, while the color of the tails of Comets Arend-Roland (1965h) and Mrkos (1957d) are redder than the color of the Sun.

The spectrum of the tail of Comet Ikeya-Seki was obtained on November 1 and 2 of 1965, on the high-transmission nebular spectrograph of the P.K. Shternberg State Astronomical Institute [1, 2]. The observations were carried out before sunrise during early twilight ($h_\odot = -8°$). The tail of the comet was seen clearly over the mountains against the background of a relatively bright sky, and the head of the comet was still below the horizon. The conditions for the photometric observations were extremely disadvantageous because of the relatively high brightness of the sky background and low position of the tail over the horizon. The coordinates of the regions of the tail observed were the following: /142

Date	UT	α	δ, °	Distance from Head	z, °
1.XI	23 48	11.31	−17	13 °	80
2.XI	23 50	11.07	−16.5	16 °	78

The high luminosity (1/0.7) of the nebular spectrograph and the low dispersion (1500 Å/mm for λ5000 Å) yielded spectra of the tail with short exposures (5-20 m). The design of the spectrograph made it possible to observe the spectra of the tail and neighboring regions of the sky simultaneously, since the nebular slit with width of 32 cm cut a band of 9 × 1° in the sky. During the observations, the slit was set in horizontal position and the center of the slit was directed toward the middle of the tail.

The spectra were photographed on a film of the DK type, which was preliminarily illuminated by a short bright flash of light ($1/100^s$) in order to increase its sensitivity. For standardization in absolute units, we obtained spectra of a continuous-duty luminophore which was attached to the ends of the slit at the same time as the photographs of the tail. For the calibration photograph, we took the spectra of the same luninophore with different widths of the nebular slit, and the calibration curves were constructed for

eleven wavelengths in the interval of 4300 - 6300 Å.

In order to determine the transmission coefficient, spectra of the star β Ori were taken on the same spectrograph. The energy distribution in the spectrum of this star was investigated by A.V. Kharitonov [3] and obtained in absolute units. These spectra were also used in order to determine the spectral sensitivity of the receiving apparatus in the wavelength interval of 4800 - 4200 Å, where the spectrum of the luminophore was not convenient because of the bright reference peak (λ4762) and the substantial decrease in brightness of the luminophore in the wavelength interval of 4400 - 4200 Å. /143

The spectrograms were analyzed on the MF-2 microphotometer by the ordinary method. Two photometric sections were divided in the region of the cometary tail on the spectrogram, and then averaged graphically. The sky was scanned photometrically on both sides of the tail. The spectral intensity observed in the spectrum of the tail was

$$b_k(\lambda) = b_{ks}(\lambda) - \frac{b_s^1(\lambda) + b_s^2(\lambda)}{2}, \qquad (1)$$

where $b_{k_s}(\lambda)$ is the total brightness observed in the tail of the comet and the sky (center of the slit), $b_s^1(\lambda)$ and $b_s^2(\lambda)$ are the brightness of the sky on both sides of the tail, and the values of $b(\lambda)$ are expressed in units of the calibration curve. The spectral sensitivity of the apparatus was found from observations of the spectra of β Ori and the luminophore according to the following relationships:

$$C_1 K(\lambda) = \frac{E_*(\lambda)}{b_*(\lambda) P(\lambda)^{-m}}, \quad C_2 K(\lambda) = \frac{E_{\text{lum}}(\lambda)}{b_{\text{lum}}(\lambda)}. \qquad (2)$$

The energy distribution in the luminophore spectrum was also investigated in August of 1965 in absolute units. (The value of the constants C_1 and C_2 in (2) varied, since the spectra of the star and luminophore were taken with different exposures). As already mentioned, the spectra of β Ori were used only in order to obtain the relative change in spectral sensitivity in the interval of wavelengths of 4800 - 4200 Å. The values of the spectral brightness of the cometary tail were obtained in absolute units according to the following formula:

$$E_k(\lambda) = b_k(\lambda) C_2 K(\lambda) P(\lambda)^{-m}, \qquad (3)$$

where $P(\lambda)^{-m}$ is the correction for absorption of light in the Earth's atmosphere.

The results of the observations are given in the Table. The accuracy of the values obtained was on the order of 15-20%.

For a comparison with photometric observations, the brightness of one square degree of a tail was computed in a number of fifth-magnitude stars according to the following formulas:

$$2.512^{m_*(V)-m_k(V)} = \frac{1}{3283} \cdot \frac{\int E_k(\lambda)\, v(\lambda)\, d\lambda}{\int E_*(\lambda)\, v(\lambda)\, d\lambda}, \qquad (4)$$

/144

$$\log n_5{}^m = 0.4\,[5 - m_k(V)], \qquad (5)$$

TABLE: ENERGY DISTRIBUTION IN THE SPECTRUM OF THE TAIL OF COMET IKEYA-SEKI

λ, Å	1.XI 1965	2.XI 1965	λ, Å	1.XI 1965	2.XI 1965
[illegible]	88.0	75.0	5400	109.0	84.0
4900	92.0	87.0	5500	106.0	75.0
4500	89.0	110.0	5600	101.0	68.0
4600	86.9	111.5	5700	90.0	65.5
4700	87.0	102.5	5800	80.0	68.0
4800	91.0	87.0	5900	72.0	65.0
4900	90.0	86.0	6000	68.0	55.0
5000	85.0	95.0	6100	65.0	49.5
5100	85.0	82.0	6200	63.0	49.0
5200	94.0	70.0	6300	58.0	40.0
5300	102.0	78.0	6400	53.0	33.0

in which $m_*(V)$ is the magnitude of the reference star α Lyr, $m_k(V)$ is the solar magnitude of one square degree of the cometary tail in system V of Johnson-Morgan, $E_*(\lambda)$ and $E_k(\lambda)$ are the energy in the spectrum of the cometary tail and in the star α Lyr. The energy distribution in the spectrum of α Lyr was taken from [3]. The coefficient 1/3283 converts the steradians into square degrees. The following results were obtained for the regions of the tail under investigation:

	$m_k(V)$	$n_5{}^m$
1 November	3.02	6.17
2 November	2.66	8.71

The results of a comparison of the energy distribution obtained and that found in the solar spectrum are shown in Figure 1. As can be seen, the energy distribution in the spectrum of the tail is close to the solar distribution. In the range of wavelengths of 4300 - 5000 Å, two relatively weak details can be seen, but it is not certain that they are emission bands, since the observations were not precise because of the weak contrast of the tail against the sky background and the low position of the comet over the horizon.

Let us compare the spectrum of the tail of Comet Ikeya-Seki /145
to the spectra of other comets, for example, Arend-Roland (1957 III) and Mrkos (1957 V). The spectrophotometric observations of these comets which Liller [5] carried out showed that the spectrum of the tail was mainly continuous and characterized by an excess of red color compared to the solar spectrum. Figure 2 gives a comparison of the color of Comets Arend-Roland, Mrkos, Ikeya-Seki (average for November 1 and 2) and the Sun. As was done in Liller's study [5], the wavelengths were selected where there were no CO^+ emission bands and the intensity of λ4790 was taken as unity. It follows from the curves in Figure 2 that the color of the tail of Comet Ikeya-Seki differs widely from the color of Comets Arend-Roland and Mrkos, and is close to the color of the Sun, as has already been mentioned. The slight difference in color for Comet Ikeya-Seki and the Sun can be the result of uncertainty in the observations in the red spectral region and the substantial brightness of the background of the twilight sky.

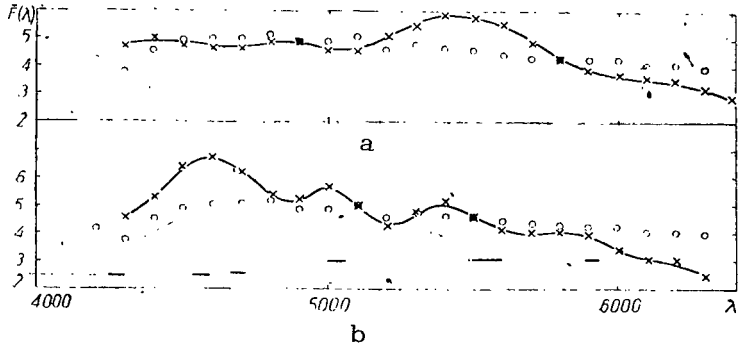

Fig. 1. Energy Distribution in the Spectrum of the Tail of Comet Ikeya-Seki, 1965 (×) and the Sun ( ) in Units, November 1 (a) and 2 (b) (the Regions where the CO^+ Bands are Observed are Marked by Short Horizontal Lines).

Unfortunately, the results we obtained relate only to two days of observations and two regions of the tail. It can be expected that the color of the tail changes in dependence on the distance from the head, and in the course of time. Ceplecha [4] showed that the color index of the tail of Comet Mrkos changed to a rather great extent in the course of time (from +0.93 to $-0^m.05$). The changes of the continuous spectrum could be the reasons for these /146
variations, as well as the appearance of the CO^+ emission bands in the wavelength range of 4300 - 5000 Å.

Possibly, the color of the tail of Comet Ikeya-Seki indicates that dust particles predominate.

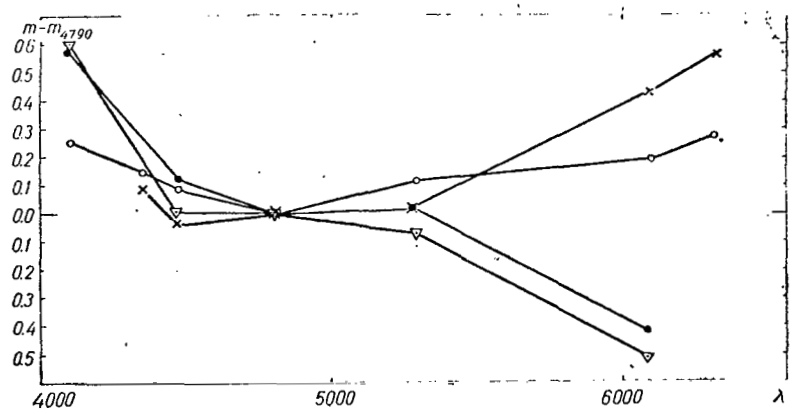

Fig. 2. Energy Distribution in the Continuous Spectrum of the Tails of Comets Arend-Roland (Δ), Mrkos (●), Ikeya-Seki (×) and the Sun (○).

References

1. Karyagina, Z.V.: Astron. Zhur., Vol. 37, p. 822, 1960.
2. Pariyskiy, N.N. and L.M. Gindilis: In the book: Sbornik trudov MGU po MGG (Astronomiya) [Collection of the Proceedings of Moscow State University on the IGY (Astronomy)]. Moscow University Press, No. 3, 1962.
3. Kharitonov, A.V.: Astron. Zhur., Vol. 40, p. 339, 1963.
4. Ceplecha, Z.: Publ. Czech. Acad. Sci. Astr. Inst. Vol. 34, p. 31, 1958.
5. Liller, W.: Astrophys. J., Vol. 132, o. 867, 1960.

POLARIMETRIC AND PHOTOMETRIC OBSERVATIONS OF COMET IKEYA-SEKI 1965f

T.A. Polyakova and T.K. Pisareva

ABSTRACT: The results of photographic and photoelectric observations of the light polarization of Comet Ikeya-Seki (1965f) are given, as are the results of photographic photometry of the head of the comet in the region of the C_2 and C_3 bands.

The comet Ikeya-Seki was observed at the Byurakan station of the Astronomical Observatory of Leningrad State University in October and November of 1965. The AFM-6 electrophotometer installed in the Cassegrainian focus of the AZT-14 telescope (D = 480 mm, D/f = 1:15) was used for the electropolarimetric observations [1]. The observation methods and the analyses are described in a study by V.A. Dombrovskiy [2]. /148

TABLE 1

№	Observation Time, UT		P, %	θ_E, °	φ, °	d	$(\theta_E-\varphi)$°
1	October 1965	2.069	6.5	172	81	54.4	91
2		3.078	8.5	178	81	54.4	97
3		5.085	6	13	82.5	136	110.5

Before the passage of the comet through the perihelion, the polarization of its light was determined three times. The results of these observations are given in Table 1, where P is the degree of polarization; θ_E is the position angle of the plane of preferential oscillations of the electric vector in the equatorial system of coordinates; ϕ is the position angle of the direction comet-to-Sun; d is the diameter of the diaphragm with which the observation is carried out (in seconds of arc). Only the central section of the comet with the nucleus were fixed in the diaphragm of 54.4"; with a diaphragm of 136", the entire comet was visible in the Cassegrainian focus of AZT-14. Observation No. 3 has somewhat lower weight because of the rather unreliable consideration of the sky background.

After the passage of the comet through the perihelion, there were two more photoelectric determinations of the light polarization in the tail of the comet at a distance of about 8 (No. 1) and 2° (No. 2) from the head of the comet. The results are given in Table 2.

Moreover, two series of photographs of the comet (three each) were obtained on November 3 and 4 (3.078 and 4.093) with the aid of

an Exacta camera, with a polaroid in front of the objective. The camera was attached to the parallactic arrangement of an AST-453 telescope. An RF-3 film was used, for which λ_{eff} = 4600 Å. The polaroid was turned by 60° between exposures, and the polarization /149 parameters were then calculated according to Fesenkov's formulas [3].

TABLE 2

№	Observation Time, UT	P, %	θ_P, °	d''
1	November 3.078	1	11	136
2	3.092	17	173	136

Extrafocal photographs (exposure of 8 min) were obtained in the first series (3.078), and focal photographs (exposure of 7 min) were obtained in the second (4.094). The photographs were measured on the MF-2 microphotometer. The calibration was carried out according to the photographs of the tubular photometer. A diaphram which described an almost square area with side of 6′ on the plate was used in the measurements. The cross section of the comet's tail in which the measurements were carried out were a distance of 0.6 or 0.9 mm from each other in the first series; in the second series, they were a distance of 1.0 or 0.7 mm. The diaphragms in each cross section were set up against each other.

Corrections for reduction to one zenith distance were introduced into the measurements. The regions of the tail around the head of the comet were not analyzed, since their zenith distance $z \geq 87°$.

If the somet was extended by more than 20° on the photographs without polaroid, its image was roughly 16° on photographs with polaroid.

In the series with focal photographs, the polarization in the tail of the comet was determined for distances from 2.7 to 16° from the head of the comet. In the other series, it was determined for distances from 3.4 to 13.4°.

These photographic measurements were tied in with the photoelectric measurements of polarization in the tail of the comet (see Table 2) by introducing additional coefficients. The values obtained for the polarization parameters, which were averaged in each section over several points, are represented in Figure 1.

Moreover, a series of three photographs of the head of the comet was obtained on ORWO ZU-2 plates on November 3 (3.101) on the AST-453 telescope in straight focus. Each photograph was taken with exposure of 5 min. Because of the difficulties in guiding along the nucleus of the comet, which was on the horizon itself, the images of the head of the comet were irregular for the short exposures. Because of this, it was impossible to investigate the

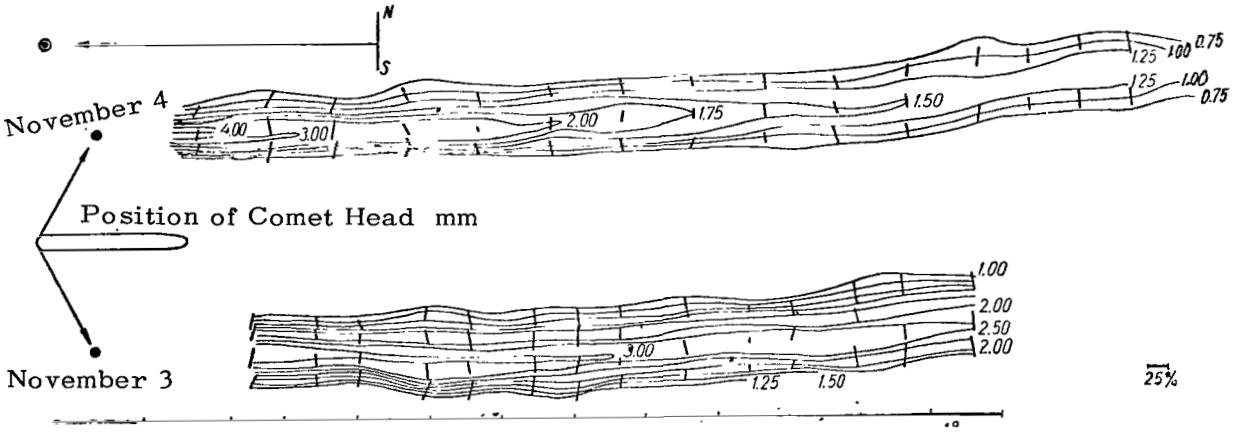

/150

Fig. 1. Isophotes and Polarization Distribution Obtained by Photographs of the Comet on November 3 and 4 with the "Exacta" Camera.

distribution of polarization over the image of the cometary head. /151
Therefore, the measurements were taken on the automatic recording microphotometer MF-4 with a diaphragm cutting a square with side of 0.5 mm on the plate (scale: 100″ is 1 mm), which was selected so that the image of the head of the comet would decrease in full in the diaphragm. The polarization was determined with the same diaphragm at four points of the brightest part of the tail obtained on the photographs. The furthest point was a distance of roughly 14′ from the center of the head. The results of the measurements were the following (r is the distance from the head of the comet on the plate):

r, mm	0.0	1.4	3.6	5.9	8.2
P, %	52	44	35	40	38
θ_E, °	20	0	12	8	6

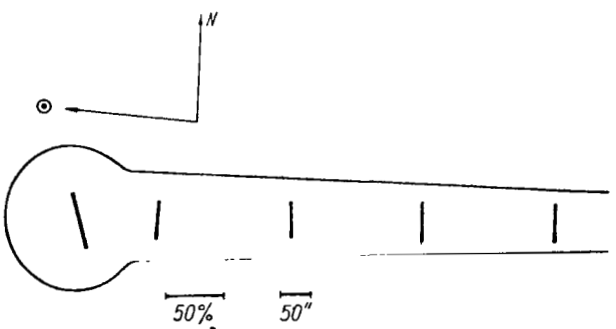

Fig. 2. Polarization Distribution in the Region of the Head of the Comet, Obtained according to Photographs on November 3, in the Straight-Line Focus of the AST-453 Telescope.

The position angle of the direction comet-Earth was equal to 88° in this case. These photographic observations were not tied in with the photoelectric polarization observations. In addition, the error in determining the polarization by the photographic method, which was great in itself, increased in this case because of the difficulty in taking account of the changes in atmospheric conditions. The photographs were taken with a two-level magazine, but only one extrafocal disk of the star at the very edge of the plate was used, and that was fuzzy because of the guiding over the comet. Thus, the error in determining the degree of polarization in the head of the comet reached 20%, and it can be considered that the values obtained for the polarization in the region of the comet's head were linked with the values for polarization in those regions of the tail of the comet which were a distance of 3° from the head. /152 In the two preceding series, the polarization at this distance was greater than 20%. In general, the average values for the degree of ionization and the position angle for the first series (3.078) were 20% and 195°, and those for the second series (4.094) were 17% and 192°. The position angle of the radius vector comet-Sun for the first and second series was equal to 88 and 93°, respectively. All the polarization observations were carried out without light filters.

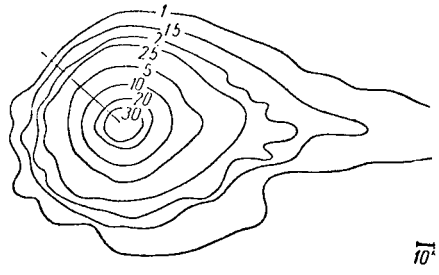

Fig. 3. Isophotes of the Image of the Comet's Head in the C_2 Lines (The Straight Line Shows the Section for Which the Intensity Distribution Law was Selected).

The photometric measurements were carried out for two photographs which were obtained with interference filters on November 4 (4.0930) and 5 (5.0954), 1965, in straight-line focus of the AST-453 telescope on the ARWO ZU-2 plates. A filter with transmission band of 100 Å ($\lambda\lambda$467 - 477 mμ) was used on November 4; the

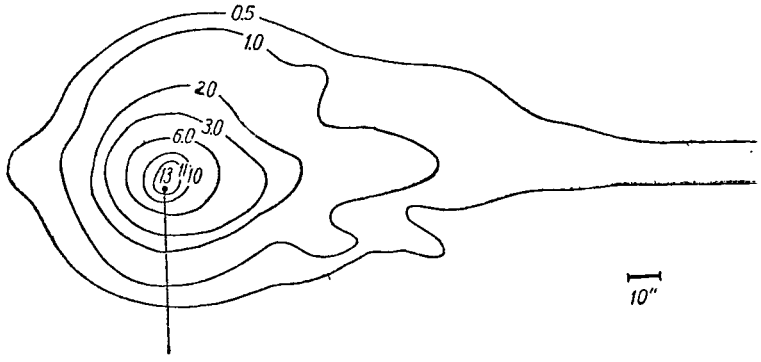

Fig. 4. Isophotes and Image of the Comet's Head in the C_3 Lines (The Straight Line Shows the Section for Which the Intensity Distribution was Constructed).

image of the comet's head was obtained in this case in the light of the C_2 band. The photograph was taken with exposure of 27.5 min, with the aid of a two-level magazine. The photograph of the tubular photometer was less dense than the image of the central regions of the comet's head; therefore, the intensity was not determined /153 for them. The isophotes are given in Figure 3. The intensities are designated in relative units, since the guiding was carried out over the comet and the images of the extrafocal stars were obtained in the form of series of superposed disks, which were not suitable for photometry.

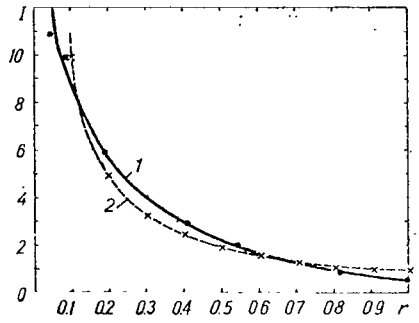

Fig. 5. Dependence of I on r for Photograph in the C_3 Lines (1) $I = f(r)$; (2) $y = 1/x$.

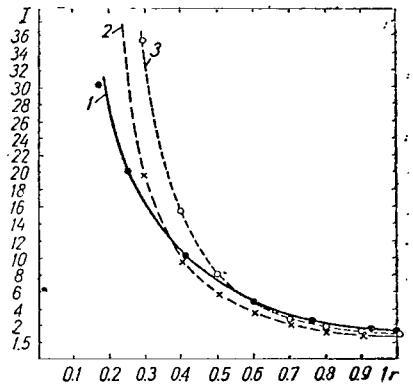

Fig. 6. Dependence of I on r for Photograph in the C_2 Lines. (1) $I = f(r)$; (2) $y = s^{-5/2}$; (3) $y = x^{-3}$

On November 5, the cometary head was photographed with a filter for which the transmission band was 140 Å ($\lambda\lambda 400 - 414$ mμ), which guaranteed an image of the comet in the light of the C_3 line (exposure of 25 min). The isophotes are given in Figure 4.

As for the isophotes, we attempted to find the law for the intensity distribution I as a function of the distance from the center of the comet's head r in the sections depicted in Figure 3 and 4.

The intensity distribution curve for the isophotes of the comet image in the light of the C_2 band is obviously most similar to the curve of $y = x^{-5/2}$, while that in the light of the C_3 band is close to the curve of $y = x^{-1}$. These curves are represented in Figures 5 and 6.

References

1. Dombrovskiy, V.A. et al: Trudy Astron. Observ. Leningradsk. Gosudarstv. Universit., Vol. 22, p. 83, 1965.
2. Dombrovskiy, V.A.: Astron. Zhur., Vol. 30, p. 603, 1953.
3. Martynov, D.Ya.: Kurs prakticheskoy astrofiziki (A Course in Practical Astrophysics). Moscow, "Nauka", 1965.

THE DENSITY OF SODIUM IN COMET IKEYA-SEKI (1965f)

E.A. Gurtovenko

ABSTRACT: Resonance scattering of photospheric radiation is the only mechanism which brings about emissions of the D_1 and D_2 lines of comets. This mechanism, and the data of spectral observations at Sacramento Peak, were used in order to estimate the number of atoms N and the mass of the sodium M in the head of Comet 1965f. The values obtained, $N \approx 0.25 \cdot 10^{32}$ and M $1 \cdot 10^9$ g, are almost equal to the corresponding estimates deduced from the emissions of other elements and compounds in ordinary comets (at a great distance from the Sun). This indicates that comets consist of heavy elements (Na, Fe, etc.) to a considerable extent. These elements can be released from the nucleus of the comet only when they are near the Sun.

In a rather cold and loose gas cloud, the mechanism of fluo- /155
rescence in the sodium D_1 and D_2 lines under the conditions of the interplanetary medium (photoionization from the ground level with subsequent recombination [2]) plays practically no part in comparison with the mechanism of resonance scattering of photospheric radiation. The lower limit to the total number of sodium atoms in the head of Comet Ikeya-Seki (1965f) can be evaluated from the equation of resonance scattering. According to the spectral observations of the comet at Sacramento Peak [5], the total number of sodium N_2 particles excited on the $^2P_{3/2}$ level (D_2 line) in a column of 1 cm^2 on the line of sight in the head and the part of the tail of the comet near the head is roughly identical, about $3 \cdot 10^7$.

For resonance scattering, we have the following relationship:

$$n_1 Q_{12} B_{12} W r_c = n_2 A_{21}, \qquad (1)$$

where r_c is the central intensity in the photospheric D_2 line, and W is the dilution factor.

Disregarding the self-absorption, the same relationship can be obtained by replacing n_1 and n_2 with N_1 and N_2 (N_1 is the total number of sodium particles in the ground state in a unit column). When there is self-absorption, (1) gives the lower limit to N_1 and N_2.

At the moment of observation in Sacramento Peak (October 20, 1920 UT) according to the epheneris data [3], the comet was a distance of about 7.5 million kilometers from the Sun. Consequently, $W \approx 2.2 \cdot 10^{-3}$. Since the D_0 and D_2 emission of the comet is displaced considerably, with respect to the solar spectrum, by a value corresponding to the radial velocity $v_r \approx +99$ km.sec [2, 6], then the absorption of photospheric radiation by sodium has originated from the continuum near D_2, i.e., $r_c = 1$. The density of the field $\rho = \frac{4\pi I}{c}$, and $I = 2.7 \cdot 10^{14}$. From (1), $N_2 \approx 7 \cdot 10^{-5} N_1$, so that $N_1 \approx 0.5 \cdot 10^{12}$.

A substantial amount of the sodium atoms near the Sun may be ionized. The equation of ionization equilibrium is the following:

$$n_1 C_1 = \sum_{k=1}^{\infty} R_k n_e n_{Na^+}. \qquad (2)$$

The coefficient of photoionization C_1, which was calculated for ionization temperature of $T_i = 4800°$ at the series limit $\lambda = 2140$Å and $W = 2.2 \cdot 10^{-3}$ is equal to $3.7 \cdot 10^{-3}$. An evaluatino of ΣR_k according to the data of [4] or the manual of K. Allen [1] is $5 \cdot 10^{-2}$ for $T_e = 100°$K. We took the value $T_e = 100°$K, considering the condition $T_e \geq T_{exc}$. According to the data of [5], $T_{exc} = 103°$K in the comet. In general, the dependence of the recombination coefficients on the temperature is weak; ΣR_k decreases by a large factor when T_e increases by a factor of 10. The value of n_e in the comet was unknown, but in any case $n_e \geq n_{Na^+}$. Consequently, considering that $n_e = n_{Na^+}$, we can find the upper limit to the concentration of sodium ions from (2). Under these conditions, $N_{Na+} \leq 1.6 \cdot 10^{10}$, i.e., practically all the sodium in Comet Ikeya-Seki was in a neutral state and $N_{Na} = N_1 \approx 0.5 \cdot 10^{12}$. /156

The underestimation of N_1 may be due to self-absorption. The optical thickness at the center of the line $\tau_0 = k_0 N_1$, and $k_0 \approx \frac{f_1 \lambda^2}{\Delta\lambda_D}$. If we assume that there is no macro- or micro-turbulence or gradient in the spatial velocities of individual elements of a volume, then at $T = 100°$K, $\Delta\lambda_D = 5 \cdot 10^{-3}$ Å and $k_0 \approx 6 \cdot 10^{-11}$. However, spectral observations with high dispersion [6] indicate that there is a large gradient of velocities which disturb the D_1 and D_2 profiles and extend them by a value up to several tenths of an angstrom. For this width of the profile, the optical thickness at the center of the line decreases by at least two orders so that, in all probability, the real value for the optical thickness of the comet's head in the D_2 line $\tau_0 < 1$, and the estimate of $N_1 \approx 0.5 \cdot 10^{12}$ is close to the real value.

Let us briefly discuss the effect of the splitting into two parts of the D_1 and D_2 emission in the region of the nucleus which

was observed in the spectrum obtained at Kitt Peak [6]. One of the variations for the explanation of this effect is the assumption that there could be absorption of the emission in the outer, cooler layer surrounding the nucleus. The authors of [6] incorrectly call this phenomenon self-absorption. Absorption in the outer layer is possible on the condition that the emission in the central region arises because of intrinsic excitation sources (for example, an electron impact), which is not realistic in this case. The mechanism of resonance scattering can yield a splitting (double-humped curve) of the profile for the cases when $\tau_0 \geq 1$. In this regard, there is a mechanism of self-absorption which is connected with multiple re-emission of the primary radiation of the comet, caused by the scattering of photospheric emission. This mechanism is hardly probable since, obviously, $\tau_0 < 1$. /157

Since there is no abrupt decrease in the D_1 and D_2 emission from the nucleus to the periphery, we can calculate the average sodium concentration in the head of the comet as $n_{Na} = \frac{N_1}{d}$ with sufficient accuracy for the estimate. According to the Kitt Peak observations, the principal percentage of the sodium emission is concentrated in a region with dimension of $d \approx 2'$, or $d \approx 10^{10}$ cm, $n_{Na} \approx 0.5 \cdot 10^2$, the total number of sodium particles in the comet's head is equal to $0.25 \cdot 10^{32}$, and the mass of sodium in the comet's head is about 10^9 g.

The estimates obtained for the sodium concentration, the total number of particles and the mass in the head of Comet 1965f are very close to the estimates of the corresponding values which are obtained from an analysis of the emission of atoms and molecules of various light compounds (CN, C_2, CO^+, etc.). Obviously, under the corresponding physical conditions, the nucleus of the comet can release an approximately equal amount of heavier elements (sodium, iron, etc.), i.e., the nucleus of the comet has the regular chemical composition characteristic of the majority of heavenly bodies of the solar system.

References

1. Allen, K.W.: Astrofizicheskiye velichiny (Astrophysical Magnitudes). Moscow, Foreign Literature Publishing House, 1960.
2. Gurtovenko, E.A.: In the book: Voprosy astrofiziki (Problems of Astrophysics). Kiev, "Naukova Dumka", 1967.
3. Mamedov, M.A.: In the book: Aktivnyye protsessy v kometakh (Active Processes in Comets). Kiev, "Naukova Dumka", 1967.
4. Moskvin, Yu.V.: Optika i Spektroskopiya, Vol. 15, No. 5, p. 582, 1963.
5. Curtis, G.W. et al: Astron, Journ., Vol. 71, No. 3, p. 194, 1966.
6. Livingston, W. et al: Sky and Tel., Vol. 31, No. 1, p. 24, 1966.

PHOTOGRAPHIC PHOTOMETRY OF THE TAIL OF COMET IKEYA-SEKI

E.S. Yeroshevich

ABSTRACT: The results of photometric measurements of the tail of Comet Ikeya-Seki are given. The data were obtained from observations with a Schmidt camera. The isophotes of the head and tail of the comet are plotted. The quantity of dust is determined according to these data.

During the period of the passage of Comet Ikeya-Seki near the Sun in 1965, the brightness of the tail was studied as a function of the distance from the head of the comet. The observations were carried out by D.A. Rozhkovskiy on the night of November 26-27. During this period, not only the tail, but also the head of the comet could be observed, with its very low position over the horizon before sunrise. The observations were carried out on the Schmidt camera constructed at the Astrophysical Institute of the Academy of Sciences of the Kazakh S.S.R. (D = 170 mm; $\frac{D}{F} = \frac{1}{1}$; field of view 10°). Three photographs were obtained on the A-500 film, with exposure of 1 min. /159

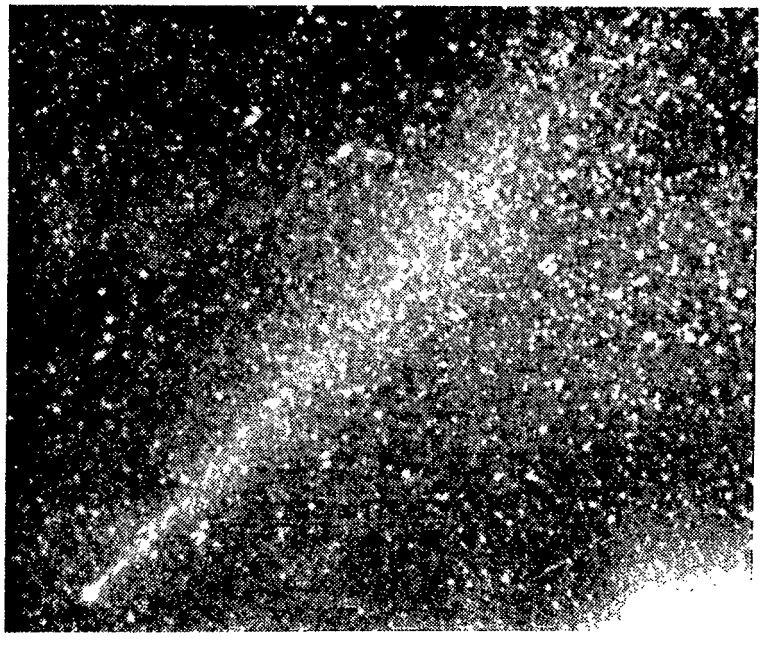

Fig. 1. Comet Ikeya-Seki.

TABLE 1

/160

Sections	34′	32′	30′	28′	26′	24′	22′	20′	18′	16′	14′	12′	10′	8′	6′	4′	2′
I										9.96	9 11	9.11	0.00	8.77	8.45	7.37	6.31
II										9.98	9.11	9.11	8.77	8.77	8.04	7.45	7.41
III										9.98	0.00	0.00	8.77	8.16	9.11	8 01	7.70
IV										9.96	9.52	8.77	8.45	8.01	8.21	7.85	7.70
V										9.96	9.52	0.00	9.11	9.11	9.21	8.11	8 45
VI						9.98	9.11		0.00	9.11		8 21		8.21		8.21	7.85
VII						0,00		8.45	8.45	8.45		8 45	8.21		8.01	7.70	
VIII	0.00	9.96		9.96	9.96	9.96		8 77		0.00		8.21		8.21		8.45	
IX		9.96		9.96		0.00		9.52		9.52		8.45		8.45		9.11	
X		9.96		9.96		9.52		9 52		9.11		8.77		9.11		8.01	
XI		9 96		9.52		9.52		9.52		8.77		8.77		8.45		8.45	
XII		9.96		9.96		9.96		9.96		8 45		8.45		8.77		9.11	
XIII		9 96		9.52		9.52		9.52		9.52		9.52		9.52		9.11	
XIV		9.96		0.00		9.52		9.52		9.52		9.11		9.11		9.11	

Sections	0′	2′	4′	6′	8′	10′	12′	14′	16′	18′	20′	22′	24′	25′	28′	30′	32′
I	5.26	6.38	7.46	8.01	7.57	8.21	9.96	9.96	0.00	9.96							
II	7.44	7.09	7.85	8.04	8.21	9.96	9.59	9.96	9.59	9.96							
III	7.70	7.16	7 85	9.11	8.21	9.52	0.00	0.00	0 00	9 96							
IV	7.70	7.08	8.45	8.21	8.45	8 45	9.52	9.96	9.96	9.96							
V	7.70	7.57	8.01	8.21	9.11	8.45	0.00	9.52	9.96	9.96							
VI	7 85		8.01		7.46		7.85		7.45		8.21		8.45	9.96			
VII	7.46		7.85		7.86		8.45		8.77		8.77		9.11	9.96			
VIII	7.85			8.45			8.45		9.52		9.11		9.52		9.96		9.96
IX	8.21			8.77			8.45		9 11		9.11		9.52		9.52		9 96
X	8.21			8.45			9 52		9.11		8.77		9 11		9.52		9.96
XI	8.45			8.77			9 11		9.52		9 52		9.96		9.52		9 96
XII	9.11			8.77			8.77		9.52		9.52		9.52		9 96		9.96
XIII	8.77			9.52			9.52		9 52		9.96		9.96		9.96		9.96
XIV	8.77			9.52			9.52		9.52		9.96		9.96		9.96		9.96

/161

The general appearance of the comet is presented in Figure 1. The photographs were calibrated with the aid of a tubular photometer. The photographs were standardized over the extrafocal stellar images obtained in the same region; therefore, there was no more need for correcting the observational data for the transmission coefficient of the atmosphere.

The blackenings of the images of the comet's tail were measured on the MF-4 microphotometer with 27 enlargement, and a spherical diaphragm of 0.11 ± 0.01 mm, which corresponds to 2.2′ in the sky, was used. Fourteen sections perpendicular to the radius vector of the comet's tail were made in equal spaces of 30′ on each photograph. In each section, we took that number of points for which detailed isophotes could be plotted. In all, 240 points were scanned photometrically in each photograph, and the mean arithmetic value for the intensities was taken from the three photographs.

The results of measurements of all 14 sections are given in Table 1 (in stellar magnitudes with 1□°) and Figure 2. The integral brightness was determined according to the brightness distribution in each section with area of 32 × 2′.

TABLE 2

Section No.	α	δ	r, a.u.	m
	$10^h\ 36^m\ 5^s$	$-32°\ 50'$	0.000	6.43
I	10 36 2	−32 48	0.006	9.64
II	34 3	36	0.021	10.73
III	32 4	24	0.037	11.03
IV	30 5	12	0.052	10.78
V	28 6	00	0.067	10.95
VI	26 7	−31 48	0.082	10.80
VII	24 8	36	0.097	10.81
VIII	22 9	24	0.112	11.68
IX	21 0	10	0.128	11.65
X	19 2	−30 56	0.144	11.65
XI	17 4	42	0.161	11.63
XII	15 6	28	0.177	11.89
XIII	13 8	14	0.195	12.22
XIV	12 0	−30 00	0.212	12.38

Table 2 gives the coordinates of the centers of each photometric section, the distance from the nucleus along the radius vector, and the integral brightness corresponding to the given section. In order to determine the distance r from the nucleus of the comet, we used the formulas of S.V. Orlov and O.V. Dobrovol'skiy [2,1].

Figure 3 shows the change in brightness of the tail along the radius vector as a function of the distance from the nucleus (the brightness values were taken from Table 1 for the middle of each section, beginning with the second).

The brightness m is the function of 2.5 log r, where r is the distance from the head of the comet (the values were taken from Table 2). It can be seen from Figure 3 that the decrease observed in the brightness along the radius vector of the comet's tail to the side opposite to the Sun obeys the law $1/r^2$ near the head, and the law $1/r^4$ at greater distances from the head.

The isophotes characterizing the brightness distribution in the tail and coma were constructed according to the data of Table 1. Ten isophotes were plotted, and the brightness interval between neighboring isophotoes was from 0.3 to 0.5. The general appearance of the isophotes of the tail and coma is represented in Figures 4 and 5 (the isophotes of the coma in Fig. 5 were constructed with an enlargement by a factor of five). The values for the brightness of the isophotes were the following:

Isophote No.	1	2	3	4	5	6	7	8	9	10
Stellar Magnitude	4.52	4.85	5.51	6.27	7.02	7.36	8.21	8.77	8.98	9.51

/162

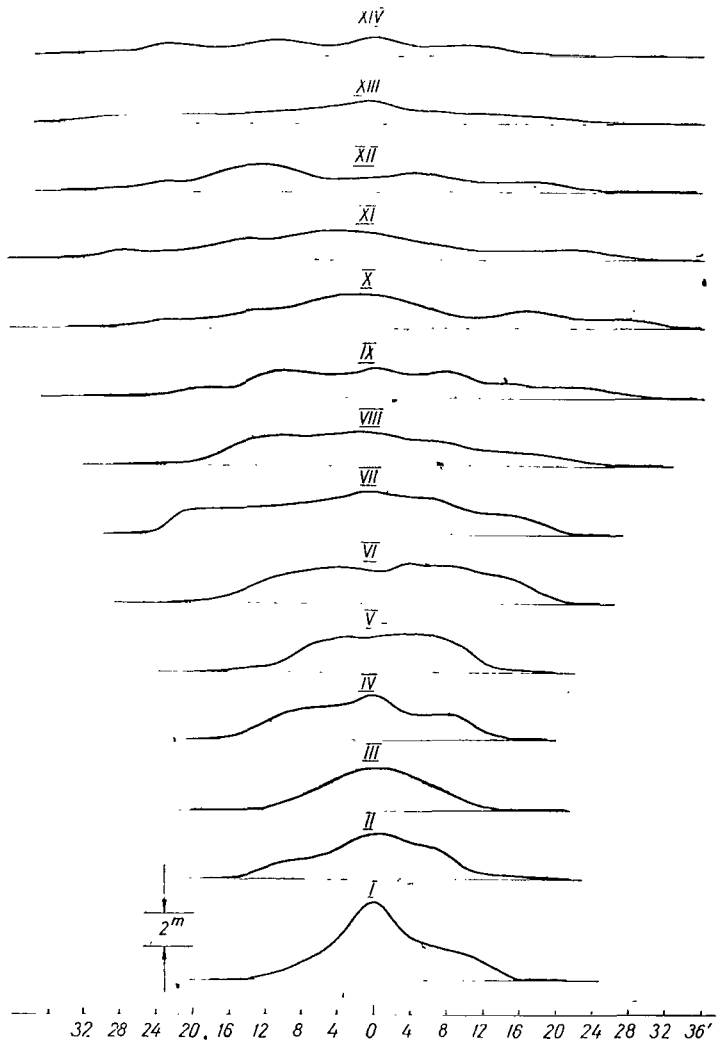

Fig. 2. Brightness Distribution in Comet Tail, in Stellar Magnitudes, per Square Degree.

/163

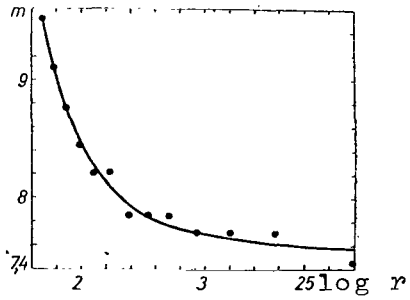

Fig. 3. Brightness Distribution in Comet Tail Along Radius Vector.

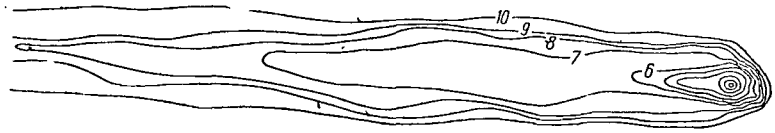

Fig. 4. Isophotes of the Coma and Tail of the Comet.

The integral brightness of the coma with diameter over radius vector of 14′ was equal to 6.43^m.

As is seen in Figures 1 and 2, the tail of the comet is slightly inclined with respect to the radius vector in the direction opposite to the motion of the comet.

The quantity of dust particles in the head of the comet and in each cross section can be determined according to the data of Table 2, which contains the integral brightnesses of each section. However, before determining the amount of dust in the comet, let us turn to the results which were previously obtained in this regard. /164

Photographs of the spectrum and polarization of the comet were obtained on October 31 and November 1. A photograph of the spectrum of a segment of the comet was obtained by Z.V. Karyagina [4]. It was found in a spectral analysis that the comet consists of dust.

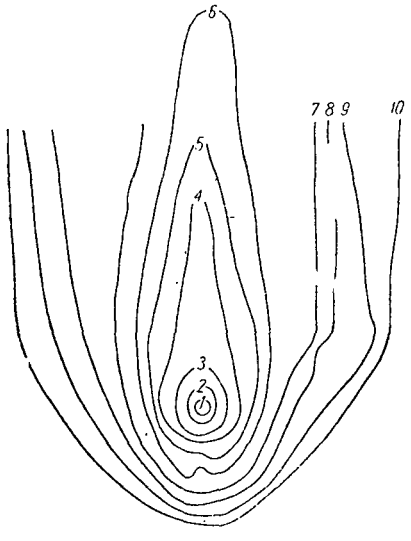

Fig. 5. Isophotes of the Coma.

The degree of polarization of the comet's tail which V.S. Matyagin, A.V. Kharitonov and Sh.N. Sabitov obtained averages about 65%, which indicates that the composition of the comet includes dust.

In order to determine the quantity of dust particles in the coma of the comet, we used the formula of A.V. Kurchakov [3]:

$$E = E_0 N \pi \rho^2 \frac{A}{4\pi\Delta^2}, \qquad (1)$$

where E_0 is the illumination produced by the Sun at the distance of the comet, A is the albedo of a particle, which is assumed to be equal to one, ρ is the effective radius of the particle, and N is the quantity of dust particles both in the head of the comet and in the tail.

The distribution of dust in the tail of the comet was calculated according to the following formula:

$$E = E_0 \frac{\mu\tau}{\sin^2\varphi} \cdot \frac{x(\bar{\Theta})}{4\pi} \sin^2\bar{\Theta}, \qquad (2)$$

from which we find that

$$\mu\tau = \frac{E}{E_0} \cdot \frac{\sin^2\varphi}{\sin^2\bar{\Theta}} \cdot \frac{4\pi}{x(\bar{\Theta})}, \qquad (3)$$

where μ is the albedo of a particle, ϕ is the angle between the comet and the Sun relative to the Earth, $\bar{\Theta}$ is the angle of visibility of the cometary tail from the Earth, $\bar{\Theta}$ is the average value for the angle between the first and last section of the tail (the average value $\bar{\Theta}$ is taken from the idea that it changes very slightly from the first to the fourteenth section and does not introduce a substantial error in the calculations), $x(\bar{\Theta})$ is the scattering indicatrix: /165

$$x(\bar{\Theta}) = \frac{1-q^2}{(1+q^2-2q\cos\bar{\Theta})^{3/2}}, \qquad (4)$$

q is the size of a particle with diameter of 0.8 at $\lambda = 10^{-5}$.

We find from (4) that $x(\bar{\Theta}) = 7.8 \cdot 10^{-2}$.

If the albedo of a particle μ is taken as one, then the optical thickness $\tau = 3 \cdot 10^{11}$ cm. Knowing the value of τ, we will find the quantity of particles in each section of the tail according to the following formula:

$$\tau = \pi\rho^2 N, \qquad (5)$$

where N is the number of particles, and ρ is the size of the particle, which is equal to $2.7 \cdot 10^{-6}$ cm. Using (5), we will find the following values for N:

№	I	II	III	IV	V	VI	VII
N	$2.3 \cdot 10^{22}$	$1.2 \cdot 10^{22}$	$5.8 \cdot 10^{21}$	$1.3 \cdot 10^{22}$	$1.3 \cdot 10^{22}$	$1.3 \cdot 10^{22}$	$1.3 \cdot 10^{22}$
№	VIII	IX	X	XI	XII	XII	XIV
N	$6.5 \cdot 10^{21}$	$6.8 \cdot 10^{21}$	$6.8 \cdot 10^{21}$	$7.2 \cdot 10^{21}$	$7.2 \cdot 10^{21}$	$2.8 \cdot 10^{20}$	$3 \cdot 10^{20}$

The number of particles N in the head of the comet was calculated according to (1). It is equal to $6 \cdot 10^{24}$.

References

1. Dobrovol'skiy, O.V.: Komety (Comets). Moscow, "Nauka", 1966.
2. Orlov, S.V.: Komety (Comets). Moscow-Leningrad, Academy of Sciences of the U.S.S.R., 1935.
3. Kurchakov, A.V.: Izvest. Astrofizicheskogo Instituta, Vol. 9,1960.
4. Karyagina, Z.V.: This Collection.

THE PROBLEM OF THE DUST COMPONENT OF THE COMETARY ATMOSPHERE

M.Z. Markovich

ABSTRACT: Certain properties of the dust component of the cometary atmosphere are considered: the mass of the dust M, the number of particles in the cometary head N, the concentration of dust near the nucleus n_{0d}, the capacity of the dust M', the distribution of dust particles by size, or $\phi(h) = A_1 h^{-p}$. It is held that the distribution by size is the same as in meteoroid showers ($p = 7$). The values of M, M', N and n_{0d} change within wide ranges for different comets.

The investigations of the nature of the dust component in the cometary atmosphere have recently been carried out in the following directions: /166

(1) Division of the emission of the cometary head into the emissions of the gas and dust components. It is held in [26, 20, 7, 8, 25] that the brightness of the dust component changes in inverse proportion to the square of the distance from the Sun. This law cannot be considered as sufficiently founded, since we do not know how the number of particles and their size change with the heliocentric distance. Z. Sekanina [23] took account of the variable photometric index n_d of the dust-containing coma, obtained a complex theoretical dependence on $r_\odot$ for it, and determined the function $n_d(r_\odot)$ from observational data.

(2) Investigations of the continuous spectrum in the head of the comet and an analysis of different types of light scattering showed that small dust particles with dimensions on the order of 0.1 - 0.7 μ predominate in the atmospheres of comets [14, 2, 19]. A study of the motion of dust particles in a flow of cometary gas [30, 9] led to diameters roughly of the same order. Thus, the problem of the size of the dust particles in cometary atmospheres obviously can be considered as solved; the diameters of the particles do not exceed a few microns or tenths of a micron.

(3) Attempts are made to link the physical characteristics of the dust component, for example its total mass, with the integral brightness of the comet and the brightness distributions and, consequently, the density of the matter in the head of the comet. For example, Whitney [32] assumed that the emission of a comet is due entirely to dust particles and found the following relationship for the total mass of particles:

$$M = \log \rho_d h + 2 \log\left[\frac{r_\odot \Delta \cdot 385 \cdot 10^5}{\Phi^{1/2}(\alpha)}\right] - 0.4\, m + 2.1, \qquad (1)$$

where m is the apparent magnitude of the comet, ρ_d is the density of the dust, h is its radius, Φ is the phase function (ratio between the brightness for phase angle of α and the brightness in opposition), r and Δ are the helio- and geo-centric distances, AU, and the remaining values are given in the CGS system.

Rozhkovskiy [15,16] recently obtained a similar formula for M, /167 using the same assumption:

$$M = \frac{128}{3\pi} 2.512^{-m+m_\odot} \frac{hr_\odot^2 \rho_d}{Ax(\vartheta)Q}, \qquad (2)$$

where $m_\odot = -26.26^m$, Q is the coefficient of the effectiveness of spherical dust particles with respect to the reduction of light, $X(\theta)$ is the scattering indicatrix, ϑ is the angle of scatter, and A is the albedo of the particles of dust. In particular, the mass of the dust component of Comet Humason ($r_\odot = 2$ AU) was estimated according to (2) for dielectric particles ($h = 10^{-5}$ cm, $A = 1$) scattering isotropically as 10^8 g.

It was found that a large quantity of dust can affect the density distribution of the luminous molecules in the head of the comet [3, 10]. The distribution of the number of molecules n in a unit volume with distance r from the center of the nucleus is usually determined by the following expression:

$$n = n_0 \left(\frac{R_0}{r}\right)^\beta, \qquad (3)$$

where R_0 is the radius of the sphere on which the observed molecules are formed. The average velocity of the molecule changes with the distance by the following law:

$$v = v_0 \left(\frac{R_0}{r}\right)^{2-\beta}, \qquad (4)$$

where v_0 is the velocity of a molecule at $r = R_0$. The index β usually acquires values from 1.5 to 2.0 [4, 10, 16]. If the concentration of dust particles is sufficient for a substantial slowing of the gas flow, then $\beta < 2$. For example, at $\beta = 1.5$ ($r_\odot = 1$ AU), the number of dust particles per cm^3 near the nucleus ($r = R_0$) is of the order of 10^9. The capacity of such a comet, i.e.,

$$Q' = R_0^2 v_{0d} n_{0d} \overline{m}_d$$

at $R_0 \sim 10^5$cm, $v_{0d} \sim 10^4 - 10^5$ cm/sec, $n_{0d} \sim 10^9$ and average particle mass $m_d \sim 10^{-15}$g, a value on the order of $10^8 - 10^9$ g/sec·steradian, which is in complete correspondence with Liller's data

for the comets Arend-Roland and Mrkos [21].

If the deceleration of the molecules is caused by the dust particles, it is determined by the following expression at $r = R_0$:

$$\left(\frac{dv}{dr}\right)_{r=R_0} = 2\sigma v_0 n_{0d} \tag{5}$$

where σ is the effective section of the molecule [10]. Observations show that in the majority of cases $\beta = 2$ (no deceleration) and, consequently, the repulsive acceleration of the Sun $(\frac{dv}{dr})_\odot$ which always occurs does not affect the value of β in the distribution of (3). The law $\beta = 2$ also follows from the so-called three-dimensional model of a comet's head developed by Mokhnach [11]. Taking account of the acceleration of solar repulsion, Mokhnach maintained that the number of luminous molecules at a given point of the reference plane $n_1 \sim r_1^{-1}$ (r_1 is the distance from the center of the nucleus in this plane), which corresponds to the law $n \sim r^{-2}$ for the number of molecules in a unit volume. Substituting the value $(\frac{dv}{dr})_\odot = 3 \cdot 10^{-6}$ sec^{-1} ($g_0 = 0.6$ cm/sec^2, $1 + \mu = 1$, $v_0 = 2 \cdot 10^5$ cm/sec, $r_\odot = 1$ AU) into (5), we will obtain a concentration of $n_{0d} = 7.5 \cdot 10^3$ cm^{-3}, for which the dust cannot be recorded over the observed distribution of the type in (3) for gaseous molecules in the head of the comet. Therefore, it can be considered that the "normal" (corresponding to the distribution in (3) at $\beta = 2$) concentration of dust near the nucleus does not exceed 10^4 cm^{-3}.

Let us examine some problems regarding the dust component which have not been discussed to a great extent in the literature.

Formulas (1) and (2) can be improved if we consider the relative percentage of dust k, which is equal to the ratio between the brightness of the dust component of the coma and that of the gas component at $r_\odot = 1$ AU, i.e.,

$$k = \frac{I_{0d}}{I_{0r}}. \tag{6}$$

Considering (6) and the expression for the absolute magnitude of the comet, i.e.,

$$m_0 = -2.5 \log I_0 = -2.5 \log (I_{0r} + I_{0d}), \tag{7}$$

we will obtain the following expression for the brightness of the dust component in stellar magnitudes:

$$m_{0\pi} = 2.5 \log \frac{1+k}{k} + m_0. \tag{8}$$

When k is known, we must take $m_{0\pi}$ according to (8) instead of m in (1) and (2). The values of k were determined in [24, 27, 7, 8]. Table 1 gives the masses of the dust components M of a number of comets for $r_{\odot}$ - 1 AU, as calculated according to (2), with a consideration of (8); as regards the values of ρ_d, A, $X(\vartheta)$ and Q, we made the same assumptions as Rozhkovskiy [16]. The values of m_0 and k were obtained by the author of [7]. The time during which the particles remain in the head of the comet can be estimated from Orlov's relationship [13], i.e., /169

$$\tau = 2.41 \sqrt{\frac{2\xi_0}{a}}, \qquad (9)$$

where $2\xi_0$ is the diameter of the cometary head, a is the repulsive acceleration of the Sun for particles of sizes ranging from 0.1 to 0.15 μ ($\frac{a}{g_0} = 1 + \mu = 2$ [2, p.50]). The capacity of the dust of the comet $M' = \frac{M}{\tau}$ is given in Table 1. The data on the diameters of the comet's heads were taken from [1].

TABLE 1

Comet	m_0	k	M, g	$2\xi_0$, cm	τ, sec	M', g/sec
1853 III	4.4	0.10	$4\cdot10^6$	$8.9\cdot10^9$	$2.1\cdot10^5$	19.0
1881 III	5.6	0.77	$2\cdot10^7$	—	—	—
1884 I	5.0	0.27	$3\cdot10^7$	$2.2\cdot10^{10}$	$3.3\cdot10^5$	91.0
1910 II*	5.7	0.07	$2\cdot10^6$	$2.04\cdot10^{10}$	$3.2\cdot10^5$	6,3
1910 II**	4.6	0.02	$2\cdot10^6$	—	—	—
1914 V	1.4	0.09	$2\cdot10^8$	—	—	—

* Before perihelion; ** After perihelion

Vanysek [28] evaluated the mass of the dust as 10^7 - 10^{11} g (assuming that the particles are distributed by size according to the law h^{-4}) on the basis of photoelectric observations of the continuous spectrum of 12 comets observed in 1954 - 1964. This agrees with the data of Table 1.

The dust particles are released from the nucleus as the ice evaporates [31]. A.Z. Dolginov pointed out the other possibility that the particles could be formed by condensation of gases in the vicinity of the nucleus. Remy-Battiau [22] discussed the scattering of solar radiation on ice particles with H_2O, CO_2, NH_3, CH_4, etc. using the Mi theory (the size of the particles is of the order of the wavelength of the light). However, ice particles of these dimensions evaporate rapidly by the effect of the photon radiation of the Sun and, consequently, can be only in the immediate neighborhood of the surface of the nucleus. This fact is corroborated by calculations. The radius of a spherical field of ice with one side turned toward the Sun which evaporates completely by the effect of

solar radiation in a time of τ_0 is determined by the following expression: /170

$$h = \frac{3\varkappa q_0 m_M \eta_i \tau_0}{4 r_\odot^2 \rho L}, \tag{10}$$

where q_0 = 2.0 cal·cm^{-2}·min^{-1} = 3.33·10^{-2}cal·cm^{-2}·sec^{-1} is the solar constant, m_M is the mass of an ice molecule, ρ is its density, L is the heat of evaporation of one molecule, cal, κ is the ice absorption factor of the solar radiation, η is the efficiency of the ice evaporation, which is equal to the ratio between the amount of heat used in evaporation and the heat of the Sun absorbed by the nucleus. For example, for ice of H_2O at $\hbar$ = 0.5 μ, κ = 0.5, η = 0.04 [8], ρ = 0.9 g/cm^3, L = 2·10^{-20} cal for $r_\odot$ = 1 AU, τ_0 = 20 sec; for ice of CH_4 (h = 0.5 μ, $\eta \cong 1$, ρ = 0.52, L = 3.67·10^{-21}) τ_0 = 0.15 sec. Thus, the particles from non-volatile ices of the H_2O type can exist in the atmosphere of a comet only at great distances from the Sun.

The distribution function of the cometary dust particles by radii has been studied insufficiently. Weigert [30] uses the following expression for the distribution function:

$$\varphi(h) = A_1 h^{-p}, \tag{11}$$

while

$$2.6 \leqslant p \leqslant 4.2 \ (h_1 \leqslant h \leqslant h_2).$$

The coefficient A_1 is determined from the normalization condition

$$I = A_1 \int_{h_1}^{h_2} h^{-p}\, dh. \tag{12}$$

At the same time, the following function of the distribution of particles by masses in meteoroid showers is well known:

$$\psi(M) = BM^{-s}. \tag{13}$$

We should mention that the distribution of (11) and (13) are differential. For the weaker and most numerous meteors, s is close to three, for example for meteors of $+12^m$ - $+15^m$ s = 3.4, while for brighter ones it is 2.9 [17], for sporadic ones 2, for Quadrantid meteors 1.7, and for Geminids 1.7 and 3.7 [18]. The identity of the orbits of the comets and the corresponding meteoroid showers, as well as the agreement between the physical data on meteors and /171 the model of the cometary nucleus, speak in favor of the theory by

which meteoritic particles consist of cometary matter [6]. It is natural to assume, that a distribution of particles by masses similar to that in (13) also occurs in the atmosphere of a comet. The indices s and p are connected by the following relationship [5]:

$$p=3s-2. \tag{14}$$

Since, ordinarily, $s \geq 2$, then $p \geq 4$ in the expression in [11]. Table 2 gives the coefficients A_1 of the distribution in [11], the mathematical expectations $M\{h\}$ and the root-mean-square deviations $\sigma\{h\}$, which were calculated for different s and p, while it was assumed that $h_1 = 0.1$ μ, $h_2 = 0.7$ μ. We should mention that A_1 depends almost solely on h_1.

TABLE 2

s	p	A_1	$M\{h\}$, μ	$\sigma\{h\}$, μ
2	4	3.10^{-15}	0.15	0.06
3	7	6.10^{-30}	0.12	0.002
4	10	9.10^{-45}	0.11	0.001

The motion of the dust particles in the stream of cometary gas which carries them along was studied in detail by Weigert [30] and the author [9] for the case of low "dustiness" of the atmosphere ($n \sim r^{-2}$). The repulsive force of the Sun not taken into account in these studies. Further, a repulsive acceleration of $(1 + \mu)g_\odot$ is made to be comparable with the acceleration due to the effect of the flow of cometary gas, and exceeds it at substantial distances from the nucleus. For the case under investigation, at $r < 10R_0$, i.e., in the immediate vicinity of the nucleus, the velocity of the dust particles rapidly reaches the critical value v_π, and its dependence on the size of the dust particles h is determined by the following expression:

$$v_d = v - b\sqrt{h}, \tag{15}$$

where v is the velocity of the gas flow,

$$b = \frac{2}{3}\sqrt{\frac{2\pi k^2 \rho_0 \rho_\pi R_0}{m_M n_0}}, \tag{16}$$

m_M is the mass of the gas molecule, ρ_0 is the density of the nucleus, and k^2 is the gravitational constant. It can be seen from (15) that v_d depends only slightly on h. The constancy in the velocity of the dust particles has been affirmed by observations [12]. Considering the uniformity in movement of the dust particles in the radial direction, we can assume that the concentration of dust (number of dust particles in a unit volume) decreases with r accord- /172

ing to the inverse square law, i.e.,

$$n_{id} = n_{0d}\left(\frac{R_0}{r}\right)^2. \qquad (17)$$

Considering the distribution of (11) and (17), we can calculate the number of dust particles in the head of the comet N and the mass of the dust component M:

$$N = 4\pi A_1 R_0^2 R n_{0d} \frac{h_2^{1-p} - h_1^{1-p}}{1-p}, \qquad (18)$$

$$M = 52.7\, A_1 \rho_{id} n_{0d} R_0^2 R \frac{h_2^{4-p} - h_1^{4-p}}{4-p} \quad \text{at} \quad p > 4,$$

$$M = 52.7\, A_1 \rho_{id} n_{0d} R_0^2 R \ln \frac{h_2}{h_1} \quad \text{at} \quad p = 4, \qquad (19)$$

where R is the radius of the cometary head, and n_{0d} depends on $r_\odot$ and the individual characteristics of the comet and changes for different comets in a very wide range. Thus, at $p = 7$, $A = 6 \cdot 10^{-30}$, $\rho_d = 0.3$ g/cm^3 (average density of the particles of meteoroid showers [29]), R_0 10^5 cm, R 10^{10} cm and M 10^6 - 10^{11} g, n_{0d} 0.3 -3.10^4 cm^{-3}. Correspondingly, the total number of dust particles in the heads of comets N is 10^{21} - 10^{26}. Additional data on the structure of the dust component of cometary atmospheres and the dust concentration can be found from observations of obscurations of stars by comets.

References

1. Vsekhsvyatskiy, S.K.: Fizicheskiye kharakteristiki komet (The Physical Characteristics of Comets). Moscow, "Fizmatgiz", 1958.
2. Dobrovol'skiy, O.V.: Nestatsionarnyye protsessy v kometakh i solnechnaya aktivnost' (Non-Stationary Processes in Comets and Solar Activity). Academy of Sciences of the Tadzhik S.S.R. 1961.
3. Yegibekov, P.: In the book: Issledovaniye komet po programme Mezhdunarodnogo goda spokoynogo Solntsa (An Investigation of Comets According to the International Quiet Sun Year Program). Kiev, "Naukova Dumka", p. 48, 1964.
4. Konopleva, V.P.: Informatsionnyy Byull., Vol. 10, pp. 77-91, 1966.
5. Levin, B.Yu.: Fizicheskaya teoriya meteorov i meteornoye veshchestvo v solnechnoy sisteme (The Physical Theory of Meteors and Meteoric Matter in the Solar System). Moscow, Academy of Sciences of the U.S.S.R., 1956.
6. McKinley, D.: Metody meteornoy astronomii (Methods of Meteoric Astronomy). Moscow, "Mir", 1964.
7. Markovich, M.Z.: Byull. Instit. Astrofiziki Akad. Nauk Tadzh, S.S.R., Vol. 28, p. 25, 1959.

8. Markovich, M.Z.: Author's Abstract of Candidate's Dissertation, 1962.
9. Markovich, M.Z.: Byull, Komissii po Kometam i Meteoram, Vol. 8, /173 No. 11, 1963.
10. Markovich, M.Z.: In the book: Aktivnyye protsessy v kometakh (Active Processes in Comets). Kiev. "Naukova Dumka", 1967.
11. Makhnach, D.O.: Byull. Instit. Teor. Astro., Vol. 6, p. 269, 1956.
12. Orlov, S.V.: Komety (Comets). Moscow-Leningrad, "ONTI", 1935.
13. Orlov, S.V.: Golova Komety i novaya klassifikatsiya kometnykh form (The Comet Head and a New Classification of Comet Forms), Moscow, "Sovetskaya Nauka", 1945.
14. Poloskov, S.M.: Vestnik Moskovs. Gosudarstv. Universit., No. 2, 1948.
15. Rozhkovskiy, D.A.: Byull. Komisii po Kometam i Meteoram, Vol. 10, No. 3, 1965.
16. Rozhkovskiy, D.A.: In the book: Fizika komet i meteorov (The Physics of Comets and Meteors). Kiev, "Naukova Dumka", p. 5, 1965.
17. Rubtsov, L.N.: Author's Abstract of Candidate's Dissertation. - Dushanbe, 1966.
18. Fialco, E.I.: Radiolokatsionnyye metody nablyudeniya meteorov (Radar Methods of Observing Meteors), 1961.
19. Houziaux, L.: University de Liege Inst. d'Astrophys. Collection in 8°, p. 407, 1959.
20. Hruska, A.: Bull. Astr. Inst. Czechoslovakia, Vol. 5, No. 4, 1954.
21. Liller, W.: Ap. J., Vol. 132, No. 3, p. 867, 1960.
22. Remy-Battiau, L.: Bull. Acad. Roy. Belg., Vol. 50, No. 2, pp. 74-89, 1964.
23. Sekanina, Z.: Bull. Astr. Inst. Czechoslovakia, Vol. 10, No. 2, 1 1959.
24. Sekanina, Z.: Bull. Astr. Inst. Czechoslovakia, Vol. 10, No. 1, p. 34, 1959.
25. Vanysek, V.: Contr. from the Astr. Inst. of the Masaryk Univers., Brno. Vol. 1, No. 9, 1952.
26. Vanysek, V., F. Hrjebik: Bull. Astr. Inst. Czechoslovakia, Vol. 5, p. 4, 1954.
27. Vanysek, V.: Publ. CSAV, Astr. Ustav., pp. 34-43, 195-211, 1958.
28. Vanysek, V.: Mem. Soc. Roy. Sci. Liege., Vol. 12, pp. 255-260, 1966.
29. Verniani, F.: Nuoro cimento, Vol. 33, No. 4, pp. 1173-1184.
30. Weigert, A.: Astr. Nachricht., Vol. 285, No. 3, pp. 117-128, 1959.
31. Whipple, F.: Ap. J., Vol. 11, p. 375, 1950; Vol. 113, p. 464, 1951.
32. Whitney, Ch.: Ap. J., Vol. 122, p. 190, 1955.

BRIGHTNESS VARIATION AND PHOTOMETRIC PARAMETERS OF COMET KILSTON (1966b)

G.A. Garazdo-Lesnykh and V.P. Konopleva

ABSTRACT: Some information is given on the observations of Comet Kilston which were carried out at the Main Astronomical Observatory of the Academy of Sciences of the Ukrainian S.S.R. (Kiev) and at the Skalnate Pleso Observatory (Czechoslovakia) from August 12 to September 15, 1966. Photographic (31 estimates) and photovisual (6 estimates) magnitudes were found. These magnitudes were reduced to the volume of the coma with radius of 25,000 km. The photographic brightness of Comet Kilston was almost invariable: $(9.9 - 9.6)^m \pm 0.3^m$. The absolute magnitude, $H_{10}(pg)$, was 4.4 ± 0.1^m. The color index of the comet was $(0.7)^m \pm 0.2^m$. Visual observations show a somewhat greater increase in the brightness of the comet during this period, and $H_{10}(v) = 4.1^m \pm 0.2^m$. The changes in appearance of this comet are described.

In order to determine the integral brightness of Comet 1966b (Kilston) in the photographic and photo-visual lines we used 37 straight-line photographs. Of these, 15 were obtained with the binary astrograph (12/70 cm) of the Main Astronomical Observatory of the Academy of Sciences of the Ukrainian S.S.R., and 22 were obtained with the astrograph of 30/150 cm of the Skalnate Pleso Observatory of the Slovakian Academy of Sciences. A list of the negatives is given in Table 1 (the following conditional designations of the observers are used: GG, G.A. Garazdo-Lesnyhh; VK, V.P. Konopleva; VS, V.I. Stupin). /174

The photometric measurements of the negatives were carried out with the aid of the microphotometers MF-2 (33 images of the comet) and MF-4, which was equipped with the automatic recorder EPP-09 (four images). Circular diaphragms with diameter from 2.47 to 7.57mm were used in the first case, and a square slit was used in the second. The photometric sections were made in the direction perpendicular to the star trails.

One of the images on plate 69-15 (exposure of 1 min) was obtained without guiding, with disconnected second control of the timer mechanism. The comet and stars have the appearance of short dashes. In deriving the stellar magnitudes, a correction was made for the varying length of the trails of the comet and the reference stars. The guiding was carried out along the comet during hourly exposures. In this case, the integral intensity of emission of the comet was

TABLE 1

/175

No. Photograph	Date, UT	Observation Site	Exposure, min.	Type of Plate	Observer	Comment
	1966 August					
60—6	12.8892	Skalnate	10.5	OPBO ZU-2	VK	—
61—7	.9029	Pleso	4.0			—
62—8	.9864		1.0			—
64—10	13.8355		1.0			1
66—12	.8482		6.5			—
—	.8892		60.0			2
67—13	.9182		4.0			—
68—14	.9238		2.0			—
18826	15.8551	Kiev	31.0	OPBO ZU-1	GG	1
1882a			31.0	Agfa Panchrome		1,3
18836	16.8105		30.0	OPBO ZU-1	VS	1
1883a			30.0	Agfa Panchrome		1,3
18846	.8417		30.0	OPBO ZU-1		1
1884a			30.0	Agfa Panchrome		1,3
69—15	17.8623	Skalnate	1.0	OPBO ZU-2	VK	1
	.8659	Pleso	0.5			—
	.8678		0.5			—
70—16	.8996		60.0			—
72—18	.9416		6.0			—
74—20	18.8545		6.0			—
	.8579		0.5			—
75—21	.8864		60.0			—
76—22	.9208		1.0	OPBO ZU-1		—
	.9230		0.5			6
18856	19.7952	Kiev	30.0	OPBO ZU-1	VS	1,4
18866	.8237		30.0			1
1886a			30.0	Agfa Panchrome		1,3
81—26	19.9385	Skalnate Pleso	6.0	OPBO ZU-2	VK	—
18876	20.8251	Kiev	30.0	OPBO ZU-1	VS	1,5
1887a			30.0	Agfa Panchrome		1,3,5
18886	.8668		30.0	OPBO ZU-1		1,5
88—30	28.8327	Skalnate	6.0		VK	—
89—31	.8406	Pleso	1.0			1
	.8444		2.0			—
	September					
18956	15.7524	Kiev	15.0	Kodak OaO	VS	1
18966	.7701		30.0			1
1896a			30.0	OPBO ZP-1		1,3

Comments: (1) stellar guiding; (2) the plate is broken up, but the image of the comet is not harmed; (3) photograph with orange filter; (4) the edges of the negative are illuminated preliminarily; (5) cirrus; (6) very weak image.

found according to the data of the distribution of surface brightness along the radius of the coma. The accuracy of these estimates does not exceed $\pm 0.3^m$, since the photographs were not standardized or calibrated.

Let us give a brief description of the external appearance of the comet on the negatives which were analyzed.

60-6. A very dense nuclear condensation surrounded by a clearly noticeable, slightly prolonged coma. 61-7. Dense bright nuclear condensation, weak coma. 62-8. Almost point nucleus (clearly not stellar), very weak coma. 64-10. Because of inaccurate setting of the timer mechanism, the images of the comet and stars are slightly extended (trails roughly equal to 25″). Only the circum-nuclear region of the comet was obtained. 62-12. A weak coma can be seen around a dense, non-stellar condensation. On the photograph with hourly exposure (August 13, 89), the coma is well developed, and /176 the nuclear condensation is overexposed. The tail is wide, gradually narrowing. Same for plates 72-18, 88-30 and 67-13. Prolongation of the coma is noticed on photograph 63-13. 68-14. The nuclear condensation and coma seem to be perfectly circular (same for plate 75-21). 1882a. Extrafocal photograph. Assymetric diffuse coma extended from southeast to northwest. 1882b. The images of the comet and stars are blurred. The comet has the form of a diffuse patch with concentration around the center. 1883a, 1883b. The photographs are slightly extrafocal. 1884a, 1884b. The comet is in the shape of a diffuse patch. The coma is oval and extended from southeast to northwest (same for 1885b, 1886a). 69-15. The two images of the comet (exposure of 0.5 min) are almost pointed. Only the densest segment of the nuclear condensation appeared. On the photograph with exposure of 1 min, the images of the comet and stars are prolonged. This photograph was scanned photometrically with the aid of an MF-4. 70-16. The bright nuclear condensation appears slightly eccentrically inside a rather dense coma. The coma is traced from 2.5′ from the nucleus with the aid of an MF-4. 74-20. A circum-nuclear cloud can be seen. The coma is not symmetric. 81-26. Only the nuclear condensation can be seen, and the trails of the coma are hardly noticeable. 1887a. Same as for 1884a. The condensation is shifted toward the south. 1887b, 1888b, 1895b. 1896a, 1896b. The nuclear condensation is slightly extended. 89-31. The circum-nuclear condensation has a clearly non-stellar appearance. On the photograph with exposure of 1 min, there are no traces of the coma, and on the photograph with exposure of 4 min, there is a weak coma.

On the photographs with short exposures (0.5, 1.0 and 2.0 min), a small, dense and practically round nuclear condensation of a clearly non-stellar appearance is very noticeable. It is surrounded by a very weak coma. The tail cannot be seen. The photographs with somewhat longer exposures (4 or 6 min) give more distinguishable images of the coma. The nuclear condensation has an almost circular shape as before. However, it is found that it is distributed asymmetrically with respect to the "center" of the slightly

extended coma. A small and extremely bright nuclear condensation ($d \approx 10''$) surrounded by a rather dense cloud ($D \sim 30''$) is clearly distinguished on the photograph of August 13.89 with exposure of 1 hour. It is clearly displaced with respect to the center of this cloud. The coma is weak, but very extended. A weak tail can be traced up to 5.5-6′ from the nucleus. On the two other photographs with exposure of 1 hour, the coma seems to have even larger apparent dimensions (it is traced up to 2.5′ from the nucleus with the aid of the MF-4); however, it is very weak.

The magnitudes of the reference stars were taken from [1, 4, 5] and from the AGK_2 catalogues. They are given in Table 2, while the results of an analysis of the straight-line photographs of the comet are given in Table 3 (d is the diameter of the densest part of the circum-nuclear region, D is the diameter of the apparent coma in seconds of arc, m_{ob} is an estimate of the integral luminosity of the comet as derived from observations). /177

It can be seen that m_{ob} clearly depends on the duration of the exposure, i.e., on the apparent diameter of the coma. In this regard, we found it necessary to reduce the observed estimates of the luminosity of the comet to some defined volume of the coma. Having constructed graphs representing the dependence of the average values of the stellar magnitude of a comet from one square second on the dimensions of the visible coma (the observations of 2-3 dates were combined), we found the values of m which corresponded to a diameter of the head equal to 50,000 km. They are given in Table 3. It was found that the estimates of the brightness of the comet in the photographic lines which were derived according to the photographs of Skalnate Pleso differ systematically from those of Kiev. At Skalnate Pleso, the comet seemed to be 0.9^m brighter than at Kiev, although the zero-point of both photometric systems practically coincided. A comparison of the brightness of two stars of the G5 type and two stars of the K0 type derived from plates obtained at Kiev and Skalnate Pleso showed that the systems differ on the average by 0.07^m. At the same time, the accuracy of the observed estimates of the brightness does not exceed $\pm 0.1 - \pm 0.2^m$. The higher estimates of the comet's brightness at Skalnate Pleso, compated to those at Kiev, are easily explained since the difference in altitudes over sea level for these observation sites is very substantial (1783, 150 m).

The data of Table 3 were used to obtain approximate value of the color index and photometric parameters of Comet Kilston. It follows from the observations conducted at Kiev that the average value of the color index at the coma of Comet Kilston is equal to $+(0.7 \pm 0.2)^m$.

In order to determine the photometric parameters, the stellar magnitudes of the comet in the photographic lines were reduced to the system of Skalnate Pleso by introducing corrections equal to -0.9^m to all the brightness estimates of Kiev. A graphic balancing

TABLE 2

/178
/179

No.	BD	m_{pg} (B)	m_{pv} (V)	Sp	Source	No. by Source
1	6°3767	(10.^{m}61)	(9.^{m}95)	—	[1],NGC6633	46
2	3769	(9.03)	(8.21)	—		56
3	3806	(10.72)	(10.12)	—		152
4	3809	(10.1)	(9.5)	—		153
5	3812	(11.43)	(10.55)	—		157
6	3996	(10.00)	(8.96)	—		134
7	3998	(9.85)	(8.79)	—		140
8	7 3553	8.1	—	G5	AGK_2	7°2330
9	3613	9.3	—	G5		2367
10	3653	10.3	—	G0		2392
11	3661	8.5	—	K2		2399
12	13 3497	9.4	—	K2		13 1751
13	3503	10.2	—	G5		1754
14	3505	10.4	—	K0		1755
15	3508	(12.37)	(11.77)	—	[2],1800,15°	7
16	3509	10.3	—	G0	AGK_2	13 1756
17	3514	9.0	—	K0		1757
18	3517	9.7	—	K0		1758
19	3519	10.0	—	K0		• 1760
20	3525	10.1	—	K0		1763
21	14°3382	9.2	—	K0		14°1812
22	3390	9.1	—	K2		1817
23	3401	9.4	—	K0		1822
24	3407	10.1	—	G5		1825
25	14 3413	10.1	—	K2	AGK_2	14°1827
26	3417	9.8	—	G5		1830
27	3464	10.71	—	—	[3],ПК86	416
28	3468	11.08	—	—		135
29	15 3418	9.49	—	—		254
30	3419	10.49	—	—		280
31	16 3312	8.6	—	K0	AGK_2	16°1755
32	3313	9.3	—	G0		1756
33	3330	10.2	—	G5		1763
34	3345	9.0	—	G5		1771
35	3347	7.8	—	G0		1773
36	3349	9.0	—	K0		1775
37	17 3349	9.9	—	G5		17°1770
38	3364	(9.82).	(9.64)	—	[2],1800,15°	2
39	3386	9.9	—	G0	AGK_2	17°1782
40	3390	9.2	—	G5		1784
41	3402	10.4	—	K2		1789
42	3414	9.7	—	K0		1794
43	3417	10.3	—	G5		1795

TABLE 2 (cont'd)

No.	BD	m_{pg} (B)	m_{pv} (V)	Sp	Source	No. by Source
44	18°3501	10.^{m}3	—	G5		18°1628
45	3503	10.0	—	K0		1630
46	3506	10.2	—	K5		1632
47	3510	10.1	—	K2		1633
48	3525	10.2	—	K0		17 1792
49	3526	11.1	—	G5		18 1640
50	3530	9.9	—	K0		1642
51	18 3531	11.4	—	K0	AGK$_1$	18 1643
52	3532	11.1	—	G5		1644
53	3549	10.1	—	G5		1654
54	19 3452	9.7	—	K0		19 1664
55	3455	9.0	—	K0		1665
56	3460	10.4	—	K0		1669
57	3466	9.0	—	K0		1672
58	3472	10.7	—	K2		
59	3475	10.4	—	K5		1675
60	3478	10.4	—	K2		1677
61	3495	9.3	—	K0		1683
62	3506	8.9	—	K2		1687
63	3507	11.6	—	K5		1688
64	20 3606	9.23	8^m.15	G5	HD	163469
65	3613	8.1	8.0	A2		163790
66	3617	8.60.	7.60	K0		163908
67	3626	8.7	8.7	A0		164200
68	—	(7.96)	(7.45)	—	[2],1800,15°	3
69	-	(11.28)	(10.23)	—		5

of the summary system was then carried out. The values of $\bar{m}_{50}$ thus derived (Table 3) were used for calculating the average value of the absolute magnitude of the coma (Table 4).

The brightness of the comet changes very slowly in the photographic lines. As can be seen from the description of the negatives, its structure also did not undergo any significant changes. This conclusion agrees well with the data of other observers (I AUC, 1965, 1967, 1971, 1972, 1976, 1981; Kometnyy Tsirkulyar, 46).

A very dense circum-nuclear condensation with diameter of 50-60" (possibly slightly oval) is clearly seen on the reproduction of the photograph which Wirtanen [6] obtained (August 12.256) with the 20" refractor of Lick Observatory (USA, exposure of 36 min, blue spectral region). It is positioned asymmetrically with respect to the center of the coma. The densest part of the coma is almost circular (diameter of about 100"). The coma is traced up to 70-80" from the nucleus. It passes into the very wide tail, which is clearly seen up to 2' from the nucleus.

On August 10 at 0852 UT, L. Aller [6] photographed the spectrum of the comet with the nebular spectrograph of the Lick reflector. The spectrum of the head was mainly continuous. Only the cyanin band λ3883Å can be examined. Aller notes that a very bright circular

TABLE 3

/180
/181

Date, UT	Diaphragm	System	m_{ob}	d	D	m_{50}	$\bar{m}_{50}$	Reference Stars
August								
12.89	49″.5	pg	$10^m.0 \pm 0^m.1$	16″	34″	$9^m.9 \pm 0^m.3$	$9^m.90$	54—57, 59, 60, 61, 63—67
.90	31 .9		10.6± 0.2	10	20			54—56, 59—61, 63—67
.99	16 .2		11.2± 0.1	4	11			54—57, 59, 60, 64, 66, 67
13.84	49 .5		10.2± 0.2	—	14		9.88	54—57, 59, 60, 63—67
.85	49 .5		9.5± 0.1	15	28			54—56, 59, 61, 63—67
.89	3.3·118		9.0(?)	30	82			59, 61, 64—66
.92	49 .5		9.8± 0.2	14	28			54—56, 59—61, 63—67
.92	24 .5		10.4± 0.3	9	12			54—57, 64, 66, 67
15.86	106 .3		10.5± 0.2	—	59	10.9± 0.3	9.87	27—30, 37, 38, 45, 47, 52—54, 57, 58, 61, 62
.86	83 .5	pv	10.1± 0.2	—	37	10.1± 0.2	—	37, 38, 44, 45, 47, 52—54, 57, 58, 61, 62, 69
16.81	58 .0	pg	11.3± 0.2	9	30	10.9± 0.3	9.85	27—30, 37, 38, 45, 47, 52—54, 57, 58, 61, 62, 69
.81	83 .5	pv	10.1± 0.2	18	37	10.1± 0.2	—	37, 38, 44, 45, 47, 52—54, 57, 58, 61, 69
.84	58 .0	pg	10.8± 0.2	28	40	10.9± 0.3	9.85	27—30, 37, 38, 44, 45, 47, 52—54, 57, 58, 61, 62, 69
.84	83 .5	pv	10.1± 0.2	15	32	10.1± 0.2	—	37, 38, 44, 45, 47, 52—54, 57, 58, 61, 62, 69
17.86	—	pg	10.7± 0.2	5	7	9.8± 0.3	9.84	39, 41—43, 45—52, 58, 60, 61, 63
.87	19 .6		10.9± 0.1	5	7			39, 41—44, 46—52, 61, 63
.87	19 .6		11.1∓ 0.1	5	7			39, 41—44, 46—52, 61, 63
.90	—		9.0(?)	27	85			39, 41—43, 45—49, 51, 52, 58, 60, 61, 63
.94	31 .9		10.2∓ 0.2	14	27			39, 41—43, 45—48, 50—52, 58, 60, 61, 63
August								
18.85	49″.5	pg	$9^m.8 \pm 0^m.1$	15″	29″	$9^m.8 \pm 0^m.3$	$9^m.83$	33, 35, 39—44, 46, 48,
.85	24 .5		10.5± 0.1					49, 51, 52, 60
.86	24 .5		9.8± 0.1					
.89	—		9.3(?)	28	~95			39, 41—43, 46, 47, 49, 51, 52, 60
18.92	16 .2		11.1± 0.1	3	~ 9			41—43, 45, 47—49, 51, 52, 58
19.80	83 .5		11.0± 0.2	—	~33	10.7± 0.3	9.82	27—30, 31, 32, 34, 35, 37—41, 44, 52, 53
.82	106 .3		10.1± 0.2	21	~40			27, 29, 30—32, 34, 36, 37—40, 44, 52, 53, 69
.82	83 .5	pv	10.2± 0.2	15—30	40	10.1± 0.2	—	31, 32, 34, 35, 37—41, 44, 52, 53, 69
.94	49 .5	pg	10.7± 0.1	10	12	9.9± 0.3	9.82	33, 35, 39—41, 46, 49, 51, 52
20.83	106 .3		10.5± 0.2	3—4	37	10.7± 0.3	9.79	27—32, 34, 35, 37—41, 44, 52, 53, 69
.83	83 .5	pv	10.2± 0.2	4—6	40	10.1± 0.2	—	31, 32, 34, 35, 37—41, 44 53, 69
.87	106 .3	pg	10.9± 0.2	12	37	10.7± 0.3	9.79	27—32, 35—41, 44, 53, 69
28.83	49 .5		10.1± 0.1	13	38	10.1∓ 0.3	9.73	13—16, 18, 20, 23—26, 68
28.84	31 .9	pg	11.2± 0.3	12	14	10.1± 0.3	9.73	13, 14, 16, 20, 21, 23, 24—26
.84			11.2± 0.3	12	14			13, 14, 16, 20, 21, 23, 24—26
September								
15.75	106 .3		10.2± 0.2	14—30	48	10.5± 0.3	9.61	1—11
.77	106 .3		10.1± 0.2	30	42			1—11
.77	83 .5	pv	10.1± 0.2	15—21	52	10.0± 0.2	—	1, 2, 4, 6—11

NOTE: Tail Length: August 13.89 ~5.5'; August 17.90 ~6.5'; August 18.89 ~5.0'.

TABLE 4 /182

System	H_{10}	H_y	y	Interval of Observations	log r	Observation
m_{pg} ($25 \cdot 10^3$ км)	$4.^m4 \pm 0.^m1$	—	—	12.VIII—15.XI	0.403—0.386	Kiev, Skalnate Pleso
m_V I	4.1 ± 0.2	—	—	8.VIII— 8.XII	0.406—0.378—0.385	All Observations
$\bar{m}_V$ II	4.0 ± 0.1	$0.^m7 \pm 1.^m1$	19 ± 3	10.VIII— 8.XII	0.404—0.378—0.385	Antal, Bakharev (smoothed curve)
$\bar{m}_V$ III	4.1 ± 0.2	$-2. \pm 70.1$	28 ± 0			Same without brightness flashes

condensation with diameter of 10-15″ surrounded by a weak halo can be observed visually. According to observations of V.P. Konopleva on August 17/18 with the guide of the 30-centimeter astrograph of Skalnate Pleso (13/195 cm), an almost pointed luminous nucleus was distinguished inside a rather bright and diffuse condensation. V. S. Houston (August 14) noticed a weak halo with diameter of about 0.5° and a weak tail with length of about 1° with the aid of a 10″ wide-angle telescope. The diameter of the brightest part of the coma was no more than 1′. E. Bortle (August 13) gives the same estimate for the diameter of the circum-nuclear condensation. According to the measurements of E. Bortle, the diameter of the weak diffuse coma was equal to 2′. A wide straight tail with length of 10′ can be seen on the high-contrast print of the photograph which J. Young obtained on the same night (exposure of 60 min) with the aid of a 250-millimeter telephoto-objective. During the following night, a tail with length of 15′ was observed visually (IAUC, 1967). The comet has the appearance of a spherical nebula with diameter of about 1′ and overexposed central condensation on the photographs from the 40-centimeter astrograph of the Crimean Astrophysical Observatory of the Academy of Sciences of the U.S.S.R. (August 13- /183
23) which were obtained with exposure of one hour. The weak tail is traced to distances of 2-3′ from the nucleus. For an exposure of 10-20 min, the image of the comet is spherical, with a sharply pronounced condensation (Kometnyy Tsirkulyar, 45). S.K. Vsekhsvyatskiy, who observed the comet in Kiev visually with a 25-centimeter refractor (F = 4.3 m) of the Astronomical Observatory of Kiev State University, and photographically with the Astropettsval' camera (12/60 cm), noted that the comet reached $8.5\text{-}9.0^m$ on September 20-25. It had a dense central condensation, the nucleus was of $11.5\text{-}12^m$, and there was a weak fuzzy tail with length of about 2′. The comet diminished around October 6-7. Its brightness was $11\text{-}11.5^m$ during this time (possibly the effect of atmospheric haze). It became more diffuse (D = 30-40″) (Kometnyy Tsirkulyar, 44).

The visual estimates of the brightness of Comet Kilston in August of 1966 which have been published by different observers sometimes differ by 1^m. Therefore, to construct the brightness

curve and derive the photometric parameters, we used only those estimates which were derived by A.M. Antol and A.M. Bakharev, who observed the comet during the entire visibility period.

A.M. Bakharev observed the comet with the "Assembi" binocular from August 12 to 17 at the Gissar Observatory of the Institute of Astrophysics of the Academy of Sciences of the Tadzhik S.S.R., and from October 11 to 19 at the main base of the institute at Dushabne. En enlargement of a factor of 40 was used in August-September, and one of 20 was used in October.

The observations of M. Antal (Kometnyy Tsirkulyar, 53 and IAUC, 2009) in August of 1966 were carried out in the territory of Bulgaria and Rumania with a refractor of 20 × 50, and in September-December at Skalnate Pleso with a "Somet" binocular (25 × 100). Antal's estimates differ systematically from those of Bakharev (the comet seemed brighter to the latter). In order to obtain a summary system, a correction of -0.4^m was introduced into all of Antal's estimates; this correction was equal to the difference in estimates of these observers in September-October, 1966. Then, by averaging three successive values for the summary system, which were reduced to a distance of $\Delta = 1$ AU from the Earth, we constructed a smoothed curve for the integral brightness of the comet in the visual lines (Figure). An analysis of this curve showed that there were two brightness flare-ups in Comet Kilston during the observation period (August 13-25 and September 4-12). The amplitude of the first outburst was about $(0.9 \pm 0.3)^m$, and that of the second was $(0.5 \pm 0.2)^m$. The reality of the outburst has been confirmed by the data of the photoelectric observations conducted by I. Tremko (Skalnate Pleso) [2] /184 and A. Mrkos (station in the city of Klet, Czechoslovakia) [2]. The interval between outbursts was roughly equal to two revolutions of the Sun. A small increase in brightness was also observed 25-28 days after the maximum of the first outburst. This gives us reason to assume that the cited brightness flare-ups of the comet were apparently connected with processes occurring on the Sun (this problem needs additional investigation). The color of the comet also changed with time. According to the data of photoelectric observations (Kometnyy Tsirkulyar, 53) [2], in August of 1966 it was equal to $+(0.98 \pm 0.12)^m$ (Skalnate Pleso), to $+(0.68 \pm 0.07)^m$ in September (Klet, Ondrejov), to $+(0.76 \pm 0.01)^m$ in October (Klet), and to $+0.83^m$ in November (Byurakan). According to photographic observations in Kiev, the color index was equal to $+(0.8 \pm 0.2)^m$ in August and $+(0.5 \pm 0.2)^m$ in September. Consequently, despite the fact that the comet was a substantial distance from the Sun (2.38 - 2.55 AU), it was very active.

In order to determine the physical characteristics of Comet Kilston, we found the photometric parameters H_{10}, y and H_y. These values were calculated with the aid of the "Promin" computer according to the following well-known reduction formulas:

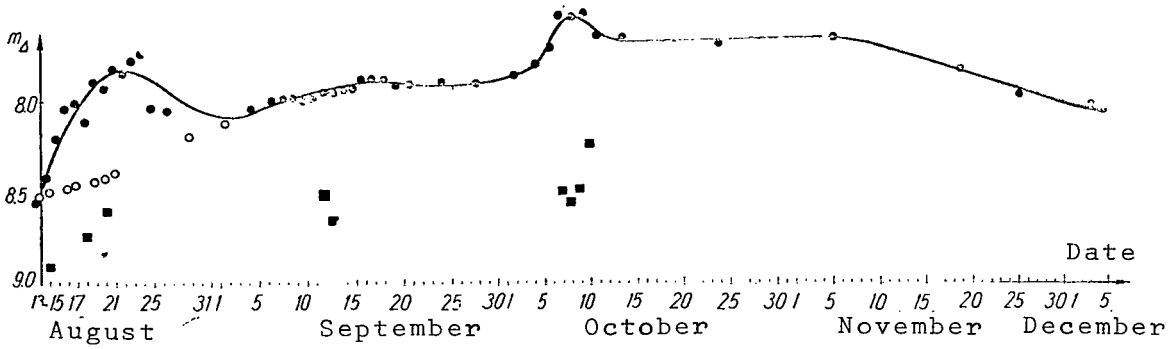

Change in Brightness of Comet 1966b. (●) Visual Observations, Smoothed Curve; (○) Photographic Observations; (□) Photoelectric Observations.

$$m_\Delta = H_y + y \log r,$$
$$m_\Delta = H_{10} + 10 \log r,$$

where $m_\Delta = m - 5 \log \Delta$, m is the observed stellar magnitude, r and Δ are the distances of the comet from the Sun and the Earth calculated by G.R. Kastel' (August 8-October 2, 1966) and Marsden (after October 2) with the elements of Marsden (IAUC, 1972). We did not use other formulas to determine the photometric parameters, since the change in distance of the comet from the Sun did not exceed 0.2 AU during the observations. For the same reason, the true error in the parameters y and H_{10} may be much higher than that calculated. /185

The following groups of estimates of the brightness of Comet Kilston were investigated:

(1) photographic magnitudes of the comet m_{pg} with respect to a coma with radius of $25 \cdot 10^3$ km, determined according to observations at Kiev and Skalnate Pleso;

(2) all the visual estimates of the comet's brightness which have been published, for each day in August of 1966, with mean stellar magnitudes according to the data of all the observers (Kometnyy Tsirkulyar, 44) [3, 6], and with the summary system of M. Antal and A.M. Bakharev for September - December (system m_V, I);

(3) the smoothed brightness curve constructed by averaging the summary system of Antal-Bakharev (system m_V, II);

(4) the smoothed curve without regard for the brightness flare-ups (system m_V, III).

The values given for the absolute magnitude of the comet in the photographic and visual lines and the pronounced continuous spectrum indicate that Comet Kilston is a larger object than the famous Comet

Ikeya-Seki (1965f). Because of the distance from the Sun, this comet was a weak object and therefore did not attract the attention of observers. The photometric data collected by the authors were not sufficient for a detailed study of the physical processes which occured in this comet. The investigations showed that visual observations (particularly in conjunction with photoelectric observations) can be used successfully in order to find the variations in brightness of comets which exceed 0.2 - 0.3^m. Therefore, there must be systematic visual observations of comets at observatories carried out with the cooperation of qualified amateur astronomers.

References

1. Hiltner, W.A., B. Iriarte and H.L. Johnson: Astroph. Journ., Vol. 127, No. 3, p. 539, 1958. /186
2. Mrkos, A., J. Tremko, V. Vanysek: BAC., Vol. 19, No. 1, p. 43, 1968.
3. Rise Hvezd: Vol. 47, No. 10, p. 196, 1966.
4. Sanders, W.L.: Astro. Journ., Vol. 71, No. 8, p. 719, 1966.
5. Seares, F.H., J.C. Kapteyn and P.J. van Rhijn: Publ. Carnegie Inst. a. Washington, p. 402, 1961.
6. Sky a.Telescope, Vol. 32, No. 4, p. 191, 1966.

INVESTIGATIONS OF THE MOVEMENT OF COMETS CARRIED OUT BY THE INSTITUTE OF THEORETICAL ASTRONOMY OF THE ACADEMY OF SCIENCES OF THE U.S.S.R. (1963-1966)

N.A. Bokhan

ABSTRACT: The studies of cometary movements which were carried out by the Institute of Theoretical Astronomy of the Academy of Sciences of the U.S.S.R. during the period of 1963-1966 are reviewed. A brief summary of 37 studies is given.

The investigations of the movement of comets by the Institute /187
of Theoretical Astronomy of the Academy of Sciences of the U.S.S.R. are being carried out in cooperation with specialists working in other astronomical institutions of the Soviet Union. The studies are conducted according to a single plan which consists of the following divisions:

(1) Ephemeris survey of comets;

(2) Refinement and determination of the terminal orbits, calculation of the original and future orbits;

(3) New systematic analyses, construction of the foundations of the coordinates and ellipses of the large planets, and programs for computer calculations;

(4) Theoretical investigations;

(5) Mass study of the evolution of cometary orbits.

Let us give a brief review of the studies which were carried out in 1963-1966.

The ephemeris survey includes:

a calculation of the elements and ephemerides for forthcoming apparitions of short-period comets;

a calculation of the ephemrides of newly-discovered comets;

observation of the comets.

The following studies relate to the first point:

S.G. Makover [20, 36] calculated the elements of Comet Encke for 1964 and gave the ephemeris for 1963-1964 with a consideration of the perturbations from six planets (Mercury-Saturn).

G.R. Kastel [35] calculated the perturbations from six planets for one revolution in 1964, on the basis of the elements of Comet Encke, and gave the ephemeris for 1967.

V.K. Abalakin and N.A. Belyayev [1, 34] obtained the elements of Comet Tuttle (1790II) for 1967 and ephemeris for 1966. Using the elements which A. Crommelin obtained for 1939, the authors took account of the perturbations from eight planets (Venus-Pluto) for the period of 1939-1967. The calculations were carried out on a BESM-2 computer.

M.A. Merzlyakova [29, 37] continued the study of the movement of the Comet Ashbrook-Jackson (1956II). Using the elements obtained in 1956, she integrated the equations of motion of the comet for one revolution, considering the perturbations from six planets (Venus-Uranus) and gave the ephemeris for 1964-1965. The comet was again detected and observed by its ephemerides for more than three /188 years.

Calculations of the ephemerides of newly-discovered comets with the aid of the BESM-2 was the object of M.A. Mamedov's study. He calculated a series of preliminary orbits of Comet Ikeya-Seki (1965f) and gave a number of ephemerides for 1965 [24, 25]. The first cometary orbit he computed was very unreliable. Despite this fact, it aided Soviet astronomers in finding and observing the comet. According to this orbit, the comet should have collided with the Sun on October 23 (perihelion distance of $q = 0.003575$). Although subsequent clarifications of the orbit did not affirm that the comet would collide with the Sun, this orbit nevertheless showed that the comet is an interesting object for astronomers. Elements of the cometary orbit which were obtained were reported in "Astrosovet", "Kometnyy Tsirkulyar", "Astronomicheskiy Tsirkulyar" and a number of observatories.

Somewhat later, L. Kenning, Z. Sekanina and M. Mamedov carried out more precise computations. The elements of the cometary orbits which M.A. Mamedov calculated, as well as the daily and hourly ephemerides, were reported by different observatories of the Soviet Union.

Many observatories of the Soviet Union carried out observations of the comet according to the existing information, both near the perihelion and after the passage of the comet through the perihelion, using the ephemerides calculated at the Institute of Theoretical Astronomy.

M.A. Mamedov [23, 27, 28] also determined preliminary orbits and gave ephemerides of Comets Alcock (1965h), Kilston (1966b), Barbon (1966c) and Ikeya-Everhardt (1966d). The orbits and ephemerides are reported in a number of observatories of the Soviet Union and published in "Kometnyy Tsirkulyar".

Observations of comets are being conducted in cooperation with the Crimean Astrophysical Observatory of the Academy of Sciences of the U.S.S.R.

N.S. Chernykh observed Comets Ikeya-Seki (1965f), Alcock (1966h), Kylston (1966b), Barbon (1966c), Ikeya-Everhardt (1966d) and Van Biesbroeck (1954IV).

S.A. Feoktistova (Institute of Theoretical Astronomy) constructed a program for the BESM-2 in order to obtain the spherical coordinates of an object according to the rectilinear coordinates of the object measured on the plate. Using this program, the Institute of Theoretical Astronomy systematically calculates the coordinates α and δ according to the measurements of plates which the Crimean Astrophysical Observatory and some other Soviet observatories send. The studies on calculations of the coordinates α and δ of newly discovered comets are being conducted exceptionally hurriedly. On the /189 day the letters or photo-telegrams with the results of plate measurements are obtained (or the following day in the extreme case), we calculate the requisite values on the electronic computer, use these values for a hurried determination of the orbit and ephemeris, and send them for publication in "Kometnyy Tsirkulyar".

For an example of the quick analysis of cometary positions, we can mention the measurement of plates and determination of orbits of Comet Ikeya-Seki. Four hours after the telegrams were obtained from the Crimean Astrophysical Observatory, we had distributed information on the ephemeris of this comet to all interested institutions, so that it could be observed further. This work is done by N.V. Ashkova.

The studies on calculations of the orbits can be divided into these three groups:

Refinement of the orbits of short-period comets with a determination of the anomalies in their movement;

Calculation of the ultimate orbits of long-period comets;

Calculation of the original and future orbits of long-period comets.

The following investigations involve refinements of the orbits of short-period comets:

S.G. Makover and S.I. Luchich [19] refined the orbit of Comet Encke on the basis of observations of this comet in 1947, 1950-1951, 1953-1954 and 1957 and obtained a good idea of the future observations of the comet in 1960. The perturbations from eight planets (Mercury-Neptune) were taken into account for the period of 1947-1957, while those from six planets (Mercury-Saturn) were considered for the period of 1954-1960. The authors determined the coefficient of secular acceleration during this period, which was equal to 12.6".

F.B. Khanina [33] used the system of elements of Comet Faye and, in 1959, connected four apparitions of the comet in 1932, 1936, 1947 and 1954. She also considered the disturbances from seven planets (Mercury-Uranus). The average error was +2.2".

M.P. Imnadze [11] made the orbital elements of Comet Wirtanen (1947XIII) which G. Merton obtained in 1948 more precise, for two apparitions in 1948 and 1954, considering the disturbances from five planets (Venus-Saturn). Integration over the more precise elements was conducted on the "Ural-1" computer, with a consideration of the disturbances from Jupiter and Saturn during the periods of 1948-1922 and 1954-1972. Two convergences of the comet with Jupiter in 1923 and 1971 were established.

The following authors studied computations of the ultimate orbits of comets: /190

I.V. Galibina and O.N. Barteneva [10] determined the ultimate orbit of Comet Johnson (1950I) on the basis of 97 observations with a consideration of the disturbances from seven planets (Venus-Neptune).

M.A. Mamedov [26] gave the ultimate orbit of Comet Kenning (1941I). He used 400 observations and considered the perturbations from five planets (Venus-Saturn). The calculations were carried out on the BESM-2. Mamedov also obtained the ultimate orbit of Arend-Roland (1957III), using 600 observations and considering the disturbances from five planets. The average error in unit weight was ±2.0".

L.M. Belous [4] determined the terminal orbit of Comet Bappu-Boch-Newkirk (1949IV), using 83 observations from June 29, 1949 to May 15, 1940, with a consideration of the disturbances from four planets (Venus, Earth, Jupiter, Saturn).

L.M. Belous [5] also calculated the ultimate orbit of Comet Mrkos (1953II), using 71 observations from December 10, 1952 to July 18, 1953, with a consideration of the disturbances from the same four planets. The average error in unit weight was ±0.56".

O.N. Barteneva [3], using the elements of Dubyago in 1943, calculated the ultimate orbit of Comet 1943I (Whipple-Fedke-Tezvadze). She analyzed 550 observations, taking account of the disturbances from six planets (Mercury-Saturn). The average error in unit weight was ±1.7". The calculations were carried out without a computer, therefore, a control computation was made according to the program of M.A. Mamedov.

The following authors investigated original and future orbits:

I.V. Galibina [8, 9] investigated the original and future orbits of long-period comets, applying the method of considering the dis-

turbances in elements with the real anomaly as the independent variable. She obtained 20 original (16 elliptical and 4 hyperbolic) and 17 future orbits (9 elliptical and 4 hyperbolic included). For the majority of the comets, the disturbances from four planets (Jupiter-Neptune) were considered.

O.N. Barteneva [2] calculated the original and future orbits of Comet Johnson (1950I) on the basis of the ultimate orbit which she and I.V. Galibina had obtained.

As for the systematic analyses and construction of programs for computer calculations, there are a number of different studies.

Development of a new method to take account of the disturbances from the contraction of Jupiter. /191

G.R. Kastel' [18] investigated the movement of Comet Brooks during the course of three years before its discovery (1889-1886) with a consideration of the disturbances from five planets (Venus-Saturn) and from the contraction of Jupiter in the neighborhood of the perijovian; as a result, she obtained the shortest distance of the comet from Jupiter as 0.000985 AU. The radius of the disturbing effect of contraction of Jupiter was 0.02 AU. The results of this study will prove to be of substantial aid in investigations of large-scale transformations of cometary orbits in the sphere of the effect of Jupiter for more precise determinations of its mass, as well as for launching artificial satellites.

Construction of the foundation of coordinates for all the large planets, development of a new method for integration of the equations of motion in particular coordinates with double accuracy, taking all the planetary disturbances and deviations from Newton's law of gravity into account, and construction of programs for the BESM-2.

Ye.I. Kazimirchak-Polonskaya [13, 14] clarified the theory of the motion of Comet Wolf I which M.M. Kamenskiy constructed for revolution 1918-1925, which includes its passage through the effective sphere of Jupiter in 1922, on the basis of the methods and program developed for calculations on the BESM-2. This study was undertaken in order to eliminate the discontinuity in the theory of the motion of Comet Wolf I and as a preparation stage for more precise determinations of the mass of Jupiter.

Construction of the foundation of osculating ellipses of eight planets for the interval 1660-2060 and construction of the program (for the BESM-2) of integration by the Cowell method.

N.A. Belyayev studied this theme. The program was constructed in cooperation with G.M. Sitarskiy of the Polish Academy of Sciences.

Construction of a library of standard and typical programs for electronic computers.

All the scientists at the Division of Small Planets and Comets directed by N.A.Bokhan are working on this theme. As a result, programs which provide for the principal calculations connected with investigations of the movement of comets have been constructed.

The following authors are carrying out theoretical investigations:

N.S. Yakhontova [32] gave a review of the studies on the movement of comets which were carried out up to 1963.

F.B. Perlin [30, 31] made a brief review of the methods of calculating the perturbations of comets moving along ellipses with great eccentricities, and proposed a method of varying arbitrary constants, with the eccentric anomaly as the independent variable. She also described the auxiliary tables she had constructed. /192

S.G. Makover pointed out in [21] that the disturbances in orbits of long-period comets from fixed stars could be calculated if the eccentric anomaly were taken as the independent variable.

In [22], it was suggested that the capture hypothesis could not explain the passages of at least several short-period comets.

The evolution of cometary orbits was investigated by Ye.I. Kazimirchak-Polonskaya and N.A. Belyayev.

Ye.I. Kazimirchak-Polonskaya [15, 16] continued the studies of M.M. Kamenskiy, investigating the evolution of Comet Wolf I in an interval of 400 years (1660-2060) with a consideration of the disturbances from eight planets and the secular deceleration in movement of this comet. She studied the movement of Comet Bernard (1892V) during the course of 90 years before its discovery, and found that a generality in the passage of comets Wolf I and Bernard could be possible.

N.A. Belyayev [6, 7] investigated the evolution of orbits for 400 years (1660-2060) with respect to Comets Daniel (1909IV), Neujmin 2 (1916II), Comas Sola (1927III) and Schwassmann-Wachmann 2 (1929I) in order to determine the regularities in the transformations of the orbits of these comets by the effect of large disturbances from Jupiter and in order to calculate the effect of convergences with Jupiter on the detection of comets.

Ye.I. Kazimirchak-Polonskaya [12, 17] studied the evolution of the orbits of 15 comets (1660-2060) belonging to different planet groups, with a consideration of the disturbances of from six to eight planets (Venus-Uranus, Venus-Pluto). Using the results which she and N.A. Belyayev had obtained, she concluded that the outer

planets (particularly Jupiter) and their effective spheres are powerful transformers of cometary orbits, which determine their evolution to a considerable extent, move the comets from one planet group to another, and in some cases carry them beyond the boundaries of the solar system.

The Institute of Theoretical Astronomy of the Academy of Sciences of the U.S.S.R. is obtaining telegraph messages from the International Center in the USA on newly discovered comets, and is ready to send this information to the "Kometnyy Tsirkulyar" as well as all interested observatories.

References

1. Abalkin, V.K. and N.A. Belyayev: Kometnyy Tsirkulyar, Vol. 38, 1966.
2. Barteneva, O.N.: Byull. Instit. Teoret. Astron., Vol. 10, No. 6(119) p. 443, 1965.
3. Barteneva, O.N.: Byull. Instit. Teoret. Astron., 1968.
4. Belous, L.M.: Byull. Instit.Teoret.Astron., Vol. 9 No. 8(111), p. 569, 1964.
5. Belous, L.M: Byull. Instit.Teoret. Astron., Vol. 10, No. 8(121), 1966; Kometnyy Tsirkulyar, Vol. 24, 1965.
6. Belyayev, N.A.: Byull.Instit.Teoret.Astron., Vol. 10, No. 123, 1966.
7. Belyeyev, N.A.: Astron.Zhur., Vol. 44, No. 2, p. 461, 1967.
8. Galibina, I.V.: In the book: Materialy konferentsii po issledovaniyu dvizheniya malykh planet i komet (Materials of the Conference on the Motion of Small Planets and Comets), Baku, 1962. Academy of Sciences of the Azerb.S.S.R., Baku, p. 145, 1966.
9. Galibina, W.V.: Byull. Instit.Teoret.Astron., Vol. 9, No. 7(110), p. 465, 1964.
10. Galibina, I.V. and O.N. Barteneva: Byull. Instit. Teoret. Astron. Vol. 10, No. 3(116), p. 192, 1965.
11. Imnadze, M.P.: In the book: Trudy Vychislitel'nogo tsentra AN GruzSSR (Proceedings of the Computer Center of the Academt of Sciences of the Georgian S.S.R.), Vol. 3, p. 269, 1963; Soobshcheniya Akad.Nauk GruzSSR, Vol. 30, No. 2, p. 157, 1963.
12. Kazimirchak-Polonskaya, Ye.I.: In the book: Materialy konferentsii po issledovaniyu dvizheniya malykh planet i komet (Materials of the Conference on the Motion of Small Planets and Comets), Baku, 1962. Academy of Sciences of the Azerb S.S.R., Baku, p. 90, 1966.
13. Kazimirchak-Polonskaya, Ye.I.: Trudy Instit.Teoret.Astron., Vol. 12, 1967.
14. Kazimirchak-Polonskaya, Ye.I: Trudy Instit.Teoret.Astron., Vol. 12, 1967.
15. Kazimirchak-Polonskaya, Ye.I.: Trudy Instit.Teoret.Astron., Vol. 12, 1967.
16. Kazimirchak-Polonskaya, Ye.I.: Trudy Instit. Teoret. Astron., Vol. 12, 1967.

17. Kazimirchak-Polonskaya, Ye.I.: Astron.Zhur., Vol. 44, No. 2, p. 439, 1967.
18. Kastel', G.R.: In the book: Materialy konferentsii po issledovaniyu dvizheniya malykh planet i komet (Materials of the Conference on the Motion of Small Planets and Comets) Baku, 1962. Academy of Sciences of the Azerb.S.S.R., Baku, 1966 p. 153; Byull. Instit.Teoret. Astron., Vol. 10, No. 2(115) p. 118, 1965.
19. Makover, S.G. and S.I. Luchich: Byull.Instit. Teoret. Astron., Vol. 9, No. 4(107), p. 224, 1963.
20. Makover, S.G.: Kometnyy Tsirkulyar, Vol. 4, 1963; International Astronomical Union Publications, No. 1852, 1964.
21. Makover, S.G.: Byull.Instit.Teoret.Astron., Vol. 9, No. 8(111), p. 525, 1964.
22. Makover, S.G.: Byull. Instit.Teoret.Astron., Vol. 11, No. 2(125), 1966.
23. Mamedov, M.A.: Astron.Tsirkulyar, No. 346, 1965; Kometnyy Tsirkulyar, Vol. 32, 1965.
24. Mamedov, M.A.: Kometnyy Tsirkulyar, Vol.20, 1965.
25. Mamedov, M.A.: Izvest. Akad.Nauk Azerb.S.S.R. No. 3, 1966.
26. Mamedov, M.A.: Izvest.Akad.Nauk Azerb.S.S.R., No. 5, 1966.
27. Mamedov, M.A.: Izvest.Akad.Nauk Azerb.S.S.R., No. 6, p. 57, 1965.
28. Mamedov, M.A.: Byull.Instit.Teoret.Astron., Vol. 10, No. 8(121), p. 41, 1965.
29. Merzlyakova, M.A.: Astron. Tsirkulyar, No. 263, 1968.
30. Perlin, F.Kh.: In the book: Materialy konferentsii po issledovaniyu dvizheniya malykh planet i komet (Materials of the Conference on the Movement of Small Planets and Comets), Baku, 1962. Academy of Sciences of the Azerb.S.S.R., Baku, p. 62, 1966.
31. Perlin, F.Kh.: Byull.Instit.Teoret.Astron., Vol. 9, No. 9(112), p. 607, 1964.
32. Samoylova-Yakhontova, N.S.: In the book: Materialy konferentsii po issledovaniyu dvizheniya malykh planet i komet (Materials of the Conference on the Movement of Small Planets and Comets), Baku, 1962. Academy of Sciences of the Azerb.S.S.R., Baku, p. 54, 1966.
33. Khanina, F.B.: In the book: Materialy konferentsii po issledovaniyu dvizheniya malykh planet i komet (Materials of the Conference on the Movement of Small Planets and Comets), Baku, 1962. Academy of Sciences of the Azerb.S.S.R., Baku, p. 69, 1966.
34. Abalakin, V.K. and N.A. Belyayev: International Astronomical Union Publications, No. 1953, 1966.
35. Kastel, G.R.: Hand.Brit.Astr.Assoc., p. 64, 1967.
36. Makover, S.G.: Hand.Brit.Astr.Assoc., p. 58, 1964.
37. Merzlyakova, M.A.: International Astronomical Union Publications, No. 1853, 1963.

THE ACCELERATION OF COMETARY IONS BY RANDOM MAGNETIC FIELDS OF THE SOLAR WIND

(Abstract)

A.Z. Dolginov

The high accelerations in cometary tails of the first type are /195
usually explained in terms of the capture of ions by the regular magnetic fields of the solar wind. The assumption that the ions are accelerated by a regular field is confronted with a number of difficulties connected with the problem of the possibility of this field penetrating into the cometary plasma, and with the absence of a correlation between the field direction and the direction of the cometary tail. These difficulties are not encountered if the random component of the interplanetary magnetic field entrained by the solar wind is taken into account. Although we cannot solve the system of the kinetic equation and the Maxwellian equation which describes the movement of cometary ions, we can state that the self-consistent magnetic field has a random component which is comparable to the random component of the field outside the coma. We examined the movement of ions in the random magnetic field during the interaction of the plasma of the solar wind and that of the coma. It is seen that the traveling non-uniformities of the random magnetic field entrain cometary ions in the direction in which the solar wind moves. The estimates obtained for the acceleratino of the ions coincide with the observed values.

† Fiziko-tekhnicheskiy institut imeni Ioffe, Akad. Nauk SSSR.

MODELING THE MOVEMENT OF COMETS IN THE OORT CLOUD (Abstract)

I. Zal'kalne†

A program was constructed for the quick-response electronic computer BESM-2 in order to model the movement of comets in the cloud of Oort. The following scheme was examined. A sphere with radius of 1 *pc* was described around the Sun. One star enters the sphere along straight lines in the course of 20,000 years at a velocity given in the Gliyeze catalogue. The disturbances on the part of the stars and Sun changing the movement of comets are considered in the form of impulses according to the formula of Rissel. In the intervals between impulses, the comet moves along undisturbed orbits, i.e., along an ellipse or hyperbola. The coordinates of the comet x, y, z are determined with accuracy up to eight signs. Five minutes of machine time are needed for one revolution of the comet around the Sun (a = 50,000 AU).

/196

† Astronomicheskaya observatoriya Latviyskogo universiteta.

STREAMER SYSTEMS IN THE TAILS OF COMETS
(Abstract)

V.P. Tarashchuk†

A complex structure is observed in well-developed cometary /197
tails of the first type: single streamers, bunches of streamers and flows from the head of the comet.

The matter in the tail moves with accelerations whose nature is still not completely clear. The changes in the streamer structure occur during very short periods of time. They are the result of processes occurring in the interplanetary medium, as well as the interactions between the cometary matter and the interplanetary plasma.

The changes in structure of the tail during an increase in distance from Sun was examined in the example of Comet Mrkos (1957V). Original photoplates obtained at the Main Astronomical Observatory in Pulkovo and the Main Astronomical Observatory of the Academy of Sciences of the Ukrainian S.S.R., as well as reproductions published in Soviet and foreign presses, were used for this study.

The changes in the streamer system of the tail were examined from August 8 to August 30. The change in position of the axis of a tail of the first type was examined with respect to the extended radius vector. In all cases, the axis of the tail deviated from the extended radius vector in the direction opposing the movement of the comet. There were no regularities established in these deviations for the comet Mrkos, or in the case of comet's Morehouse, Brooks and Daniel.

† Glavnaya Astronomicheskaya observatoriya Akad. Nauk Ukrainskoy SSR.

TEMPERATURE OF THE ICE NUCLEUS OF A COMET NEAR THE SUN (Abstract)

M.Z. Markovich and L.N. Tulenkova†

In 1966, Ye.A. Kaymakov and V.A. Sharkov carried out experiments at the Physico-Technical Institute of the Academy of Sciences of the U.S.S.R. (Leningrad) to determine the rate of evaporation of pure and contaminated water ice under conditions which were close to those of a comet (vacuum on the order of 10^{-5} - 10^{-6} mm Hg). As a result, it was found that the rate of evaporation of ice under vacuum is described rather well by the classic Hertz formula. /198

The average temperature of the surface and inner layer of a nucleus of water ice at a distance of 1 AU from the Sun and closer (orbit of Comet Ikeya-Seki, 1965f) is determined by a numerical solution to the equation of thermal conductivity, with a consideration of the thermal balance on the surface of the nucleus. The substantial decrease in dimensions of the ice nucleus resulting from intensive sublimation at distances from the Sun less than 0.5 AU is also taken into account. The temperatures calculated are in good correspondence with the experimental results of Kaymakov and Sharkov.

The complete text of this report is published in a collection of the proceedings of Kalinin Polytechnical Institute.

† Kalininskiy politekhnicheskiy institut.

ONE REGULARITY IN THE MECHANICAL THEORY OF COMETARY FORMS (Abstract)

O.V. Dobrovol'skiy†

It was found from a large number of observations that the acceleration of particles in dust atmospheres a_0, reduced to a unit distance from the Sun according to the quadratic law, as well as the initial velocity of the particles v_0, obey the relationship $a_0 = Cv_0^2$, which is valid in a wide range of values of a_0 and v_0 both for the head and for the tail of the comet. The relationship corresponds to the ice model of the nucleus.

/199

† Institut Astrofiziki Akad. Nauk Tadzhikskoy SSR.

A NEW METHOD OF CALCULATING PROPERTIES OF COMETARY TAILS (Abstract)

O.V. Dobrovol'skiy and Kh. Ibadinov†

A new formula was obtained in order to determine the true anomaly in the nucleus of a comet v' at the moment t' in which dust particles of the cometary tail are ejected from the nucleus of the comet according to a preset true anomaly of the nucleus v at the moment of observation t and the cometocentric coordinates of the particle of the tail ξ and η: /200

$$v' = v - \frac{\varphi}{\varkappa},$$

where $\tan \phi = \frac{\eta}{\xi}$, $\kappa = 0.670 - 0.00025\, v$. According to our studies, κ does not depend on the perihelion distance of the comet q.

The formula which was found simplifies a solution to the inverse problem of the mechanical theory of cometary forms, i.e., reduces the solution to a few arithmetic operations. It is completely applicable at $v - v' \leq 60°$, which is the interval most used. At $v - v' > 60°$, the error in determining v' increases and reaches several degrees.

A more detailed presentation of this method is given in a report which will be published in the "Byulleten Instituta Astrofiziki AN Tadzh. S.S.R."

† Institut Astrofiziki Akad. Nauk Tadzhikskoy SSR.

A NEW STATISTICAL REGULARITY IN COMETS
(Abstract)

O.V. Dobrovol'skiy and R.S. Osherov†

The many years of observations of Beyer, who determined the apparent brightness I and apparent diameter of comets d in angular dimensions according to a single method for more than thirty years, are analyzed. It was found that individual pairs of the values of I and d can be observed in the most diversified combinations, but the following rather pronounced statistical dependence exists: /201

$$I=Ad^{B},$$

where A and B are constant. This dependence is discussed briefly within the framework of the isophote theory.

† Institut Astrofiziki Akad. Nauk Tadzhikskoy SSR.

THE TAIL OF COMET IKEYA-SEKI BEFORE PERIHELION (Abstract)

Kh. Ibadinov†

Two pre-perihelion photographs of Comet 1965f for October 21. /202
0972 and 21.1438 (r = 0.015 and 0.01 AU) were studied by the methods of the mechanical theory of cometary forms. The values of the effective acceleration $1 + \mu$ were determined. It was found that the tail was neither syndynamic nor synchronous, but was formed by the continuous ejection of particles. Approximately, the tail of 21.0972 corresponded to types I and II, and that of 21.1438 corresponded to type III.

In the interval between photographs, i.e., in 1 hour and 7 minutes, the tail was almost completely reconstructed, and the particles of the tail of 21.0972, which were ejected later, passed by the slower particles which formed the tail of 21.1438 and those of 21.0872 in the circum-nuclear zone with $\xi < 0.001$ AU.

† Institut Astrofiziki Akad. Nauk Tadzhikskoy SSR.

ONE OF THE POSSIBLE REASONS FOR THE ASYMMETRY IN THE BRIGHTNESS CURVES OF COMETS WITH RESPECT TO THE PERIHELION (Abstract)

P. Yegibekov†

A numerical integration of the equation of heat conductivity /203 was carried out for the revolving nucleus of a comet on the assumption that the axis of rotation was directed along the radius vector and perpendicular to it. Under otherwise equal conditions, the difference in brightness of the comet before and after perihelion can reach several stellar magnitudes. The effect is partly due to the different effective heating area and the temperature differential thus arising, and partly to the increase in efficiency of the solar radiation with an increase in temperature.

† Institut Astrofiziki Akad. Nauk Tadzhikskoy SSR.

THE OBSERVATIONS OF COMET IKEYA-SEKI (1965f) AT DUSHABNE (Abstract)

A.M. Bakharev[†]

Comet 1965f was found by the author at 00 UT on September 25, /204
1965, with the aid of the "Asembi" binocular. It had the appearance of a hazy object of 7.5^m with a sharply pronounced bright planetary nucleus. All the observations were carried out at the Gissar Astronomical Observatory of the Institute of Astrophysics of the Academy of Sciences of the Tadzhik S.S.R. Before passage of the perihelion, a planetary nucleus of comparatively large dimensions was clearly singled out in telescopic observations. On September 28 and 29, 1965, the brightness of the comet was equal to 6.20^m. A straight tail with length of about 15′ was noticed.

On September 30, the comet seeking was unsuccessful; it was hidden in the rays of the Sun.

Starting on November 1, 1965 (after perihelion), the comet was photographed many times with the aid of small-size cameras. The photographs were obtained by Ye.V. Struk, O.Mamadov and the author. Two tails can be seen on them, and the larger one had length on the order of 45°. Many fibers, jet flows from the head of the comet, bright transverse light bands, etc. can be seen in the tail.

It is suggested that the movements of single formations in both tails of the comet be examined according to the photographs. The results will be published in the publications of the Institute of Astrophysics of the Academy of Sciences of the Tadzhik S.S.R.

[†] Institut Astrofiziki Akad. Nauk Tadzhikskoy SSR.

THE COMET IKEYA-SEKI ACCORDING TO OBSERVATIONS AT ALMA ATA (Abstract)

Sh.N. Sabitov[†]

In November of 1965, during the period of the convergence of /205
Comet Ikeya-Seki with the Sun, a number of photographs and the spectrum of the tail of this comet were obtained at the Astrophysical Institute of the Academy of Sciences of the Kazakh S.S.R.

Polarimetric Observations. Sixteen photographs of the tail of the comet were obtained for different positions of the polaroid, which varied by 60° (method of Academician V.G. Fesenkov). The observations were carried out on the meniscus telescope of the system of D.D. Maksutov (aperture ratio 1:2.5), as well as on the Schmidt camera constructed at the Astrophysical Institute of the Academy of Sciences of the Kazakh S.S.R. (Aperture ratio 1:1). The exposure was from 2 to 4 min. The atmospheric conditions were advantageous for observations, and the quality of the photographs was good. The analysis of the photographs obtained on the meniscus telescope of Maksutov's system was carried out with the aid of the M-20 computer. An independent analysis of the photographs obtained on the two instruments gave consistent results. Radial polarization of the light of the cometary tail with respect to the Sun was found. The degree of polarization changed from 10 to 50% as the distance to the tip of the comet decreased.

Photographs on Both Lines. Photographs of the cometary tail were obtained on the Schmidt camera, and later, when the brightness of the comet decreased substantially, photographs of the entire comet. This aided in constructing the brightness distribution in absolute units.

The spectrum of the cometary tail was obtained. The energy distribution in the wavelength interval from 4000 to 6400 Å was found.

[†] Astrofizicheskiy Institut Akad. Nauk Kazakhskoy SSR.

INVESTIGATION OF THE TAIL OF COMET IKEYA-SEKI
(Abstract)

N.S. Chernykh†

The comet Ikeya-Seki was photographed at the Crimean Astrophysical Observatory of the Academy of Sciences of the U.S.S.R. on the dual 40-centimeter astrograph from September 26 to December 3, 1965 with astrometric targets. Twenty-six photographs were obtained. The photographs of September 29, October 2 and November 5 were used for determining the type of the tail. /206

On the photographs for September 29 and October 2, the tail of the comet, with length of about 1°, was oriented almost precisely along the continuation of the radius vector; therefore, it should belong to the first type in the classification of Bredikhin.

On the photographs of November 5 (2 photographs with the 40-centimeter astrograph and 2 with the "zenit" camera), the insignificantly curved tail extends to 20°, inclining notably from the continued radius vector. A number of points in the axis of the tail and two synchrones were projected on the plane of the cometary orbit. In the cometocentric system of coordinates, the position of the axis of the tail relative to the radius vector and the syndynames $1 + \mu = 1$ indicate that the tail belongs to the second type. The repulsive forces, which were calculated for points on the axis of the tail, were found to be equal to $1 + \mu = 0.55$. Calculations of the lifetime of the particles at the points of the tail under investigation showed that all the particles composing the tail of the comet on November 4 were ejected from the nucleus after the passage of the comet through perihelion.

The escape velocity of the particles leaving the nucleus was determined according to the width of the synchrones and their lifetime. It was found to be equal to 0.4 km/sec.

This report will be published in "Izvestiya Krymskoy Astrofizicheskoy Observatorii AN SSSR in Volume 37.

† Krymskiy Astrofizicheskiy institut, Akad. Nauk SSSR.

THE CLUSTER OF OORT COMETS
(Abstract)

S.K. Vsekhsvyatskiy†

In a famous study of J. Oort (B.A.N., 1950, p. 408), the effects of stellar disturbances on the component clusters of comets which extended, according to Oort, from 25,000 to 200,000 AU, were examined. It was first assumed that the comets, just as all small bodies, could be formed as the result of the disruption of a hypothetical planet. At present, it is postulated (1963) that the comets were condensed during the first period of existence of the solar system in the region of large planets and, becoming the ejected perturbations of the latter, were preserved in this cluster, moving around the Sun. Oort maintained that the perturbations of the stars will limit the dimensions of the cluster of comets. Recently, G.A. Chebotarev (Astron. Zhur., Vol. 43, No. 2, p. 435, 1966) showed that the disturbances from the galactic nucleus should limit the dimensions of the cluster to distances of 60,000 - 100,000 AU. According to Oort, the velocities of the comets in the cluster are always less than the escape velocities for the given distance, i.e., less than 250 m/sec for the inner boundary of the cluster. However, calculations show that the comets could not preserve angular velocities in it during the prolonged existence of the cluster, but should have acquired substantial hyperbolic velocities as a result of repeated stellar passages through the region of the cluster. /207

It was shown earlier (Astron. Zhur., Vol. 31, p. 587, 1954) that, during 10^9 years existence of a cluster, there should be passages of stars through it tens of thousands of times, and no less than one thousand times for a distance of 10,000 AU from the Sun. The average value for the relative velocities of the stars closest to the Sun was roughly equal to 35 km/sec. The star encounters the comets in the cluster almost at its relative velocity.

Newton's famous relationship

$$\frac{1}{a} - \frac{1}{a_{\text{н}}} = \frac{1.M\cos\varphi\sin\alpha}{PS},$$

in which a_{in} is the initial semiaxis of the cometary orbit (roughly equal to the radius R), M is the mass of the star, P is a value roughly equal to the parameter of the cometary orbit relative to the star ($P < R$), S is the velocity ratio of the comet relative to the star and that of the star relative to the Sun (practically equal to one), 2α is the angle between the asymptotes of the relative hyperbolic cometary orbit, and ϕ is the angle between the direction of /208

† Kiyevskiy gosudarstrenniy universitet imeni T.G. Shevchenko.

the velocity of the star and the direction of the periastron of the relative cometary orbit, is always negative, since the velocity of the star is two orders greater than the relative velocities in the cluster. Consequently, as a result of the passages of stars, the overwhelming majority of the comets should acquire substantial hyperbolic velocities and go into interplanetary space in a time no longer than 10^8 years.

THE SUBLIMATION OF H_2O ICE AT LOW TEMPERATURES
(Abstract)

Ye.A. Kaymakov and V.I. Sharkov†

The results of experiments carried out in order to determine /209
of heats of sublimation of H_2O ice at low temperatures are given in this study. The experiments were carried out in a liquid-nitrogen cooled vacuum chamber under a residual gas pressure of $5 \cdot 10^{-6}$ mm Hg. The cuvette with the ice under investigation were attached to a spring balance. Each value for the power input corresponded to a value determined for the steady-state teimperature of the ice surface. The power losses not connected with sublimation were taken into account. The steady-state temperature and yield of ice were measured in the experiments as a function of the energy flux supplied to a unit surface of the ice (specific power).

In changes of the specific capacity from 0.142 to $2 \cdot 10^{-3}$ $W \cdot cm^{-2}$, the temperature of the ice surface changed from -66 to -103°C, while the flux of sublimation changed from $0.47 \cdot 10^{-4}$ to $0.3 \cdot 10^{-6}$ $g \cdot cm^{-2} \cdot sec^{-1}$, In the temperature range of -(57-77)°C, the heat of sublimation was about 670 cal per gram.

† Fiziko-tekhnicheskiy Institut imeni Ioffe, Akad. Nauk SSSR.

THE BEHAVIOR OF DUST PARTICLES IN THE SUBLIMATION OF ICE IN THE SYSTEM H_2O ICE-DUST (Abstract)

Ye.A. Kaymakov and V.I. Sharkov[†]

The results of experiments investigating the conditions for /210 the formation and disruption of matrices, determining the velocities and angular distribution for escape of the dust particles, and defining the albedo of the ice-dust system are given in this report.

The experiments were carried out in a vacuum chamber under residual gas pressure of the order of 10^{-5} mm Hg. The energy was supplied to the sample either with the aid of a miniature electric heater or with a light beam. The temperature of the sample varied from -49 to -77°C. The ice and dust, which was of electrocorundum and nickel metal with grain size from 3 to 20 μ, was studied for different weight ratios between the ice and the dust.

It was shown that a low temperature of the ice, as well as high concentration and small dimensions of the dust particles, bring about the formation of matrices. The discarding of matrices occurs during changes in the intensity of the light beam.

The escape velocity of the dust particles is determined mainly by the temperature of the ice and depends little on the size of the particles.

[†] Fiziko-tekhnicheskiy Institut imeni Ioffe, Akad. Nauk SSSR.

THE EMISSION SPECTRA OF NITROGEN, OXYGEN AND AIR ($\lambda\lambda$7000-11500Å) EXCITED BY FAST ELECTRONS (Abstract)

A.M. Fogel', A.G. Koval', V.T. Koppe and V.V. Gritsyna[†]

The spectra of rarefield nitrogen, oxygen and air excited by /211 electrons with energy of 13 keV in the wavelength range of 7000-11500Å were obtained and analyzed. The spectrograph IPS-51 and an image converter were used for recording the spectra. The relative intensities of all the emissions observed were determined. The bands of Meynel's N_2^+ system and the first positive N_2 system are the most intensive in the nitrogen in this spectral region. In this regard, the intensity of the bands of the N_2 system are two or three times weaker than for Meynel's system for identical v and v''. In the oxygen spectrum, relatively intensive bands of the first negative system and four intensive lines λ = 7775, 8447, 9286 and 11295Å are observed. For nitrogen and oxygen, a large number of weaker emissions (NI, NII, OII and OI) was recorded. The spectra obtained were compared to those of gases disturbed in a gaseous discharge and to those of aurorae.

[†] Fiziko-tekhnicheskiy Institut Akad. Nauk Ukrainskoy SSR.

OBSERVATIONS OF COMET IKEYA-SEKI IN NOVEMBER OF 1965 ON AN ELECTRONIC-TELESCOPIC DEVICE (Abstract)

P.G. Petrov, K.L. Mench and V.S. Rylov[†]

Observations of Ikeya-Seki were carried out in November of 1965 on the electronic-telescopic device of the Physico-Technical Institute at the base of the Crimean Observatory in Simeiz. More than 40 photographs of the comet were taken with exposures from 0.1 to 10 sec. The photographs of the comet with interference light filters were found to be unsuccessful because of the large dark background of the image converter.

/212

[†] Fiziko-tekhnicheskiy Institut imeni Ioffe, Akad. Nauk SSSR.

ULTIMATE, INITIAL AND FUTURE ORBITS OF COMET ALCOCK (1959IV) (Abstract)

G.T. Yanovitskaya†

The ultimate orbit of Comet Alcock (1959IV) was determined on the basis of all the available observations. A system of elements which Marsden calculated and which used eight observations encompassing the period from August 27 to September 22, 1959 (NAS, 1446), was selected as the preliminary system for further refinement. August 20, 1959 was taken as the time of osculation. All the calculations were carried out on the computer BESM-2M with the aid of the complex of programs constructed in order to determine the near-parabolic orbits of the comets. The disturbances from Venus, Earth, Mars, Jupiter, Saturn, Uranus and Neptune were taken into account. The integration of the differential equations relative to the elements of the cometary orbit was conducted by the quadratic method, with interval of ten days, and the changes in elements were taken into account in the right-hand parts of the differential equations. As a result of the refining, the following ultimate system of elements was obtained: /213

$$T = 1959\ \text{August}\ 7.607\ 54\ \text{E. T.}$$

$$\left.\begin{aligned} \omega &= 124°.706\ 16; \\ \Omega &= 159.225\ 73; \\ i &= 48.262\ 84; \\ q &= 1.150\ 3541; \\ e &= 1.000\ 9192; \end{aligned}\right\} 1950.0,$$

$$\frac{1}{a} = -0.000\ 799 \pm 0.000\ 043.$$

As regards the hyperbolic form of the orbit of Comet 1959IV, it was decided that its initial and future orbits should be calculated.

The integration of the differential equations was carried out before and after the time of osculation (foreward and backward) until the elements of its orbit changed so insignificantly, because of the rather great distance of the comet from the disturbing bodies, that the nature of the orbit could be discussed. In this regard, the program constructed for the BESM-2M required a calculation of the corrections for the barycenter in the rectilinear heliocentric equatorial coordinates, as well as the velocities of the comet, which allowed us to calculate the inverse value of the major semi-axis of the cometary orbit in the barycentric system of coordinates. /214

† Glavnaya Astronomicheskay Observatoriya, Akad. Nauk Ukrainskoy SSR.

It was found that the orbit of Comet 1959 IV (Alcock) was hyperbolic in the heliocentric system of coordinates and elliptical in the barycentric system during the osculation. The initial orbit of this comet was elliptical, while the future one was hyperbolic.

The results obtained will be published in "Byulleten Instituta Teoreticheskoy Astrofiziki".

ALL-UNION CONFERENCE ON THE PHYSICS OF COMETS

V.I. Ivanchuk†

ABSTRACT: A brief review is given of the studies and decisions of the All-Union Conference on the Physics of Comets which was held in Kiev on October 26-29, 1966.

On October 26-29, 1966, a regular conference on comets was held in Kiev under the direction of Professor B.A. Vorontsov-Vel'yaminov. The conference was organized by the group for the study of comets in the IQSY, the commission on comets and meteors of the Astrosovet of the Academy of Sciences of the U.S.S.R., Kiev State University imeni T.G. Shevchenko and the Main Astronomical Observatory of the Academy of Sciences of the Ukrainian S.S.R. /215

More than 70 people, representing about 30 science-research institutes and universities, took part in the work of the conference. Forty-nine addresses and reports were given. A rather wide range of timely problems in the physics of comets was discussed: the processes in heads and tails, the interaction between comets and the interplanetary medium and solar radiation, the modeling of cometary processes under laboratory conditions, the problems of the origination of comets and other groups of small bodies, the problems of the observation techniques, etc.

Professor B.A. Vorontsov-Vel'yaminov, the director of the group on the study of comets in the IQSY S.K. Vsekhsvyatskiy, and Academician of the Academy of Sciences of the Tadzhik S.S.R. O.V. Dobrovol'skiy mentioned the increasing significance of cometary investigations at this stage in space research. S.K. Vsekhsvyatskiy emphasized that, in addition to the generally-accepted role of comets as natural probes of interplanetary space and indicators of the solar activity, the possibility of using comets in order to understand the past of the solar system and the evolution of planetary bodies is becoming more and more apparent.

The heating of the nucleus of a comet, which consists of H_2O ice, and some accompanying physical processes in nuclei at short distances from the Sun were examined by M.Z. Markovich and A.M. Al'khovskiy (Kalinin). The authors concluded that there could be melting of the ice at a distance of 0.5 AU from the Sun; this brought forth objections, because they did not take account of the process of sublimation and the effect of the cometary atmosphere. M.Z. Markovich examined different methods of estimating the amount of dust in the heads of comets. It was found that the concentration of dust particles changes with the distance from the center of the nucleus according to an inverse square law. Assuming that the

† Kiyeskiy Gosudarstrenniy Universitet imeni T.G. Shevchenko.

distribution of dust particles by radii in the heads of comets is analogous to the distribution of particles in meteor streams, the masses of dust in cometary heads were found to be equal to 10^8 - 10^{13} g (at r = 1 AU) for heads with varying degrees of "dustiness". /216

L.M. Shul'man (Kiev, Main Astronomical Observatory of the Academy of Sciences of the Ukrainian S.S.R.) studied the near-nucleus region of the cometary head, for which molecular collisions are substantial. It follows from a gas-dynamics investigation that there can be a supersonic flow region in which the nucleus is surrounded by a fixed shock wave which has the appearance of a halo.

O.V. Dobrovol'skiy (Dushanbe) found from an analysis of the data in the literature that the acceleration of dust particles in cometary atmospheres is proportional to the square of their initial velocity. This corroborates the ice model of the cometary nucleus. In the discussion, L.M. Shul'man mentioned that the regularity he found can be understood as the result of acceleration of the dust by a gas flow.

New and convenient formulas for calculating the moments of the ejection of dust particles of the cometary tail from the cometary nucleus according to present coordinates and observation site were suggested in the address by O.V. Dobrovol'skiy and Kh. Ibadinov.

Ye.B. Kostyakova (P.K. Shternberg State Astronomical Institute) determined the distribution of matter in the head of Comet Arend-Roland (1957III). She showed that the density decreases according to an inverse square law.

Z. Sekanina (Prague) studied the dynamic effect of the forces of a non-gravitational nature resulting from outflows from the nucleus or eruptions, and found the changes in orbital elements as a function of the rotation of the nucleus. The method he developed aided in evaluating the decrease in mass (for example, Halley's comet lost up to 10^{13} g of the mass of the nucleus in one outburst). The effect of the rotation of the nucleus on the characteristics of the brightness curve was examined by P. Yegibekov (Dushanbe). Because of the varying effective heating area for different positions of the axis of rotation with respect to the radius vector of the comet, the asymmetry of the brightness curves can reach several stellar magnitudes.

The studies on the modeling of physical processes in comets (Ye.A. Kaymakov, V.I. Sharkov) which were carried out at the Physico-Technical Institute imeni Ioffe of the Academy of Sciences of the U.S.S.R. aroused great interest. The values for the heat of sublimation of H_2O ice were determined here for low temperatures. In a change in specific capacity from $4 \cdot 10^{-1}$ to $5 \cdot 10^{-4}$ W·cm^{-2}, the flux of sublimation changed from 10^{-4} to 10^{-6} g·cm^{-2}·sec^{-1}. It was found that the escape velocity of the dust particles from the ice-dust system, put under vacuum of 10^{-5} mm Hg at T = 200-235°K, is determined mainly by the temperature of the sample and changes

little with the size of the dust particles (3.5μ). A change in intensity of illumination of the sample by a light beam brings about a discarding of the matrices (dust skin), which may be connected with outbursts in cometary heads. /217

Arguments in favor of the idea that the parabolic shells of bright comets, the tails of type II, and also the spherical comas of comets which are far removed from the Sun, are different forms of the same formation, which has an identical gaseous nature (C_2, CN molecules), were given in the report of V.G. Riyves (Tartu). According to B.Yu. Levin (as follows from the theses mentioned at the conference), the repulsive accelerations, the great thickness of the tail in the direction perpendicular to the planet of the orbit, the nature of the deviations in the energy distribution from the solar spectrum, and a number of other factors affect the gaseous nature of tails of type II.

V.P. Tarashchuk (Kiev, Main Astronomical Observatory of the Academy of Sciences of the Ukrainian S.S.R.) analyzed the changes in structure of the tail of Comet Mrkos (1957V). No regularities were found in the oscillations in position of the axis of the tail with respect to the radius vector of the comet. G.K. Nazarchuk (Kiev) compared the brightness distribution in the tail of comet Arend-Roland (1957III) to some theoretical models. This aided in evaluating a number of the physical characteristics of the cometary tail, including the particle flux. The expansion of the matter occurs anisotropically, which is explained by the presence of a longitudinal magnetic field with $H = 10^{-5}$ G. It was shown that the parameters of corpuscular streams interacting with comets could be investigated.

A.Z. Dolginov (Physico-Technical Institute of the Academy of Sciences of the U.S.S.R.) pointed out a number of problems encountered in the acceleration of cometary ions in tails of type I with the regular magnetic field of the solar wind. After an examination of the movement of ions in a random magnetic field, it was concluded that the non-uniformities moving in the magnetic field are responsible for the acceleration of the ions arising in the interaction of the solarwind plasma with the plasma of the comet. A.Z. Dolginov and A.S. Dvoryashin (Crimean Astronomical Observatory) presented some reviews of the most recent data on interplanetary magnetic fields, solar corpuscular radiation, and the interaction of the solar wind with the Earth's magnetosphere.

O.V. Dobrovol'skiy and R.S. Osherov studied the deviations from the ordinary photometric formula for comets. The supplementary parameter k, which characterizes the deviations from the inverse square law at geocentric distances, acquires a value from 5 to -2 (the standard value $k = 2$ signifies preservation of the inverse square law) for different comets. An analysis of Beyer's series showed a rather clear statistical dependence between the apparent brightness and diameter of the comet $I = Ad^B$, where A and B are constants. /218

V.I. Cherednichenko (Kiev) examined a number of basic problems in the spectroscopy of comets. It was shown that a detection of the hydrogen (H_α) emission in the spectrum of comets is made difficult because of the weakness and blending with the hydrogen emission of the geocorona. The most probable parent molecules, which coincide with the products of volcanic eruptions on the Earth, were found. The mechanisms for emission of the forbidden lines λλ5577 and 6300 of oxygen and the yellow sodium line (λ5890) were examined, and the total quantity of these elements was estimated for the head of Comet Mrkos (1957V). The continuous spectrum can be partly due to the processes of recombination of cometary ions with the electrons of the solar wind. It was mentioned in the discussion that the author uses increased values for the density of the corpuscular streams, compared to the data of rocket measurements.

D.A. Mokhnach (Leningrad) developed new concepts on the processes of dissociation and ionization of cometary molecules by the ultraviolet radiation of the Sun. Z. Sekanina spoke of the studies of V. Vanysek (Prague) on the photoelectric scanning of comets.

Ya.M. Fogel', A.G. Koval', V.T. Koppe and V.V. Gritsyna (Khar'kov) studied the infrared emission spectrum of evacuated nitrogen and oxygen of the air excited by electrons with energy of 13 keV. A close agreement was found between these spectra and those of aurorae. The importance and necessity of an experimental investigation of the spectra for conditions close to those of the cometary atmospheres were mentioned in the discussion.

There were eleven reports on Comet Ikeya-Seki, 1965f. Z. Sekanina studied the motion of two components of the nucleus of this comet and established the time of their division near the perihelion (October 21). N.S. Chernykh (Crimean Astronomical Observatory), Kh. Ibadinov (Dushanbe), S.K. Vsekhsvyatskiy, A.A. Demenko (Kiev) and A.M. Bakharev (Dushanbe) determined the type of tail and discussed the changes occuring with the comet. Sh.N. Sabitov (Alma Ata, Astrophysical Institute), E.Ye. Khachikyan (Byurakan), A.A. Demenko and V.T. Khrapach (Kiev, Astronomical Observatory of Kiev State University) gave data on the photometry of the tail. Before the passage of the comet through the perihelion (September, 1965), it had a straight tail of type I. Near the perihelion (at heliocentric distances of r = 0.01 AU), substantial and rapid changes of the tail from type I to type III were noted in a few hours. The shape of the tail cannot be described in full within the framework of the mechanical theory. After perihelion, at the end of October and the beginning of November, the comet had a strong tail of type II which extended by more than 20°. Unusual "synchrones" were sometimes noted, where the filamentary structure of the tail was similar to a twisted rope. The rate of escape from the nucleus was equal to 0.4 km/sec, according to N.S. Chernykh.

B.A. Vorontsov-Vel'yaminov pointed out the great losses which Soviet astronomy suffered by the sensational and hasty remarks made

in the press on the collision of Comet Ikeya-Seki with the Sun; these remarks were based on the first, not very accurate data on the elements of the orbit.

According to the photographs obtained in Alma Ata on November 1-2, 1965 (Schmidt camera 1:1 and Maksutov camera 1:2.5), there was radial polarization relative to the Sun which increased from the head to the tip of the tail (10-60%). This conclusion of Sh. M. Sabitov agrees qualitatively with the results of the polarimetric measurements carried out at Byurakan (E.Ye. Khachikyan) and at the station of Leningrad University (T.A. Polyakova and T.K. Pisareva).

The report of G.G. Petrov, P.S. Rylov and K.L. Mench treated the results of observations with the electronic telescope of the Physico-Technical Institute imeni Ioffe of the Academy of Sciences of the U.S.S.R. in the Crimea. The photographs of Comet Ikeya-Seki with exposures of 0.1 - 10 sec were not completely satisfactory because of the large dark background of the image converter.

In the address of V.P. Konopleva, G.A. Garazdo-Lesnykh and Ye. M. Sered (Kiev), there were reports on different observations of comets during the IQSY which were carried out in the U.S.S.R. and abroad, as well as the work of the Main Astronomical Observatory of the Academy of Sciences of the Ukrainian S.S.R. as the World Data Center. Twenty-eight comets were observed in 1957-1965. The large number of investigations carried out at the Main Astronomical Observatory on the collection of the data of comet observations was mentioned in the discussion.

V.P. Konopleva (Main Astronomical Observatory), A.M. Bakharev (Dushanbe, Astrophysical Institute), Ye.B. Kostyakova (P.K. Shternberg State Astronomical Institute), N.S. Chernykh (Crimean Astronomical Observatory), S.K. Vsekhsvyatskiy (Kiev State University), E. Ye. Khachikyan (Byurakan), Z. Sekanina (Czechoslovakia) and others reported on the observations of comets carried out in different institutions in 1966. E.A. Dibay and V.P. Yesipov (P.K. Shternberg State Astronomical Institute) studied the spectra in the visible region of three comets 1966 b,c,d with the aide of an image converter in the Cassegrainian focus of the 125-centimeter reflector (dispersion of 270 Å/mm, exposure of 30 min - 2 hours). Changes were noted in the C_2 bands in the heads.

N.A. Bokhan (Institute of Theoretical Astronomy), Ye.A. Novikova (Kazan') and A. Yanovitskaya (Main Astronomical Observatory of the Academy of Sciences of the Ukrainina S.S.R.) reported on calculations of the orbits and the theory of motion of comets. The total catalogue of 81 initial and 50 future cometary orbits was presented and analyzed by Z. Sekanina. /220

The importance of the studies conducted at the Institute of Theoretical Astronomy and the new qualitative stage of these investigations were pointed out. In the second half of 1965, the program

for computer calculations of parabolic orbits and ephemerides, as well as the ultimate orbits, was developed at the ITA. The ITA also distributes information on the first orbits and periodic ephemerides to the institutions which survey comets. It was suggested that studies on the theory of the movement of comets could be expanded with a consideration of the non-gravitational effects in the movement of comets and investigations of the convergences of short-period comets with Jupiter.

The problems of the cosmogony of comets and small bodies was given great significance at the conference. Using calculations of the conditions for convergence of the solar system with the nearest stars, S.K. Vsekhsvyatskiy showed the impossibility of the existence of the stationary Oort cloud. A number of substantial contradictions were found in the modern hypotheses of Koiper, Whipple and others, and numerous data were given in favor of the disruption hypotheses for the formation of all groups of small bodies. The total mass of the substance which is lost by the planets of the solar system as a result of the eruptive activity is 10^{30} - 10^{31} g. I. Zal'kalne (Riga) reported an interesting experiment on the modeling of the movement of comets in the Oort cloud on a BESM-2, with a consideration of the disturbances from stars and the Sun. The first experimental results were obtained; they indicated that the comets are ejected from the cloud. Z. Sekanina discussed the methods and results of a recent study by L. Kresak. He again affirmed that the secular decrease in brightness of Comet Encke is from 2 to 4^m per century. He also examined the regularity in the distribution of orbital elements of comets with an extremely short perihelion distance (family of Kreuze comets). A hypothesis was given on the passage of these comets as a result of a cosmic collision occuring with a hyperbolic body. The orbits of the body and the time of the collision were determined.

N.B. Divari (Odessa) studied the possibility of the formation of zodiacal light due to the disintegration of different groups of small bodies. It follows from a comparison of the brightness distribution and polarization system of zodiacal light and the calculated distribution that none of the groups of small bodies can completely satisfy the characteristics observed in zodiacal light. /221

Ye.N. Kramer (Odessa) examined a number of characteristic features and anomalies in the movement and structure of some meteor bodies. He considered them to be bodies of a cometary origin which preserve partially "volatile" compounds. It was pointed out that there are difficulties in explaining the preservation of volatile compounds in such small bodies as the meteoric dust particles which exist in the field of solar emission.

The general increase in observations and investigations of comets which have recently been carried out in the U.S.S.R. was noted in the resolutions of the conference. The successful studies on the modeling of cometary processes which were carried out at

the Physico-Technical Institute imeni Ioffe of the Academy of Sciences of the U.S.S.R. were mentioned in particular, as they aided in solving the problem of plotting the ephemeris of a cometary surveying site. The calculations of orbits and discussions of the theory of the movement of comets (Institute of Theoretical Astronomy of the Academy of Sciences of the U.S.S.R.) were also given particular mention.

At the same time, it was noted that the observations of comets lag a great deal behind the contemporary level. Thus, almost all the stations in the USA use extremely large telescopes for observations of comets. In October-November, 1965, unique data were obtained in many observations of the USA and France on the spectrum of Comet Ikeya-Seki during its approach to the Sun; lines of Fe, Na, K, Ca^+ and others were observed. Spectrograms of the ultraviolet region (1100-2300 Å) were obtained with the aid of rockets launched on October 19 and 21.

For measures needed to increase the level of cometary observations in the U.S.S.R., the conference recommended that studies of large telescopes of Soviet observatories be included in the cometary observation program, as well as the rapid completion of the observatory of the Astrophysical Institute of the Academy of Sciences of the Tadzhik S.S.R. (with a sub-station at Sanglok) and the cometary station of Kiev State University at Lesniki, and the development of cometary observations at the Main Astronomical Observatory of the Academy of Sciences of the Ukrainian S.S.R. In particular, it was recommended that spectral observations of comets be included in the program for the 2-meter reflector of the Shemakhin Observatory of the Academy of Sciences of the Azerbaidzhan S.S.R.

The participants supported the plan of starting an International Photoelectric Survey of Comets in 1967-1968 in order to record the brightness of all the accessible comets (brighter than $11\text{-}12^m$), considering it necessary for this purpose to use the instruments of the Byrakan station of the Astronomical Observatory of Leningrad State University, the Astrophysical Institute of the Academy of Sciences of the Kazakh S.S.R., the Abastumani Astrophysical Observatory, the Main Astronomical Observatory of the Academy of Sciences of the Ukrainian S.S.R. and the observatory of Odessa University. /222
In this regard, it was noted that the system of magnitudes must be developed for photoelectric observations; before constructing a new system, it was recommended that the method and system used in Czechoslovakia be tested.

The organization of photoelectric surveying of comets is also very important to provide for observations of artificial comets. The results of the studies carried out by astronomers of the USA and the Federal Republic of Germany on observations of artifical comets have shown the great potentials of such experiments for testing the role of solar photon and corpuscular radiation in inter-

planetary space and for solving a number of other cometary and combined problems. Therefore, the conference turned to the Astrosovet of the Academy of Sciences of the U.S.S.R. with a petition for the realization of the previously-developed plan of cometary investigations in the U.S.S.R. in every way possible.

It was decided that comet-seeking services must be organized in the very near future, considering the experience of the Czechoslovakian astronomers. Amateur astronomers in different divisions of the All-Union Astronomical and Geodetic Society could be of great aid in this study.

It was mentioned that the following conference would be held in Kiev in October-November, 1967, and at the Summer School on the Physics of Comets in 1968.

Translated for the National Aeronautics and Space Administration by:
Aztec School of Languages, Inc.
Research Translation Division (457)
Maynard, Massachusetts and McLean, Virginia
NASW-1692

NASA-Langley, 1970 —— 30 F-599

"The aeronautical and space activities of the United States shall be conducted so as to contribute . . . to the expansion of human knowledge of phenomena in the atmosphere and space. The Administration shall provide for the widest practicable and appropriate dissemination of information concerning its activities and the results thereof."

—NATIONAL AERONAUTICS AND SPACE ACT OF 1958

NASA SCIENTIFIC AND TECHNICAL PUBLICATIONS

TECHNICAL REPORTS: Scientific and technical information considered important, complete, and a lasting contribution to existing knowledge.

TECHNICAL NOTES: Information less broad in scope but nevertheless of importance as a contribution to existing knowledge.

TECHNICAL MEMORANDUMS: Information receiving limited distribution because of preliminary data, security classification, or other reasons.

CONTRACTOR REPORTS: Scientific and technical information generated under a NASA contract or grant and considered an important contribution to existing knowledge.

TECHNICAL TRANSLATIONS: Information published in a foreign language considered to merit NASA distribution in English.

SPECIAL PUBLICATIONS: Information derived from or of value to NASA activities. Publications include conference proceedings, monographs, data compilations, handbooks, sourcebooks, and special bibliographies.

TECHNOLOGY UTILIZATION PUBLICATIONS: Information on technology used by NASA that may be of particular interest in commercial and other non-aerospace applications. Publications include Tech Briefs, Technology Utilization Reports and Technology Surveys.

Details on the availability of these publications may be obtained from:

SCIENTIFIC AND TECHNICAL INFORMATION DIVISION

NATIONAL AERONAUTICS AND SPACE ADMINISTRATION

Washington, D.C. 20546